

*Response of the photosynthetic  
system to altered protein composition  
and changes in environmental  
conditions*

*Tünde Tóth*

## **Thesis committee**

### **Promotor**

Prof. Dr H. van Amerongen  
Professor of Biophysics  
Wageningen University

### **Co-promotors**

Dr G. Garab  
Group leader, Institute of Plant Biology  
Biological Research Centre, Szeged, Hungary

Dr L. Kovács  
Senior research associate, Institute of Plant Biology  
Biological Research Centre, Szeged, Hungary

### **Other members**

Prof. Dr O. van Kooten, Wageningen University  
Dr J.C.P. Matthijs, University of Amsterdam  
Dr J.P. Dekker, VU University Amsterdam  
Prof. Dr C. Mullineaux, Queen Mary University of London, United Kingdom

This research was conducted under the auspices of the Graduate School of Experimental Plant Sciences

**Response of the photosynthetic system to altered  
protein composition and changes in  
environmental conditions**

Tünde Tóth

**Thesis**

submitted in fulfilment of the requirements for the degree of doctor  
at Wageningen University  
by the authority of the Rector Magnificus  
Prof. Dr M.J. Kropff,  
in the presence of the  
Thesis Committee appointed by the Academic Board  
to be defended in public  
on Wednesday 3 September 2014  
at 11 a.m. in the Aula.

Tünde Tóth

Response of the photosynthetic system to altered protein composition  
and changes in environmental conditions,  
150 pages.

PhD thesis, Wageningen University, Wageningen, NL (2014)  
With references, with summaries in Dutch and English

ISBN 987-94-6257-050-4

*"Life is bottled sunshine"*

*Winwood Reade, 1874*

# *Table of contents*

<b><i>Abbreviations</i></b>	<b>2</b>
<b><i>Chapter 1</i></b>	<b>4</b>
<i>Introduction</i>	
<b><i>Chapter 2</i></b>	<b>27</b>
<i>Carotenoid deficiency induces structural and functional changes in the phycobilisomes and photosystems of Synechocystis PCC 6803</i>	
<b><i>Chapter 3</i></b>	<b>68</b>
<i>The PsbW protein stabilizes the supramolecular organization of Photosystem II in higher plants</i>	
<b><i>Chapter 4</i></b>	<b>101</b>
<i>The role of light-harvesting complex II in the macro-organisation of thylakoid membranes, as revealed by circular dichroism spectroscopy in vivo</i>	
<b><i>Chapter 5</i></b>	<b>132</b>
<i>Cadmium exerts its toxic effects on photosynthesis via a cascade mechanism in the cyanobacterium, Synechocystis PCC 6803</i>	
<b><i>Chapter 6</i></b>	<b>157</b>
<i>General discussion</i>	
<b><i>Chapter 7</i></b>	<b>168</b>
<i>Algemene discussie</i>	
<b><i>Acknowledgement</i></b>	<b>177</b>
<b><i>List of Publications</i></b>	<b>178</b>

# Abbreviations

$\tau_{av}$	average lifetime
$\Phi_{PSII}$	operational PSII quantum yield
APC	allophycocyanin
asPsbW	antisense PsbW
BN-PAGE	blue-native polyacrylamide gel electrophoresis
CA	carbonic anhydrase
Car	carotenoid
CCM	carbon-concentrating mechanism
CD	circular dichroism
C-PC	C-Phycocyanin
DAS	decay associated spectrum/spectra
DCMU	3-(3,4-dichloro-phenyl)-1,1-dimethylurea
FNR	ferredoxin/NADP <sup>+</sup> -oxidoreductase
EET	excitation energy transfer
EM	electron microscopy
ET	electron transport
FLIM	fluorescence lifetime imaging microscopy
koPsbW	knock-out PsbW
LAHG	light activated heterotrophic growth
LHC	light harvesting complex
LMW	low molecular weight
L <sub>R</sub> <sup>33</sup>	33 kDa rod linker protein
MV	methyl viologen
NPQ	non-photochemical quenching
PAG	photoautotroph growth
PBS	phycobilisome
pBQ	p-benzoquinone
PC	phycocyanin
PSI and PSII	photosystem I and II
qP	photochemical quenching
PQ	plastoquinone
RC	reaction centre
RC47	PSII monomeric core complex lacking CP43
ROS	reactive oxygen species

PPFD	photosynthetic photon flux density
Rubisco	ribulose biphosphate carboxylase-oxygenase
TE	terminal emitter of the phycobilisome
TL	thermoluminescence
WOC	water oxidising complex

# Chapter 1

## *Introduction*

## Scope of the thesis

Photosynthesis is one of the fundamental processes on Earth, which is responsible for the transformation of inorganic carbon to organic forms and it also determines to a large extent the composition of the atmosphere. Therefore, there is a large interest to understand the basic processes of photosynthesis and the organization of the photosynthetic apparatuses as well as the impact of environmental factors on their performance. Photosynthesis research represents a broad and diverse field and many aspects have been studied intensively for over more than two centuries. After many aspects have been investigated at the molecular level *in vitro* for several decades, there is now a renewed interest in the study of the performance of the various complexes *in vivo*, trying to couple the obtained knowledge of isolated complexes to the overall performance *in situ*.

The thylakoid membranes, where virtually all light reactions of photosynthesis take place, is a well-organised hierarchic system, but the interaction between complexes might be relatively instable and possibly change upon membrane isolation. Therefore, in this thesis we have tried to apply mostly *in vivo* spectroscopic (absorption and fluorescence spectroscopy/microscopy) methods to investigate the photosynthetic apparatus of various organisms under various conditions.

In this thesis we used photosynthetic organisms with modified pigment- or protein-compositions to investigate their effect on the organisation and function of the photosynthetic pigment-protein complexes. We also studied the responses of the photosynthesis apparatus to the toxic heavy metal pollutant cadmium.

## 1.1 Oxygenic photosynthesis

### 1.1.1 General phenomenon

Oxygenic photosynthetic organisms reduce  $\text{CO}_2$  to synthesize sugars using light energy and this process is accompanied by  $\text{O}_2$  evolution. Light is captured by pigments of the light-harvesting antennae associated with Photosystem I (PSI) and Photosystem II (PSII), and the excitation energy forwarded to the photochemical reaction centers induces primary charge separation and drives the linear electron transport, which leads to the production of ATP and NADPH (Fig. 1.1).

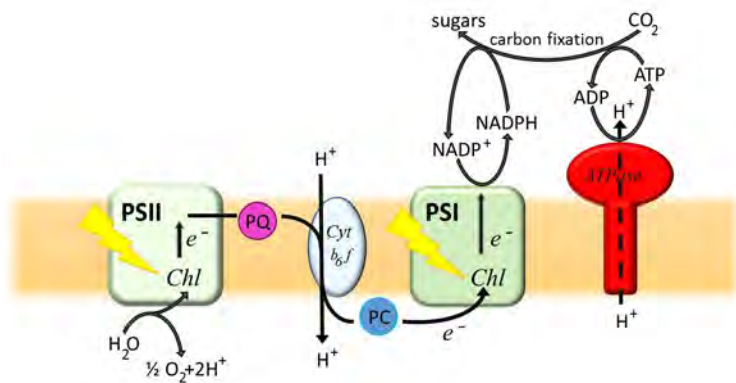


**Figure 1.1.** Simplified model of the photosynthetic electron transport chain of oxygenic photosynthetic organisms. Abbreviations: PSI, Photosystem I; PSII, Photosystem II; PQ, plastoquinone; PC, plastocyanin; Cyt  $b_6f$ , cytochrome  $b_6f$  complex; ATPase, ATP synthase.

The key components of photosynthetic energy conversion system are PSI, PSII, the cytochrome  $b_6f$  (Cyt  $b_6f$ ) and the ATP synthase (ATPase), protein complexes, which are embedded in the thylakoid membranes [1-3]. The intersystem electron transport occurs by the use of electron carriers, i.e., the lipid soluble pool of plastoquinone (PQ) molecules, the membrane-intrinsic cyt  $b_6f$  protein complex and the water-soluble small plastocyanin (PC) protein, which is localised in the thylakoid lumen (Fig. 1.1). The light reactions of photosynthesis reduce  $\text{NADP}^+$  to NADPH on the stromal side, and generate a proton gradient across the membrane and a transmembrane electrical field, components of the electrochemical potential gradients for protons. This is used by the ATP synthase to convert ADP to ATP and the process known as photophosphorylation.

## 1.1.2 Photosynthetic model organisms

The cyanobacterial *Synechocystis* PCC 6803 strain and the higher plant *Arabidopsis thaliana* used in this thesis are commonly applied model organisms in photosynthesis research. Their entire genomes have been sequenced [4, 5] and extensive mutant collections are available for these organisms.

Cyanobacteria are ancient prokaryotes with a relatively small genome size (3.6 Mbp) [4] and low degree of complexity. Due to their relative simplicity cyanobacteria are commonly used model organisms to study basic photosynthetic processes. In the presence of adequate carbon sources some of the cyanobacterial strains, including *Synechocystis* PCC 6803, are able to grow heterotrophically without operating photosynthesis [6]. This property makes *Synechocystis* PCC 6803 strain suitable to study several photosynthesis-related mutations which otherwise would be lethal [7, 8].

Higher plants possess a bigger genome size, with more complex organisation and combined physiological responses. One of the most widely studied model plants is *Arabidopsis thaliana* (*Arabidopsis*). Its relatively small genome (125 Mbp) makes it advantageous to work with *Arabidopsis*, but the results obtained on these plants can be also relevant for crops.

## 1.2 Photosynthetic pigments

In photosynthetic organisms pigments are responsible for the absorption of light. They are positioned close together in the pigment-protein complexes to provide efficient energy transfer. The different photosynthetic taxa possess different pigment species owing to evolutionary adaptation to various environmental conditions. In this section the pigments occurring in cyanobacteria and higher plants are described in details.

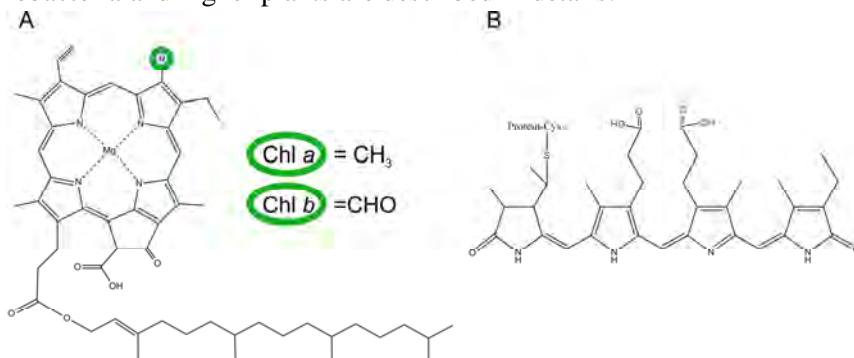


**Figure 1.2.** Molecular structure of chlorophyll a, chlorophyll b (A) and phycocyanobilin (B) pigments

## 1.2.1 Chlorophylls

Chlorophylls are cyclic tetrapyrrole molecules, and more precisely, belong to the group of reduced porphyrins. Their porphyrin ring contains a magnesium atom in the centre and is associated with a phytol tail consisting of four isoprene units. All photosynthetic organisms contain chlorophyll-type pigments, but their fine structure is characteristic for the taxa [3]. Cyanobacteria contain only chlorophyll *a* (Chl *a*), while higher plants also contain chlorophyll *b* (Chl *b*) (Fig. 1.2). These two types of chlorophylls are different only in one functional group, which is a methyl group in Chl *a* and a formyl group in Chl *b*. In spite of their structural similarity, Chl *a* and Chl *b* have distinct spectral properties. The chlorophylls show most absorption in the near-UV region, the Soret ( $B_y$  and  $B_x$ ) bands, and in the near-IR, the  $Q_y$  and  $Q_x$  bands. Chl *a* absorbance peaks are found in the  $\sim 350$ - $450$  nm and  $\sim 650$ - $700$  nm regions and Chl *b* around  $\sim 400$ - $500$  nm and  $\sim 625$ - $675$  nm (Fig. 1.3).

There are some special chlorophylls in photosynthetic systems. In photosystem I complexes a special Chl *a* stereoisomer is present, the so called Chl *a'*, which forms one half of the special P700 Chl pair. The pheophytins are metal-free chlorophylls, where the magnesium is replaced by hydrogens. Two pheophytin molecules are present in photosystem II where they have important function in the process of charge separation. On the other hand the pheophytin can also be a product of chlorophyll degradation.

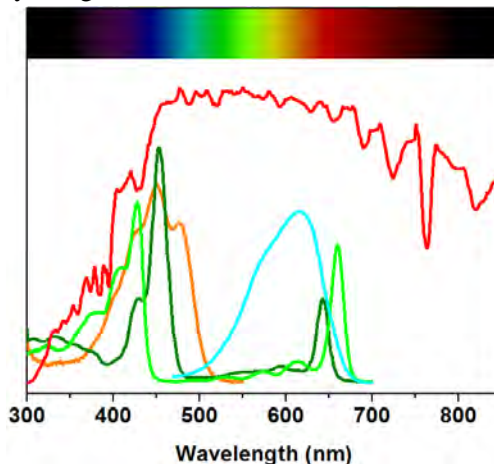


**Fig 1.3.** The absorption spectra of various photosynthetic pigments:  $\beta$ -carotene (orange), chlorophylls *a* (light green) and *b* (dark green), dissolved in non-polar solvents. Phycocyanin is a protein containing phycocyanobilin pigments covalently bound to the peptide, it was measured in aqueous buffer (cyan). Red curve, represents the solar spectrum incident on the surface of Earth.

## 1.2.2 Bilins

Bilins are open-chain tetrapyrrole molecules. They are present in the phycobilisome antennae of cyanobacteria, red algae, glaucophytes and some cryptophytes. They are unique in a way that they are covalently bound to the proteins via thioether bonds. The most common bilins are phycocyanobilin and phycoerythrobilin (Fig. 1.3). In *Synechocystis* PCC 6803 strain, used in this thesis, phycocyanobilin is present only (Fig. 1.2), but exists in two spectrally different forms depending on the phycobiliprotein to which it is bound. Phycocyanobilin in allophycocyanin has more red-shifted absorption and fluorescence spectra than in phycocyanin.

## 1.2.3 Carotenoids

Carotenoids (Cars) are the most wide-spread pigments in nature. Cars are tetraterpenes comprising eight isoprene units. They contain double bonds in a conjugated system, which is responsible for the colour and rod-shape of the molecules. Carotenes and xanthophylls form the two main classes of Cars. Carotenes, such as  $\beta$ -carotene, are pure hydrocarbon molecules containing a cyclohexene ring (ionone ring) at one or both ends. They are extremely hydrophobic, non-polar molecules. Xanthophylls carry one or more oxygen-containing functional groups, generally attached to their terminal ionone rings (e.g., echinenone, zeaxanthin). In Cars glycosides, a sugar group is attached to the molecule at one side instead of the ionone ring (e.g., myxol-dimethyl-fucoside) (Fig. 1.4 A). In photosynthetic organisms, carotenoids are typically localised in protein complexes and lipid membranes and their location is highly influenced by the polarity of Cars and direct environment. Both photosynthetic reaction centre core complexes (PSI and PSII) contain Cars and this is also the case for light-harvesting complexes of higher plants (see section 1.3). Cars have various functions in photosynthetic organisms [9]. They can serve as accessory light-harvesting antenna pigments by absorbing in the blue-green region of the solar spectrum (Fig. 1.3) [10]. Cars have also protective roles exerted by quenching of singlet or triplet excited state Chl upon excess light conditions and by directly scavenging the singlet excited state oxygen [11, 12]. Cars also decrease the susceptibility of lipid-membranes to oxidative degradation [13]. In lipid bilayers the Car molecules seem to significantly influence the membrane fluidity and form penetration barrier of small molecules, including oxygen [14].

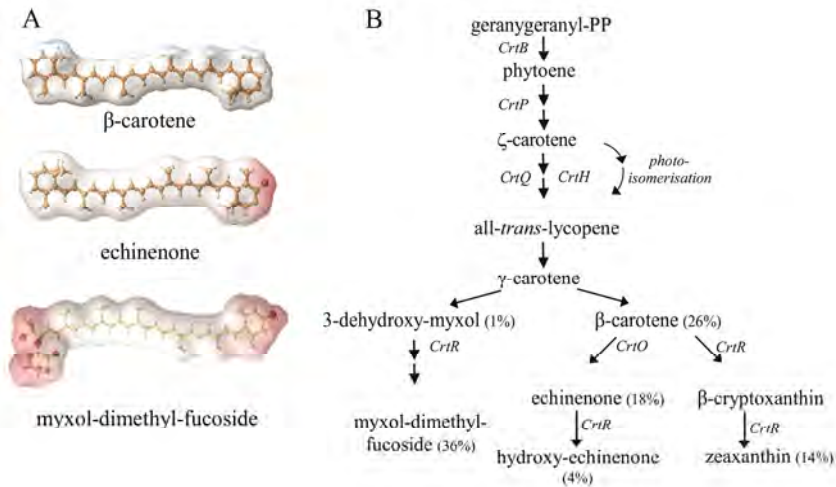


**Figure 1.4.** Chemical structure of three carotenoid molecules (A) adapted from Domonkos et al. (2013)[9], and a simplified scheme of the biosynthesis pathways of the most abundant carotenoids of *Synechocystis* PCC 6803 (B). White colour represents the non-polar parts of the molecule and red colour, the polar regions. Relative amounts are shown in parantheses. *CrtB*, phytoene synthase; *CrtP*, phytoene desaturase; *CrtQ*,  $\zeta$ -carotene desaturase; *CrtH*, *cis-trans* carotene isomerase; *CrtR*, carotene  $\beta$ -hydroxylase; *CrtO*, carotene  $\beta$ -ketolase.

In *Synechocystis* the main Car forms are as follows:  $\beta$ -carotene (~26% of total carotenoid content), echinenone (~18%), zeaxanthin (~14%) and myxoxanthophyll (~36%) (present as myxol 2'-dimethyl-fucoside) [15]. The biosynthesis of Cars was recently reviewed by Domonkos and co-workers [9]. Figure 1.4 B shows the key steps of the synthesis and the catalysing enzymes. The first step of Car synthesis is the condensation of two geranylgeranyl-diphosphates by the phytoene synthase (*CrtB*) enzyme [16]. The produced *cis*-phytoene is transformed to all-*trans*-lycopene via multiple steps, which include desaturation and isomerisation. The desaturation steps are catalysed by phytoene desaturase (*CrtP*) and  $\zeta$ -carotene desaturase (*CrtQ*). Until now only one *cis-trans* carotene isomerase (*CrtH*) has been characterized from cyanobacteria. Masamoto and co-workers [17] demonstrated that the presence of the *CrtH* enzyme or light is essential for the isomerisation steps, and thus for the production of all-*trans*-lycopene. Subsequent steps require the presence of cyclases. Formation of one ionone ring results in the production of  $\gamma$ -carotene, which is a branching point of the synthesis.  $\gamma$ -carotene can be used to synthesize myxoxanthophyll, which, in *Synechocystis*, is myxol 2'-dimethyl-fucoside [15].  $\gamma$ -carotene is also used for the production of  $\beta$ -carotene by the formation of the

ionone ring on the other side of the molecule.  $\beta$ -carotene is an intermediate product for echinenone and zeaxanthin synthesis. The final form of the xanthophylls require the presence of carotene  $\beta$ -hydroxylase (CrtR) and carotene  $\beta$ -ketolase (CrtO) [18].

## 1.3 Photosynthetic pigment-protein complexes

### 1.3.1 Photosynthetic reaction centres

Photosynthetic reaction centres (RCs) are special pigment-protein complexes where light induces electron transfer reactions, which results in charge separation across the membrane. The basic structure of the photosystems is evolutionary highly conserved and rather similar for cyanobacteria and higher plants [1, 3].

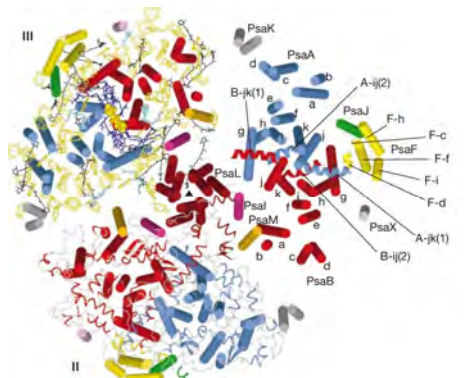


**Figure 1.5.** Photosystem I trimer of *Synechococcus elongatus* as seen from the stromal side; copied from Jordan et al. (2001) [19] with permission. In each monomer (I, II and III) different structural aspects are emphasized. In monomer I the transmembrane  $\alpha$ -helices are represented by cylinders and different subunits are labelled. In monomer II the luminal loop regions are represented by ribbons. In monomer III the complete set of cofactors is presented; quinones and Chls (blue), iron and sulphur atoms of the three  $Fe_4S_4$  clusters (orange and yellow spheres), antenna system Chls (yellow), carotenoids (black), lipids (turquoise).

### Photosystem I

Photosystem I has a FeS type reaction centre, in which the terminal electron acceptor is a  $[4Fe_4S]$  cluster. The monomeric PSI of cyanobacteria (Fig. 1.5) contains 12 protein subunits and 127 cofactors, i.e., 96 Chl *a*, 22 carotenoids, two phylloquinones, three  $[4Fe_4S]$  clusters and four lipids [20, 21]. The central part of the monomeric complex is a heterodimer of PsaA



## 1.3.2 Light-harvesting antennae

In photosynthetic organisms there are specialized pigment-protein complexes to increase the light-harvesting capacity of reaction centres. These complexes are also called photosynthetic antennae. Unlike the strong RC homology between species, the light-harvesting antennae are evolutionarily rather diverse. Cyanobacteria and red algae possess hemidiscoidal phycobilisome antennae attaching to the stromal side of PSs while green algae and plants have membrane-embedded light-harvesting complexes (LHCs) [3, 29].

### *Phycobilisome*

Phycobilisomes (PBSs) are water-soluble pigment-protein complexes, which contain open-chain tetrapyrroles, i.e., phycobilins, as pigments. In general, PBSs consist of rods radially attached to a central core. The rods capture the light energy and funnel it to the PBS core complex, from where the excitation energy is transferred to the RCs [30]. Despite the similarities of the general structure, the detailed composition and organisation of the PBSs shows a wide variety among different species [30-32]. In the *Synechocystis* PCC 6803 strain the PBSs have six radial phycocyanin (C-PC) rods. Each rod comprises typically three hexameric disks and each hexamer contains 18 phycocyanobilin pigments. The PBS core consists of three allophycocyanin (APC) cylinders. Each APC cylinder is composed of four trimeric disks and six allophycocyanobilin pigments per trimer [33]. Both core cylinders closest to the membrane plane have two special trimers, which function as terminal emitter (TE) and transfer the energy toward the photosynthetic RCs [34]. Specific linker polypeptides are responsible for the assembly of the PBSs and for the connection between the PBS and the PSs [33, 35].

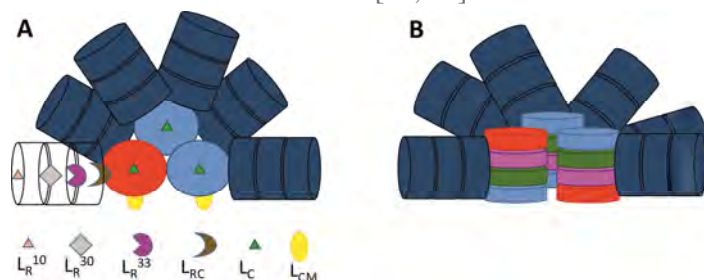


**Figure 1.7.** Model of phycobilisome of *Synechocystis* PCC 6803 (based on [33, 36]). (A) side view, linker proteins are represented by various colours as labelled; (B) luminal view, phycocyanin rods are dark blue, differential colouring of APC units represent their distinct compositions. APC units with magenta and red represent the terminal emitters of the PBS.

These linkers can be separated into functional groups according to the units they are connecting (Fig. 1.7). The rod linkers ( $L_R$ ) are responsible for the attachment of the rod hexameric units, the rod-core linker ( $L_{RC}$ ) for the connection of the rods to the PBSs core and the core linker ( $L_C$ ) for the assembly of the core cylinders [33, 37].

## *Light-harvesting complexes I and II*

The light-harvesting complexes (LHCs) of plants and green algae are membrane-embedded proteins containing both Chl *a* and *b* pigments and possess somewhat different structures for PSI and PSII antennae.

The PSI supercomplex of plants contains in total 168 chlorophylls, 2 phylloquinones, 3 FeS<sub>4</sub> clusters and around 30 carotenoids. Like the PSI core, LHCI antennae contain some long-wavelength (“red”) Chl *a* pigments, but the role of these antenna pigments has not been clarified yet [38]. The PSI antenna in plants is made up of five LHCI (Lhca1-Lhca5) proteins organised on one side of the core complex [39, 40]. These proteins form Lhca2/3 and Lhca1/4 or occasionally Lhca1/5 functional heterodimers under physiological conditions, in which each monomers contributes almost equally to the energy transfer to the core [41, 42].

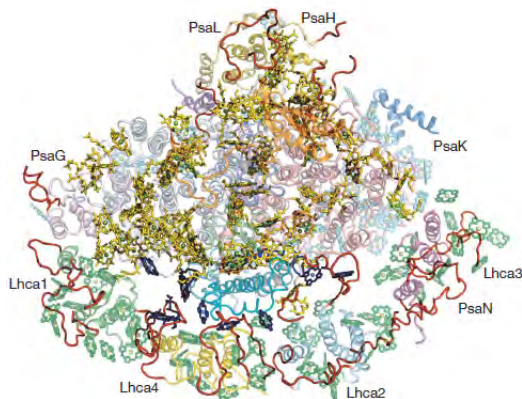


**Figure 1.8.** Stromal side view of a PSI complex isolated from pea, based on Amunts et al. (2007) [39] with permission. Chlorophylls with resolved phytol side chains are represented in yellow, the rest of the reaction centre chlorophylls in cyan, the gap chlorophylls in blue and chlorophylls of LHCI in green, respectively. The positions of PsaG, H, K, L, N and the various LHCI monomers are indicated.

The dimeric PSII core together with monomeric and trimeric light-harvesting proteins form PSII supercomplexes in green algae and plants [43,

44]. The light-harvesting antenna of PSII is encoded by *lhcb1-lhcb6* genes which show strong sequence homology. The monomeric components, the CP24, CP26 and CP29, are encoded by *lhcb6*, *lhcb5* and *lhcb4*, respectively. These minor complexes connect the LHCII trimers to the core and stabilise the supercomplex structure [45, 46]. Each monomeric subunit of the LHCII trimer contains eight Chl *a*, and six Chl *b* molecules, two lutein molecules, one neoxanthin and one violaxanthin pigment. In excess light the violaxanthin molecule can be converted into zeaxanthin via the reversible xanthophyll cycle, which is an important element of the protective non-photochemical quenching process. The trimeric LHCII is composed of Lhcb1, Lhcb2 and Lhcb3 proteins, occurring in variable ratios but their exact function is still under investigation [47, 48]. The dimeric PSII core has two high and two low affinity binding sites for LHCII trimmers, and the trimers bound to them are called S and M trimmers, respectively. Accordingly, we can distinguish various supercomplexes based on their LHCII composition.

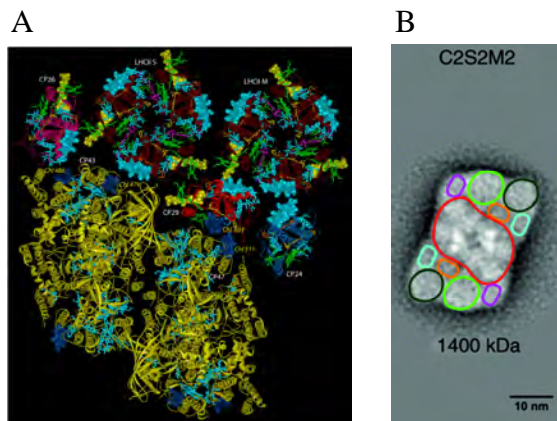


**Figure 1.9.** PSII supercomplex structure of *Arabidopsis thaliana* adapted from Caffarri *et al.* (2009)[43]. The model (A) was obtained by fitting the single-particle images of PSII supercomplex (B) with the crystal structure of PSII and LHCII trimeric and monomeric complexes. Colours represents M trimer (dark green), S trimer (light green), CP29 (orange), CP26 (purple) and CP24 (cyan) respectively.

## 1.4 Macro-organisation of the photosynthetic complexes

The supercomplexes of the thylakoid membrane can be organised into higher associations in order to optimise the photosynthetic processes. Folea and co-workers [49] observed the arrangement of several PSII core complexes into parallel rows in the partially solubilised, thylakoid membranes of cyanobacteria, which were negatively stained for electron-microscopy measurements. Although

there are several models to describe the functional role of these PSII arrays, e.g., avoiding spillover or increasing excitation probability, their exact role still needs to be elucidated. Recently PSII-PBS-PSI complexes were purified from cyanobacteria by cross-linking [50], which might indicate the *in vivo* presence of this megacomplex.

Based on circular dichroism spectroscopy, existence of long range ordered macroassemblies of chlorophyll containing proteins localised in the granal thylakoids of higher plants were suggested several decades ago [51-53]. In addition, PSII arrays were also observed in plants thylakoid membranes [44, 54-56] and especially well studied in *Arabidopsis thaliana* and spinach [44, 56]. In plants these arrays might even have a diameter of a few hundred nm and cover a quite extended area of the grana and they often contain over one hundred PSII supercomplexes resulting in a semi-crystalline structure. Recent finding shows that the formation of the PSII domains depends largely on the local homogeneity of the PSII supercomplexes [57]. It was proposed that these highly organised PSII domains are necessary to provide sufficient diffusion capability of the PQ molecules [58]. Moreover, the PSII reaction centres within the PSII arrays can efficiently transfer excitation energy toward another open RC in case of re-excitation of PSII with already closed RCs [59]. Several factors were reported to influence the PSII domain organisation using various mutant lines [45, 60-62]. The organisation of the PSII arrays depends on the relative abundance of the LHCII components in the complexes, and different supercomplexes give rise to altered PSII macro-structures, in which the position of the PSII cores varies. The properties of the PSII arrays in the membrane can also determine the macro-organisation of the adjacent membrane layer [44, 56]. The PSII arrays in adjacent membranes, which are attached to each other at their stromal side, are present in preferred orientations manifested by a specific angle between the PSII rows running in the two membranes. At these angles the overlap of LHCII trimers is believed to be maximal in the centre of the domains [56]. Somewhat different preferential angles were observed in spinach (~3° or ~46°) [63] than in *Arabidopsis* (~32° or ~58°) [44, 56, 57, 64]. The differences originate most likely from the distinct basic PSII supercomplex units [57].

## 1.5 Responses to environmental changes

Photosynthetic organisms can be found nearly everywhere where sufficient light is present. What makes photosynthetic organisms so successful is the fact that their photosynthetic apparatuses have a highly dynamic structure,

capable to adapt to highly different and highly variable environmental conditions [65-68].

Light is one of the most frequently changing factors in Nature, which can dynamically vary in intensity and spectral composition. Different adaptation mechanisms exist in short-term and long-term exposure to altered light access [69]. At low light intensities the change of the light quality would drastically decrease the photosynthetic efficiency due to induced imbalance between the two photosystems based on their spectral differences [70]. Therefore, plants are able to redistribute a mobile antenna pool through the so called state transition [70-72]. Moreover, there is also an efficient and relatively fast process to avoid overexcitation upon excess light [73]. Within minutes the effective antenna size can be decreased by antenna detachment and strong non-photochemical quenching [73]. However, if the modified environmental conditions are maintained for longer time periods then the organisms may modify their protein synthesis patterns according to the requirements [57, 74-76]. The presence of extremely unfavourable conditions evokes stress responses and if the organisms are not capable to avoid serious damage by various regulation processes they might be destroyed. Some of the most harmful stressors are the heavy metals. Most organisms are capable to tolerate the presence of heavy metals only in a low concentration range. However, due to the environmental pollution the concentration of these toxic metals are drastically increased in some localized areas. Cadmium is one of the most toxic heavy metal, especially for aquatic photosynthetic organisms [77-80]. The primary target of cadmium is the photosynthetic apparatus.

## 1.6 Experimental techniques

### 1.6.1 Chlorophyll fluorescence spectroscopy

There are several techniques based on the detection of the auto-fluorescence from chlorophyll molecules of photosynthetic organisms upon light excitation. Fluorescence measurements can provide a unique tool to monitor the functional integrity and physiological responses of the photosynthetic machinery. One of the main advantages of these techniques is that most of them can also be applied *in vivo*.

The so-called Pulse-Amplitude-Modulation (PAM) fluorometry is one of the most commonly used technique to monitor the photosynthetic responses to altered light quality (state transitions) or stress conditions, such as excess light (non-photochemical quenching, photoinhibition), drought, or heavy metal

poisoning. The method is based on the continuous recording of the fluorescence yield using high frequency of short, low-intensity pulses in combination with some high-intensity saturation pulses in the presence or absence of continuous illumination. The parameters derived from values of cardinal points of fluorescence induction curve provide information on the primary photochemistry of PSII, maximal and operative efficiency of PSII energy conversion, the state of photosynthetic electron transport and related processes [81].

With non-modulated techniques better time resolution of fluorescence kinetics can be achieved. The different phases of fast fluorescence transient kinetics of dark-adapted photosynthetic samples upon high intensity illumination followed at  $\mu\text{s}$  time-resolution are related to the reduction of various electron transport components. For the corresponding fluorescence induction curve each phase represents different steps of the electron transport chain [82, 83].

With advanced time-resolved fluorescence spectroscopy, the kinetics of fluorescence emission can be detected with picosecond time resolution. The picosecond fluorescence kinetic traces obtained upon excitation with short laser pulses are capable to provide information about the dynamical processes that occur in the excited state [84-86].

The streak-camera system detects the fluorescence decay kinetics simultaneously for a broad wavelength interval at subpicosecond time resolution. Detailed information about a given system can be obtained by global analysis of the streak camera data. In global analysis the set of decays is fitted assuming that each component has the same lifetime throughout, and only the relative amplitude is wavelength-dependent [87]. The obtained wavelength distribution of the amplitudes for each lifetime component is represented as Decay Associated Spectra (DAS). From the lifetime values and the spectral features of DAS components we may deduce information on the excitation energy migration and trapping (charge separation) time in various photosynthetic organisms. However, streak-camera measurements are bulk experiments and provide information only about the ensemble averages.

Fluorescence Lifetime Imaging Microscopy (FLIM) is a combination of microscopy with time-correlated single-photon counting (TCSPC) detection. In this way the FLIM setup is capable to record the fluorescence decay kinetics from individual pixels with sub- $\mu\text{m}$  resolution [84] at the selected emission wavelength region. FLIM is a powerful tool to investigate the homogeneity of cell populations and to reveal variations in pigment composition or energy transfer processes within the cell or the leaf tissue [85, 86].

## 1.6.2 Circular dichroism spectroscopy

Circular dichroism (CD) is the difference in absorption of right- and left-circularly polarized light by chromophores having chiral properties, either in their own structure or in their organization. CD spectroscopy is very sensitive non-invasive method to detect structural changes of pigment-protein complexes and their macro-assemblies (reviewed by [88, 89]). In thylakoid membranes CD signals can originate from different levels of structural complexity. The intrinsic CD arises from the asymmetry of the electronic structure of the individual pigments molecules and results in only a very weak signal for most chromophores. The excitonic CD bands originate from asymmetries in short-range intermolecular interactions and dominate the CD spectra of all isolated pigment-protein complexes. The so called psi-type (polymer- and salt-induced) CD signal arises from chirally organized macroarrays of pigment-containing proteins and exhibits intense, anomalously-shaped bands. The psi-type CD signals have been recorded for granal thylakoids, artificial LHCI aggregates, and several algal cells, where they typically dominate the CD spectra. Psi-type CD carries significant information on the *in vivo* macro-organisation of thylakoid membranes although its practical application demands further elucidation of the origin and the assignment of these signals to macro-structures.

## 1.7 Aims and outline

An important feature of the photosynthetic thylakoid membrane is that it contains many pigment-protein complexes embedded in a lipid membrane. Besides chlorophylls, carotenoids are the most abundant pigments in the thylakoids and the carotenoids are even the most widespread pigments in Nature. In photosynthetic organisms carotenoids have important structural and functional roles, they contribute for instance to light harvesting and photoprotection, influence the membrane fluidity, and stabilize the membrane structure and pigment-protein complexes. Although crystallisation studies demonstrate the presence of relatively high amounts of carotenoids in both photosystems, we have little information about their structural importance. Despite the fact that the carotenoid composition is known to respond to changing environmental conditions, the direct consequences of the modified carotenoid levels are more or less unknown.

- In this thesis we aim to study which carotenoids contribute to which extent to the structural and functional integrity of the photosynthetic apparatuses in cyanobacteria (**Chapter 2**).

- Since for photoautotrophic organisms the complete lack of carotenoids is lethal, we have used the *Synechocystis* PCC 6803 strain that is also capable of growing heterotrophically, allowing studies on various carotenoid biosynthesis mutants in which the carotenoid composition is altered. Besides a completely carotenoid-deficient mutant, also xanthophyll-deficient cells were studied in order to distinguish between the roles of the different carotenoid classes. We used *in vivo* time-resolved techniques in combination with biochemical methods.

- Our results confirm recent literature data and also provide unexpected findings, which have not been observed before. We found an effect of carotenoids on phycobilisome stability and a contribution of xanthophylls to the stabilisation of the oligomeric states of both photosystems.

In higher plants thylakoid membranes and the photosynthetic complexes are organised in a different way than in cyanobacteria, and PSI and PSII are localised in spatially clearly distinct regions, the stroma lamellae and the stacked grana membranes, respectively. The PSII complexes are arranged into supramolecular assemblies, most probably to maintain optimal efficiency.

- However, it is not completely clear which factors determine the PSII macro-organisation. The low-molecular-weight PsbW protein is part of the PSII supercomplex and was thought to contribute to the macrodomain organisation, but its exact role has not been elucidated so far.

- Structural and functional aspects of the decrease in its amount or the complete lack of PsbW protein were examined by the use of biochemical and biophysical methods (**Chapter 3**).

- The PsbW protein appears to be one of the key elements for the macro-organisation of the plant thylakoid membrane, which is stabilising the PSII-LHCII complex. In the PsbW deficient mutant the redox states and the redox regulated processes are also altered as a result of the modified PSII supercomplex structure.

To study PSII macro-structures one can almost only make use of *in vitro* techniques. However, circular dichroism spectroscopy is a potentially useful non-invasive technique to study the macro-organization *in vivo*. Although it has previously been observed that granal thylakoids give rise to strong circular dichroism signals that reflect the presence of long-range ordered chiral macrodomains, relatively little information is available about the nature of the *in vivo* structures that lead to these signals.

- In this thesis we attempt to develop and provide *in vivo* fingerprinting for the various macrodomains using circular dichroism spectroscopy on intact leaves (**Chapter 4**).
- The presented study compares various plant species and mutants for different growth conditions in order to elucidate the factors that contribute to the formation of chirally-ordered macrodomains, which are responsible for the CD signal.
- We show that CD is a potentially useful technique to detect the PSII macrodomains *in vivo*. In **Chapter 4** we show a correlation between the previously observed PSII semi-crystalline arrays and the CD signal characteristic for granal thylakoids.

We have also studied the effect of cadmium on photosynthesis in cyanobacteria. Due to environmental pollution the concentration of heavy metals has substantially increased in many places during the last decades. Cadmium is one of the most toxic heavy metals and photosynthetic processes of aquatic organisms are especially susceptible to it. Despite extensive research the primary and secondary effects of cadmium on photosynthesis have not been distinguished yet.

- This thesis also aims to identify the primary targets of cadmium toxicity and to distinguish its direct effects from the indirect ones in *Synechocystis* PCC 6803 (**Chapter 5**).
- We used increasing concentration of cadmium and studied the time-dependence of the toxic effects under various conditions.
- We separated the toxic effects of cadmium and determined the cadmium-concentration dependence of these individual effects. Based on the results we propose a cascade mechanism, in which as a first step the dark-cycle of the photosynthesis is blocked and, as a secondary effect, the level of PSII decreases.

## 1.8 Reference list

- [1] Hohmann-Marriott, M.F., Blankenship, R.E., Evolution of Photosynthesis, *Annu. Rev. Plant Biol.*, 62 (2011) 515-548.
- [2] Eberhard, S., Finazzi, G., Wollman, F.A., The dynamics of photosynthesis, *Annu. Rev. Genet.*, 42 (2008) 463-515.
- [3] Blankenship, R.E., Molecular Mechanisms of Photosynthesis, Wiley, 2002.
- [4] Kaneko, T., Sato, S., Kotani, H., Tanaka, A., Asamizu, E., Nakamura, Y., Miyajima, N., Hirose, M., Sugiura, M., Sasamoto, S., Kimura, T., Hosouchi, T., Matsuno, A., Muraki, A., Nakazaki, N., Naruo, K., Okumura, S., Shimpo, S., Takeuchi, C., Wada, T., Watanabe, A., Yamada, M., Yasuda, M., Tabata, S., Sequence analysis of the genome of the unicellular

- cyanobacterium *Synechocystis* sp. strain PCC6803. II. Sequence determination of the entire genome and assignment of potential protein-coding regions, *DNA Res.*, 3 (1996) 109-136.
- [5] **Kaul, S., Koo, H.L., Jenkins, J., Rizzo, M., Rooney, T. et al.**, Analysis of the genome sequence of the flowering plant *Arabidopsis thaliana*, *Nature*, 408 (2000) 796-815.
- [6] **Anderson, S.L., McIntosh, L.**, Light-activated heterotrophic growth of the cyanobacterium *Synechocystis* sp strain PCC 6803 - A blue-light-requiring process, *J. Bacteriol.*, 173 (1991) 2761-2767.
- [7] **Sozer, O., Komenda, J., Ughy, B., Domonkos, I., Laczko-Dobos, H., Malec, P., Gombos, Z., Kis, M.**, Involvement of carotenoids in the synthesis and assembly of protein subunits of photosynthetic reaction centers of *Synechocystis* sp PCC 6803, *PCP*, 51 (2010) 823-835.
- [8] **Laczko-Dobos, H., Ughy, B., Toth, S.Z., Komenda, J., Zsiros, O., Domonkos, I., Parducz, A., Bogos, B., Komura, M., Itoh, S., Gombos, Z.**, Role of phosphatidylglycerol in the function and assembly of photosystem II reaction center, studied in a *cdsA*-inactivated PAL mutant strain of *Synechocystis* sp. PCC6803 that lacks phycobilisomes, *Biochim. Biophys. Acta*, 1777 (2008) 1184-1194.
- [9] **Domonkos, I., Kis, M., Gombos, Z., Ughy, B.**, Carotenoids, versatile components of oxygenic photosynthesis, *Prog. Lipid Res.*, 52 (2013) 539-561.
- [10] **van Amerongen, H., van Grondelle, R.**, Understanding the energy transfer function of LHCII, the major light-harvesting complex of green plants, *J. Phys. Chem. B*, 105 (2001) 604-617.
- [11] **Schodel, R., Irrgang, K.D., Voigt, J., Renger, G.**, Quenching of chlorophyll fluorescence by triplets in solubilized light-harvesting complex II (LHCII), *Biophys. J.*, 76 (1999) 2238-2248.
- [12] **Polivka, T., Sundstrom, V.**, Ultrafast dynamics of carotenoid excited states - From solution to natural and artificial systems, *Chem Rev*, 104 (2004) 2021-2071.
- [13] **Gruszecki, W.I., Strzalka, K.**, Carotenoids as modulators of lipid membrane physical properties, *Biochim. Biophys. Acta*, 1740 (2005) 108-115.
- [14] **Berglund, A.H., Nilsson, R., Liljenberg, C.**, Permeability of large unilamellar digalactosyldiacylglycerol vesicles for protons and glucose - influence of alpha-tocopherol, beta-carotene, zeaxanthin and cholesterol, *Plant Physiol. Biochem.*, 37 (1999) 179-186.
- [15] **Takaichi, S., Maoka, T., Masamoto, K.**, Myxoxanthophyll in *Synechocystis* sp. PCC 6803 is myxol 2'-dimethyl-fucoside, (3R,2'S)-myxol 2'-(2,4-di-O-methyl-alpha-L-fucoside), not rhamnoside, *PCP*, 42 (2001) 756-762.
- [16] **Martinezferez, I., Fernandezgonzalez, B., Sandmann, G., Vioque, A.**, Cloning and expression in *Escherichia coli* of the gene coding for phytoene synthase from the cyanobacterium *Synechocystis* sp PCC6803, *Biochim. Biophys. Acta*, 1218 (1994) 145-152.
- [17] **Masamoto, K., Wada, H., Kaneko, T., Takaichi, S.**, Identification of a gene required for cis-to-trans carotene isomerization in carotenogenesis of the cyanobacterium *Synechocystis* sp PCC 6803, *PCP*, 42 (2001) 1398-1402.
- [18] **Schafer, L., Vioque, A., Sandmann, G.**, Functional in situ evaluation of photo synthesis-protecting carotenoids in mutants of the cyanobacterium *Synechocystis* PCC 6803, *J. Photochem. Photobiol. B: Biol.*, 78 (2005) 195-201.
- [19] **Jordan, P., Fromme, P., Witt, H.T., Klukas, O., Saenger, W., Krauss, N.**, Three-dimensional structure of cyanobacterial photosystem I at 2.5 angstrom resolution, *Nature*, 411 (2001) 909-917.
- [20] **Fromme, P., Jordan, P., Krauss, N.**, Structure of photosystem I, *Biochim. Biophys. Acta*, 1507 (2001) 5-31.
- [21] **Grotjohann, I., Fromme, P.**, Structure of cyanobacterial photosystem I, *Photosynth Res.*, 85 (2005) 51-72.
- [22] **El-Mohsnawy, E., Kopczak, M.J., Schlodder, E., Nowaczyk, M., Meyer, H.E., Warscheid, B., Karapetyan, N.V., Rögner, M.**, Structure and function of intact photosystem I monomers from the cyanobacterium *Thermosynechococcus elongatus*, *Biochemistry*, 49 (2010) 4740-4751.
- [23] **Ben-Shem, A., Frolow, F., Nelson, N.**, Crystal structure of plant photosystem I, *Nature*, 426 (2003) 630-635.

- [24] **Nelson, N.**, The structure of plant photosystem I - The first membrane supercomplex solved by X-ray crystallography, *FASEB J.*, 20 (2006) A489-A489.
- [25] **Guskov, A., Kern, J., Gabdulkhakov, A., Broser, M., Zouni, A., Saenger, W.**, Cyanobacterial photosystem II at 2.9-angstrom resolution and the role of quinones, lipids, channels and chloride, *Nat. Struct. Mol. Biol.*, 16 (2009) 334-342.
- [26] **Vinyard, D.J., Ananyev, G.M., Dismukes, G.C.**, Photosystem II: the reaction center of oxygenic photosynthesis, *Annu. Rev. Biochem.*, 82 (2013) 577-606.
- [27] **Umena, Y., Kawakami, K., Shen, J.R., Kamiya, N.**, Crystal structure of oxygen-evolving photosystem II at a resolution of 1.9 angstrom, *Nature*, 473 (2011) 55-U65.
- [28] **Nickelsen, J., Rengstl, B.**, Photosystem II assembly: From cyanobacteria to plants, *Annu. Rev. Plant Biol.*, 64 (2013) 609-635.
- [29] **Fromme, P.**, Photosynthetic protein complexes: A structural approach, Wiley, 2008.
- [30] **Sidler, W.A.**, Phycobilisome and Phycobiliprotein Structures, in: D. Bryant (Ed.) The Molecular Biology of Cyanobacteria, Springer Netherlands, 2004, pp. 139-216.
- [31] **Apt, K.E., Collier, J.L., Grossman, A.R.**, Evolution of the Phycobiliproteins, *J. Mol. Biol.*, 248 (1995) 79-96.
- [32] **Adir, N.**, Structure of the phycobilisome antennae in cyanobacteria and red algae, in: P. Fromme (Ed.) Photosynthetic Protein Complexes, Wiley, 2008, pp. 243-274.
- [33] **Arteni, A.A., Ajlani, G., Boekema, E.J.**, Structural organisation of phycobilisomes from *Synechocystis sp* strain PCC6803 and their interaction with the membrane, *Biochim. Biophys. Acta*, 1787 (2009) 272-279.
- [34] **Ashby, M.K., Mullineaux, C.W.**, The role of ApcD and ApcF in energy transfer from phycobilisomes to PSI and PSII in a cyanobacterium, *Photosynth Res.*, 61 (1999) 169-179.
- [35] **Watanabe, M., Ikeuchi, M.**, Phycobilisome: architecture of a light-harvesting supercomplex, *Photosynth Res.*, 116 (2013) 265-276.
- [36] **Tian, L., Gwizdala, M., van Stokkum, I.H., Koehorst, R.B., Kirilovsky, D., van Amerongen, H.**, Picosecond kinetics of light harvesting and photoprotective quenching in wild-type and mutant phycobilisomes isolated from the cyanobacterium *Synechocystis* PCC 6803, *Biophys. J.*, 102 (2012) 1692-1700.
- [37] **Ughy, B., Ajlani, G.**, Phycobilisome rod mutants in *Synechocystis sp* strain PCC6803, *Microbiology*, 150 (2004) 4147-4156.
- [38] **Croce, R., van Amerongen, H.**, Light-harvesting in photosystem I, *Photosynth Res.*, 116 (2013) 153-166.
- [39] **Amunts, A., Drory, O., Nelson, N.**, The structure of a plant photosystem I supercomplex at 3.4Å resolution, *Nature*, 447 (2007) 58-63.
- [40] **Melkozernov, A.N., Barber, J., Blankenship, R.E.**, Light harvesting in photosystem I supercomplexes, *Biochemistry*, 45 (2006) 331-345.
- [41] **Wientjes, E., Oostergetel, G.T., Jansson, S., Boekema, E.J., Croce, R.**, The role of Lhca complexes in the supramolecular organization of higher plant photosystem I, *J. Biol. Chem.*, 284 (2009) 7803-7810.
- [42] **Wientjes, E., van Stokkum, I.H.M., van Amerongen, H., Croce, R.**, Excitation-energy transfer dynamics of higher plant photosystem I light-harvesting complexes, *Biophys. J.*, 100 (2011) 1372-1380.
- [43] **Caffarri, S., Kouril, R., Kereiche, S., Boekema, E.J., Croce, R.**, Functional architecture of higher plant photosystem II supercomplexes, *EMBO J.*, 28 (2009) 3052-3063.
- [44] **Kouril, R., Dekker, J.P., Boekema, E.J.**, Supramolecular organization of photosystem II in green plants, *Biochim. Biophys. Acta*, 1817 (2012) 2-12.
- [45] **Kovacs, L., Damkjaer, J.T., Kereiche, S., Illoia, C., Ruban, A.V., Boekema, E.J., Jansson, S., Horton, P.**, Lack of the light-harvesting complex CP24 affects the structure and function of the grana membranes of higher plant chloroplasts, *Plant Cell*, 18 (2006) 3106-3120.
- [46] **Yakushevskaya, A.E., Keegstra, W., Boekema, E.J., Dekker, J.P., Andersson, J., Jansson, S., Ruban, A.V., Horton, P.**, The structure of photosystem II in Arabidopsis: Localization of the CP26 and CP29 antenna complexes, *Biochemistry*, 42 (2003) 608-613.

- [47] **Damkjaer, J.T., Kereiche, S., Johnson, M.P., Kovacs, L., Kiss, A.Z., Boekema, E.J., Ruban, A.V., Horton, P., Jansson, S.**, The photosystem II light-harvesting protein Lhcb3 affects the macrostructure of photosystem II and the rate of state transitions in *Arabidopsis*, *Plant Cell*, 21 (2009) 3245-3256.
- [48] **Leoni, C., Pietrzykowska, M., Kiss, A.Z., Suorsa, M., Ceci, L.R., Aro, E.M., Jansson, S.**, Very rapid phosphorylation kinetics suggest a unique role for Lhcb2 during state transitions in *Arabidopsis*, *Plant J.*, 76 (2013) 236-246.
- [49] **Folea, I.M., Zhang, P., Aro, E.M., Boekema, E.J.**, Domain organization of photosystem II in membranes of the cyanobacterium *Synechocystis* PCC6803 investigated by electron microscopy, *FEBS Lett.*, 582 (2008) 1749-1754.
- [50] **Liu, H.J., Zhang, H., Niedzwiedzki, D.M., Prado, M., He, G.N., Gross, M.L., Blankenship, R.E.**, Phycobilisomes supply excitations to both photosystems in a megacomplex in cyanobacteria, *Science*, 342 (2013) 1104-1107.
- [51] **Garab, G., Wells, S., Finzi, L., Bustamante, C.**, Helically Organized Macroaggregates of Pigment Protein Complexes in Chloroplasts - Evidence from Circular Intensity Differential Scattering, *Biochemistry*, 27 (1988) 5839-5843.
- [52] **Faludi-Daniel, A., Mustardy, L.A.**, Organization of chlorophyll a in the light-harvesting chlorophyll a/b protein complex as shown by circular dichroism - liquid crystal-like domains, *Plant Physiol.*, 73 (1983) 16-19.
- [53] **Demeter, S., Mustardy, L., Machowicz, E., Gregory, R.P.F.**, Development of intense circular dichroism signal during granum formation in greening etiolated maize, *Biochem. J.*, 156 (1976) 469-472.
- [54] **Simpson, D.J.**, Freeze-Fracture Studies on Barley Plastid Membranes .2. Wild-Type Chloroplast, *Carlsberg Res Commun*, 43 (1978) 365-389.
- [55] **Miller, K.R.**, A particle spanning the photosynthetic membrane, *Journal of ultrastructure research*, 54 (1976) 159-167.
- [56] **Dekker, J.P., Boekema, E.J.**, Supramolecular organization of thylakoid membrane proteins in green plants, *Biochim. Biophys. Acta*, 1706 (2005) 12-39.
- [57] **Kouril, R., Wientjes, E., Bultema, J.B., Croce, R., Boekema, E.J.**, High-light vs. low-light: Effect of light acclimation on photosystem II composition and organization in *Arabidopsis thaliana*, *Biochim. Biophys. Acta*, 1827 (2013) 411-419.
- [58] **Kirchhoff, H.**, Diffusion of molecules and macromolecules in thylakoid membranes, *Biochim. Biophys. Acta*, 1837 (2013) 495-502.
- [59] **Stirbet, A.**, Excitonic connectivity between photosystem II units: what is it, and how to measure it?, *Photosynth Res.*, 116 (2013) 189-214.
- [60] **Garcia-Cerdan, J.G., Kovacs, L., Toth, T., Kereiche, S., Aseeva, E., Boekema, E.J., Mamedov, F., Funk, C., Schroder, W.P.**, The PsbW protein stabilizes the supramolecular organization of photosystem II in higher plants, *Plant J.*, 65 (2011) 368-381.
- [61] **Goral, T.K., Johnson, M.P., Duffy, C.D.P., Brain, A.P.R., Ruban, A.V., Mullineaux, C.W.**, Light-harvesting antenna composition controls the macrostructure and dynamics of thylakoid membranes in *Arabidopsis*, *Plant J.*, 69 (2012) 289-301.
- [62] **Kereiche, S., Kiss, A.Z., Kouril, R., Boekema, E.J., Horton, P.**, The PsbS protein controls the macro-organisation of photosystem II complexes in the grana membranes of higher plant chloroplasts, *FEBS Lett.*, 584 (2010) 759-764.
- [63] **Boekema, E.J., van Breemen, J.F.L., van Roon, H., Dekker, J.P.**, Arrangement of photosystem II supercomplexes in crystalline macrodomains within the thylakoid membrane of green plant chloroplasts, *J. Mol. Biol.*, 301 (2000) 1123-1133.
- [64] **Yakushevskaya, A.E., Jensen, P.E., Keegstra, W., van Roon, H., Scheller, H.V., Boekema, E.J., Dekker, J.P.**, Supermolecular organization of photosystem II and its associated light-harvesting antenna in *Arabidopsis thaliana*, *Eur. J. Biochem.*, 268 (2001) 6020-6028.
- [65] **Drozak, A., Romanowska, E.**, Acclimation of mesophyll and bundle sheath chloroplasts of maize to different irradiances during growth, *Biochim. Biophys. Acta*, 1757 (2006) 1539-1546.

- [66] Andaluz, S., Lopez-Millan, A.F., Rivas, J.D.I., Aro, E.-M., Abadia, J., Abadia, A., Proteomic profiles of thylakoid membranes and changes in response to iron deficiency, *Photosynth Res.*, 89 (2006) 141-155.
- [67] Garstka, M., Drozak, A., Rosiak, M., Venema, J.H., Kierdaszuk, B., Simeonova, E., van Hasselt, P.R., Dobrucki, J., Mostowska, A., Light-dependent reversal of dark-chilling induced changes in chloroplast structure and arrangement of chlorophyll-protein complexes in bean thylakoid membranes, *Biochim. Biophys. Acta*, 1710 (2005) 13-23.
- [68] Oquist, G., Huner, N.P.A., Photosynthesis of overwintering evergreen plants, *Annu. Rev. Plant Biol.*, 54 (2003) 329-355.
- [69] Dietzel, L., Braeutigam, K., Pfannschmidt, T., Photosynthetic acclimation: State transitions and adjustment of photosystem stoichiometry - functional relationships between short-term and long-term light quality acclimation in plants, *FEBS J.*, 275 (2008) 1080-1088.
- [70] Haldrup, A., Jensen, P.E., Lunde, C., Scheller, H.V., Balance of power: a view of the mechanism of photosynthetic state transitions, *Trends Plant Sci.*, 6 (2001) 301-305.
- [71] Galka, P., Santabarbara, S., Thi Thu Huong, K., Degand, H., Morsomme, P., Jennings, R.C., Boekema, E.J., Caffarri, S., Functional analyses of the plant photosystem I light-harvesting complex II supercomplex reveal that light-harvesting complex II loosely bound to photosystem II is a very efficient antenna for photosystem I in state II, *Plant Cell*, 24 (2012) 2963-2978.
- [72] Wientjes, E., Drop, B., Kouril, R., Boekema, E.J., Croce, R., During state 1 to state 2 transition in *Arabidopsis thaliana*, the photosystem II supercomplex gets phosphorylated but does not disassemble, *J. Biol. Chem.*, 288 (2013) 32821-32826.
- [73] Horton, P., Optimization of light harvesting and photoprotection: molecular mechanisms and physiological consequences, *Phil. Trans. R. Soc. B*, 367 (2012) 3455-3465.
- [74] Bauer, H., Nagele, M., Comploj, M., Galler, V., Mair, M., Unterpertinger, E., Photosynthesis in cold-acclimated leaves of plants with various degrees of freezing tolerance, *Physiol. Plant.*, 91 (1994) 403-412.
- [75] Anderson, J.M., Horton, P., Kim, E.H., Chow, W.S., Towards elucidation of dynamic structural changes of plant thylakoid architecture, *Phil. Trans. R. Soc. B*, 367 (2012) 3515-3524.
- [76] Wientjes, E., van Amerongen, H., Croce, R., LHCI is an antenna of both photosystems after long-term acclimation, *Biochim. Biophys. Acta*, 1827 (2013) 420-426.
- [77] Nagel, K., Voigt, J., Impaired photosynthesis in a cadmium-tolerant *Chlamydomonas* mutant strain, *Microbiol. Res.*, 150 (1995) 105-110.
- [78] Pawlik, B., Skowronski, T., Ramazanow, Z., Gardestrom, P., Samuelsson, G., pH-dependent cadmium transport inhibits photosynthesis in the cyanobacterium *Synechocystis aquatilis*, *Environ. Exp. Bot.*, 33 (1993) 331-337.
- [79] Clijsters, H., Van Assche, F., Inhibition of photosynthesis by heavy metals, *Photosynth Res.*, 7 (1985) 31-40.
- [80] Vanassche, F., Clijsters, H., Effects of metals on enzyme-activity in plants, *Plant Cell and Environment*, 13 (1990) 195-206.
- [81] Schreiber, U., Pulse-Amplitude-Modulation (PAM) fluorometry and saturation pulse method: An overview, in: G.C. Papageorgiou, Govindjee (Eds.) *Chlorophyll a Fluorescence*, Springer Netherlands, 2004, pp. 279-319.
- [82] Strasser, R.J., Tsimilli-Michael, M., Srivastava, A., Analysis of the chlorophyll a fluorescence transient, in: G.C. Papageorgiou, Govindjee (Eds.) *Chlorophyll a Fluorescence*, Springer Netherlands, 2004, pp. 321-362.
- [83] Toth, S.Z., Schansker, G., Strasser, R.J., A non-invasive assay of the plastoquinone pool redox state based on the OJIP-transient, *Photosynth Res.*, 93 (2007) 193-203.
- [84] van Munster, E.B., Gadella, T.W.J., Fluorescence lifetime imaging microscopy (FLIM), in: J. Rietdorf (Ed.) *Microscopy Techniques*, 2005, pp. 143-175.
- [85] Krumova, S., Laptinok, S., Borst, J., Ughy, B., Gombos, Z., Ajlani, G., van Amerongen, H., Monitoring photosynthesis in individual cells of *Synechocystis sp.* PCC 6803 on a picosecond timescale, *Biophys. J.*, 99 (2010) 2006-2015.

- [86] **Laptenok, S., Mullen, K.M., Borst, J.W., van Stokkum, I.H.M., Apanasovich, V.V., Visser, A.**, Fluorescence Lifetime Imaging Microscopy (FLIM) data analysis with TIMP, *Journal of Statistical Software*, 18 (2007).
- [87] **van Stokkum, I.H.M., van Oort, B., Mourik, F., Gobets, B., van Amerongen, H.**, (Sub)-picosecond spectral evolution of fluorescence studied with a synchroscan streak-camera system and target analysis, in: T. Aartsma, J. Matysik (Eds.) *Biophysical Techniques in Photosynthesis*, Springer Netherlands, 2008, pp. 223-240.
- [88] **Garab, G., Mustardy, L.**, Role of LHCII-containing macrodomains in the structure, function and dynamics of grana, *Aust. J. Plant Physiol.*, 26 (1999) 649-658.
- [89] **Garab, G., van Amerongen, H.**, Linear dichroism and circular dichroism in photosynthesis research, *Photosynth Res.*, 101 (2009) 135-146.

# Chapter 2

## ***Carotenoid deficiency induces structural and functional changes in the phycobilisomes and photosystems of *Synechocystis* PCC 6803***

Tünde Tóth<sup>1,2</sup>, Volha Chukhutsina<sup>1</sup>, Ildikó Domonkos<sup>2</sup>, Josef Komenda<sup>3</sup>, Bettina Ughy<sup>2</sup>, Mihály Kis<sup>2</sup>, Zsófia Lénárt<sup>2</sup>, Győző Garab<sup>2</sup>, Zoltán Gombos<sup>2</sup>, László Kovács<sup>2\*</sup> and Herbert van Amerongen<sup>1,4</sup> *In preparation*

<sup>1</sup> *Laboratory of Biophysics, Wageningen University, Wageningen, The Netherlands*

<sup>2</sup> *Institute of Plant Biology, Biological Research Centre of Hungarian Academy of Sciences, Szeged, Hungary*

<sup>3</sup> *Laboratory of Photosynthesis, Institute of Microbiology, Trebon, Czech Republic*

<sup>4</sup> *MicroSpectroscopy Centre, Wageningen University, Wageningen, The Netherlands*

## 2.1 Abstract

Carotenoids are the most widespread pigments in nature and especially important in photosynthetic organisms. We have studied structural and functional characteristics of wild-type and mutants of *Synechocystis* PCC 6803 cells, which are deficient in various carotenoid biosynthetic enzymes. Here we show that xanthophyll deficiency lowers the stability of photosystem II dimers and increases the photosystem I monomer to trimer ratio without impairing the transfer of excitation energy. Moreover, our results demonstrate that, although the phycoblisome (PBS) does not contain any carotenoid, however it contains a substantial amount of unconnected phycocyanin units, far away from the PBS core and the thylakoid membranes, whereas the phycocyanin rods of the PBSs that are connected to the photosystems are reduced to mostly one hexameric unit. We propose that dissociation of the rods occurs in the absence or limited availability of  $\beta$ -carotene only after the PBSs are first fully assembled.

## 2.2 Introduction

In all living systems carotenoids (Cars) are the most abundant pigments with important structural and functional roles. These pigments can be essential for assembly of protein complexes [1] or to maintain intact membrane structure [2] and they might contribute to the regulation of the membrane fluidity [3]. In photosynthetic organisms Cars can also assist in the light-harvesting process [4-6] or serve as photoprotective agents, especially when the organisms are exposed to excess light [7]. The Car pigments are capable to quench the triplet excited state chlorophylls and directly scavenge the singlet excited oxygen. Due to their hydrophobic characteristics the Cars are mostly localized in thylakoid membranes often in the vicinity of or inside the photosynthetic complexes. It is interesting to note that while  $\beta$ -carotenes molecules mostly present in protein complexes, the xanthophylls can be also found in the membranes [8]. The photosynthetic machinery of higher plants shows strong homology to the cyanobacterial, therefore cyanobacteria are excellent tools to study the role of various carotenoid species on photosynthetic complexes. The cyanobacteria are prokaryotic photosynthetic organisms in which the most abundant Cars are  $\beta$ -carotene and various xanthophylls, i.e. synechoxanthin, canthaxanthin, caloxanthin, echinenone, myxoxanthophyll nostoxanthin and zeaxanthin [8, 9]. X-ray crystallographic studies have revealed that in the cyanobacterium *Thermosynechococcus elongatus* 22  $\beta$ -carotenes molecules are located in photosystem I (PSI) [10, 11] and 12  $\beta$ -carotenes are present in

# Role of carotenoids in thylakoid organisation

photosystem II (PSII) [12] monomers, respectively. Also the electron transport component, the cytochrome *b<sub>6</sub>f* (cyt *b<sub>6</sub>f*) complex, contains one Car molecule [13]. In addition, one Car serves as a switch to activate the photoprotective orange carotenoid protein (OCP) which is responsible for non-photochemical quenching in cyanobacteria [14-16]. In the commonly used model organism, *Synechocystis* PCC 6803 (*Synechocystis*) strain, the most important Cars are the  $\beta$ -carotene, echinenone, 3'-hydroxy-echinenone, zeaxanthin, synechoxanthin and myxoxanthophyll (myxo-2'-fucosid) (Table 2.1).

**Table 2.1.** Location and function of different carotenoid forms in cyanobacteria

Type	Location (# Car molecules)	Function	Refs
<i><math>\beta</math>-carotene</i>	PSII (12/monomer) PSI (22/monomer) cyt <sub>b6f</sub> (1/protein)	accessory pigment, structure stabilizing element, ROS scavenger, photoprotective agent	[10, 12, 13]
<i>Echinenone</i>	OCP (1/protein) Membranes	NPQ unknown	[17]
<i>Zeaxanthin</i>	Membranes	photoprotective agent, membrane rigidifying substance	[18] [19]
<i>Myxo- xanthophyll</i>	Membranes Cell wall	cell wall component, membrane rigidifying substance	[2, 20]

The biosynthesis of carotenoids in cyanobacteria have been intensively studied for long and several mutants deficient in various steps of biosynthesis are available [8, 9] allowing to investigate the role of various Car classes.

In *Synechocystis crtR/O* double mutant strain almost complete loss of xanthophylls were obtained by inactivation of two biosynthetic enzymes (carotene  $\beta$ -ketolase and carotene  $\beta$ -hydroxylase). These cells contain only  $\beta$ -carotene and some precursors of myxoxanthophyll. However, the lack of xanthophylls increases the light sensitivity of the cells upon high light intensities, while the basic photosynthetic processes and membrane integrity seems to be unaffected [21, 22]. The *crtH* mutant strain is deficient in an enzyme catalysing the *cis* to *trans* isomerization of carotenoids, which is a rather early step of Car biosynthesis. These isomerisation steps can also occur via photo-isomerisation process in *crtH* mutant cells upon continuous light illumination during photoautotrophic (PAG) or photoheterotrophic (PHG) growth conditions [23]. However, the photo-isomerisation does not replace completely the enzyme catalysing the *cis* to *trans*

isomerisation. Consequently the Car composition and ratio of various Car species of light grown *crtH* cells is not completely restored to the values obtained from wild-type cells [23]. The *crtH* cells, which are grown in the dark under light-activated heterotrophic (LAHG) conditions [24] are not able to synthesize trans-carotenoids due to the lack of both enzymatic and photo-isomerisation. These cells can produce only some Car precursors, primarily *cis*-lycopenes and a small amount of all-*trans* carotenes, but no xanthophylls [23, 25].

**Table 2.2.** *Synechocystis* PCC 6803 mutant strains and growth conditions used in this study

Mutation		Carotenoid content	Consequences	Refs
<b>Photoautotroph growth (PAG)</b>				
<i>WT</i>		$\beta$ -carotene, zeaxanthin, echinenone, myxoxanthophyll		
<i>crtR/O</i>	$\beta$ -carotene ketolase, $\beta$ -carotene hydroxylase	deoxymyxol 2'-dimethyl-fucoside (myxoxanthophyll), $\beta$ -carotene	WT-like thylakoid structure, sensitive to light and oxidative stress	[8, 21, 26]
<i>crtH</i>	<i>cis</i> to <i>trans</i> isomerase	all kinds of Cars, but different ratios	more PSI (PsaA), less PSII (D1) on Chl basis than in WT	[23]
<b>Light-activated heterotrophic growth (LAHG)</b>				
<i>WT</i>		normal Car content	less thylakoid, interthylakoid distances are larger, free PBs, fraction of nonfunctional PSII, high PSI activity	[23, 27]
$\Delta$ <i>crtB</i>	phytoene synthase	no Car	for $\Delta$ <i>crtH/B</i> : Few thylakoid membranes, no detectable O <sub>2</sub> evolution, only small amount of assembled PSII core complexes, cyt <i>b<sub>6</sub>f</i> formed, PSI is in monomeric form	[8, 28]
<i>crtH</i>	<i>cis</i> to <i>trans</i> isomerase	almost no Car, just a small amount of car precursors	High PSI activity, almost no detectable PSII (D1), no detectable O <sub>2</sub> evolution	[23]

Recently a  $\Delta$ *crtH/B* mutant *Synechocystis* strain that is completely without Cars has been generated [28]. This mutant strain is deficient in enzymes catalysing the early steps of Car biosynthesis. In the corresponding cells the phytoene synthetase encoding *crtB* gene was inactivated in the *CrtH* deficient mutant. The phytoene synthetase catalyses one of the first enzymatic steps in the Car biosynthesis pathway,

## Role of carotenoids in thylakoid organisation

while the *crtH* gene coding the *cis* to *trans* isomerase enzyme which contributes to the later synthesis steps (see also [8]). These mutant cells do not contain carotenoid precursors or intermediate products what would make difficult separate the role of the different carotenoid classes. The  $\Delta crtH/B$  cells are extremely light sensitive and only able to grow in the dark under light-activated heterotrophic growth (LAHG) conditions [24]. In the  $\Delta crtH/B$  mutant cells oxygen-evolving activity cannot be observed, suggesting the absence of photochemically active PSII complexes and/or the absence of functional water splitting complex. Only a small amount of a non-functional, partially assembled PSII core complex can be detected. However, the formation of *cyt b<sub>6</sub>f* complexes has been detected in these cells [28]. The thylakoid structure of the cells is also influenced by the mutations; only a few fragmented thylakoids were observed [8]. Most recently  $\Delta crtB$  have become available mutant (this work) this mutant is essentially the same as  $\Delta crtH/B$ .

In photosynthetic organisms the pigment-protein complexes localised in the thylakoid membrane are responsible for the transformation of light energy into chemical energy. The various pigments embedded in photosynthetic complexes have distinct spectroscopic properties to ensure the funnelling of the excitation energy toward photosynthetic reaction centres (RCs). The two membrane-embedded chlorophyll-containing photosystems (PSII and PSI) both have an evolutionarily highly conserved protein structure. In the cyanobacterial thylakoid membrane PSII, like in higher plants, occurs in dimeric form. Each PSII monomer containing two inner antennae CP43 and CP47 attached to the PSII RC, together forming the PSII core with a total of 35 chlorophyll *a* (Chl *a*)/monomer. Interestingly, PSI of cyanobacteria, although being very similar to PSI of higher plants, exists instead of monomer (96 Chl *a*/PSI monomer), as trimers. There are some small molecular weight proteins which are proved to be important for attaching the PSI monomers into trimer. The most important small subunit is the PsaL protein, which is necessary for the trimerisation, while the PsaM and PsaI has trimer stabilising function. Three out of the 22  $\beta$ -carotene molecules are localised in the trimerisation domain, but not in close contact with any Chl molecule, these Cars are predicted to stabilise the trimeric form of PSI. Both photosystems contains only Chl *a* pigment molecules beside the Cars. Chl *a* has absorption maximum typically at ~680 nm and emits fluorescence at ~685 nm except for a few long-wavelength Chl *a* molecules (LWCs) in PSI emitting at longer (~730 nm) wavelengths. The LWC molecules are more abundant in PSI trimers than in monomers due to some pigment-pigment interactions which are only present in the trimer. Although the exact position and role of LWCs are controversial, the emitted long-wavelength fluorescence is often used as an *in vivo* sign of the presence of PSI trimers.

In cyanobacteria, peripheral antenna complexes, the phycobilisomes (PBS) serve as light-harvesting antennae for the photosynthetic complexes [29]. In PBSs the phycobilin pigments (phycocyanobilin, phycourobilin, phycoerythrobilin, phycobiliviolin) attached to phycobliproteins (phycocyanin, allophycocyanin, phycoerythrin, phycoerythrocyanin) are responsible for light harvesting. In *Synechocystis* each PBS contains approximately six C-phycocyanin (C-PC) rods attached to the three allophycocyanin (APC) core cylinders. Each C-PC rod comprises typically three hexameric disks (18 bilins/hexamer) while all the APC core cylinders consist of four trimeric disks (6 bilins/trimer). There are various linker proteins which are responsible for maintaining the PBS structure, and these linkers can be divided into groups according to their function [30]. The rod linker ( $L_R$ ) proteins attach to the hexameric rod units and organise them into rods [31]. The  $L_R$  proteins are named according to their molecular mass. The  $L_R^{10}$  protein is believed to be localized at the end of the rods as a cap and has a stabilising function. The  $L_R^{30}$  attaches the last hexamer unit to the middle one, while the  $L_R^{33}$  is required for the linkage of the first and the second unit. The rod-core linkers ( $L_{RC}$ ) bind the rods to the core cylinders. The small core linkers ( $L_C$ ) stabilise the core cylinders. Two of the four terminal emitters (TE) contain the APC monomer part of the membrane-core linker ( $L_{MC}$ ), which attaches the PBS to the PSs.

The incident light is absorbed mainly by the pigments of the PC rods, which have maximum absorbance at around 620 nm and fluorescence emission at 640-650 nm. As a next step, the absorbed energy is transferred to the pigments of the APC in the PBS core with 650 nm absorption. Both of the two APC core cylinders closest to the membrane contain two special trimers [32] responsible for the energy transfer towards the RCs [33]. They function as TE of the PBS because they contain either one or two bilins that are responsible for the fluorescence at 680 nm for these particular APC trimers ( $APC_{680}$ ) as opposed to the other trimers that fluoresce at 660 nm ( $APC_{660}$ ) and in this way they ensure the continuous energy transfer from PBSs to the PSs. The TE are responsible for direct excitation energy transfer (EET) to the Chl *a*-containing core of the photosystems [33].

The fluorescence emitted by the pigment-protein complexes can provide information about the rate and efficiency of photosynthetic processes. Although a wealth of information is available about the roles of Cars (Table 2.1), until recently, no comparative study has been done in cyanobacteria about their functional impact on photosynthetic energy transfer processes. *Synechocystis* PCC 6803 (*Synechocystis*) strains have been mutated at various Car biosynthetic steps, which resulted in partial or complete elimination of Cars and provided a tool to investigate the effect of Car-depletion on various photosynthetic processes (Table 2.2). The

# Role of carotenoids in thylakoid organisation

present study focuses on the role of the various Cars in the energy transfer processes and the organisation of the photosynthetic complexes of *Synechocystis* cells. To this end, different Car biosynthesis mutants grown under various conditions have been studied with the use of picosecond fluorescence spectroscopy/microscopy in combination with standard biochemical methods and electron microscopy. Our results show that the xanthophylls influence the oligomeric states of PSI and PSII although they are not modelled in the crystal structure. Furthermore, the PBSs structure is strongly altered in response to the Car composition, despite the fact that they are thought not to be part of the PBS structure.

## 2.3 Materials and methods

### *Cell culturing*

*Synechocystis* PCC 6803 cells were cultivated in BG11 medium [34] buffered with 5 mM HEPES (pH 7.5) on a rotary shaker at 30 °C. Under photoautotrophic growth (PAG) conditions WT, *crtR/O* and *crtH* [23] cells were illuminated with continuous white light using 35  $\mu\text{mol photons m}^{-2} \text{s}^{-1}$  PPFD.  $\Delta\text{crtB}$ , *crtH* and WT strains were grown under light-activated heterotrophic growth (LAHG) conditions [24] in BG11 in the presence of 10 mM glucose using 10 min illumination per day with 15  $\mu\text{mol photons m}^{-2} \text{s}^{-1}$  PPFD. The mutant cells were cultured in the presence of the appropriate antibiotics. The cells used for the measurements were in the logarithmic growth phase.

### *Construction of *Synechocystis* PCC 6803 $\Delta\text{crtB}$ and *crtR/O* mutant strains*

A construct containing part of the *crtB* gene and an omega cassette [28] was used to transform WT cells of *Synechocystis* PCC 6803. Transformants were selected under LAHG conditions on BG11 agar plates supplemented with glucose and increasing amounts of spectinomycin by several restreaking of single colonies.

The *crtR/O* mutant was a gift from Kazumori Masamoto (Kumamoto University, Japan). This mutant was created by introducing kanamycin and spectinomycin cassettes into the coding regions of the *crtR* and *crtO* genes, respectively. Complete segregation of the mutant cells was confirmed by PCR.

### *Electron-microscopy analysis*

The collected cells were fixed in 1% paraformaldehyde and 1% glutaraldehyde for 4 h at 4°C and post-fixed in 1% osmium tetroxide [35]. The

samples were dehydrated in aqueous solutions of increasing ethanol concentrations, and then embedded in Spurr resin. Following polymerization, 85–90 nm ultrathin sections were cut out by a Reichert Ultracut E ultramicrotome (Leica, Wetzlar, Germany). According to the standard procedure the sections were treated with uranyl acetate and lead citrate and subjected to electron microscopy in a Zeiss EM 902 electron microscope (Carl Zeiss AG, Oberkochen, Germany).

### *Isolation of phycobilisomes*

Phycobilisomes were prepared from *Synechocystis* PCC 6803 wild-type and mutant cells according to [36] with some modifications. Cells were pre-treated by 0.2% lysozyme at 37 °C and following centrifugation resuspended in 0.75 M K-Na phosphate buffer (pH 7.0). All subsequent steps were carried out at room temperature. The cells were disrupted with 0.1 mm diameter glass beads in a Bead Beater homogenizer. After 5% Triton X-100 treatment for 50 min at room temperature the thylakoid membranes were pelleted by centrifugation at 15,000 g. The supernatant was treated again with 3% Triton X-100 for 20 min and loaded onto a discontinuous sucrose density gradient. After 20 hours of centrifugation at 90,000 g 14 °C the PBS containing blue-coloured layers were removed from the gradients and stored at room temperature until spectroscopic and protein analysis.

### *Protein analysis*

Membranes for two-dimensional BN/SDS-PAGE were isolated by breaking cells in 25 mM MES/NaOH buffer (pH 6.5) containing 10 mM CaCl<sub>2</sub>, 10 mM MgCl<sub>2</sub> and 25% glycerol using glass beads in a beadbeater. The thylakoid membranes were collected by centrifugation and solubilized with 1% dodecyl- $\beta$ -D-maltoside. First-dimension, blue-native electrophoresis was performed at 4 °C in a 4–14% polyacrylamide gel. 5  $\mu$ g Chl containing samples were loaded onto each lane. The protein composition of the complexes was assessed by a second dimension electrophoresis in a denaturing 12 to 20% linear gradient polyacrylamide gel containing 7 M urea. The lanes from the native gel were excised along their entire length, incubated for 20 min in 25 mM Tris/HCl (pH 7.5) containing 1% SDS and 1% dithiothreitol (w/v) and placed on top of the denaturing (SDS) gel. Proteins separated in the gel were stained with Coomassie Blue [37].

Protein composition of isolated PBSs was studied using Tricine–SDS-PAGE [38]. The isolated PBSs were precipitated by adding an equal volume of 20% trichloroacetic acid and incubating on ice for 5 min. After centrifugation the pellet was resuspended in loading buffer and heated for 5 min at 85 °C. Denaturing gel electrophoresis of samples was performed in a 10 to 16% linear gradient

# Role of carotenoids in thylakoid organisation

polyacrylamide gel. 40 µg total protein containing samples were loaded onto each lane. The separated proteins were stained with Coomassie Blue.

## *Picosecond time-resolved measurements*

Two-photon excitation (860 nm) FLIM measurements were performed according to [39]. Fluorescence was recorded via non-descanned single photon counting detection, through two band-pass (BP) filters of 700 nm with 75 nm bandwidth (BP 700/75) or through one BP 647/58 (see also Fig. Supplementary Information 2.11). The time resolution was 12 ps per time channel; 64 x 64 pixel images were collected, with 0.2 µm/pixel resolution. To minimize photodamage, low excitation power (60 µW average power at 860 nm) in combination with long integration times (20-30 min) was used. Cells were immobilized in 3% low gelling temperature agarose, type VII (Sigma-Aldrich) dissolved in BG11 media and pressed between microscopy and cover glasses. Pinacyanol in methanol with a 6 ps lifetime was used as a reference [40] to determine the instrument response function (IRF). FLIM images were analysed using Glotaran as graphical user interface for the R-package TIMP (glotaran.org) [41, 42]. Only pixels with fluorescence intensity above 75 counts per second were selected for global analysis. Global analysis of the image results in the same set of lifetimes for all selected pixels with different amplitudes. The fit quality was judged by singular value decomposition of the residual matrix associated with each FLIM image [42]. Average lifetimes were calculated using the following equation:

$$\tau_{avr} = \sum_{i=1}^n \alpha_i \tau_i$$

Time-resolved emission spectra were recorded at room temperature (293 K) using a synchroscan streak-camera system [40, 43, 44]. The average of 100 images, each measured for 10 s, was used while the time window was either 800 ps or 2 ns. The laser repetition rate was 250 kHz and the laser power was typically 70 µW. The excitation light was vertically polarized and a spot size diameter of ~100 µm was used. The wavelength of the excitation pulses was either 590 nm or 400 nm. Cells with an optical density of 0.3-0.6 cm<sup>-1</sup> at the excitation wavelength were used for the measurements. In order to keep the RCs open the cells were dark-adapted for 10 min and circulated in a 1 mm flow cell during measurements.

The streak images were analysed using the Glotaran graphical user interface for TIMP [45]. The images were corrected for background signal and detector sensitivity and sliced up into traces of 5 nm. Streak images obtained with the 800 ps and 2 ns time window were linked during the analysis. A Gaussian-shaped IRF was used for the analyses and its width was a free fitting parameter. The synchroscan

period (13.17 ns) results in a back and forth sweeping of long-lived components and leads to some signal before time zero in the streak-camera images [46], which was used for estimation of amplitudes and lifetimes of long-lived components. The fit quality was judged by singular value decomposition of the residuals matrix [45].

## 2.4 Results

### *Electron microscopy analysis*

The effect of the Cars on thylakoid membrane organisation was investigated by standard transmission electron microscopy. The three-dimensional structure of wild-type *Synechocystis* cells were extensively studied with special consideration to the arrangement of thylakoid membranes [47, 48]. The photoautotrophically grown (PAG) xanthophyll-deficient *crtR/O* and the *crtH* mutant cells showed similar morphology that of the WT *Synechocystis* cells (Fig. 2.1 A-C). All strains contained multilayered membrane sheets of 3–6 pairs of thylakoid running mostly parallel to the cytoplasmic membrane within the peripheral region of the cell and occasionally some thylakoid membrane pairs traversed the central cytoplasm. The average distance between the adjacent membrane pairs was approximately 40 nm. The central cytoplasmic region contained carboxysomes and ribosomes; lipid drops were located at the interthylakoid part of the cells.

The Car deficient  $\Delta$ *crtB* strain is extremely light sensitive similar to the  $\Delta$ *crtH/B* cells [28], therefore these cells can be cultured only in darkness with organic carbon source and daily pulse of light, so-called LAHG conditions [24]. In order to distinguish the Car effects from the structural and functional changes induced by the growth conditions the WT cells were also cultivated under the same (LAHG) conditions. These WT cells (Fig. 2.1 D) exhibited a reduced number of thylakoid layers in a less-ordered structure than under PAG conditions. Only short sections of membrane pairs were located parallel to the cell wall with slightly increased inter-thylakoid distances (~ 50 nm) and more thylakoid sheets were penetrating into the central region of the cell. The presence of cytoplasmic inclusions, like carboxysomes and polyhydroxybutyrate (PHB) granules appeared to be characteristic for these cells.

# Role of carotenoids in thylakoid organisation

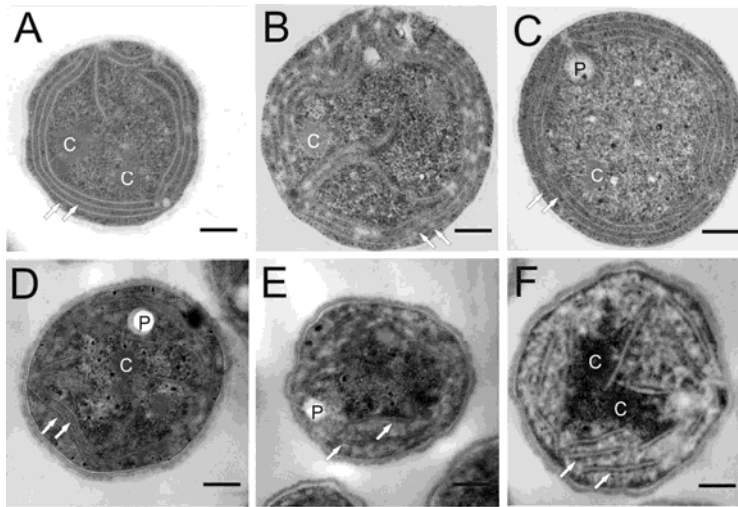


**Figure 2.1.** Electron micrographs of *Synechocystis* PCC 6803 WT PAG (A), *crtR/O* PAG (B), *crtH* PAG (C), WT LAHG (D),  $\Delta$ *crtB*(E) and *crtH* LAHG (F) cells. White arrows show thylakoid membrane pairs. C: carboxysome; P: polyphosphate bodies. Bars: 0.25  $\mu$ m.

The complete lack of Cars in the  $\Delta$ *crtB* cells (Fig. 2.1 E), similar to the heterotrophic growth conditions (LAHG) of *crtH* mutant cells (Fig. 2.1 F), resulted in disintegrated thylakoid membrane structures. These cells possess less thylakoid membrane pairs than the WT<sub>LAHG</sub> cells and the thylakoid layers do not form multilayer membranes parallel to the cell wall but only membrane pairs dispersed in the cell. The distance between the adjacent thylakoid sheets increased to 60-140 nm and the membrane pairs enclosed slightly inflated thylakoid lumen. Carboxysomes and PHB granules were frequently present. There was an interesting characteristic of these cells: they showed a highly electron-dense central cytoplasm with inclusions but the peripheral regions were electron-transparent apart from the thylakoid layers.

## *Protein analysis of thylakoid membranes*

The presence of membrane proteins and their complexes in various Car biosynthesis mutant strains were investigated by two-dimensional (2D) gel electrophoresis (Fig. 2.2). In the first dimension, native protein complexes, obtained by mild solubilisation of thylakoid membranes, were separated and in the second dimension, the subunit composition of the complexes was determined by denaturing SDS-PAGE. This method allowed us to assess the effect of Car biosynthesis mutations on the amount of various oligomeric forms of PSI and PSII and other membrane proteins.

Under PAG conditions the PSII complex in WT thylakoid samples predominantly occurred in the form of the dimeric core complex (RCC(2), Fig. 2.2 A arrows 1) closely followed by the PSII core monomer (RCC(1) while the amount of RC47 (PSII monomeric core complex lacking CP43) was negligible (Fig. 2.2 A arrows 2). PSI predominantly existed as trimer (Fig. 2.2 A arrows 3 and 4) while the level of PSI monomer was much lower (Fig. 2.2 A arrow 7 and 8) and the amount of PSI dimers (PSI(2)) was negligible (Fig. 2.2 A arrow 5 and 6). Interestingly, the PSI trimer (PSI(3)) complex (unlike the monomer and dimer) showed a strong resistance to SDS-induced decomposition and only small subunits PsaF and PsaE were significantly released from the complex during SDS-PAGE while both large PsaA and PsaB subunits remained bound together with majority of PsaD and PsaL.

The absence of CrtR and CrtO proteins in *crtR/O* double mutant cells resulted just in a slightly lower level of PSII dimer (Fig. 2.2 B arrow 1) as compared to the WT and the amount of PSI monomer relative to the PSI trimer increased (Fig. 2.2 B arrow 2 and 3), which suggests some destabilization of the structure of both photosystems in the absence of xanthophylls. In contrast, the *crtH* strain grown under PAG conditions contained much lower amount of PSII dimer in comparison to monomer and also the level of RC47 was higher than in the WT (Fig. 2.2 B). In these cells the ratio of PSI(3) to PSI(2) was much lower than in the WT and the complexes including PSI(3) were more efficiently decomposed by SDS indicating that the stabilization effect of Cars is decreased in the absence of CrtH. In both mutants we also observed a significantly increased level of phosphate transporter PstS1 (sll0608) (Fig. 2.2 B and 2.2 C, arrows 10) and partly also ChlP, geranyl-geranyl reductase involved in the reduction of geranyl-geranyl to phytol (Fig. 2.2 B and 2.2 C, arrows 10).

We assessed the membrane complexes and their protein composition also in the control WT LAHG strain (Fig. 2.2 D) and mutant  $\Delta$ *crtB* and *crtH* strains (Figs. 2.2 E and 2.2 F). Unlike PAG cells, in the cells of WT grown in the presence of glucose in the dark the dimeric PSII core complex was almost completely absent while a higher amount of RC47 was detected in the gel (Fig. 2.2 D). The levels and stability of PSI complexes remained similar to those of PAG cells. In both  $\Delta$ *crtB* and *crtH* LAHG mutants the amount of PSII complexes was drastically reduced in comparison to WT with RC47 as the only detectable complex by protein staining in both mutants (Figs. 2.2 D-F).

# Role of carotenoids in thylakoid organisation

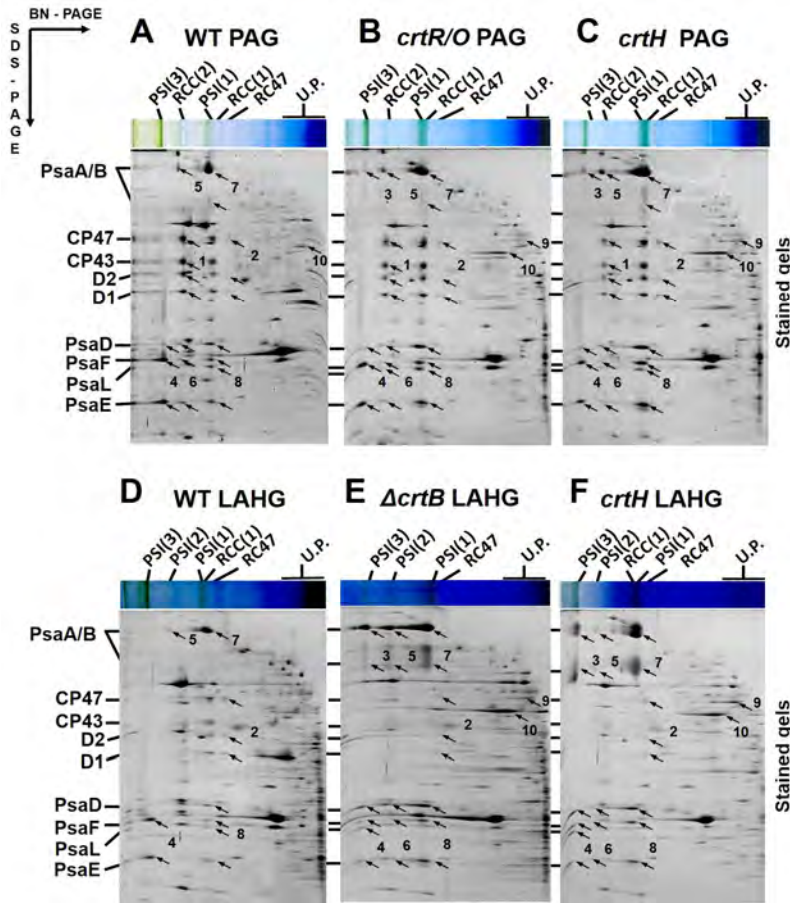


**Figure 2.2.** Two dimensional BN/SDS-PAGE analysis of membranes isolated from WT, *crtR/O* and *crtH* cells grown under PAG conditions (A-C) and WT,  $\Delta$ *crtB* and *crtH* cells grown under LAHG conditions (D-F). The 2D gels were stained with Coomassie Blue. Designation of complexes: PSI(3), PSI(2) and PSI(1), trimeric, dimeric and monomeric PSI complexes, respectively; RCC(2) and RCC(1), dimeric and monomeric PSII core complexes, respectively; RC47, PSII core complex lacking CP43, and U.P. indicates unassembled proteins. Arrows 1 – large subunits of RCC(2) CP47, CP43, D2 and D1 proteins (from top to bottom); arrows 2 - large subunits of RC47 CP47, D2 and D1 proteins (from top to bottom); arrows 3 - large subunits of PSI(3); arrows 4 - small subunits of PSI(3); arrows 5 – large subunits of PSI(2); arrows 6 - small subunits of PSI(2); arrows 7 - large subunits of PSI(1); arrows 8 - small subunits of PSI(1); arrow 9 - ChlP, geranyl-geranyl reductase; arrow 10 - *PstS1* phosphate transporter.

The strong depletion (*crtH* LAHG) or absence ( $\Delta$ *crtB*) of Cars also led to the conversion of most of the PSI trimers to monomers. The stability of PSI complexes was also largely affected as indicated by their decomposition into subunits during 2D SDS-PAGE (Figs 2.2 D-F). Interestingly, the PSI monomer

lacked the PsaL subunit while the trimer contained it. The PsaL subunit was easily released from the mutant trimer unlike the trimer of WT. This result indicates that the insertion of PsaL into trimer-forming domain is destabilized in the absence of Car and PsaL is released from the monomer during BN-PAGE, while it is still retained inside the trimer. Both mutants showed drastic overexpression of the PstS1 phosphate transporter (Sll0680) and ChlP (arrows 9 and 10), which might indicate that in the absence of Cars cells require more phosphate and reduction of geranylgeranyl might be affected.

### *Fluorescence lifetime imaging microscopy measurements*

The efficiency of photosynthetic energy transfer processes can be monitored by various fluorescence methods especially by time-resolved techniques. Photosynthetic systems have relatively short fluorescence decay times at room temperature if both the excitation energy transfer and the charge separation are efficient. In cyanobacteria the light energy is mainly captured by PBSs and excitation energy is transferred towards the RCs, where it is used for charge separation, thereby leading to fast fluorescence lifetime components. When PSII RCs are open no long lifetimes can be expected if only the energy transfer is blocked at some point. Therefore, measurements of (average) fluorescence lifetime of photosynthetic cells, obtained in the presence of predominantly open PSII RCs, can provide information about the functional integrity of the photosynthetic systems within the cells. In addition, the spatial distribution of the average lifetime values detected by fluorescence lifetime imaging microscopy (FLIM) can uncover structural alterations inside the cells. Calculated average lifetimes ( $\tau_{av}$ ) of Car-deficient *Synechocystis* PCC 6803 mutant strains detected through a 700/75 nm BP filter upon 860 nm (two-photon) excitation, are shown in Figure 2.3. 860 nm illumination was proved to preferentially excite PBSs [49]. The WT cells (Fig. 2.3 A) showed a value of  $\sim 200$  ps for  $\tau_{av}$  in all cells. Close to the cell wall higher fluorescence intensity was detected (Fig. Supplementary Information 2.3), but the value of  $\tau_{av}$  did not differ significantly. This is caused by the fact that the thylakoid membranes mainly arrange along the cell wall and thus increase the local pigment concentration but this does not lead to variation in composition and efficiency of the photosynthetic processes.

The xanthophyll-less *crtR/O* mutant showed a significant increase of  $\tau_{av}$  (Fig. 2.3 B); the fluorescence typically decayed with a 275 to 300 ps lifetime (see also Fig. Supplementary Information 2.4) with only limited variation of  $\tau_{av}$  within and between cells. In our experiment *crtH* PAG cells had significantly longer  $\tau_{av}$  values than WT PAG (Fig. 2.3 C). In *crtH* PAG cells significant inhomogeneity

# Role of carotenoids in thylakoid organisation

could be observed with an average lifetime of  $\sim 370$  ps along the cell wall, and  $\sim 500$  ps in the central regions of the cells.

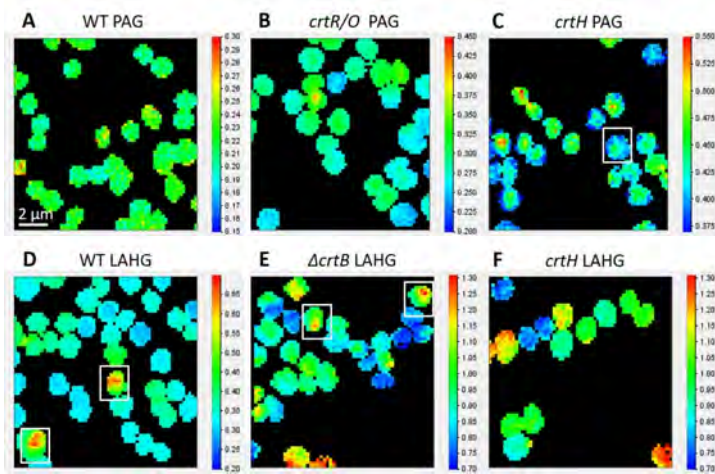


**Figure 2.3.** Fluorescence lifetime images of *Synechocystis* PCC 6803 cells. Color-coded average lifetime images are presented for WT PAG (A), *crtR/O* (B), *crtH* PAG (C), WT LAHG (D),  $\Delta$ *crtB* (E) and *crtH* LAHG (F). The fluorescence was collected through a 700/75 nm bandpass filter. Fluorescence average lifetimes were calculated from a multi-exponential fit of the decay traces for each pixel. Colour codes are different for each strain according to the minimum and the maximum values of the obtained average lifetimes. Lifetimes are given in ns. The white frames of certain cells emphasize a substantial variation of average lifetimes within the cells.

The complete Car deficiency (Fig. 2.3 E) in  $\Delta$ *crtB* cells caused a drastic increase of  $\tau_{av}$  to above 1 ns, which suggests a serious distortion of energy transfer processes. The calculated  $\tau_{av}$  values were much higher than observed for WT cells grown under the same LAHG conditions (Fig. 2.3 D).  $\Delta$ *crtB* cells showed high variation in  $\tau_{av}$  from 700 ps up to 1.2 ns. Furthermore, in the  $\Delta$ *crtB* cells in most cases the presence of high-intensity fluorescence spots was observed (Fig. Supplementary Information 2.3) close to the cell membrane with larger values of  $\tau_{av}$  in most cases (white outlined cells). In WT LAHG there were also a few cells showing long-lived fluorescence ( $\tau_{av} \sim 700$  ps, cells with white frames) but in these cells the area of this fluorescence is more expanded and almost occupies the whole cell. The *crtH* cells cultivated at LAHG conditions (Fig. 2.3 F) give similar results as observed for  $\Delta$ *crtB* cells. The observed long  $\tau_{av}$  in  $\Delta$ *crtB* and *crtH* LAHG probably originates from disconnected PBSs in the absence of active PSII (Fig. 2.2).

### Streak-camera measurements of whole cells

In order to further investigate the origin of the large differences in the values of  $\tau_{av}$  streak-camera measurements were performed (Fig. 2.4) on the same strains for two different excitation wavelengths. The 590 nm excitation light is absorbed mainly by the PBSs (90%) and the 400 nm excites Chl and PBSs as well (see also Fig. Supplementary Information 2.2). The recorded streak images were globally analysed, resulting in decay-associated spectra (DAS) which show the spectral features of individual lifetime components. The spectrum of such a component indicates which pigment-protein complex it might originate from.

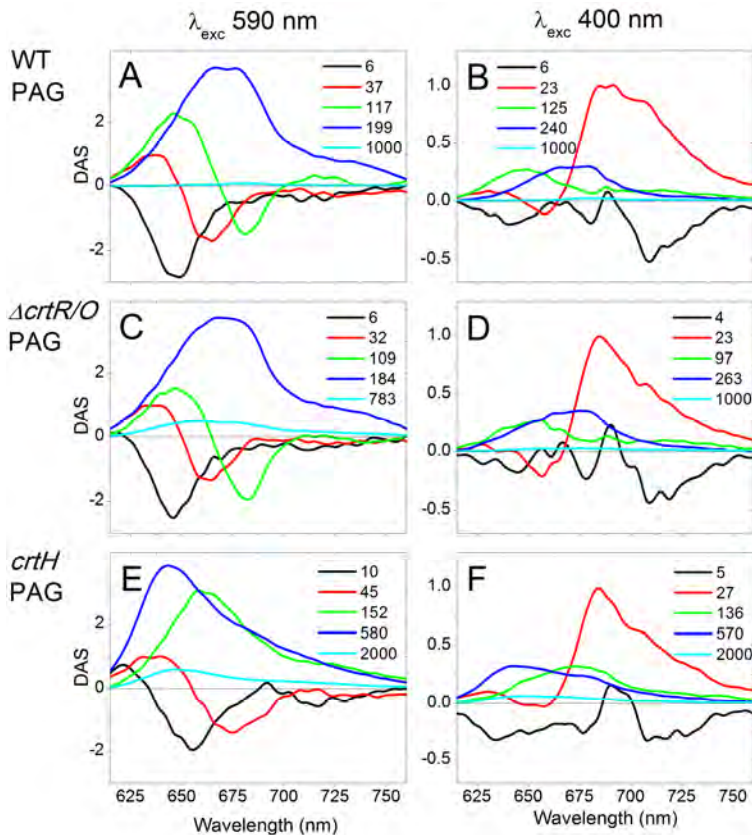


**Figure 2.4.** Decay associated spectra of WT PAG (A, B), *crtR/O* (C, D) and *crtH* PAG (E, F) cells. DAS were estimated from global fitting of the time-resolved fluorescence data obtained with the streak camera. The corresponding lifetimes are given in the figures in ps. The excitation wavelength was 590 nm (left panels) and 400 nm (right panels), respectively. Spectra have been normalized to the second (red) lifetime component.

## Role of carotenoids in thylakoid organisation

Global analysis of streak-camera data obtained for WT PAG cells (Figs. 2.4 A and B) resulted in similar DAS observed and discussed in detail before [15]. Upon 590 nm excitation (Fig. 2.4 A) five components were observed: the 6-8 ps (black DAS) reflects excitation equilibration within the C-PC rods of PBS, the 30 ps (red DAS) shows downhill EET from C-PC to APC<sub>660</sub> with the typical positive sign on the short-wavelength side (corresponding to overall fluorescence decay at those wavelengths) and the negative sign at longer wavelengths (corresponding to a rise of fluorescence due to energy transfer to the corresponding pigments). The 117 ps (green DAS) component reflects down-hill (from high to low energy) EET, in this case from APC<sub>660</sub> to APC<sub>680</sub> + Chls and the 199 ps (blue DAS) component is due to excitation trapping by the RCs (charge separation). Also a long-lived component (~1 ns) can be observed (cyan DAS), which has very low amplitude and probably reflects competition between secondary charge separation and charge recombination [15, 50].

Upon 400 nm excitation (Fig. 2.4 B) the fluorescence components originate from different pigment-protein complexes and they are less clearly separated into various processes: the 6 ps component (black DAS) reflects both equilibration within the C-PC rods (see above) and EET within PSI from bulk to red Chls [49]. The dominating 21 ps (red DAS) component represents mainly charge separation in PSI (leading to decay of Chl fluorescence but it also shows some contribution of the ~30 ps PBSs component which is observed upon 590 nm excitation. The 125 ps component (blue DAS) shows characteristics of the 117 ps (downhill EET) and 199 ps components (charge separation in PSII), which are observed upon 590 nm excitation. The 240 ps component is rather similar to the 199 ps DAS in Figure 2.2 A and is most probably entirely due to charge separation in PSII.

Although the DAS of *crtR/O* cells (Fig. 2.4 C) were similar to those of WT cells grown under the same conditions, a fraction of long-lived (783 ps) fluorescence could be observed (upon 590 nm excitation) with PBS spectral characteristics (max 650 nm), which was not observed for WT cells. This component reflects a small fraction of distorted PBSs or PBSs which are functionally not fully attached to the PSs. The 400 nm excitation of the cells did not show strongly altered components as compared to the results of WT cells since the detached PBSs which were responsible for the main difference upon 590 nm excitation, were hardly excited at 400 nm. Although, a decreased amount of PSII dimers was observed by 2D-PAGE (Fig. 2.2), *in vivo* the fluorescence emitted by PSII was not influenced in the mutant. However, the PSI DAS (~23 ps) shows relatively less contribution on the long-wavelength side (700 nm and above), suggesting a lower level of red pigments in PSI.

In *crtH* PAG cells the obtained DAS and corresponding lifetimes were entirely different from those of WT (Figs. 2.4 E and F), which is consistent with the longer average lifetimes observed by FLIM (Fig. 2.3 C). Upon 590 nm excitation (Fig. 2.4 E) there was no clearly separated component for EET from the PBSs to the pigments fluorescing around 675-680 nm (Chls and some red-shifted bilins in the core of the PBSs) [16]. In these cells a dominant ~600 ps and less pronounced ~2 ns lifetime component were present with fluorescence maximum around 640-650 nm. These components originate from energetically disconnected C-PC units, showing that the PBSs are to a large extent disassembled. In addition, the ~580 ps component also has a shoulder around 680 nm which is more pronounced upon 400 nm excitation (Fig. 2.4 F) demonstrating that it is partly due to Chl *a*. This long living Chl fluorescence might originate from the high level of RC47 observed on 2D-PAGE (Fig. 2.2 C) due to the incomplete assembly of PSII. Furthermore, based on the spectra obtained upon 400 nm excitation, the PSII related component has a shorter, 136 ps lifetime instead of the ~250 ps lifetime, characteristic for WT. This might explain the appearance of the EET component upon 590 nm excitation in spite of the fact that no free PBS related TE fluorescence was observed. The PSI signal is similar to that obtained for *crtR/O* cells (red DAS).

For WT LAHG cells upon 590 nm excitation (Fig. 2.5 A) a lower fraction of functionally coupled PBS-PSII complexes was detected than for cells grown in normal light, which is reflected in the smaller negative amplitude of the green DAS and the smaller amplitude of the blue DAS. In addition a fraction of long-lived ~1.3 ns fluorescence was observed originating from PBSs which do not transfer energy toward the PSs. Upon 400 nm excitation the PSI signal had a similar shape as observed for WT PAG, i.e. with the pronounced shoulder above 700 nm. Similar to the FLIM images, the lack or strong decrease of Cars induced drastic changes in the DAS (Figs. 2.5 C and D) of the *Synechocystis* cells ( $\Delta crtB$  and *crtH* LAHG) when compared to WT LAHG. The obtained DAS were very similar for  $\Delta crtB$  LAHG and *crtH* LAHG cells. Upon 590 nm excitation the dominating blue DAS with ~700 ps lifetime had spectral features that are very similar to those of *crtH* PAG cells and they are characteristic for C-PC rods. The three faster components all showed downhill EET characteristics somewhat similar to those of WT cells, but there was no clear proof of EET to PSII and no ~200 ps PSII decay component was present, which reflects an undetectable level of PSII proteins. The longest lifetime components probably represent the fluorescence emitted predominantly from the terminal emitter of the non-transferring PBSs in the absence of PSII. As it was also observed for the other Car mutants, the red shoulder in the PSI emission decreases significantly upon 400 nm excitation. The fraction of the long-lived (2 ns)

# Role of carotenoids in thylakoid organisation

component was higher upon preferential excitation of Chl molecules at 400 nm (as compared to the 700 ps signal) implying that the emission arises from non-functional parts of PSII and/or from the APC core of PBSs after direct excitation. Since the protein analysis revealed only trace amounts of PSII proteins a PBS-origin of this component is more likely.

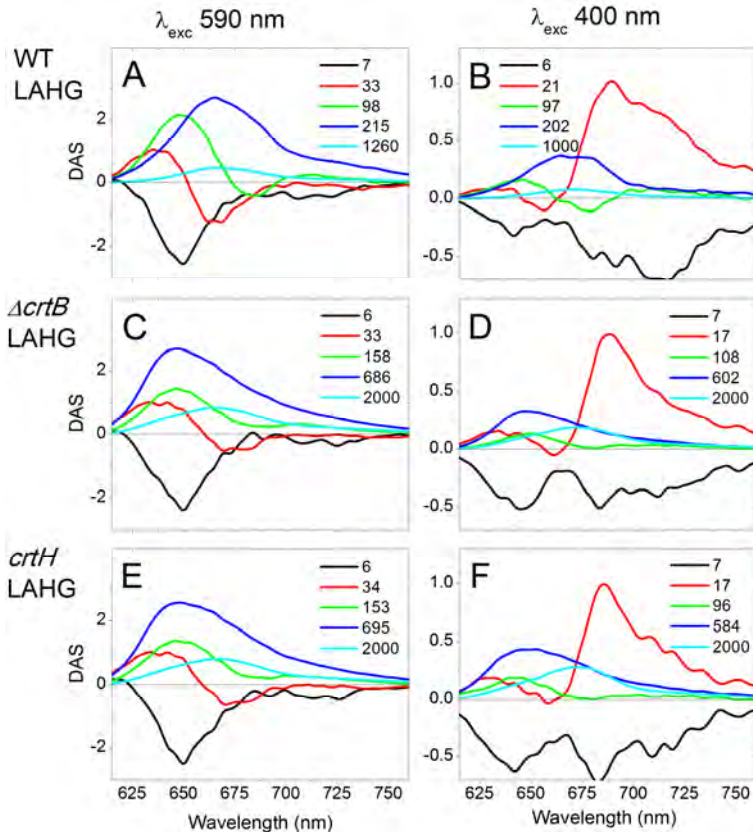


**Figure 2.5.** Decay associated spectra (DAS) of WT LAHG (A, B),  $\Delta crtB$  LAHG (C, D) and  $crtH$  LAHG (E, F) cells. DAS were estimated from global fitting of the time-resolved fluorescence data obtained with the streak-camera setup. The corresponding lifetimes are given in the figures in ps. The excitation wavelength was 590 nm (left panels) and 400 nm (right panels). Spectra have been normalized to the positive peak of the second (red) lifetime component.

## Identification of phycobilinprotein fractions separated by sucrose gradient

In order to determine to which extent PBSs assemble in the absence or limited availability of Cars, PBSs were isolated from the Car mutant strains. Assembled PBSs was possible to be purified from all cells using the sucrose

density gradient centrifugation procedure. However, the PBs band from *crtH* PAG,  $\Delta crtB$  and *crtH* LAHG cells was shifted to lower densities suggesting reduced size and two additional low density subfractions appeared (Fig. 2.8 B inset).

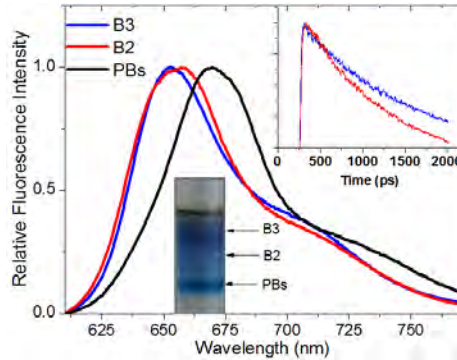


**Figure 2.6.** Steady-state fluorescence spectra of the phycobiliprotein complexes from  $\Delta crtB$  LAHG strains, separated by sucrose gradient. B3 represents the upper band, B2 represents the middle band and the PBs form the lower band on the gradient. Fluorescence decay of B3 and B2 at their fluorescence maxima are represented in the inset.

The two low density subfractions showed very similar PC-like fluorescence spectra with maximum intensities at ~650 nm suggesting that the fluorescence is emitted from the same pigments. However, the fluorescence decay recorded at 650 nm was different for the two fractions. The smallest size (B3) fraction (Fig. 2.6) showed a much longer fluorescence decay time than the bigger size (B2) fraction, which implies different energy transfer processes in the two fractions. These results suggest that detached PC rods in two different aggregation states are responsible for the unconnected PC-originated fluorescence signal in the  $\Delta crtB$  and *crtH* cells *in vivo*.

# Role of carotenoids in thylakoid organisation

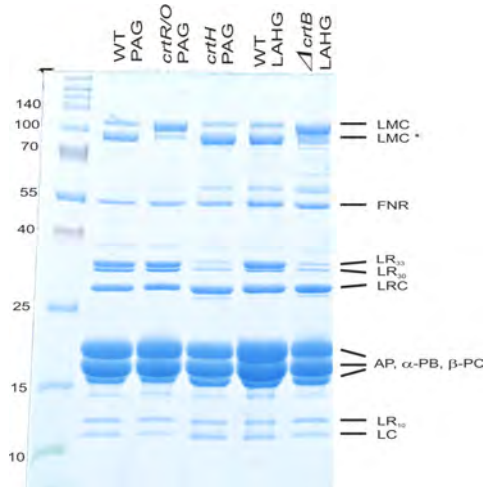


**Figure 2.7.** Tricine SDS-PAGE of the isolated phycobilisomes of WT PAG, *crtR/O* PAG, *crtH* PAG, WT LAHG,  $\Delta$ *crtB* LAHG cells, respectively, as is indicated with the labels. The identities of polypeptides are indicated on the right, masses of the molecular marker are indicated in kDa on the left.

In order to obtain structural information about the assembled PBSs of the  $\Delta$ *crtB* and *crtH* mutants, the protein composition of the isolated PBSs was analysed by denaturing gel electrophoresis (Fig. 2.7). The applied Tricine-SDS gel electrophoresis allows to estimate the amount of PBS linker proteins. Our results show that levels of the rod linkers LR30 and LR33 is drastically reduced in PBSs from  $\Delta$ *crtB* LAHG and *crtH* PAG. This suggests that C-PC rods have predominantly been reduced, containing only one PC hexameric unit instead of three as characteristic to the WT.

## Streak-camera measurements of phycobilisomes

Using the streak camera, EET upon 590 nm excitation (Fig. 2.8) was studied in PBSs isolated from WT and  $\Delta$ *crtB* LAHG cells. The calculated DAS of WT PBSs (Fig. 2.8 A) were similar to those presented by Tian *et al.* [16] with an extra component of ~250-300 ps in our case. A similar extra component (maximum ~660 nm) was observed previously [49] which was considered to originate from some distorted PBSs. The remaining components for WT PBSs were as follows; the 6 ps component reflects energy redistribution within C-PC rods, 20 ps corresponds to EET from C-PC to APC<sub>660</sub> and 80 ps to EET from APC<sub>660</sub> to APC<sub>680</sub>. The ~1.6 ns lifetime corresponds to the excited-state lifetime of equilibrated PBSs.

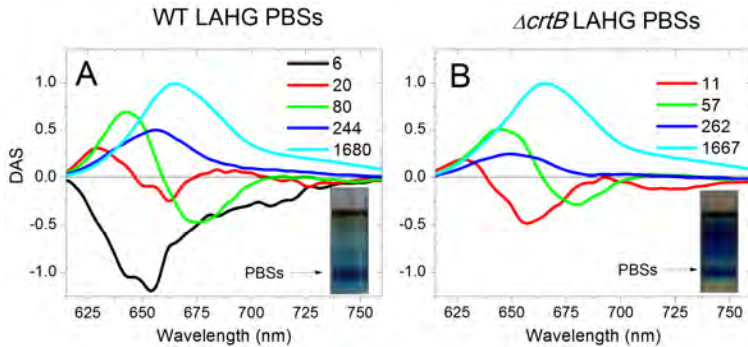


**Figure 2.8.** DAS of isolated phycobilisomes of WT LAHG (A) and  $\Delta crtB$  LAHG (B) strains obtained with the streak-camera setup using 590 nm excitation light. The corresponding lifetimes are given in the figures in ps. The spectra have been normalized to the longest (cyan) lifetime component. The sucrose gradient profiles of the phycobilisomes are presented in the right corner.

However, in  $\Delta crtB$  PBSs (Fig. 2.8 B) we were only able to resolve 4 components with different spectra. The  $\Delta crtB$  PBSs showed reduced fluorescence in the C-PC region as compared to WT PBSs (see also Fig. Supplementary Information 2.6), which can be explained either by the presence of less C-PC rods per PBS or by a shortening of the rods.

### *Fluorescence lifetime imaging microscopy measurements with two detection wavelengths*

To get better insight into the fate of the detached rods, FLIM images of *crtH* PAG cells were collected using a 647/57 nm BP filter (Fig. 2.9). In this strain the fluorescence is mainly emitted by the unconnected PC rods of the PBSs, and therefore using a filter that preferentially detects PBSs can provide more details about the locations of the detached C-PC rods within the cells. The calculated average lifetimes in these FLIM images were significantly longer in the centre of the cells, similar to what was previously observed using the 700/75 nm BP filter (Fig. 2.4). Global analysis of the images allowed separation of three individual lifetime components; 66 ps, 264 ps and 764 ps, respectively (Fig. 2.9). Although the observed FLIM components differed from the streak component obtained upon PBS excitation due to the different time resolution and detection window, some correlation is clearly present.

# *Role of carotenoids in thylakoid organisation*

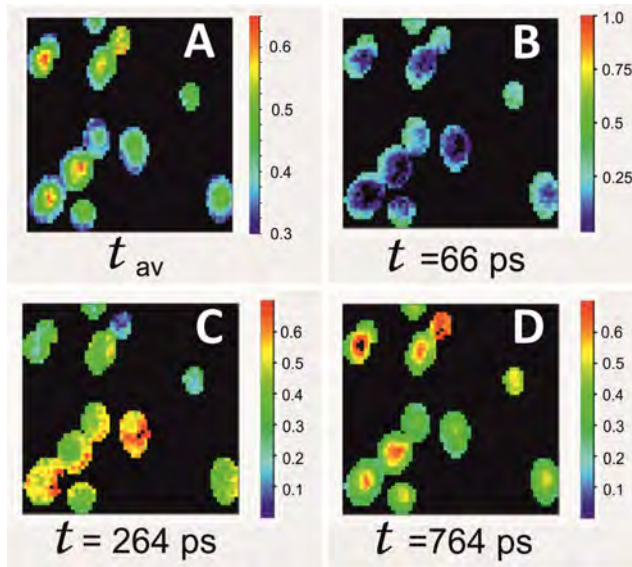


**Figure 2.9.** FLIM images of *crtH* PAG cells detected through a 647/57 nm bandpass filter. Images of calculated average lifetimes are given in ns (A). Distribution of the individual lifetime components as obtained from the global analysis result (B, C and D). Colours represent the relative contribution.

The 66 ps component probably originates from energy transfer in assembled PBSs. The 264 ps is a relatively short lifetime, and therefore it could arise from quenched PBSs or from PSII components. The longer 764 ps component represents the detached rod fractions; its corresponding distribution is represented in Figure 2.9 D. This component had a relatively high (up to 0.7) contribution in the central region of the cells while it is clearly lower (0.3-0.4) along the cell wall. In contrast, the two short components show opposite behaviour, they have the highest contribution along the cell wall. This indicates that the detached C-PC rod fractions (with 764 ps lifetime) are not co-localised with the thylakoid membranes, but are present in the centre of the cells.

## **2.5 Discussion**

### *Thylakoid membrane integrity*

The importance of Cars for thylakoid integrity was previously demonstrated using mutants, in which Car biosynthesis is interrupted at the early steps. [2, 8]. The Car-deficient  $\Delta crtH/B$  [8] and  $\zeta$ -carotene desaturase (CrtQ) enzyme-deficient mutants [2] contain reduced amounts of (only fragmented) thylakoid membrane sheets as compared to WT, cultivated under the same LAHG conditions. We could observe similar changes for the Car-deficient  $\Delta crtB$  and *crtH* LAHG strains (Fig

2.1), where a higher amount of thylakoid sections penetrates into the central part of the cells and the thylakoid membrane sheets are 60-140 nm apart instead of the ~50 nm as observed in WT cells. We have to note that the heterotrophic growth itself introduces some alterations in the morphology of the thylakoid membranes [8, 27, 51]. Recently it was observed that also the lack of both PSs results in reduced amounts and more fragmented thylakoid membranes [52], but a mutant that is only deficient in PSII has normal thylakoid sheets [53]. Therefore, it is unlikely that the effect on the thylakoid organisation is only due to the observed decrease in PSII protein content (Fig 2.2).

Moreover, Cars are known to modulate the physical properties of the membranes, e.g. the membrane fluidity [3]. Mohamed and co-workers [2] observed that the lack of the fucosylated form of myxoxanthophyll results in more fragmented thylakoid membranes, which suggests a membrane-stabilising function of myxoxanthophyll when it contains the fucose functional group. In our experiments, the xanthophyll-deficient *crtR/O* mutant possesses properly organised thylakoid membranes (Fig 2.1), [8] consistent with the fact that these cells in addition to  $\beta$ -carotene also contain the deoxymyxol-2'-dimethyl-fucoside intermediate product of myxoxanthophyll biosynthesis [22, 26]. The *crtH* PAG cells, which contain all Car species even though in an altered ratio [23] also have a similar thylakoid structure as wild-type cells (Fig 2.1). It is interesting to note that in cyanobacterial thylakoids most of the  $\beta$ -carotenes are in the PSs [54].

These findings suggest a basic role of fucosylated myxoxanthophyll to maintain the thylakoid organisation intact but a contribution of  $\beta$ -carotene cannot be excluded.

One might argue for the presence of normal respiratory function in lack of the normal WT-like thylakoid membranes in the Car-deficient mutant. Seriously impaired respiratory functions would lead to slower growing rate in carotenoid deficient mutant compare to the WT cells grown also under LAHG conditions. However, previous experiments demonstrated that the carotenoid deficient cells possess identical growth rate as observed in WT cells [28].

Interestingly in Car-deficient cells the geranylgeranyl reductase (ChlP) protein is overexpressed. This enzyme catalyses the reduction of geranylgeranyl pyrophosphate to phytyl pyrophosphate, which is required for synthesis of chlorophylls, phylloquinone and tocopherols [55]. Although our measurements are not providing any direct explanation for the overexpression of ChlP, but it might be caused by the accumulation of geranylgeranyl pyrophosphate in Car-deficient cells which is a common target molecule of CrtB and ChlP enzymes. Moreover, due to the overlapping function of tocopherol with Car synthesis [56], the lack of Cars can

# Role of carotenoids in thylakoid organisation

indirectly enhance the synthesis of tocopherol to protect the cells. Although even the complete lack of tocopherol has only slight influences on the photoautotrophically grown cells [56, 57], tocopherol seems to be important at photomyxotrophic conditions for proper macronutrient homeostasis [57].

## *Photosystem I*

In WT cyanobacteria PSI is mainly present in trimeric form (~90%) under normal growth conditions [58]. The high-resolution (2.5 Å) crystal structure of PSI trimer (*Thermosynechococcus elongatus*) has been obtained and modelled including 22  $\beta$ -carotene molecules/PSI monomer [10, 11] although one of the peripheral Car molecules is not completely resolved and might not be a  $\beta$ -carotene. Despite the relative abundance of Cars in cyanobacterial PSI the basic PSI functions are retained in a Car-deficient mutant and only slight changes in reoxidation of the primary electron acceptor ( $A_1$ ) and in the rate of charge recombination were observed [59]. In Car-deficient ( $\Delta crtH/B$ ) cells the PSI complexes were mostly observed as monomers instead of trimers, which are characteristic for WT cells [28]. In the present study we confirm by two-dimensional gel electrophoresis that the Car-deficient mutant ( $\Delta crtB$ ) contains predominantly PSI monomers (Fig. 2.2). Our results also show that in the absence of Cars in the  $\Delta crtB$  mutant the remaining PSI trimers are less stable and the interaction of the PsaL subunit with the PSI complex seems to be weaker than in WT cells and the PsaL protein is missing in mutant PSI monomers (Fig. 2.2). PsaL is necessary for PSI trimer formation [11, 60] and according to the trimeric PSI crystal structure the PsaL protein is in close contact with three  $\beta$ -carotenes, which are believed to be involved in trimer stabilisation [10, 61]. Probably the lack of those structurally important “linker” Cars leads to the destabilisation of PsaL binding and thus to destabilisation of the PSI trimer. Furthermore, the *in vivo* detected picosecond PSI fluorescence results (Fig. 2.5 C red DAS upon 400 nm excitation) indicate significantly less long-wavelength Chls (LWCs) in Car-deficient cells than in WT cells. This is in line with the decrease of PSI trimers since the amount of LWCs is higher in cyanobacterial PSI trimers than in monomers [58, 62]. In our experiments the *crtH* LAHG cells behave similarly to Car-deficient  $\Delta crtB$  cells, and only contain a slightly higher amount of PSI trimers, probably due to the presence of intermediate products of Car biosynthesis [23].

Previously xanthophyll molecules have also been observed in PSI preparations [59, 63]. This might be explained by co-purification of xanthophyll molecules localised in the close vicinity of PSI trimers in the membrane or the presence of xanthophyll molecules in the PSI trimers which were lost upon crystallization. Interestingly, in the xanthophyll-deficient *crtR/O* cells, protein

analysis also showed less stable PSI trimers and relatively more PSI monomers than in WT cells (Fig. 2.2) together with a decrease in the PSI LWC signal (Fig. 2.3 B red DAS upon 400 nm excitation). Unlike in  $\Delta crtB$  cells, in  $crtR/O$  cells the PsaL protein binds with similar stability as in WT cells, and thus it is also present in the monomeric PSI complex (Fig. 2.2). In our experiments the light-grown  $crtH$  (PAG) cells (Fig. 2.2) also show increased amount of monomeric PSI and the binding of PsaL to monomeric PSI is slightly weaker. This is consistent with the limited availability of Cars including  $\beta$ -carotene in light grown  $crtH$ .

The different behaviour of the PsaL protein in the Car-deficient ( $\Delta crtB$ ) and xanthophyll-depleted ( $crtR/O$ ) cells might suggest that the increase of PSI monomers can occur due to different reasons. Our results confirm the prediction [61] that, in addition to the PsaL [11, 60] and a phosphatidylglycerol molecule [64], the  $\beta$ -carotenes are also necessary for stabilisation of the trimerisation domain, most probably via stabilizing the binding of the PsaL protein to PSI. The xanthophyll deficiency also influences the PSI complex: it might indirectly cause the increase in the fraction of the naturally occurring PSI monomers, or directly by influencing protein-protein interaction.

### *Photosystem II*

Although the PSII complex contains less Cars than PSI (12  $\beta$ -carotenes/PSII monomer, in *Thermosynechococcus elongatus*) [12, 65], Cars are essential for the assembly of the PSII dimeric complex [28, 66]. Accordingly, in the Car-less  $\Delta crtB$  cells and  $crtH$  LAHG cells only trace amounts of partially assembled (CP43 depleted) RC47 PSII subcomplex can be detected (Fig. 2.2), similarly as previously demonstrated in the  $\Delta crtH/B$  strain [8, 28]. In line with the protein analysis, we could not obtain a clear PSII fluorescence signal from the Car-deficient  $\Delta crtB$  and  $crtH$  LAHG cells (Fig. 2.5).

By the use of xanthophyll-deficient mutants Schafer and co-workers [21] previously showed that even upon complete elimination of xanthophylls ( $crtR/O$ ) the PSII functions seems to be unaffected under normal light conditions. However, xanthophyll depletion might lead to PSII damage upon high light intensities in an indirect way due to the substantial sensitivity of the cells to light stress [14, 21]. In our experiments the protein analysis showed a significant decrease in stability of the PSII dimers (Fig. 2.2), but no corresponding alteration in PSII related fluorescence (Fig. 2.4 blue DAS upon 400 nm excitation) was observed by streak-camera measurements. However, a small fraction of energetically disconnected PBSs was observed in  $crtR/O$  cells with the streak camera but with a shorter lifetime (Fig. 2.4) than characteristic for the unconnected whole PBSs in WT LAHG cells (Fig. 2.5).

## Role of carotenoids in thylakoid organisation

This kind of fluorescence emission might originate from the improper docking of PBSs to PSII when the PSII dimers, which are prerequisite of attaching PBSs, are not stable.

In contrast to an earlier prediction [25] the *crtH* cells cultivated in the presence of light have severely impaired PSII functions (Fig. 2.4). However, the average fluorescence lifetime obtained for *crtH* cells (Fig. 2.3) is not as long as for *ΔcrtB* cells, indicating photochemical and/or non-photochemical quenching of the excitation energy. Accordingly, in addition to the increased level of monomeric PSII and RC47 a clear fraction of PSII dimers was also detected by two-dimensional gelelectrophoresis (Fig. 2.2), supporting a significant fraction of functioning PSII which is capable for photochemical quenching. The *crtH* PAG related PSII changes suggest a somewhat decreased β-carotene level relative to the Chl.

The above-mentioned observations support the fact that fully assembled functional PSII requires the presence of β-carotene while xanthophylls seem to have some minor stabilising function in low-light conditions.

### *Phycobilisomes*

Although there is no sign of the presence of Car molecules in PBSs we found a strong influence of the presence of Cars on PBS integrity. In WT cells PBSs are well assembled even under LAHG condition, where a significant fraction of unattached, photochemically unquenched PBSs is observed (Figs. 2.5 and 2.8) in agreement with [27]. In Car-deficient (*ΔcrtB*) (Fig. 2.5) cells a high level of energetically disconnected, non-transferring C-PC units was observed at room temperature by time-resolved fluorescence.

Recently the existence of a special rod-like PBS was proposed in *Synechocystis* PCC 6803, which contains only phycocyanin and believed to transfer energy towards the PSI [67, 68]. However, this PBS is hardly expressed in the dark [67], therefore it is quite unlikely that the observed unattached rods would originate from released rod-like PBSs.

Disassembled PBS were also observed *in vivo* upon high light or temperature treatment [69, 70] or upon nutrient limiting conditions [71, 72]. Further measurements pointed out that a fraction of the assembled PBSs is also present in these mutants, but they are reduced in size as reflected also by the change in their location in the sucrose density gradient. Based on the time-resolved fluorescence measurements (Fig. 2.8) it is tempting to conclude that the C-PC rods become shorter leading to faster equilibration between rods and core. These observations are in line with those on intact cells although in that case differences in lifetimes might also have been influenced by a change in docking of the PBSs onto the

photosystems. Also protein analyses (Fig. 2.7) confirm that the PBSs isolated from *ΔcrtB* strain possess predominantly shorter rods as apparent from the reduced level of the rod linker LR<sub>30</sub> and LR<sub>33</sub> proteins in the protein gels of the isolated PBSs (Fig. 2.7). The LR<sub>30</sub> and LR<sub>33</sub> proteins are necessary for the binding of the C-PC units to each other. The parallel decrease of these two linker proteins indicate that the PBSs contain predominantly rods with only one hexameric unit but full length rods with three hexameric units is also present at low frequency.

The step-wise sucrose density gradient centrifugation has separated two further fractions of phycobiliprotein complexes localised at the upper region of the gradient (Fig. 2.6). The steady-state fluorescence of these fractions shows their C-PC origin (Fig. 2.6) but their size dependent separation implies a difference in aggregation level. The different aggregation states of the unconnected C-PC units also influence the fluorescence properties as reflected by the faster fluorescence decay of the C-PC units in higher aggregation state (Fig. 2.6). Protein analysis of the C-PC fraction with bigger size also demonstrates the presence of the LR<sub>30</sub> protein which connects the two peripheral C-PC units (data not shown). These results suggest that in *ΔcrtB* cells two hexameric units stay connected in a certain fraction of the detached C-PC units. We conclude that in Car-deficient cells most of the PBSs possess reduced rods and the missing two C-PC units are present as unconnected C-PC units in two aggregation forms in the cells. It should be noted that the xanthophyll-less *crtR/O* mutant contains properly assembled PBSs. In the sucrose density gradient pattern no significant difference with WT is observed and the protein analysis also does not imply any structural differences of the *crtR/O* PBSs (Fig. 2.7). However, in the *crtR/O* strain the presence of WT-like PBS assembly due to the intermediate products e.g. myxoxanthophyll biosynthesis intermediate deoxymyxol-2'-dimethyl-fucoside cannot be excluded. Therefore we conclude that the lack of β-carotene or the fucosylated myxoxanthophyll is responsible for PBS distortion in the Car-deficient cells.

The lack of the last two peripheral rod units observed in Car-deficient cells also occurs in the mutant deficient in the 33 kDa rod linker, the LR<sub>33</sub>, which is responsible for binding the last two hexamers to the basal C-PC rod unit [31]. Surprisingly, the LR<sub>33</sub> deficient mutant exhibits only one fraction of the detached rods [31, 73]. However, in the Car-deficient mutant the last two peripheral C-PC units are attached together in high amounts and appeared in two aggregation forms represented by two distinct sucrose density gradient fractions. The different behaviour of the C-PC units might be explained by distortion of the PBSs after the assembly is completed in lack of Cars.

## Role of carotenoids in thylakoid organisation

Cars should either have a direct or indirect effect on the PBS structure. The direct PBS-stabilising role of Cars would predict a Car molecule inside the PBS rods or in the vicinity of the PBS rods, but up to now there is no evidence for their presence in the PBS structure. Therefore an indirect effect of Cars on PBSs via some mediator proteins or processes is most likely.

Disassembly of PBSs has often been observed under limited nutrient supply [71, 72, 74, 75]. In our experiments the lack or limited availability of Cars enhanced the level of the PstS1 phosphate transporter in all studied Car mutants (Fig. 2.2), especially in  $\Delta crtB$  and  $crtH$  cells. It was demonstrated that the long-term adaptation to low inorganic phosphate availability provokes an increase in the level of PstS1 in *Synechocystis* and a decrease of the level of all PBSs constituents [76]. However, in spite of the apparent change in the level of the PstS1 transporter, it is difficult to justify that a disturbed phosphate metabolism would eventually lead to the detachment of the PC units, but it is one plausible explanation.

In  $crtH$  PAG and in  $crtH$  LAHG cells the phycobilisomes are distorted to a similar extent as in  $\Delta crtB$  cells as demonstrated by the various measurements (Fig. 2.4, 2.5 and 2.7). It is rather surprising since in light-grown  $crtH$  (PAG) cells the Car content is restored to a large extent [23]. However, the synthesis might be insufficient, because the necessary *cis* to *trans* isomerisation step can occur only through photo-isomerisation when the parallel enzymatic pathway is absent [23, 25]. The sucrose density gradient centrifugation of  $crtH$  cells shows a similar ratio of the distorted PC fractions to the intact PBSs, and in the isolated PBSs the amount of  $L_R^{30}$  and  $L_R^{33}$  proteins is decreased to similar extent (Fig. 2.7) as in  $\Delta crtB$ . In the  $crtH$  PAG cells a normal WT-like thylakoid organisation is present (Fig. 2.1) and no clear signal from disconnected PBSs (TE) is detected (Fig. 2.4); therefore, these cells provide an excellent tool to study the location of the detached rod units. FLIM experiments demonstrated that the lifetime component originating from PC (Fig. 2.4) has higher relative contribution in the middle of the cells (Fig. 2.3 and Fig. 2.9). Therefore, we can conclude that the detached rod units do not stay in close vicinity of the thylakoid membranes but they are accumulated separately from the thylakoid membranes in the centre of the cells. Similar dislocation of disconnected rod units was observed by Tamary *et al.* [70] upon extreme-high light intensity treatment.

PBS disassembly occurs in  $crtH$  PAG and LAHG cells to a similar extent (Fig. 2.4, 2.5 and 2.7), and therefore the assembly/disassembly is not directly related to presence/absence of light. The reactive oxygen species (ROS) production is usually enhanced upon light illumination. Therefore, in case of ROS-induced PBS distortion, the presence of detached rod units should be light dependent. In addition, although it is known that ROS might cause PBS disassembly [77], the PSs are more

sensitive to it than the PBSs. Accordingly, we can exclude that light-induced ROS formation leads to the detachment of certain rod fragments in our case.

The lack of PSII itself cannot be the reason for the disassembly, since PBSs are assembled in a PSII deficient mutant [78] and even in a mutant, which contains only a trace amount of Chl [77]. However, in the total absence of Chl *a* a slight decrease in PBS stability was observed [79]. Moreover, the lack of PSII cannot explain such a high amount of unconnected PC units in *crtH* PAG, where a significant amount of PSII is still around (Fig. 2.2). Therefore we conclude that the structure of the PBS depends on the Car content of the cells, but the exact reason for the presence of unconnected C-PC rod units of PBSs in the lack of Cars need to be further elucidated.

## 2.6 Conclusions

Although the xanthophylls do not appear to have a vital physiological role in cyanobacteria under normal light conditions, their absence lowers both PSII dimer and PSI trimer stability. The fucosylated myxoxanthophyll has general importance in thylakoid membrane stabilisation but its effect on photosynthetic complexes is not clarified yet. However, the  $\beta$ -carotene seems to be essential for the assembly of PSII and for stabilisation of the PSI trimer and also crucial for the proper assembly of PBSs. In the absence or limited availability of Cars the two peripheral units of most PBSs rods are not attached. The detached rods can be found in the thylakoid-free parts of the cells and they are present in two aggregation forms, i.e. in a single hexameric unit and in two hexameric units associated together. It seems that PBS PC units most probably detach after the PBS assembly is completed, rather than appear as a result of improper assembly of the PBS.

## 2.7 Acknowledgements

This work was supported by the Sandwich PhD program of Wageningen University and (to T.T.), by HARVEST Marie Curie Research Training Network (PITN-GA-2009-238017) (to V.C.) and by a grant from the Hungarian Science Foundation (OTKA K82052 to I.D.) and Social Renewal Operational Programmes (TAMOP-4.2.2/B-10/1-2010-0012 to T.T., TAMOP-4.2.2.A-11/1/KONV-2012-0047 to K.L) and A\*STAR Singapore (NIH-A\*STAR TET\_10-1-2011-0279 to G.G.). The authors thank Arie van Hoek for technical help with the time-resolved measurements, and Prof. Arpad Parducz for preparing electron micrographs. Special thanks go to Anna Sallai Kunne for the phycobilisome preparation.

# *Role of carotenoids in thylakoid organisation*

## 2.8 Reference list

- [1] **Sozer, O., Kis, M., Gombos, Z., Ughy, B.**, Proteins, glycerolipids and carotenoids in the functional Photosystem II architecture, *Frontiers in Bioscience-Landmark*, 16 (2011) 619-643.
- [2] **Mohamed, H.E., van de Meene, A.M.L., Roberson, R.W., Vermaas, W.F.J.**, Myxoxanthophyll is required for normal cell wall structure and thylakoid organization in the cyanobacterium, *Synechocystis sp* strain PCC 6803, *J. Bacteriol.*, 187 (2005) 6883-6892.
- [3] **Gruszecki, W.I., Strzalka, K.**, Carotenoids as modulators of lipid membrane physical properties, *Biochim. Biophys. Acta*, 1740 (2005) 108-115.
- [4] **van Amerongen, H., van Grondelle, R.**, Understanding the energy transfer function of LHCII, the major light-harvesting complex of green plants, *J. Phys. Chem. B*, 105 (2001) 604-617.
- [5] **Stamatakis, K., Tsimilli-Michael, M., Papageorgiou, G.C.**, On the question of the light-harvesting role of beta-carotene in photosystem II and photosystem I core complexes, *Plant Physiol. Biochem.*, (2014).
- [6] **Polivka, T., Frank, H.A.**, Molecular factors controlling photosynthetic light harvesting by carotenoids, *Accounts of chemical research*, 43 (2010) 1125-1134.
- [7] **Schafer, L., Sandmann, M., Woitsch, S., Sandmann, G.**, Coordinate up-regulation of carotenoid biosynthesis as a response to light stress in *Synechococcus* PCC 7942, *Plant Cell and Environment*, 29 (2006) 1349-1356.
- [8] **Domonkos, I., Kis, M., Gombos, Z., Ughy, B.**, Carotenoids, versatile components of oxygenic photosynthesis, *Prog. Lipid Res.*, 52 (2013) 539-561.
- [9] **Takaichi, S., Mochimaru, M.**, Carotenoids and carotenogenesis in cyanobacteria: unique ketocarotenoids and carotenoid glycosides, *Cell. Mol. Life Sci.*, 64 (2007) 2607-2619.
- [10] **Jordan, P., Fromme, P., Witt, H.T., Klukas, O., Saenger, W., Krauss, N.**, Three-dimensional structure of cyanobacterial photosystem I at 2.5 angstrom resolution, *Nature*, 411 (2001) 909-917.
- [11] **Fromme, P., Jordan, P., Krauss, N.**, Structure of photosystem I, *Biochim. Biophys. Acta*, 1507 (2001) 5-31.
- [12] **Guskov, A., Kern, J., Gabdulkhakov, A., Broser, M., Zouni, A., Saenger, W.**, Cyanobacterial photosystem II at 2.9-angstrom resolution and the role of quinones, lipids, channels and chloride, *Nat. Struct. Mol. Biol.*, 16 (2009) 334-342.
- [13] **Kurisu, G., Zhang, H.M., Smith, J.L., Cramer, W.A.**, Structure of the cytochrome b(6)f complex of oxygenic photosynthesis: Tuning the cavity, *Science*, 302 (2003) 1009-1014.
- [14] **Kirilovsky, D., Kerfeld, C.A.**, The Orange Carotenoid Protein: a blue-green light photoactive protein, *Photochem. Photobiol. Sci.*, 12 (2013) 1135-1143.
- [15] **Tian, L., van Stokkum, I.H., Koehorst, R.B., Jongerius, A., Kirilovsky, D., van Amerongen, H.**, Site, rate, and mechanism of photoprotective quenching in cyanobacteria, *J. Am. Chem. Soc.*, 133 (2011) 18304-18311.
- [16] **Tian, L., Gwizdala, M., van Stokkum, I.H., Koehorst, R.B., Kirilovsky, D., van Amerongen, H.**, Picosecond kinetics of light harvesting and photoprotective quenching in wild-type and mutant phycobilisomes isolated from the cyanobacterium *Synechocystis* PCC 6803, *Biophys. J.*, 102 (2012) 1692-1700.
- [17] **Punginelli, C., Wilson, A., Routaboul, J.M., Kirilovsky, D.**, Influence of zeaxanthin and echinenone binding on the activity of the Orange Carotenoid Protein, *Biochim. Biophys. Acta*, 1787 (2009) 280-288.
- [18] **Kilian, O., Steunou, A.-S., Fazeli, F., Bailey, S., Bhaya, D., Grossman, A.R.**, Responses of a thermophilic *Synechococcus* isolate from the microbial mat of octopus spring to light, *Appl. Environ. Microbiol.*, 73 (2007) 4268-4278.
- [19] **Masamoto, K., Zsiros, O., Gombos, Z.**, Accumulation of zeaxanthin in cytoplasmic membranes of the cyanobacterium *Synechococcus sp.* strain PCC 7942 grown under high light condition, *J. Plant Physiol.*, 155 (1999) 136-138.
- [20] **Subczynski, W.K., Markowska, E., Gruszecki, W.I., Siewiesiuk, J.**, Effects of polar carotenoids on dimyristoyl-phosphatidylcholine membranes - a spin label study *Biochim. Biophys. Acta*, 1105 (1992) 97-108.

- [21] **Schafer, L., Vioque, A., Sandmann, G.**, Functional in situ evaluation of photo synthesis-protecting carotenoids in mutants of the cyanobacterium *Synechocystis* PCC 6803, *J. Photochem. Photobiol. B: Biol.*, 78 (2005) 195-201.
- [22] **Lagarde, D., Vermaas, W.**, The zeaxanthin biosynthesis enzyme beta-carotene hydroxylase is involved in myxoxanthophyll synthesis in *Synechocystis* sp. PCC 6803, *FEBS Lett.*, 454 (1999) 247-251.
- [23] **Masamoto, K., Wada, H., Kaneko, T., Takaichi, S.**, Identification of a gene required for cis-to-trans carotene isomerization in carotenogenesis of the cyanobacterium *Synechocystis* sp PCC 6803, *PCP*, 42 (2001) 1398-1402.
- [24] **Anderson, S.L., McIntosh, L.**, Light-activated heterotrophic growth of the cyanobacterium *Synechocystis* sp strain PCC 6803 - A blue-light-requiring process, *J. Bacteriol.*, 173 (1991) 2761-2767.
- [25] **Masamoto, K., Hisatomi, S., Sakurai, I., Gombos, Z., Wada, H.**, Requirement of carotene isomerization for the assembly of Photosystem II in *Synechocystis* sp PCC 6803, *PCP*, 45 (2004) 1325-1329.
- [26] **Takaichi, S., Maoka, T., Masamoto, K.**, Myxoxanthophyll in *Synechocystis* sp. PCC 6803 is myxol 2'-dimethyl-fucoside, (3R,2S)-myxol 2'-(2,4-di-O-methyl-alpha-L-fucoside), not rhamnoside, *PCP*, 42 (2001) 756-762.
- [27] **Barthel, S., Bernat, G., Seidel, T., Rupprecht, E., Kahmann, U., Schneider, D.**, Thylakoid membrane maturation and PSII activation are linked in greening *Synechocystis* sp PCC 6803 cells, *Plant Physiol.*, 163 (2013) 1037-1046.
- [28] **Sozer, O., Komenda, J., Ughy, B., Domonkos, I., Laczko-Dobos, H., Malec, P., Gombos, Z., Kis, M.**, Involvement of carotenoids in the synthesis and assembly of protein subunits of photosynthetic reaction centers of *Synechocystis* sp PCC 6803, *PCP*, 51 (2010) 823-835.
- [29] **Mullineaux, C.W.**, Excitation-energy transfer from phycobilisomes to photosystem I in a cyanobacterial mutant lacking photosystem II, *Biochim. Biophys. Acta*, 1184 (1994) 71-77.
- [30] **Arteni, A.A., Ajlani, G., Boekema, E.J.**, Structural organisation of phycobilisomes from *Synechocystis* sp strain PCC6803 and their interaction with the membrane, *Biochim. Biophys. Acta*, 1787 (2009) 272-279.
- [31] **Ughy, B., Ajlani, G.**, Phycobilisome rod mutants in *Synechocystis* sp strain PCC6803, *Microbiology*, 150 (2004) 4147-4156.
- [32] **Jallet, D., Gwizdala, M., Kirilovsky, D.**, ApcD, ApcF and ApcE are not required for the Orange Carotenoid Protein related phycobilisome fluorescence quenching in the cyanobacterium *Synechocystis* PCC 6803, *Biochim. Biophys. Acta*, 1817 (2012) 1418-1427.
- [33] **Ashby, M.K., Mullineaux, C.W.**, The role of ApcD and ApcF in energy transfer from phycobilisomes to PSI and PSII in a cyanobacterium, *Photosynth Res.*, 61 (1999) 169-179.
- [34] **Allen, M.M.**, Simple conditions for growth of unicellular blue-green algae on plates, *J. Phycol.*, 4 (1968) 1-&.
- [35] **Laczko-Dobos, H., Ughy, B., Toth, S.Z., Komenda, J., Zsiros, O., Domonkos, I., Parducz, A., Bogos, B., Komura, M., Itoh, S., Gombos, Z.**, Role of phosphatidylglycerol in the function and assembly of photosystem II reaction center, studied in a *cdsA*-inactivated PAL mutant strain of *Synechocystis* sp. PCC6803 that lacks phycobilisomes, *Biochim. Biophys. Acta*, 1777 (2008) 1184-1194.
- [36] **Ajlani, G., Vernotte, C., Dimagno, L., Haselkorn, R.**, Phycobilisome core mutants of *Synechocystis* PCC 6803, *Biochim. Biophys. Acta*, 1231 (1995) 189-196.
- [37] **Komenda, J., Reisinger, V., Muller, B.C., Dobakova, M., Granvogl, B., Eichacker, L.A.**, Accumulation of the D2 protein is a key regulatory step for assembly of the photosystem II reaction center complex in *Synechocystis* PCC 6803, *J. Biol. Chem.*, 279 (2004) 48620-48629.
- [38] **Schagger, H.**, Tricine-SDS-PAGE, *Nat Protoc*, 1 (2006) 16-22.
- [39] **Borst, J.W., Hink, M.A., van Hoek, A., Visser, A.**, Effects of refractive index and viscosity on fluorescence and anisotropy decays of enhanced cyan and yellow fluorescent proteins, *Journal of Fluorescence*, 15 (2005) 153-160.

# *Role of carotenoids in thylakoid organisation*

- [40] van Oort, B., Amunts, A., Borst, J.W., van Hoek, A., Nelson, N., van Amerongen, H., Croce, R., Picosecond fluorescence of intact and dissolved PSI-LHCI crystals, *Biophys. J.*, 95 (2008) 5851-5861.
- [41] Snellenburg, J.J., Laptanok, S.P., Seger, R., Mullen, K.M., van Stokkum, I.H.M., Glotaran: A Java-based graphical user interface for the R package TIMP, *Journal of Statistical Software*, 49 (2012) 1-22.
- [42] Laptanok, S.P., Snellenburg, J.J., Bucherl, C.A., Konrad, K.R., Borst, J.W., Global analysis of FRET-FLIM data in live plant cells, *Methods in molecular biology* 1076 (2014) 481-502.
- [43] van Oort, B., Ereemeeva, E.V., Koehorst, R.B.M., Laptanok, S.P., van Amerongen, H., van Berkel, W.J.H., Malikova, N.P., Markova, S.V., Vysotski, E.S., Visser, A.J.W.G., Lee, J., Picosecond fluorescence relaxation spectroscopy of the calcium-discharged photoproteins aequorin and obelin, *Biochemistry*, 48 (2009) 10486-10491.
- [44] van Stokkum, I.H.M., van Oort, B., Mourik, F., Gobets, B., van Amerongen, H., (Sub)-picosecond spectral evolution of fluorescence studied with a synchroscan streak-camera system and target analysis, in: T. Aartsma, J. Matysik (Eds.) *Biophysical Techniques in Photosynthesis*, Springer Netherlands, 2008, pp. 223-240.
- [45] Mullen, K.M., van Stokkum, I.H.M., TIMP: An R package for modeling multi-way spectroscopic measurements, *Journal of Statistical Software*, 18 (2007).
- [46] van Stokkum, I.H.M., Gobets, B., Gensch, T., van Mourik, F., Hellingwerf, K.J., van Grondelle, R., Kennis, J.T.M., (Sub)-picosecond spectral evolution of fluorescence in photoactive proteins studied with a synchroscan streak camera system, *Photochem. Photobiol.*, 82 (2006) 380-388.
- [47] van de Meene, A.M., Hohmann-Marriott, M.F., Vermaas, W.F., Roberson, R.W., The three-dimensional structure of the cyanobacterium *Synechocystis sp.* PCC 6803, *Arch. Microbiol.*, 184 (2006) 259-270.
- [48] Liberton, M., Howard Berg, R., Heuser, J., Roth, R., Pakrasi, H.B., Ultrastructure of the membrane systems in the unicellular cyanobacterium *Synechocystis sp.* strain PCC 6803, *Protoplasma*, 227 (2006) 129-138.
- [49] Krumova, S., Laptanok, S., Borst, J., Ughy, B., Gombos, Z., Ajlani, G., van Amerongen, H., Monitoring photosynthesis in individual cells of *Synechocystis sp.* PCC 6803 on a picosecond timescale, *Biophys. J.*, 99 (2010) 2006-2015.
- [50] Broess, K., Trinkunas, G., van Hoek, A., Croce, R., van Amerongen, H., Determination of the excitation migration time in photosystem II consequences for the membrane organization and charge separation parameters, *Biochim. Biophys. Acta*, 1777 (2008) 404-409.
- [51] Kurian, D., Jansen, T., Maenpaa, P., Proteomic analysis of heterotrophy in *Synechocystis sp.* PCC 6803, *Proteomics*, 6 (2006) 1483-1494.
- [52] van de Meene, A.M., Sharp, W.P., McDaniel, J.H., Friedrich, H., Vermaas, W.F., Roberson, R.W., Gross morphological changes in thylakoid membrane structure are associated with Photosystem I deletion in *Synechocystis sp.* PCC 6803, *Biochim. Biophys. Acta*, 1818 (2012) 1427-1434.
- [53] Nilsson, F., Simpson, D.J., Jansson, C., Andersson, B., Ultrastructural and biochemical characterization of a *Synechocystis* 6803 mutant with inactivated Psba genes, *Archives of Biochemistry and Biophysics*, 295 (1992) 340-347.
- [54] Ashikawa, I., Miyata, A., Koike, H., Inoue, Y., Koyama, Y., Light-induced structural-change of beta-carotene in thylakoid membranes, *Biochemistry*, 25 (1986) 6154-6160.
- [55] Shpilyov, A.V., Zinchenko, V.V., Shestakov, S.V., Grimm, B., Lokstein, H., Inactivation of the geranylgeranyl reductase (ChlP) gene in the cyanobacterium *Synechocystis sp.* PCC 6803, *Biochim. Biophys. Acta*, 1706 (2005) 195-203.
- [56] Maeda, H., Sakuragi, Y., Bryant, D.A., DellaPenna, D., Tocopherols protect *Synechocystis sp.* strain PCC 6803 from lipid peroxidation, *Plant Physiol.*, 138 (2005) 1422-1435.
- [57] Sakuragi, Y., Maeda, H., DellaPenna, D., Bryant, D.A., alpha-tocopherol plays a role in photosynthesis and macronutrient homeostasis of the cyanobacterium *Synechocystis sp.* PCC 6803 that is independent of its antioxidant function, *Plant Physiol.*, 141 (2006) 508-521.

- [58] El-Mohsnawy, E., Kopczak, M.J., Schlodder, E., Nowaczyk, M., Meyer, H.E., Warscheid, B., Karapetyan, N.V., Rögner, M., Structure and function of intact photosystem I monomers from the cyanobacterium *Thermosynechococcus elongatus*, *Biochemistry*, 49 (2010) 4740-4751.
- [59] Bautista, J.A., Rappaport, F., Guergova-Kuras, M., Cohen, R.O., Golbeck, J.H., Wang, J.Y., Beal, D., Diner, B.A., Biochemical and biophysical characterization of photosystem I from phytoene desaturase and  $\zeta$ -carotene desaturase deletion mutants of *Synechocystis* sp PCC 6803, *J. Biol. Chem.*, 280 (2005) 20030-20041.
- [60] Chitnis, V.P., Chitnis, P.R., PsaL subunit is required for the formation of photosystem I trimers in the cyanobacterium *Synechocystis* sp PCC 6803, *FEBS Lett.*, 336 (1993) 330-334.
- [61] Grotjohann, I., Fromme, P., Structure of cyanobacterial photosystem I, *Photosynth Res.*, 85 (2005) 51-72.
- [62] Gobets, B., van Grondelle, R., Energy transfer and trapping in photosystem I, *Biochim. Biophys. Acta*, 1507 (2001) 80-99.
- [63] Coufal, J., Hladik, J., Sofrova, D., The carotenoid content of photosystem I pigment-protein complexes of the cyanobacterium *Synechococcus elongatus*, *Photosynthetica*, 23 (1989) 603-616.
- [64] Domonkos, L., Malec, P., Sallai, A., Kovacs, L., Itoh, K., Shen, G.Z., Ughy, B., Bogos, B., Sakurai, I., Kis, M., Strzalka, K., Wada, H., Itoh, S., Farkas, T., Gombos, Z., Phosphatidylglycerol is essential for oligomerization of photosystem I reaction center, *Plant Physiol.*, 134 (2004) 1471-1478.
- [65] Loll, B., Kern, J., Saenger, W., Zouni, A., Biesiadka, J., Towards complete cofactor arrangement in the 3.0 angstrom resolution structure of photosystem II, *Nature*, 438 (2005) 1040-1044.
- [66] Bautista, J.A., Tracewell, C.A., Schlodder, E., Cunningham, F.X., Brudvig, G.W., Diner, B.A., Construction and characterization of genetically modified *Synechocystis* sp. PCC 6803 photosystem II core complexes containing carotenoids with shorter  $\pi$ -conjugation than beta-carotene, *J. Biol. Chem.*, 280 (2005) 38839-38850.
- [67] Kondo, K., Geng, X.X., Katayama, M., Ikeuchi, M., Distinct roles of CpcG1 and CpcG2 in phycobilisome assembly in the cyanobacterium *Synechocystis* sp. PCC 6803, *Photosynth Res.*, 84 (2005) 269-273.
- [68] Kondo, K., Ochiai, Y., Katayama, M., Ikeuchi, M., The membrane-associated CpcG2-phycobilisome in *Synechocystis*: A new photosystem I antenna, *Plant Physiol.*, 144 (2007) 1200-1210.
- [69] Stoitchkova, K., Zsiros, O., Javorfi, T., Pali, T., Andreeva, A., Gombos, Z., Garab, G., Heat- and light-induced reorganizations in the phycobilisome antenna of *Synechocystis* sp PCC 6803. Thermo-optic effect, *Biochim. Biophys. Acta*, 1767 (2007) 750-756.
- [70] Tamary, E., Kiss, V., Nevo, R., Adam, Z., Bernat, G., Rexroth, S., Roegner, M., Reich, Z., Structural and functional alterations of cyanobacterial phycobilisomes induced by high-light stress, *Biochim. Biophys. Acta*, 1817 (2012) 319-327.
- [71] Ivanov, A.G., Krol, M., Sveshnikov, D., Selstam, E., Sandstrom, S., Koochek, M., Park, Y.I., Vasil'ev, S., Bruce, D., Oquist, G., Huner, N.P.A., Iron deficiency in cyanobacteria causes monomerization of photosystem I trimers and reduces the capacity for state transitions and the effective absorption cross section of photosystem I in vivo, *Plant Physiol.*, 141 (2006) 1436-1445.
- [72] Collier, J.L., Grossman, A.R., A Small polypeptide triggers complete degradation of light-harvesting phycobilliproteins in nutrient-deprived cyanobacteria, *EMBO J.*, 13 (1994) 1039-1047.
- [73] Ughy, B., Phycobilisome assembly in *Synechocystis* sp. strain PCC6803. PhD dissertation, in: Plant biology Institute of HAS Biological Research Centre, *University of Szeged, Hungary*, Szeged, 2006.
- [74] Collier, J.L., Herbert, S.K., Fork, D.C., Grossman, A.R., Changes in the cyanobacterial photosynthetic apparatus during acclimation to macronutrient deprivation, *Photosynth Res.*, 42 (1994) 173-183.
- [75] Richaud, C., Zabulon, G., Joder, A., Thomas, J.C., Nitrogen or sulfur starvation differentially affects phycobilisome degradation and expression of the nblA gene in *Synechocystis* strain PCC 6803, *J. Bacteriol.*, 183 (2001) 2989-2994.

## *Role of carotenoids in thylakoid organisation*

- [76] Fuszard, M.A., Ow, S.Y., Gan, C.S., Noirel, J., Ternan, N.G., McMullan, G., Biggs, C.A., Reardon, K.F., Wright, P.C., The quantitative proteomic response of *Synechocystis sp.* PCC6803 to phosphate acclimation, *Aquatic biosystems*, 9 (2013) 5.
- [77] Liu, X.G., Zhao, J.J., Wu, Q.Y., Oxidative stress and metal ions effects on the cores of phycobilisomes in *Synechocystis sp.* PCC 6803, *FEBS Lett.*, 579 (2005) 4571-4576.
- [78] Bittersmann, E., Vermaas, W., Fluorescence lifetime studies of cyanobacterial Photosystem II mutants, *Biochim. Biophys. Acta*, 1098 (1991) 105-116.
- [79] Yu, J.J., Wu, Q.Y., Mao, H.B., Zhao, N.M., Vermaas, W.F.J., Effects of chlorophyll availability, on phycobilisomes in *Synechocystis sp.* PCC 6803, *Iubmb Life*, 48 (1999) 625-630.

## 2.9 Supplementary Information

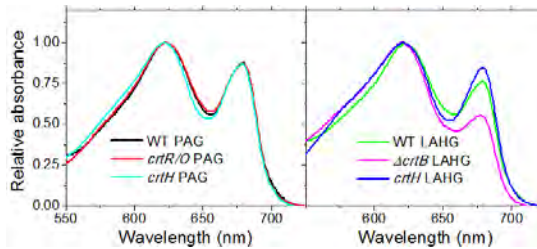


**Figure Supplementary Information 2.1.** Absorption spectra of cells measured with an integrating sphere. The spectra were normalised to the phycobilisome peak.

The intensity of the chlorophyll-related band (~675 nm) relative to the PBS peak absorption band (~625 nm) seems to be hardly affected in the various mutants except in  $\Delta crtB$  LAHG, which contains less Chl. The colour of  $\Delta crtB$  cells is bluish while the other strains are green.

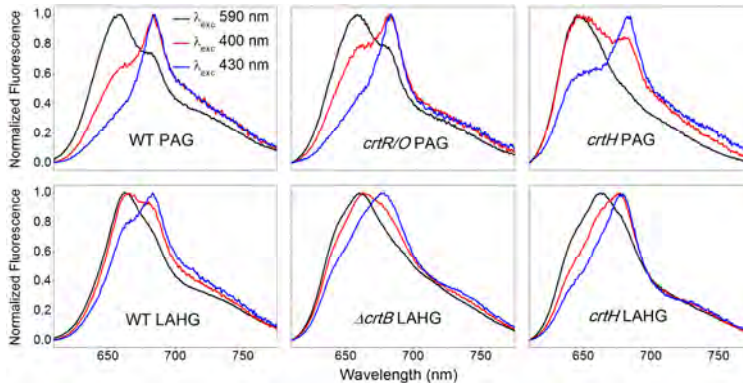


**Figure Supplementary Information 2.2.** Room-temperature steady-state fluorescence spectra upon 590 nm (black), 400 nm (red) and 430 nm (blue) excitation.

It is clear from the room-temperature fluorescence emission spectra that at 400 nm the PBs and the Chl containing PSI and PSII are excited. Spectra show the same differences as observed with streak measurements, but a detailed understanding of the changes requires the usage of time-resolved measurements.

# Role of carotenoids in thylakoid organisation

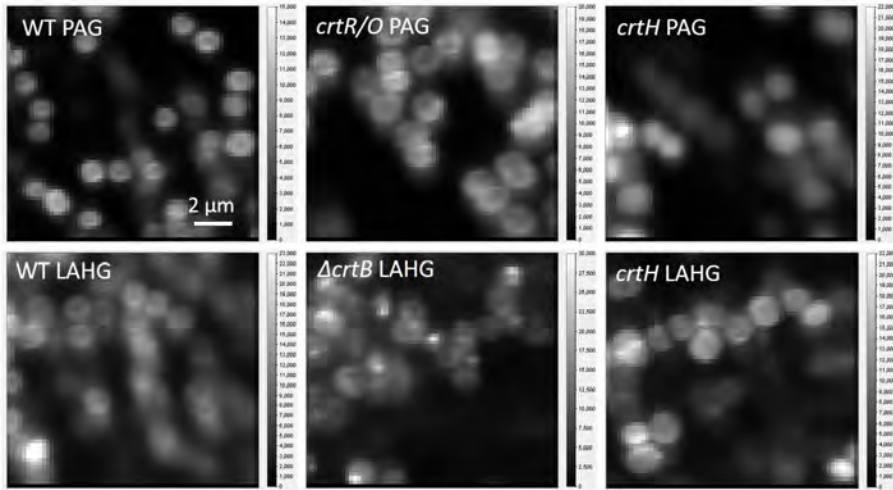


**Figure Supplementary Information 2.3.** Fluorescence intensity images of different strains obtained by the FLIM setup.

WT and *crtR/O* PAG cells show increased fluorescence around the cell wall, but the *crtH* PAG cells show even higher fluorescence in the centre of the cells. Most  $\Delta$ *crtB* and several *crtH* LAHG cells have bright spots within the cell where the fluorescence intensity is higher.

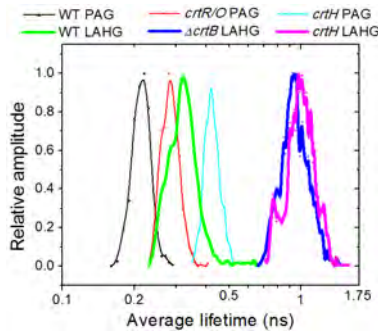


**Figure Supplementary Information 2.4.** Distribution histogram of the average lifetimes for different *Synechocystis* strains, obtained from multi-exponential fits of the FLIM results. The various colours represent WT PAG (black), *crtR/O* (red), *crtH* PAG (cyan), WT LAHG (green),  $\Delta$ *crtB* (blue) and *crtH* LAHG (pink) strains, respectively; the values are plotted on a logarithmic time scale. WT, *crtR/O*, *crtH* cells grown at photoautotrophic conditions are represented by narrow lines and the WT,  $\Delta$ *crtB*, *crtH* cells grown under light-activated heterotrophic growth conditions are shown by a thick line.

This figure summarizes the obtained distribution of  $\tau_{av}$  for each strain. The fastest  $\tau_{av}$  is observed for WT PAG cells ( $\sim$ 230 ps), whereas it is  $\sim$ 280 ps for *crtR/O* and  $\sim$ 420 ps for *crtH* PAG cells. The  $\Delta$ *crtB* and *crtH* LAHG show a long average lifetime of

~1 ns, far longer than ~310 ps, the average value found for WT cells grown in the same light conditions. Both  $\Delta crtB$  and  $crtH$  LAHG cells show a wide range of lifetime values, reflecting pronounced heterogeneity

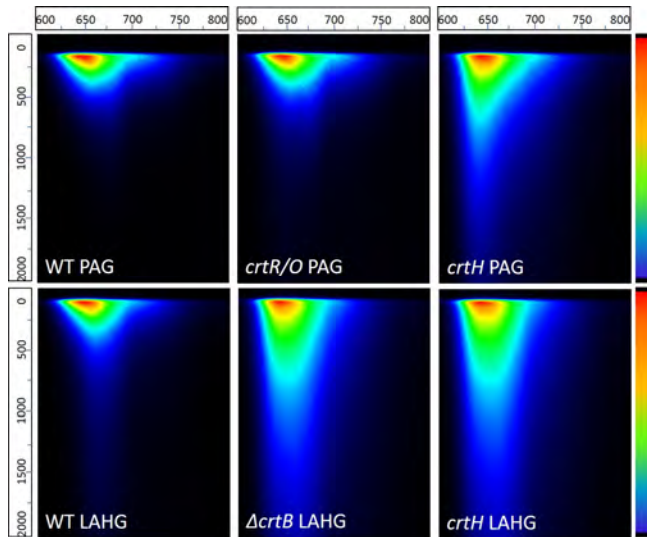


**Figure Supplementary Information 2.5.** Streak-camera images of whole cells for 590 nm excitation, using a 2000-ps time window, obtained for different strains as indicated by the labels. Images represent the fluorescence intensity (using a linear colour gradient) as a function of time (vertical axis) and wavelength (horizontal axis).

It is apparent that the WT and  $crtR/O$  show similar images, but the  $crtH$  PAG shows longer-lived fluorescence below 650 nm. The WT LAHG shows pronounced long-lived fluorescence, but only above 675 nm.  $\Delta crtB$  and  $crtH$  LAHG show similar streak images; in these cells long-lived fluorescence is emitted from 640-675 nm, indicating severely distorted energy transfer.

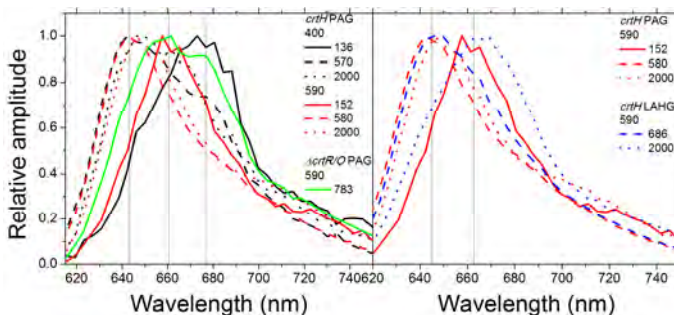


**Figure Supplementary Information 2.6.** Normalized DAS of selected streak-camera components obtained by global analysis of streak images. The corresponding DAS are

# Role of carotenoids in thylakoid organisation

presented in Figs. 4 and 5 in the main text. Excitation wavelengths are 590 and 400 nm as presented in the figures. The name of the strain and the fluorescence lifetime of the DAS spectra are displayed in the labels.

The DAS of the individual lifetime components obtained from global analysis are compared in this figure; the spectra are normalised to their maximum.

The *crtH* PAG cells show a ~600 ps and a 2ns fluorescence component both for 590 nm and 400 nm excitation. The spectra of the components are similar and differ only slightly for the two excitation wavelengths. The spectra of both components (~600 ps, 2 ns) obtained upon 400 nm excitation show a slightly higher contribution around 680 nm. The increase of the fluorescence around 680 nm should probably be ascribed to increased Chl fluorescence due to direct Chl excitation of some distorted PSII complexes.

The fluorescence of the long, 783 ps component observed for *crtR/O* has a double maximum around 660 and 675 nm; these values are characteristic for APC of the PBS core.

The long components for *crtH* PAG and LAHG were also compared. The 600-700 ps components have similar spectra, but the 2 ns components are largely different for the two samples. In *crtH* PAG, the 2 ns component has a PC-like spectrum, while for LAHG conditions the fluorescence is emitted around 670 nm. This shows that in *crtH* PAG the 2 ns component originates from unconnected PC rods, while in *crtH* LAHG the 2 ns component originates from the APC<sub>660</sub> and the TE of the unconnected PBSs.

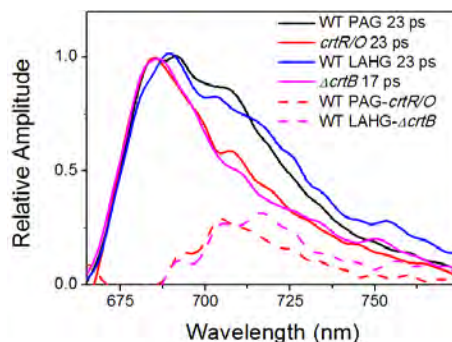


**Figure Supplementary Information 2.7.** Normalized PSI signal dominated DAS components originated from global analysis of streak-camera images obtained upon 400 nm excitation. The spectra were normalised to their maximal fluorescence intensity. The corresponding DAS are presented in Figs. 4 and 5 and discussed in the main text. The name of the strain and the fluorescence lifetime of the DAS spectra are displayed in the labels.

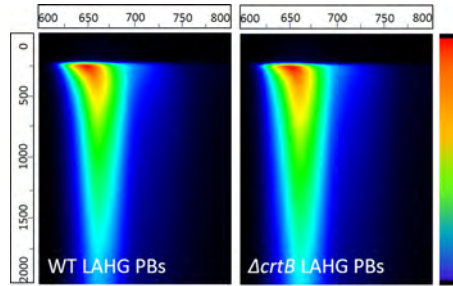


**Figure Supplementary Information 2.8.** Streak-camera images of isolated phycobilisomes of WT and  $\Delta crtB$  LAHG cells for 590nm excitation using a 2-ns (2000 ps) time window. Images represent the fluorescence intensity (using a linear colour gradient) as a function of time (vertical axis) and wavelength (horizontal axis).

Images show that the PBSs from  $\Delta crtB$  cells have a lower contribution below 650 nm than the corresponding WT PBSs, and the  $\Delta crtB$  PBSs seem to have a slightly longer lifetime.

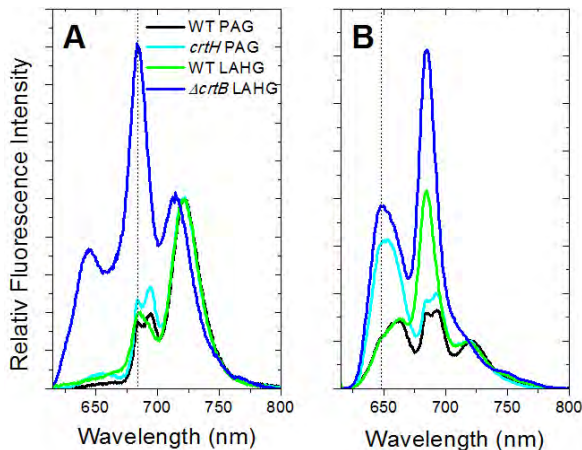


**Figure Supplementary Information 2.9.** Steady-state fluorescence emission spectra detected at 77K upon 436 (A) and 590 (B) nm excitation. Different colours represent WT PAG (black), *crtH* PAG (cyan), WT LAHG (green) and  $\Delta crtB$  LAHG (blue), respectively. The spectra were normalized to the PSI peak at ~720 nm.

77K steady-state fluorescence emission of WT and *crtH* PAG, WT and  $\Delta crtB$  LAHG cells were also recorded. The *crtH* PAG cells show only slightly higher PSII emission upon chlorophyll (436 nm) excitation than WT PAG. But upon PBS (590 nm) excitation the PBS peak at ~650 nm dominates, further supporting the presence of the unattached PC rods. It also confirms that the remaining part of the PBSs transfers energy to the RCs.  $\Delta crtB$  cells show a dominant 685 nm peak upon 436 nm

# *Role of carotenoids in thylakoid organisation*

excitation, which is probably the sum of fluorescence from the APC terminal emitter and CP47. The high contribution of PC (~650 nm peak) has also been detected upon 436 nm excitation, which reflects the high excitation probability of PBSs as compared to that of the chlorophylls. The PSI signal (~720 nm) appears to be blue-shifted as compared to WT cells. Excitation at 590 nm leads to the dominance of the 685 nm signal while the PSI signal only appears as a shoulder, demonstrating that PBSs do not transfer the absorbed energy towards the PSSs.

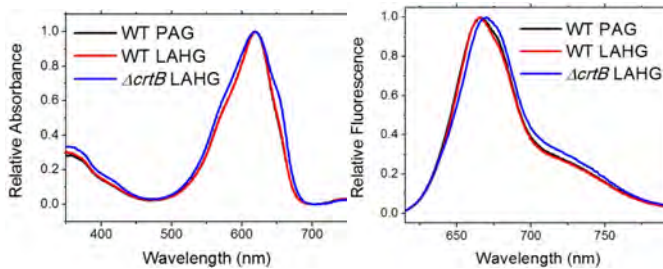


**Figure Supplementary Information 2.10.** Absorption spectra (left) and steady-state room temperature fluorescence emission spectra (right) of isolated phycobilisomes from WT PAG, LAHG and  $\Delta crtB$  cells. The spectra were normalised to their maxima.

PBSs from WT PAG and LAHG are identical, but PBSs of  $\Delta crtB$  cells have higher absorption at 650 nm and their fluorescence spectra are slightly blue-shifted. The changes in the absorption and fluorescence are due to the lower amount of C-PC as compared to APC.

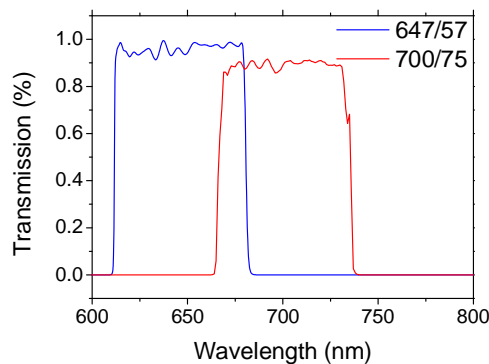


**Figure Supplementary Information 2.11.** Transmission characteristics of the bandpass filters 647/57 and 700/75 used for detection of the fluorescence lifetime imaging microscopy pictures in this study.

# Chapter 3

## ***The PsbW protein stabilizes the supramolecular organization of Photosystem II in higher plants***

José G. García-Cerdán, Tünde Tóth, László Kovács, Sami Kereïche, Elena Aseeva, Egbert J. Boekema, Fikret Mamedov, Christiane Funk and Wolfgang P. Schröder

### **Extended version of:**

J. G. García-Cerdán<sup>1</sup>, L. Kovács<sup>2</sup>, T. Tóth<sup>2</sup>, S. Kereïche<sup>3</sup>, E. Aseeva<sup>4</sup>, E. J. Boekema<sup>3</sup>, F. Mamedov<sup>5</sup>, C. Funk<sup>1</sup> and W. P. Schröder<sup>1</sup> (2011) The PsbW protein stabilizes the supramolecular organization of photosystem II in higher plants. *The Plant Journal* 65:368-381

<sup>1</sup>*Department of Chemistry and Umeå Plant Science Centre (UPSC), Umeå University, Umeå, Sweden.*

<sup>2</sup>*Institute of Plant Biology, Biological Research Center, Hungarian Academy of Sciences, Szeged, Hungary.*

<sup>3</sup>*Department of Biophysical Chemistry, Groningen Biomolecular Sciences and Biotechnology Institute, University of Groningen, Groningen, The Netherlands.*

<sup>4</sup>*Lehrstuhl für Botanik, Department Biologie I; Ludwig-Maximilians-Universität München München, Germany.*

<sup>5</sup>*Molecular Biomimetics, Department of Photochemistry and Molecular Science, Ångström Laboratory, Uppsala University, Uppsala, Sweden.*

# Role of PsbW protein in macro-organisation

## 3.1 Abstract

PsbW, a 6.1 kDa low molecular weight protein, is exclusive to photosynthetic eukaryotes and associates with the Photosystem II (PSII) protein complex. *In vivo* and *in vitro* comparison of *Arabidopsis thaliana* wild-type plants with T-DNA insertion knock-out mutants completely lacking the PsbW protein or with antisense inhibition plants exhibiting decreased amounts of PsbW demonstrated that the loss of PsbW destabilizes the supramolecular organization of Photosystem II. No PSII-LHCII supercomplexes could be detected or isolated in the absence of the PsbW protein. These changes in macro-organization were accompanied by a minor decrease in the chlorophyll fluorescence parameter  $F_v/F_m$ , and a modification of the redox state of the plastoquinone pool in dark-adapted leaves. In addition, the absence of the PsbW protein led to a faster redox changes of the PQ pool of state I to state II transition measured by changes in  $F_s$  kinetics compared to wild-type and strongly decreased PSII core protein phosphorylation. Despite these dramatic effects on macromolecular structure, the transgenic plants exhibited no significant phenotype under normal growth conditions. We suggest that the PsbW protein is located close to the minor antenna of the PSII complex and is important for the contact and stability between several PSII-LHCII supercomplexes.

## 3.2 Introduction

The light-driven water-splitting reaction of oxygen-evolving photosynthesis occurs in a multi-subunit complex called Photosystem II (PSII), which is embedded in the thylakoid membranes of cyanobacteria and the chloroplast of photosynthetic eukaryotes. Crystallographic analyses [1-7] and biochemical data obtained from cyanobacteria [8] have shown that roughly half of the protein composition of PSII consists of low-molecular-weight (LMW) proteins with molecular masses of less than 10 kDa [9]. Most of these peptides are integrated into the thylakoid membrane as single  $\alpha$ -helices. Data acquired in these studies, in addition to electron cryo-microscopic analyses [10, 11] have allowed the identification and localization of the major subunits within PSII complexes, as well as bona fide allocation for some of the LMW proteins [7]. Notably, higher plants contain three LMW proteins (PsbR, PsbTn and PsbW) that are not present in cyanobacteria [9], and consequently both their localization and functional properties remain unclear.

Although the cyanobacterial PSII reaction center is highly homologous to its higher plant counterpart in terms of intrinsic protein composition and cofactor binding, there are differences with regards to the composition of the extrinsic subunits [12] and their peripheral antenna systems. Cyanobacteria contain large

extrinsic light harvesting phycobilisomes that presumably obstruct the formation of grana stacking in the thylakoid membranes [13], whereas higher plants have integral membrane antenna complexes composed of proteins belonging to the family of light harvesting complexes (LHC) [14]. The peripheral antenna of PSII in higher plants is comprised of the major antenna LHCII, constituted by heterotrimeric complexes of Lhcb1 (*Lhcb1*), Lhcb2 (*Lhcb2*) and Lhcb3 (*Lhcb3*), and the minor antenna composed of CP24 (*Lhcb6*), CP26 (*Lhcb5*) and CP29 (*Lhcb4*). This peripheral, integral antenna permits the formation of stacked (grana) regions of the thylakoid membrane in which PSII is predominant. Grana formation in the thylakoid membrane provides PSII with an intricate macro-organization, in which PSII homodimers associate with the peripheral antenna forming so-called PSII-LHCII supercomplexes. Homogeneous preparations of various types of PSII-LHCII supercomplex from solubilized and fractionated grana membranes have been described [15]. The PSII-LHCII supercomplex from *Arabidopsis thaliana* contains a homodimeric PSII core ( $C_2$ ) with two LHCII trimers tightly bound to the core antenna protein CP43 and the minor antenna protein CP26 (trimer S), and one or two LHCII trimers, less tightly bound and in contact with the minor antenna proteins CP29 and CP24 (trimer M). This supercomplex is known as  $C_2S_2M$  or  $C_2S_2M_2$  and can form semi-crystalline arrays in the grana membrane [16]. The functional relevance of this macro-organization is not fully understood, but it has been suggested to provide PSII with a large functional antenna that facilitates excitation energy transfer between different PSII complexes. Consequently, this structure enhances the efficiency of antenna excitation energy trapping in PSII, especially in photosynthetic species such as land plants that are exposed to ever-changing environmental conditions [17].

One of the most interesting LMW proteins associated with PSII is the PsbW subunit, a 6.1 kDa protein initially described as a PSII intrinsic component in spinach [18]. The protein is exclusively associated with PSII protein complexes [19, 20] and a putative role in the stabilization of the PSII homodimer was proposed [21]. However, recently this view has been challenged by the observation that PsbW is incorporated during the later steps of PSII assembly concomitantly with Lhcb proteins [22], and that its primary location is within PSII-LHCII supercomplexes [14, 23, 24].

In this study we have investigated *Arabidopsis thaliana* T-DNA knock-out (koPsbW) and antisense (asPsbW) plants that completely lacked or exhibited decreased amounts of the PsbW protein, respectively. We show that in the complete absence of the PsbW protein, the supermolecular organization of PSII-LHCII in the grana membranes is severely compromised. Without the PsbW protein the ordered

# *Role of PsbW protein in macro-organisation*

rows of semi-crystalline macrodomains of PSII-LHCII supercomplexes cannot be formed. This in turn leads to a decrease of the efficiency in energy transfer between PSII units and slower regulation response of PSII upon light stress and decreased phosphorylation of the PSII core proteins.

## **3.3 Materials and methods**

### *Plant material*

*Arabidopsis thaliana* T-DNA insertion mutants of the *psbW* gene were generated from the Syngenta Arabidopsis Insertion Library collection (SAIL), mutant line (SAIL\_885\_A03) in Columbia ecotype (Col-O) [25], and obtained from the European stock centre (NASC) line N839813 [26]. Antisense plants were the same as described in [21]. Arabidopsis seedlings were germinated and cultivated in soil and/or in Murashige and Skoog media (MS) agar plates for 3 to 7 weeks at  $150 \mu\text{mol m}^{-2} \text{s}^{-1}$  photon flux density with a light/dark cycle of 8/16 hours respectively.

### *Isolation of thylakoid membranes and grana enriched fractions.*

Thylakoid membranes were prepared according to [27] and their chlorophyll concentrations were measured following extraction in 80% acetone according to [28]. In addition, extraction buffers were supplemented with sodium fluoride (10 mM final concentration) for measuring the extent of phosphorylation. For the preparation of grana-enriched fractions, the procedure outlined in [29] was followed.

### *Oxygen evolution measurements*

The oxygen evolving activity of thylakoid membrane preparations was measured in assay medium (25 mM Hepes, pH 7.6, 0.2 M sucrose, 10 mM NaCl, 5 mM  $\text{CaCl}_2$ ), supplemented with the artificial electron acceptors phenyl-p-benzoquinone or 2,6-dimethyl-p-benzoquinone at final concentrations of 0.25 and 1 mM, respectively. Oxygen evolution rates were measured at 20 °C under saturating light using a Clark-type electrode (Hansatech Instruments).

### *Blue native polyacrylamide gel electrophoresis (BN-PAGE)*

BN-PAGE was performed as described in [30] with modifications as in [31]. Solubilization of thylakoid membranes (concentrated to 1 mg/ml chlorophyll) was performed with one volume of 2% n-dodecyl- $\beta$ -D-maltoside. Solubilized samples were loaded onto a 1 mm thick native gel (gradient of 5-12.5 % acrylamide) and separated at 4° C.

### *Non-denaturing Deriphat-PAGE*

Non-denaturing Deriphat-PAGE was carried out according to [32] with minor modifications: Isolated thylakoid membranes were solubilised with 1% n-dodecyl- $\beta$ -D-maltoside at 1:10 chlorophyll to detergent ratio for 30 min at 4 °C. After pelleting non-solubilised material, 10  $\mu$ l aliquots of the samples were loaded onto a 1.5 mm thick acrylamide gel (38:1 acrylamide/bisacrylamide) with a 3 % stacking gel and a 4-15 % acrylamide gradient resolving gel. The electrode buffer (12.4 mM Tris-HCl, 96 mM glycine, pH 8.3) was supplemented with 0.2 % Deriphat-160 and 0.01% SDS (final concentrations). Electrophoresis was performed at 10 mA constant current at 4 °C.

### *SDS-PAGE and immunoblot analyses*

SDS-PAGE was performed on gels containing 12.5 % or 15 % acrylamide (the latter for LMW protein analyses) and 2 M urea. For immune staining, the proteins were transferred to polyvinylidene difluoride membranes (Bio-Rad Laboratories). Polyclonal antisera directed against PsbW, PsbO, D1, D2, Lhcb1, Lhcb2, Rubisco and Psal were provided by AgriSera AB (Vännas, Sweden). Antisera directed against STN7 and STN8 protein kinases were kindly provided by Professor D. Leister, Munich, Germany and phosphothreonine antibodies were purchased from Cell Signaling Technology Inc. (Danvers, MA, USA). Appropriate horse-radish peroxidase-labelled secondary antibodies were used and immunodetection was visualized by enhanced chemiluminescence (GE Healthcare) using a LAS-3000 cooled CCD camera (Fujifilm). Only samples that had been separated on the same gel were compared.

### *Sucrose density gradient ultracentrifugation*

PSII supercomplexes prepared from grana-enriched fractions were measured according to the method described in [15]. Grana membrane-enriched fractions were solubilized with n-dodecyl- $\alpha$ -D-maltoside  $\pm$  n-dodecyl- $\beta$ -D-maltoside (0.3 % or 0.45 % final concentrations respectively). Ultracentrifugation was performed using a LE-70 instrument (Beckman) at 36,000 rpm for 16 hours in a SW41 rotor.

### *Chlorophyll fluorescence measurements*

Chlorophyll *a* fluorescence was measured in intact leaves of 5-week old wild-type plants. A PAM 101/103 pulse amplitude modulated fluorometer (Heinz Walz, Effeltrich, Germany) was used to evaluate the photochemical and non-photochemical quenching parameters as described in [33]. To evaluate PSII activity

# *Role of PsbW protein in macro-organisation*

under high light ( $900 \mu\text{mol photons m}^{-2} \text{s}^{-1}$ ) and recovery under low light ( $10 \mu\text{mol photons m}^{-2} \text{s}^{-1}$ ) the typically used parameter  $F_v/F_m$  was measured in detached leaves in a time-course experiment in the presence or absence of lincomycin (1.25 mM final concentration) (Sigma-Aldrich) as follows; the leaves were immersed in water or lincomycin solution in Petri dishes under a transparent water bath connected to a cooling system in a temperature-regulated room to maintain the leaves at  $22^\circ\text{C}$ . High light treatments lasted for 22 hours and then leaves were allowed to recover in low light for 22 hours, while the maximum quantum yield of PSII ( $F_v/F_m$ ) fluorescence was measured using a portable PAM 201 fluorometer (Heinz Walz, Germany). In addition, thylakoid membranes were isolated from wild-type and koPsbW leaves that were dark-adapted for 15 minutes, lincomycin treated for 3 hours, high light treated for 22 hours and low light recovered for 22 hours.

Fast fluorescence induction curves were recorded for detached, dark-adapted leaves vacuum infiltrated with  $100 \mu\text{M}$  3-(3,4-dichloro-phenyl)-1,1-dimethylurea (DCMU). Fluorescence was measured with a DUAL DR head in a Dual PAM100 chlorophyll fluorescence photosynthesis analyzer (Heinz Walz, Germany) in fast kinetics mode. To obtain fast chlorophyll *a* fluorescence transient,  $4000 \mu\text{mol photons m}^{-2} \text{s}^{-1}$  actinic illumination was applied. The measured fluorescence induction curve was numerically fitted using the function  $F(t, I, \text{sPSII}, J)$  based on a sigmoidal fluorescence induction model [34], where  $J$  is the connectivity parameter that determines the shape of the curve, and  $\text{sPSII}$  is the functional cross-section of PSII.

Fast chlorophyll fluorescence transient kinetics were monitored on detached, dark-adapted leaves with a Handy PEA instrument (Hansatech Instruments, UK). These leaves were illuminated with continuous light (650 nm peak wavelength,  $3000 \mu\text{mol photons m}^{-2} \text{s}^{-1}$  maximum photon flux density) provided by an array of three light-emitting diodes (LEDs) focused on a circle of 5 mm diameter of the sample surface.

## *State I-state 2 transition measurements*

State transitions and state I or state II light pre-treatments were measured in intact leaves using a Dual-PAM 101 (Heinz Walz, Germany) following the method described in [35].

### *Circular dichroism (CD) spectroscopy for membrane structure analysis*

CD spectra were recorded on whole leaves or isolated thylakoid membranes between 400 and 750 nm at room temperature in a J810 dichrograph (Jasco) using a band-pass of 3 nm and a resolution of 1 nm. Detached leaves were quickly infiltrated with distilled water prior to measurement and placed perpendicular to the optical path. In order to improve the signal to noise ratio, 9 spectra were collected and averaged for each sample. Thylakoid membranes solubilised with 0.1 % n-dodecyl- $\beta$ -D-maltoside were measured at a chlorophyll concentration of 20  $\mu\text{g/ml}$  in a glass cuvette with a 1 cm optical path length.

### *Thermoluminescence*

Thermoluminescence measurements were carried out in a home-built apparatus described by [36]. After 5 min dark adaptation at 25 °C, 200  $\mu\text{l}$  thylakoid membrane suspension (equivalent to 100  $\mu\text{g}$  chlorophyll) were loaded into the sample holder and excited at -80 °C in the presence or absence of 10  $\mu\text{M}$  DCMU by a saturating single-turnover flash. Immediately after excitation, the emitted thermoluminescence was measured during heating of the sample in the dark at a heating rate of 20 °C/min using a photomultiplier (Hamamatsu Phototonics).

### *Transmission electron micrographs and electron microscopy*

Samples for chloroplast micrographs were prepared, embedded and sectioned according to [37]. For electron microscopy analyses, purified membranes, were prepared as in [38] and negatively stained with 2% uranyl acetate on glow discharged carbon-coated copper grids. Electron microscopy was performed on a Philips CM120 electron microscope equipped with a LaB6 tip operating at 120 kV. Images were recorded with a Gatan 4000 SP 4K slow-scan CCD camera at 80,000 x magnification at a pixel size (after binning the images) of 0.375 nm at the specimen level.

### *Electron paramagnetic resonance (EPR) spectroscopy*

EPR measurements were performed with a Bruker ELEXYS E500 spectrometer with a SuperX EPR049 microwave bridge and a SHQ4122 cavity, equipped with an ESR 900 liquid helium cryostat and ITC503 temperature controller (Oxford Instruments, UK). The  $S_2$  state multiline signal was induced by illumination at 200 K for 6 min and oxidation of Cytb559 was induced by illumination at 77 K for 6 min as described in [39].

# Role of PsbW protein in macro-organisation

## 3.4 Results

PsbW knock-out and antisense transgenic lines of *Arabidopsis thaliana* exhibit no significant phenotype. To investigate whether *Arabidopsis thaliana* plants depleted of the LMW PsbW protein exhibit a significant phenotype, we compared T-DNA knock-out PsbW (koPsbW) and antisense PsbW (asPsbW) with wild-type *Arabidopsis thaliana ec Columbia* plants. Seeds for koPsbW plants were obtained from the Syngenta Arabidopsis Insertion Library (SAIL) collection, asPsbW plants were described in [21]. The absence or reduction of PsbW was confirmed in isolated thylakoid membranes by immunodetection of PsbW (Fig. 3.1, top lane). As expected, no PsbW protein was detected in the koPsbW plants and the asPsbW plants displayed less than 25% of wild-type levels (Fig. 3.1). Despite the absence or reduction of the PsbW protein in the transgenic plants, there were no significant differences in photoautotrophic growth or flowering under normal growth conditions (Fig. Supplementary Information 3.1). This is in agreement with our earlier observation using asPsbW grown under reduced light ( $90 \mu\text{mol m}^{-2} \text{s}^{-1}$  photon) and normal light conditions [21]. Furthermore, plant fitness in field studies of the koPsbW plants did not differ significantly from wild type in terms of biomass, growth rate, flowering time or herbivore attack (Johansson-Jänkänpää, Schröder and Jansson unpublished results).

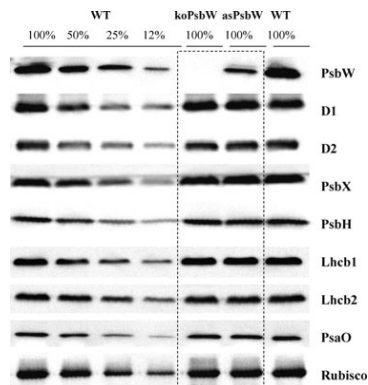


**Figure 3.1. Thylakoid membrane protein abundance of wild-type (WT), PsbW knock-out (koPsbW) and antisense (asPsbW) plants.** Immunodetection of thylakoid membrane proteins was performed with specific antibodies against PsbW, D1, D2, PsbX, PsbH, Lhcb1, Lhcb2, PsaO and Rubisco. The 100% loading control corresponds to 0.35  $\mu\text{g}$  of total chlorophyll.

The abundance of several components of protein complexes from the thylakoid membrane was determined by immunodetection: These included subunits from PSII (reaction center proteins D1 and D2, and the LMW proteins PsbX and PsbH), the light harvesting antenna subunits Lhcb1 and Lhcb2, Photosystem I (PSI)

PsaO subunit, and the stromal large subunit of the ribulose 1,5-bisphosphate carboxylase/oxygenase (Rubisco) (Fig. 3.1). No significant differences in abundance of these proteins between the knock-out, antisense or wild-type plants were observed. Moreover, the ratio of Photosystem II to Photosystem I in the thylakoid membranes measured by electron paramagnetic resonance (EPR) [40] showed no significant variation (Table 3.1). This is in agreement with comparable measurements of chlorophyll content and chlorophyll *a/b* ratio in wild-type and the transgenic *PsbW* lines (Table 3.1). Furthermore, the presence and stoichiometry of the different pigmented-protein complexes in the thylakoid membrane were investigated by non-denaturing deriphat-PAGE (Fig. Supplementary Information 3.3).

**Table 3.1.** Photosynthetic parameters of *Arabidopsis thaliana* wild-type and *PsbW* knock-out plants.

	Wild-type	koPsbW
<b>Chlorophyll <i>a/b</i> ratio</b>	$2.8 \pm 0.06^5$	$2.8 \pm 0.05$
<b>PSI/PSII ratio<sup>1</sup></b>	1.02	1.00
<b>Oxygen evolution<sup>2</sup></b>	$\mu\text{mol O}_2 / \text{mg chlorophyll h}$	$\mu\text{mol O}_2 / \text{mg chlorophyll h}$
PPBQ	$318 \pm 13$ (100%)	$222 \pm 17$ (70%)
DMBQ	$279 \pm 11$ (100%)	$238 \pm 8$ (85%)
<b>Fluorescence (PAM)</b>		
$F_v/F_m$	$0.82 \pm 0.01$	$0.78 \pm 0.01$
$F_o$ (a.u.)	$0.29 \pm 0.01$	$0.33 \pm 0.01$
<b>Antenna size<sup>3</sup></b>		
$t_{2/3}$ (ms) (fluor. rise time)	$0.115 \pm 0.011$	$0.114 \pm 0.013$
Connectivity (J)	$0.975 \pm 0.156$	$0.782 \pm 0.114$
<b>State transitions<sup>4</sup></b>		
$F_{m1}/F_{m2}$	$1.06 \pm 0.01$	$1.03 \pm 0.01$

<sup>1</sup>PSI/PSII ratio was measured by EPR in isolated thylakoid membranes according to (Danielsson *et al.*, 2004).

<sup>2</sup>Oxygen evolution rates were measured at 20 °C with 0.25 mM phenyl-p-benzoquinone (PPBQ) and 1 mM 2,5-dimethyl-p-benzoquinone (DMBQ) at saturating light intensities.

<sup>3</sup>Fluorescence transient measurements in the presence of DCMU

<sup>4</sup>State transitions were calculated as in [41].

<sup>5</sup> Errors reported are plus and minus 1 standard deviation (n= 5).

In accordance with earlier work [42, 43] seven green bands were separated in the deriphat gel, which were described from highest to lowest molecular weight as PSI-LHCI, PSII-core dimer, PSII-core monomer, antenna supercomplex (CP29-CP24-LHCII), LHCII trimer, LHCII monomer and free pigment. Interestingly, no difference was visible in any of the different pigmented protein complexes resolved by deriphat gel from samples with reduced or depleted amount of *PsbW* when compared to wild type. Thus, the *PsbW* protein seems not to be essential for the

# Role of PsbW protein in macro-organisation

organization and/or stoichiometry of the different chlorophyll-containing protein complexes found in the thylakoid membranes.

## *PsbW is important for the PSII macro-organization as shown by in vivo circular dichroism spectroscopy*

Wild-type and transgenic plants were characterized by *in vivo* circular dichroism (CD) spectroscopy, a non-invasive method to monitor structural changes of pigment-protein complexes and their higher-order associations [44] (Fig. 3.2). The CD spectra of whole leaves from wild-type plants reveal typical features; the so-called psi-type CD bands seen around 690 nm and 505 nm [44] indicate the presence of chiral LHCII-containing macrodomains of the pigment-protein complexes in thylakoid grana membranes [45, 46]. Strikingly, despite the lack of effect of PsbW levels on the organization and abundance of the pigmented protein complexes of the thylakoid membranes, whole leaves from mutant plants exhibited a CD spectrum with suppressed levels of psi-type CD bands in comparison to wild-type leaves (Fig. 3.2 A).

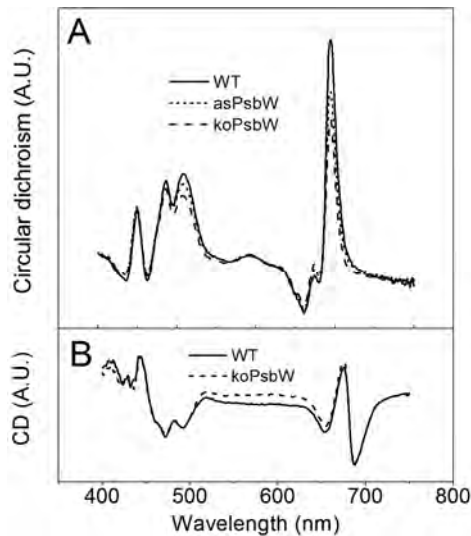


**Figure 3.2. Circular-dichroism (CD) spectra of detached leaves and solubilized thylakoid membranes.** (A) CD spectra of wild-type (WT, solid line), asPsbW (dotted line) and koPsbW (dashed line) leaves. (B) solubilised thylakoid membranes of WT (solid line) and koPsbW (dashed line) plants in the presence of 0.1% of *n*-dodecyl- $\beta$ -D-maltoside. A.U., arbitrary units

The amplitude of the psi-type band at 690 nm, measured as the difference in absorption between 690 nm and 675 nm, was decreased by 38 % in koPsbW ( $27.1 \pm 2.63$  mdeg) compared to wild-type leaves ( $43.7 \pm 3.9$  mdeg), while leaves of asPsbW

plants exhibited an intermediate decrease of 22 % ( $33.9 \pm 8.6$  mdeg). Similarly, the blue psi-type CD band in the Soret region at 505 nm was decreased in plants lacking, or with reduced amounts of PsbW. The changes in the psi-type CD are in good agreement with the level of PsbW protein determined by immunoblot analysis:

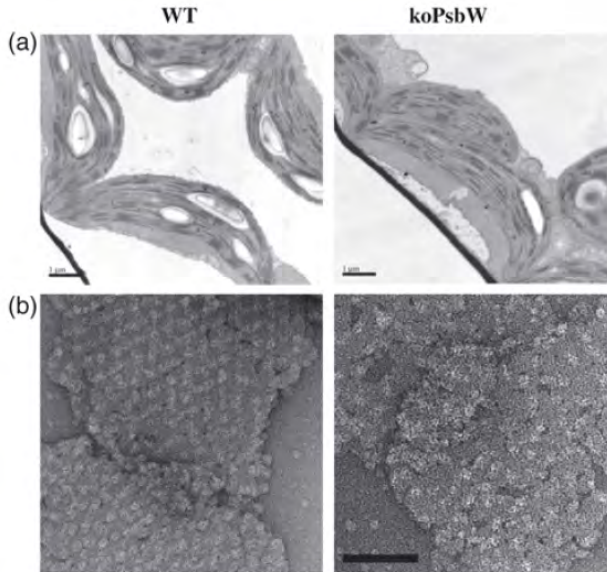


**Figure 3.3. Electron microscopy analyses.** (A) Electron microscopy images of thin sections of plastids from mesophyll cells of dark-adapted wild-type and koPsbW mutant plants. Bars = 1  $\mu$ m (B) Image of negatively-stained paired grana membrane fragments isolated from wild-type and koPsbW mutant plants. Wild-type paired grana membrane fragments exhibit crystalline arrays of PSII-LHCII supercomplexes, whereas those of koPsbW leaves show mainly disordered aggregated of PSII-LHCII supercomplexes. Scale bar represents 100 nm.

The amount of PsbW in the antisense plants is at a level intermediate between that of WT and koPsbW plants. The proportional decrease of both psi-type bands in the PsbW mutant leaves indicates a reduction in the extent of long-range order in the macro-organization of PSII-LHCII supercomplexes rather than a modification of the structure itself. Mild solubilisation of isolated thylakoids by 0.1% n-dodecyl- $\beta$ -D-maltoside eliminates the psi-type signal and uncovers the excitonic CD bands (Fig. 3.2 B). CD spectra of solubilized membranes possess excitonic CD bands characteristic for short-range interactions between chromophores bound to one polypeptide. The solubilised thylakoid membranes of WT and koPsbW lines show rather similar CD spectra suggesting that not only the pigment-protein compositions are identical, but also the orientations of the pigments within the polypeptides are unaffected in the absence of PsbW protein. The absence

## Role of PsbW protein in macro-organisation

of the PsbW protein alters the PSII macro-organization of the grana membranes as measured *in vitro* Transmission electron microscopy (EM) was used to assess whether the observed changes in macro-organization of PSII-LHCII, as indicated by the altered CD spectra of the koPsbW compared to wild-type plants, influenced the chloroplast ultra-structure, particularly the grana stacking. No obvious differences were observed in overall chloroplast membrane organization when the plants were dark-adapted (Fig. 3.3 A), or exposed to normal or high light (data not shown), before sample fixation for EM analysis. We extended our EM analyses to study the PSII macrostructure of thylakoid grana membrane fragments by means of EM combined with image analyses [47]. Negatively-stained paired grana membranes from wild-type plants exhibited well-ordered rows of semi-crystalline macrodomains of PSII supercomplexes (Fig. 3.3 B, left panel), similar to results described in [38]. However, in grana membrane fragments isolated from koPsbW plants, these ordered two-dimensional semi-crystalline domains were replaced by seemingly random aggregates in the mutant (Fig. 3.3 B, right panel).

The alteration of PSII macrostructure in the thylakoid grana membranes of the koPsbW mutant resulted in an inability to isolate PSII-LHCII supercomplexes by either blue-native (BN)-PAGE (Fig. 3.4 A) or sucrose-density gradient ultracentrifugation (Fig. 3.5 A). For the BN-PAGE (Fig. 3.4 A), thylakoid membrane protein complexes were mildly solubilised in the presence of the detergent n-dodecyl- $\beta$ -D-maltoside and were electrophoretically separated in polyacrylamide gels under native conditions in the presence of Coomassie blue dye (R-250), which provides the necessary charges for separation of the protein [30]. Typically, BN-PAGE of wild-type thylakoid membranes resolved protein complexes, in which the higher molecular weight complexes correspond to PSII supercomplexes followed by the PSI and PSII core dimers, PSII core monomers, PSII monomer without the CP43 subunit, LHCII trimers and LHCII monomers [48] (Fig. 3.4 A, left lane). 2-dimensional analysis (native BN-PAGE followed by denaturing SDS-PAGE) of wild-type thylakoid membranes followed by immunoblotting identified the PSII reaction center protein D2 in all bands corresponding to Photosystem II. Of note, PsbW was immunostained mainly in the PSII supercomplexes (Fig. 3.4 B), but was not detected in PSII monomers or PSII subcomplexes. PSII supercomplexes were drastically reduced in the absence of PsbW, as visualized after native BN-PAGE (Fig. 3.4 A, koPsbW mutant) and asPsbW membranes demonstrated reduced levels of PSII-LHCII supercomplexes. Consequently, bands in koPsbW thylakoid extracts corresponding to LHCII components (CP29-CP24-LHCII-trimers), PSII core monomer and PSII core

monomer without CP43 were increased (Figure 3.4 A, middle lane). Hence PsbW appears to facilitate PSII-LHCII supercomplex assembly.

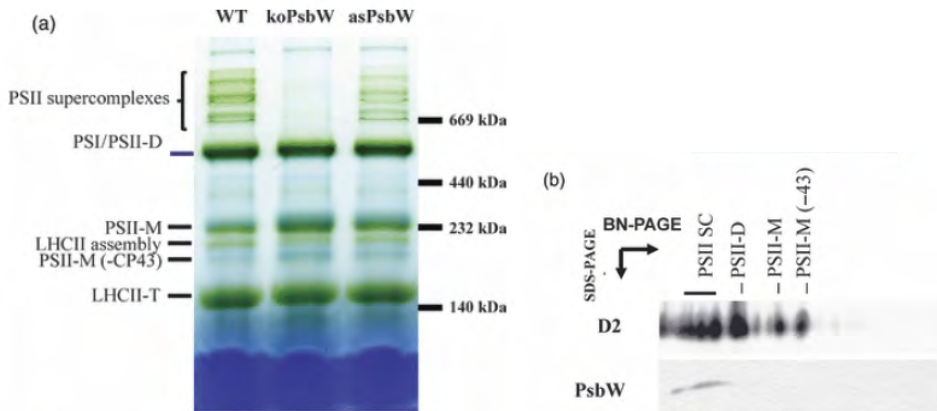


**Figure 3.4. Separation of PSII-LHCII supercomplexes from wild-type, *koPsbW* and *asPsbW* thylakoid membranes.** (A) Blue-native PAGE analysis of wild-type (WT), *koPsbW* and *asPsbW* thylakoid membranes solubilized in the presence of 1% of *n*-dodecyl- $\beta$ -D-maltoside. (B) Immunoblot of wild-type thylakoid membranes separated by 2-dimensional PAGE (BN/SDS-PAGE) using antibodies against PSII proteins D2 and PsbW. (SC: supercomplex, D: dimer, M: monomer)

Recently, [15] reported a new method for isolating and characterizing stable PSII-LHCII supercomplexes by combining sucrose-density gradient ultracentrifugation in the presence of the mild detergent (0.3% *n*-dodecyl- $\alpha$ -D-maltoside), followed by EM characterization. Several types of PSII supercomplexes were described, in which PSII core monomer (C) binds antenna trimers strongly (S) or moderately (M). The supercomplexes described are C<sub>2</sub>S<sub>2</sub>M<sub>2</sub>, C<sub>2</sub>S<sub>2</sub>M, C<sub>2</sub>S<sub>2</sub>, C<sub>2</sub>SM, C<sub>2</sub>M, C<sub>2</sub>S and CS. With the aim of characterising the supercomplexes present in the *koPsbW*, we analysed PSII-enriched membrane fractions of wild-type and mutant plants.

A total of 13 bands were resolved from wild-type, and the corresponding absorption spectra were measured (Fig. 3.5 A and 3.5 B).

# Role of PsbW protein in macro-organisation

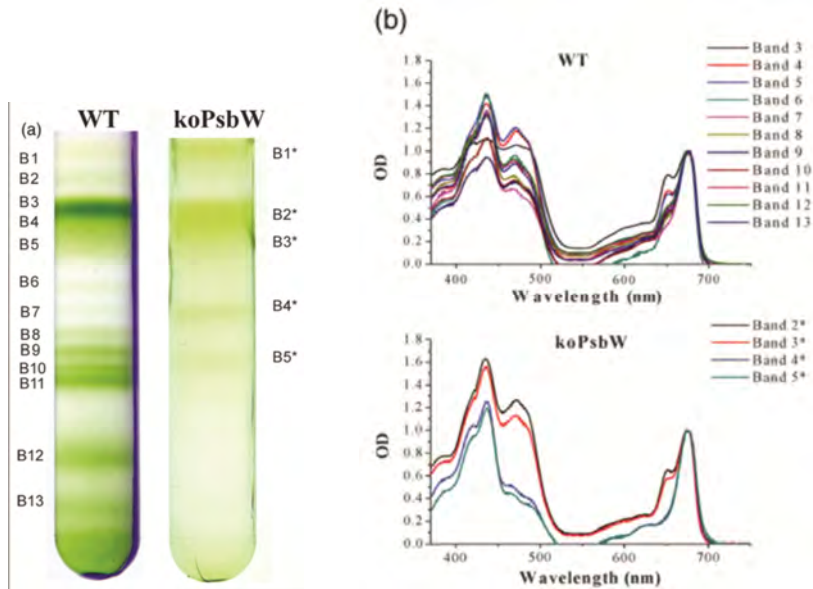


**Figure 3.5. Isolation of PSII-LHCII supercomplexes from grana-enriched membranes by sucrose density gradient centrifugation.** (A) Sucrose density gradient fractionation of wild-type and koPsbW grana-enriched membranes solubilised with 0.3% *n*-dodecyl- $\alpha$ -D-maltoside yielding bands B1-B13 or B1\*-B5\*, respectively. (B) Absorption spectra of the isolated bands. The different spectra were normalized to the maximum absorbance at 680 nm.

Of these bands, those numbered B3 to B5 were found to correspond to monomeric LHCII, trimeric LHCII and LHCII complex, respectively. B7 corresponded to dimeric PSII core and B8 to B13 corresponded to different PSII-LHCII supercomplexes containing a dimeric core complex with various numbers of bound LHCII trimers. Strikingly, only 5 bands were resolved from the PSII-enriched membrane fraction of koPsbW plants (Fig. 3.5 A, right side). From these, the absorption spectra were measured: Bands B2\* and B3\* contained antenna proteins (LHCII monomer, trimer and LHCII assembly), and the two faint bands B4\* and B5\* corresponded to monomeric and dimeric PSII complexes, respectively. Surprisingly, all of the higher molecular weight bands (B8-B13) that corresponded to various PSII-LHCII supercomplexes in wild-type were absent in the koPsbW mutant. To rule out the possibility that different solubilisation efficiencies resulted in the loss of PSII-LHCII supercomplexes in koPsbW, a higher detergent concentration of 0.45% *n*-dodecyl- $\alpha$ -D-maltoside, as well as the detergent *n*-dodecyl- $\beta$ -D-maltoside ( $\beta$ -DM) at 0.3% and 0.45%, were tested. No supercomplexes were resolved from koPsbW membranes, regardless of the detergent or concentration tested (data not shown).

## *Photosynthetic performance of transgenic plants is slightly decreased*

Despite the lack of significant changes in protein abundance of PSII subunits, the rates of oxygen evolution in isolated thylakoid membranes from koPsbW plants were 30% and 15% lower than wild-type rates when measured using the artificial electron acceptors phenyl-p-benzoquinone and 2,5-dimethyl-p-benzoquinone, respectively (Table 3.1). These results suggest that although PSII accumulates in the thylakoid membrane in similar amounts to wild-type, PSII function is slightly impaired in the absence of PsbW.

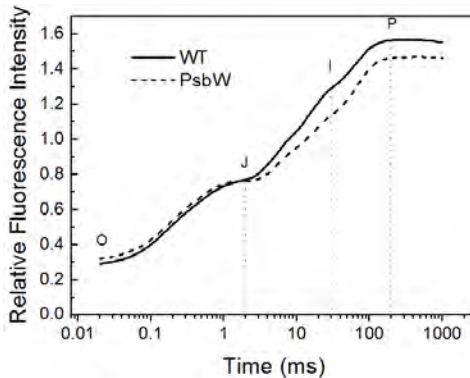


**Figure 3.6.** *Fast chlorophyll fluorescence transient kinetics of wild-type and koPsbW leaves.* Averaged curves of the chlorophyll fluorescence transient recorded in wild-type (solid line) and koPsbW (dashed line) leaves.

We further investigated the photosynthetic performance of these transgenic plants by analysing the photosynthetic chlorophyll fluorescence parameters using pulse amplitude modulated (PAM) fluorometry. The chlorophyll fluorescence parameter  $F_v/F_m$  indicates the maximum photochemical efficiency of PSII in the dark and is around 0.83 in most higher plant species [49]. In dark-adapted wild-type plants this value of 0.83 was confirmed (Table 3.1), whereas a slightly decreased value of 0.78 in koPsbW and 0.80 in asPsbW plants was measured ( $n=10$ ). The slight reduction of  $F_v/F_m$  observed in koPsbW plants was found to be due to reduced amount of variable fluorescence as a result of a decrease of the  $F_m$  value and a slight increase of the  $F_o$  value. The kinetics of the fast chlorophyll fluorescence transient can provide information about the reason for the altered fluorescence values. The kinetics of PSII reaction centre closure called the OJIP transient contains three phases, the O-J, J-I and I-P phases (Fig. 3.6). The J step at ~2 ms shows the

## Role of PsbW protein in macro-organisation

exchange of PQH<sub>2</sub> molecule with a PQ at the Q<sub>B</sub>-site, step I observed at ~30 ms implies the re-oxidation of PQH<sub>2</sub>, while the final P level (F<sub>m</sub>) at ~200 ms is due to the transient block evoked by inactive FNR. Accordingly, the O-J phase is related to the reduction of the PSII acceptor side, the slower J-I phase corresponds to a partial reduction of the PQ-pool and the I-P phase represents the reduction of the acceptor side of PSI [50]. In the koPsbW mutant the PQ pool reduction is less pronounced, as reflected by slower J-I phase and the decreased I and P levels although the amplitude of the I-P phase did not change. The F<sub>m</sub> decrease could not be observed in the fluorescence transient measured in the presence of DCMU. The reduction of Q<sub>A</sub> in the presence of DCMU is independent of the PQ pool and water oxidation. Therefore, the identical fluorescence transients of WT and koPsbW measured in the presence of DCMU indicate that the function of the PSII RC is unaffected. The suppressed J-I phase is most probably due to the faster re-oxidation of the PQ pool or a limited donor side activity of PSII.

Also a more detailed analysis of other fluorescence parameters (Table Supplementary Information 3.1) and EPR analysis (Table Supplementary Information 3.2) of the electron transport components of PSII did not reveal any dramatic effects on PSII. These results suggest that the primary PSII function is somewhat impaired in the absence of the PsbW protein.

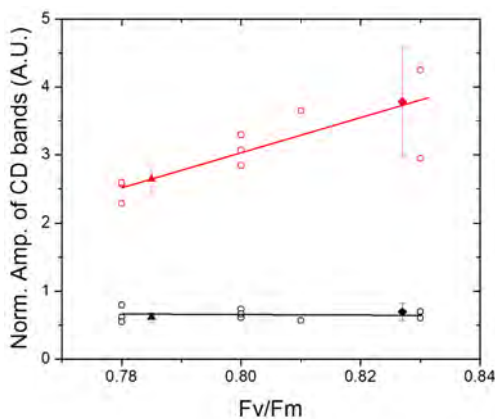


**Figure 3.7. Correlation analysis between  $F_v/F_m$  and circular dichroism in wild-type, asPsbW and koPsbW leaves.** The asPsbW( $\circ$ ) samples are represented by a set of plants (open symbols) possessing different  $F_v/F_m$  values. WT( $\blacklozenge$ ) and koPsbW( $\blacktriangle$ ) points represent typical values (average of 9 samples) for the given genotype. Red symbols represent the value of the psi-type CD band at 690 nm and black symbols represents excitonic CD band at 653 nm, respectively.

The level of PsbW protein in different asPsbW lines varies between the level of WT and koPsbW. Similarly, some of asPsbW plants possess a  $F_v/F_m$  value or psi-type CD signal close to what was observed in WT or koPsbW lines (closed symbols) while others range between them (Fig. 3.7). Since the amplitude of the red (690 nm) psi-type CD shows a linear correlation with  $F_v/F_m$  while the excitonic band is independent of  $F_v/F_m$ , we can assume that the partial depletion of PsbW protein proportionally decreases the macro-organisation of pigment-protein complexes in the thylakoid membrane which directly or indirectly modulates the PSII functions.

### *The PSII antennae size is not changed, meanwhile the connectivity is reduced*

Fast fluorescence transient measurements in the presence of 3-(3,4-dichlorophenyl)-1,1-dimethylurea (DCMU) gives information on the antenna size of PSII and the cooperation between PSII subunits. The functional antenna size can be estimated by time ( $t_{2/3}$ ) of the fluorescence induction (Table 3.1). KoPsbW exhibited a  $t_{2/3}$  of  $0.114 \pm 0.013$  ms ( $p < 0.05$ ) compared to wild-type  $0.115 \pm 0.011$  ms, indicating a similar antenna size in the studied plants, independent of the presence or absence of PsbW. The rise of fluorescence upon illumination follows a typical sigmoid kinetics, implicating cooperation between PSII complexes [51]. At the beginning of illumination, the excitation energy arriving at a closed PSII reaction center can be transferred to an open one, rather than being emitted as fluorescence, resulting in a fluorescence lag. The connectivity parameter (referred to as J), is a mathematical expression of the sigmoidicity of fluorescence transient and so measures the cooperativity of PSII units [34]. A marked change in the shape of the fluorescence curves of the transgenic plants revealed a slight but significant ( $P < 0.05$ ) difference in connectivity between the koPsbW plants ( $0.782 \pm 0.114$ ) compared to wild-type ( $0.975 \pm 0.156$ ) (Table 3.1). These measurements show that the antenna size is not changed in koPsbW, however, there is a disturbance of the macrodomain organisation of PSII subunits that lower the probability of energy transfer between PSII-LHCII supercomplexes, resulting in a less efficient cooperation of reaction centres in charring the captured light energy.

### *The redox potential of the acceptor-side of PSII is altered in koPsbW plants*

It seems reasonable to assume that a change in PSII macro-organisation would influence the interaction of PSII acceptor-side with the plastoquinone pool. In photosynthetic material, thermoluminescence occurs due to the thermally activated

## Role of PsbW protein in macro-organisation

recombination of electrons trapped on the acceptor side of PSII with positive charges stored in the water splitting complex. The thermoluminescence signal of dark-adapted sample referred to as B-band, originates from  $Q_B^-/S_{2,3}$  charge recombination [52], while the signal obtained in the presence of DCMU (preventing  $Q_A^-$  oxidation) is referred to as Q-band and arises from  $Q_A^-/S_2$  charge recombination. In thylakoid membranes isolated from both wild-type and koPsbW plants the B-band was detected at about 25°C, but interestingly the intensity was significantly lower in the koPsbW mutant (Fig. 3.8 A). The Q-band (i.e. with DCMU added), a shift towards higher temperatures was observed in the mutant (16.6°C, compared to 12.5°C in wild-type) meanwhile the intensities were the same (Fig. 3.8 B).

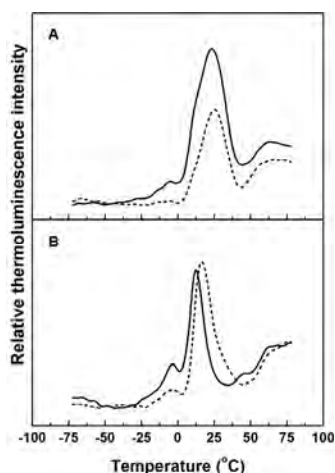


**Figure 3.8.** Thermoluminescence glow curves of thylakoid membranes isolated from wild-type (solid line) and koPsbW mutant (dotted line) leaves. Measured in the absence (A) and presence (B) of 10  $\mu$ M 3-(3,4-dichloro-phenyl)-1,1-dimethylurea (DCMU).

These results could be explained in terms of a redox shift in the Q-band ( $Q_A^-/S_2$  pair) leading to a decrease in the redox potential gap between  $Q_A$  and  $Q_B$  sites, which leads to increased stability of the charge separation in PSII. Since the B-band, which also depends on  $S_2$ , was not shifted, the redox potential of  $Q_A$  must have changed in the absence of PsbW. The unchanged amplitude of the Q-band demonstrates that the primary photochemistry (charge separation) of PSII reaction center is not altered in the mutant. A possible explanation for the decreased B-band without the concomitant decrease of the Q-band would be that the non-irradiative competitive reaction is enhanced in the koPsbW at the expense of the  $Q_B^-/S_2$  charge recombination, most probably caused by a faster exchange between the  $Q_B$  and the plastoquinone (PQ) pool in the koPsbW mutants. This conclusion is further

supported by EPR analysis of the electron transport components of PSII were the  $Q_A^-Fe^{2+}$  interaction signal was decreased, in agreement with the thermoluminescence analysis (Table Supplementary Information 3.2).

### *Altered PSII macro-organization does not influence state transitions*

A well-studied phenomenon of short term adaptation of plants are state transitions in which the amount of light energy absorbed by the two photosystems is balanced in response to changes in light quality [53]. This mechanism involves reversible phosphorylation of LHCII, mediating the redistribution of LHCII between PSII (state 1) and PSI (state 2) [41]. In this study, state transitions of wild-type and koPsbW plants were compared as in [35]. The typical chlorophyll fluorescence transient changes were measured with a Pulse Amplitude Modulated fluorimeter (Dual-PAM) on intact leaves.

Measurements of maximal relative fluorescence changes in state 1 and state 2 ( $F_{m1}$  and  $F_{m2}$ , respectively), resulted in similar  $F_{m1}/F_{m2}$  ratios for both wild-type and koPsbW plants, indicating that the extent of state 1/ state 2 transition are comparable to the wild-type (Fig. 3.9 A). However, a striking difference was observed in the level of amplitude and rate of the transient changes in chlorophyll fluorescence level (stationary fluorescence,  $F_s$ ) upon state 1 to state 2 transition, and vice versa. In wild-type, as expected, an increase in  $F_s$  was observed during the induction phase, when the far-red light was turned off. This is due to the transient accumulation of reduced  $Q_A$  and a fine-tuning of excitation energy towards the PSI protein complex, causing the re-oxidation of the plastoquinone pool and a decay of fluorescence [54]. The half-time of the  $F_s$  decay of state 1 to state 2 transitions in wild-type leaves was measured as 120 seconds, whereas in the mutant,  $F_s$  decayed much faster with a half-time of about 40 seconds (Fig. 3.9 A). This suggests that in the absence of PsbW, the PQ pool undergoes redox changes at a higher rate.

### *Loss of PsbW decreases PSII core protein phosphorylation*

Despite clear changes in  $F_s$  in koPsbW compared to wild-type upon state transitions (Fig. 3.9 A), no differences were observed in the maximal fluorescence  $F_{m1}/F_{m2}$  ratio (Table 3.1). To further investigate this phenomenon, the extent of inducible phosphorylation of LHCII was analysed in detached leaves of wild-type and koPsbW plants that had been kept in darkness or pre-treated under state 1 or state 2 light conditions (see [35]) for 25 minutes. Immediately following the light/dark treatment, thylakoid membranes were isolated, constituent proteins were

## Role of PsbW protein in macro-organisation

resolved by SDS-PAGE and immunostained using phospho-threonine antibodies (Fig. 3.9 B) or stained with Coomassie Brilliant Blue to demonstrate equal loading (Fig. 3.9 C). The band migrating at around 25 kDa corresponds to LHCII. In wild-type a very low amount of phosphorylated LHCII was detected after dark or state 1 illumination, while state 2 illuminations strongly induced LHCII phosphorylation (Fig. 3.9 B, left lanes). In the koPsbW mutant, the LHCII phosphorylation after state 1 and state 2 illuminations was comparable to the amount in wild-type. Notably however, the extent of LHCII phosphorylation of dark adapted leaves was highly elevated in koPsbW compared with wild-type.

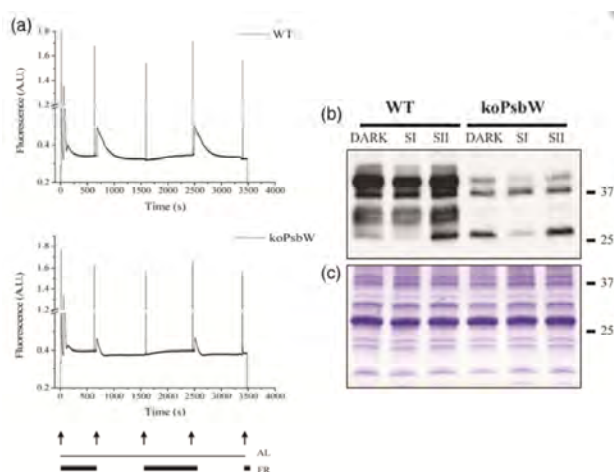


**Figure 3.9. Measurement of state transitions.** (A) Typical room temperature chlorophyll fluorescence traces of the state 1 to state 2 transitions in wild-type and koPsbW plants are shown. Arrows indicate saturating flashes and black bars indicate the presence of far red light. (B) The extent of inducible phosphorylation of the main thylakoid membrane phosphoproteins of wild-type and koPsbW leaves treated with state 1 and state 2 transition light conditions was assessed with antibodies directed against phospho-threonine (Cell Signaling Technology). Thylakoid membranes were isolated from detached leaves exposed to state 1 (SI), state 2 (SII) or dark conditions from wild-type and koPsbW plants. A total of 0.7  $\mu$ g chlorophyll was loaded per lane. (C) Reference gel (loaded as for B) stained with Coomassie Brilliant Blue R250.

The absence of the PsbW subunit strikingly reduced the extent of PSII core phosphorylation: D1 and D2, represented by the two bands around 30 kDa, were poorly phosphorylated in koPsbW (Fig. 3.9 B) compared to wild-type. The largest difference in phosphorylation between wild-type and koPsbW LHCII was in the band above 37 kDa, corresponding to CP43. CP43 was heavily phosphorylated under all light conditions in wild-type, whilst in the koPsbW mutant, phospho-threonine immunostaining was weak. PSII core phosphorylation is performed in

*Arabidopsis* mainly by the kinase STN8, whereas LHCII is phosphorylated by STN7 [55-57]. To exclude the possibility that PsbW is only indirectly involved in the observed changes in the phosphorylation pattern by affecting the amount of kinases in the cells, we quantified levels of STN8 and STN7 protein kinases in the thylakoid membrane preparations using specific antisera (Fig. Supplementary Information 3.2). The amount of each protein kinase was comparable between wild-type and koPsbW, indicating that the reduced PSII core phosphorylation observed in the mutant is not due to a lack of protein kinases.

### *Transgenic plants lacking PsbW show modest changes in photoinhibition and recovery*

PSII core phosphorylation is important in the turnover of the D1 reaction center protein, and the recycling of photoinhibited PSII complexes in the grana membranes is dependent on their dephosphorylation [58]. Since PsbW protein is important for PSII core phosphorylation and PSII-LHCII supercomplex stabilization in the grana membranes, it is likely to protect PSII from photo-damage under high light and/or to aid PSII recovery under low light. To test this, leaves from five-week old wild-type and koPsbW plants were exposed to continuous high light ( $900 \mu\text{mol photon m}^{-2} \text{s}^{-1}$ ) for 22 hours, followed by low light ( $10 \mu\text{mol photon m}^{-2} \text{s}^{-1}$ ) for another 22 hours. Changes in  $F_v/F_m$  fluorescence ratios and protein abundance in isolated thylakoid membranes were measured. Photodamage induced by high light was slightly enhanced in koPsbW plants, depicted by a decline in the  $F_v/F_m$  ratio from 0.78 to 0.63, in contrast to wild-type where the ratio only decreased from 0.82 to 0.71 (Fig. 3.10 A). These changes were corroborated by immunological analyses: Levels of PSII core proteins D1, D2 and PsbO from wild-type leaves were lower after high light treatment (HL22) compared to dark-adapted leaves (Fig. 3.10 B). Interestingly, in the koPsbW mutant, the D1 protein and to a lesser extent D2 were degraded to a greater degree than in wild-type leaves (Fig. 3.10 B). According to fluorescence measurements, low light treatment was sufficient for recovery in wild-type plants where the  $F_v/F_m$  ratio returned to 0.80, whereas in the koPsbW mutant, a lower final  $F_v/F_m$  value of 0.74 demonstrated that recovery was compromised (Fig. 3.10 A). This was accompanied by reduced amounts of PSII core protein subunits, particularly D1, which was present at levels below wild-type D1 and was decreased following low light treatment compared with dark pre-treatment (Fig. 3.10 B). Interestingly, during recovery under low light, koPsbW samples exhibited degradation fragments that were immunostained by antibodies directed against the reaction center subunits D1 and D2, suggesting an imbalance in post-translational modification.

# Role of *PsbW* protein in macro-organisation

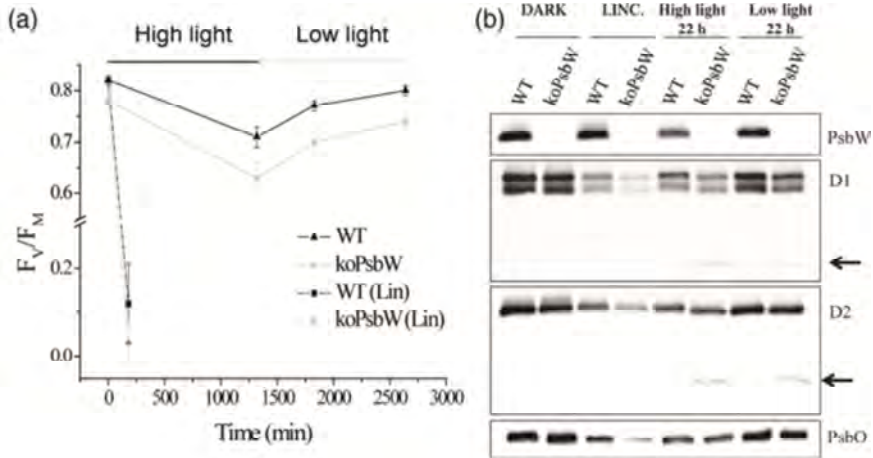


**Figure 3.10. Time course analysis of PSII photoinhibition.** (A) Detached leaves of wild-type and *koPsbW* plants were exposed to high light ( $900 \mu\text{mol photons m}^{-2} \text{s}^{-1}$ ) for 22 hours, followed by low light treatment ( $10 \mu\text{mol photons m}^{-2} \text{s}^{-1}$ ) for 22 hours at room temperature. The rate of photoinhibition and recovery was measured by the changes of the maximum quantum yield of PSII ( $F_v/F_m$ ). In addition, leaves were treated with high light in the presence of lincomycin ( $1.25 \text{ mM}$ ) for 3 hours to measure protein degradation in the absence of repair. (B) Immunodetection with specific antibodies against PsbW, D1, D2 and PsbO to monitor the extent of PSII degradation under high light, in the presence or absence of lincomycin, and recovery under low light. Samples were loaded based upon equal chlorophyll ( $0.35 \mu\text{g}$  per lane). Note the accumulation of protein degradation fragments marked by arrows.

Lincomycin inhibits *de novo* synthesis of plastid-encoded repair proteins and thus facilitates the study of photodamage in the absence of repair. As expected, following three hours of high light treatment,  $F_v/F_m$  ratios fell to 0.13 in wild-type and close to 0 in the mutant (Fig. 3.10 A). Levels of D1, D2 and PsbO were significantly lower in the presence of lincomycin, particularly for *koPsbW* (Fig. 3.10 B), indicating that PSII core protein degradation was markedly increased. Interestingly, exposure to lincomycin for 3 hours had little effect on the turnover of the PsbW protein (Fig. 3.10 B, LINC), which is nuclear-encoded and only after high-light treatment for 22 hours (Fig. 3.10 B, HL22) was the PsbW protein significantly degraded, in accordance with previous observations by [59]. Thus, the PsbW protein indeed affects the extent of PSII photo-damage under high light and/or PSII recovery under low light.

### 3.5 Discussion

#### *PSII-LHCII supercomplexes are destabilized in plants lacking the PsbW protein*

All earlier studies on the PsbW protein have been performed on antisense plants with variable residual amounts of the PsbW protein. Here, we report the first analyses of *Arabidopsis* knock-out plants completely lacking the PsbW protein. Our results conclusively show that the PsbW protein is critical for the stabilization of the PSII-LHCII supercomplexes located in the granal thylakoid membrane. All our efforts to isolate any type of PSII-LHCII supracomplex from koPsbW plants failed: Neither mild solubilisation followed by BN-PAGE (Fig. 3.4), nor density gradient ultracentrifugation (Fig. 3.5 A) could resolve any PSII-LHCII supercomplexes from thylakoid membranes of plants lacking PsbW. Furthermore, electron microscopy analyses showed that instead of the normal formation of semi-crystalline arrays of PSII-LHCII supercomplexes found in wild-type samples, koPsbW plants display random aggregates (Fig. 3.9 B). Using non-invasive CD spectroscopy of intact leaves we detected changes in the long-range order of PSII macro-organization in koPsbW plants (Fig. 3.2). Thus, using various biochemical and biophysical analyses on transgenic plants, we were able to conclusively show that PsbW must be present for PSII-LHCII supercomplex stabilization.

Antisense plants with strongly reduced levels of PsbW protein were also analysed. Compared to wild-type plants, these asPsbW plants displayed a much milder effects than the knock-out plants, which strongly supports the observed effects to be dependent on the reduction of the PsbW protein content in the plants, and not a secondary effect due to random insertion of DNA. Shi *et al.* [21] reported that the amount of PSII reaction centre proteins was reduced by almost 40% in PsbW antisense plants. In our hands no reduction of PSII or PSI proteins was detected and the PSI/PSII ratio was unchanged in both antisense and koPsbW plants. Instead our data show that plants lacking the PsbW protein are somewhat more susceptible to photoinhibition (Fig. 3.10) with the consequence that D1 and D2 degradation is increased. We therefore assume that the antisense plants used in the earlier work could have been somewhat stressed, which would have led to the reduction of the reaction centre protein content.

#### *PSII function and electron transport are slightly impaired in koPsbW transgenic plants*

Despite the changes in PSII-LHCII supercomplex organization in the koPsbW plants, chloroplast infrastructure resembled that of wild-type plants (Fig.

## *Role of PsbW protein in macro-organisation*

3.9 A). This indicates that the stabilization of PSII-LHCII super-complexes and the formation of semi-crystalline macrodomains of PSII supercomplexes is not a prerequisite for grana formation of the thylakoid membrane. In addition, no changes were measured in protein composition, pigment complex organization, PSII/PSI ratio (Table 3.1), chlorophyll content or chlorophyll *a/b* ratio. Despite these observations steady state measurements of oxygen evolution by PSII were decreased by 15-30% (Table 3.1), the S2-multiline signal was reduced by 50%, in which the formation of  $Q_A\text{-Fe}^{2+}$  signal was reduced by 30% (Table Supplementary Information 3.2), and the midpoint redox potential of the  $Q_A$  site was altered (Fig. 3.8) in comparison to wild type. The latter indicates that PSII electron transport is affected in the absence of PsbW despite the lack of an obvious phenotype in koPsbW plants and the antisense asPsbW mutants (Fig. Supplementary Information 3.1). These data supports the conclusion that the primary PSII function and composition is slightly compromised when the PSII-LHCII supercomplex organization is modified in absence of the PsbW protein.

### *How can the absence of one LMW protein affect PSII macro-organization?*

In order to have such a major effect on PSII-LHCII supercomplex formation, the low molecular weight PsbW protein must occupy a highly specific position within the PSII complex. According to the proposed model based on EM imaging analysis, the PSII-LHCII supercomplex ( $C_2S_2M_2$ ) of higher plants consists of a dimeric core ( $C_2$ ), two tightly bound LHCII trimers ( $S_2$ ) and two moderately bound trimers ( $M_2$ ) containing an unidentified small helix, located in close proximity to the S-trimer and CP26, which was assigned as an unknown “X” protein [16]. In addition, based on EM projections, the structure of the PSII-LHCII supercomplex proposed by [15] accommodates an additional small protein subunit in between CP47 of one of the dimeric PSII core complexes ( $C_2$ ) and CP24. We hypothesize that PsbW could be located in one of these regions, in close proximity to the minor antenna. In this position, PsbW could fulfill its important role in supercomplex stabilization as well as participating in contacts between different PSII-LHCII supercomplexes in the grana membranes.

An exclusive, conserved motif in the amino acid sequence of PsbW has been recognized at the C-terminus, facing the stromal side of the thylakoid membrane [18]. Of the 14 C-terminal stromal-exposed amino acids, five consecutive amino acids are negatively-charged (EEDEE), a feature that has not been observed in any other LMW protein of PSII [9]. This highly negatively charged primary fragment is well conserved in PsbW orthologues of all higher plants examined to date. Given the

net negative charge of the thylakoid membrane [60], a strong repulsive force presumably pushes this negative stretch out of the membrane, where it may provide a signal that influences protein-protein interactions within the thylakoid membrane. Clearly this feature warrants further characterization, and the generation of transgenic plants containing PsbW with modified C-terminal negative motifs could help to elucidate its function.

### *Why do higher plants form ordered rows of semi-crystalline macrodomains of PSII-LHCII supercomplexes?*

The removal of the PsbW protein affects the formation of stable PSII-LHCII supercomplexes conforming to the typical well-ordered rows of semi-crystalline macrodomains of PSII supercomplexes in the thylakoid grana. Thus, the koPsbW mutant enables us to address the role of such ordered domains in higher plant grana membranes. The data presented here point toward several important functions of these ordered domains:

- Optimisation of energy transfer between different PSII complexes

The absorbed light energy reaching a closed “occupied” PSII is not as efficiently transferred to the next photosystem in the koPsbW mutant, but instead is re-emitted as fluorescence. Basal chlorophyll fluorescence was increased in the koPsbW mutant (Fig. 3.9, Table 3.1) and energy transfer between PSII units was reduced, although differences in antenna size were not observed (Fig. 3.2). Thus, the absorption and utilisation of light energy is less efficient in disordered PSII complexes.

- Regulation of state transition of energy distribution

The lack of ordered rows of PSII supercomplexes did not influence state transitions. However, the transiently accumulated reduced  $Q_A^-$  pool seemed to relax more promptly during state 1 to state 2 transitions, reaching the steady state higher fluorescence level ( $F_S$ ) faster in the mutant. The latter indicates faster rates of which PQ undergoes redox changes. These changes observed in  $F_S$ , did not affect the extent of inducible LHCII phosphorylation in state II or the extent of transitions as measured by  $F_{m1}/F_{m2}$ . The latter indicates that the mobile LHCII experienced state transitions.

- Optimisation of the interaction between PSII and the PQ pool

The changes observed in the steady state level of chlorophyll fluorescence may well be related to changes in the redox properties of the PQ pool of the mutant thylakoid membranes. The reduction of the PQ pool in dark-adapted koPsbW thylakoid membranes correlated well with the extent of LHCII phosphorylation. Furthermore, thermoluminescence measurements of dark-adapted samples indicated higher

## *Role of PsbW protein in macro-organisation*

activation energy for the recombination of  $Q_A^-/S_2$  pairs in the mutant and a lower pool of recombining  $Q_B^-/S_{2,3}$  pairs, which seem to lose electrons faster, presumably to the PQ pool.

- Facilitation of PSII protein phosphorylation

A dramatic reduction in PSII core phosphorylation was observed in koPsbW plants. Altered and/or lower core phosphorylation has been reported to result from knock-out or antisense inhibition of other small PSII subunits in the chloroplast, e.g. PsbZ [61], PsbI [48], PsbM [62], PsbTc [63] and PsbX [64]. Two plausible scenarios could explain decreased PSII core protein phosphorylation; a reduction in the steady-state amount of PSII core subunits (as observed, for instance, in tobacco PsbI knock-out plants or PsbX antisense mutants), or changes in the PSII macro-organization, as in tobacco PsbZ, PsbTc or PsbM knock-out plants. The latter proteins are known to be intrinsic subunits of PSII, conserved in both cyanobacteria and the chloroplast. The PsbZ protein influences the interaction of the minor antenna with PSII dimers, while the location of PsbTc and PsbM has been proposed to be at the interface of the PSII dimer according to the crystal model [4, 65]. Thus, a lack of these specific subunits may affect the stability or formation of PSII dimers and/or the association of the minor antenna and consequently alter PSII macro-organization. In a similar manner, the PsbW protein may participate in the stabilization of PSII-LHCII supercomplexes in the grana stacks. A lack of ordered rows of PSII complexes in the absence of PsbW may affect specific site recognition by the protein kinase STN8 within the PSII core leading to a lower phosphorylation rate.

- Reduction of photoinhibition for fast and optimal repair

In the absence of PsbW, plants are moderately photodamaged by high light, and recover more slowly in low light than wild-type plants (Fig. 3.10 A). Such effects have been reported for several plants with mutations in LMW subunits, e.g. PsbTc [63], PsbI [48], PsbM [62] and PsbX [64]. Thus, macro-organizational changes of PSII may facilitate protease attack and repair and recycling may be delayed by the destabilized PSII macro-structure. Interestingly, small fragments of the subunits D1 and D2 accumulated during the recovery phase in the mutant, indicating abnormal post-translational processing of the main PSII core subunits undergoing repair.

The present work shows that PsbW knock-out and antisense plants are capable of photo-autotrophic growth, suggesting a non-essential role for this subunit in photosynthetic eukaryotes. However, the evolutionary origin of the PsbW subunit in the higher plant chloroplasts could have taken place during the evolution of land plants in conjunction with the presence of membrane located light-harvesting antenna pigment proteins. This low molecular weight protein may have enabled the

fine-tuning of assembly and/or stabilization of PSII-LHCII supercomplexes, and thus the formation of ordered rows of semi-crystalline macrodomains of PSII-LHCII supracomplexes within the grana stack membranes, to optimize photosynthesis for the land living eukaryotic plants facing large and fast changing environmental conditions with the need for effective regulation.

## 3.7 Acknowledgements

We thank Lenore Johansson for her assistance with the TEM work. This work was supported by grants from the Swedish Research Council for Environment, Agricultural Sciences and Spatial Planning (FORMAS, to W.P.S.), the Swedish Research Council (VR, to F.M., C.F. and W.P.S.) and the Cost action FA0603. We thank the Wallenberg and the Kempe Foundations for financial support.

## 3.8 Reference list

- [1] **Zouni, A., Witt, H.T., Kern, J., Fromme, P., Krauss, N., Saenger, W., Orth, P.**, Crystal structure of photosystem II from *Synechococcus elongatus* at 3.8 angstrom resolution, *Nature*, 409 (2001) 739-743.
- [2] **Kamiya, N., Shen, J.R.**, Crystal structure of oxygen-evolving photosystem II from *Thermosynechococcus vulcanus* at 3.7-angstrom resolution, *P Natl Acad Sci USA*, 100 (2003) 98-103.
- [3] **Ferreira, K.N., Iverson, T.M., Maghlaoui, K., Barber, J., Iwata, S.**, Architecture of the photosynthetic oxygen-evolving center, *Science*, 303 (2004) 1831-1838.
- [4] **Loll, B., Kern, J., Saenger, W., Zouni, A., Biesiadka, J.**, Towards complete cofactor arrangement in the 3.0 angstrom resolution structure of photosystem II, *Nature*, 438 (2005) 1040-1044.
- [5] **Muh, F., Renger, T., Zouni, A.**, Crystal structure of cyanobacterial photosystem II at 3.0 angstrom resolution: A closer look at the antenna system and the small membrane-intrinsic subunits, *Plant Physiol. Biochem.*, 46 (2008) 238-264.
- [6] **Adachi, H., Umena, Y., Enami, I., Henmi, T., Kamiya, N., Shen, J.R.**, Towards structural elucidation of eukaryotic photosystem II: Purification, crystallization and preliminary X-ray diffraction analysis of photosystem II from a red alga, *Biochim. Biophys. Acta*, 1787 (2009) 121-128.
- [7] **Guskov, A., Kern, J., Gabdulkhakov, A., Broser, M., Zouni, A., Saenger, W.**, Cyanobacterial photosystem II at 2.9-angstrom resolution and the role of quinones, lipids, channels and chloride, *Nat. Struct. Mol. Biol.*, 16 (2009) 334-342.
- [8] **Kashino, Y., Lauber, W.M., Carroll, J.A., Wang, Q.J., Whitmarsh, J., Satoh, K., Pakrasi, H.B.**, Proteomic analysis of a highly active photosystem II preparation from the cyanobacterium *Synechocystis* sp PCC 6803 reveals the presence of novel polypeptides, *Biochemistry*, 41 (2002) 8004-8012.
- [9] **Shi, L.X., Schroder, W.P.**, The low molecular mass subunits of the photosynthetic supracomplex, photosystem II, *Biochim. Biophys. Acta*, 1608 (2004) 75-96.
- [10] **Rhee, K.H., Morris, E.P., Zheleva, D., Hankamer, B., Kuhlbrandt, W., Barber, J.**, Two-dimensional structure of plant photosystem II at 8-angstrom resolution, *Nature*, 389 (1997) 522-526.
- [11] **Nield, J., Barber, J.**, Refinement of the structural model for the Photosystem II supercomplex of higher plants, *Biochim. Biophys. Acta*, 1757 (2006) 353-361.
- [12] **Boekema, E.J., Hankamer, B., Bald, D., Kruij, J., Nield, J., Boonstra, A.F., Barber, J., Rogner, M.**, Supramolecular structure of the Photosystem II complex from green plants and cyanobacteria, *P Natl Acad Sci USA*, 92 (1995) 175-179.

# Role of PsbW protein in macro-organisation

- [13] **Sidler, W.A.**, Phycobilisome and Phycobiliprotein Structures, in: D. Bryant (Ed.) *The Molecular Biology of Cyanobacteria*, Springer Netherlands, 2004, pp. 139-216.
- [14] **Jansson, S.**, The light-harvesting chlorophyll a/b binding-proteins, *Biochim. Biophys. Acta*, 1184 (1994) 1-19.
- [15] **Caffarri, S., Kouril, R., Kereiche, S., Boekema, E.J., Croce, R.**, Functional architecture of higher plant photosystem II supercomplexes, *EMBO J.*, 28 (2009) 3052-3063.
- [16] **Dekker, J.P., Boekema, E.J.**, Supramolecular organization of thylakoid membrane proteins in green plants, *Biochim. Biophys. Acta*, 1706 (2005) 12-39.
- [17] **Chow, W.S., Kim, E.H., Horton, P., Anderson, J.M.**, Granal stacking of thylakoid membranes in higher plant chloroplasts: the physicochemical forces at work and the functional consequences that ensue, *Photochem. Photobiol. Sci.*, 4 (2005) 1081-1090.
- [18] **Irrgang, K.D., Shi, L.X., Funk, C., Schroder, W.P.**, A nuclear-encoded subunit of the photosystem II reaction center, *J. Biol. Chem.*, 270 (1995) 17588-17593.
- [19] **Shi, L.X., Schroder, W.P.**, Compositional and topological studies of the PsbW protein in spinach thylakoid membrane, *Photosynth Res.*, 53 (1997) 45-53.
- [20] **Bishop, C.L., Purton, S., Nugent, J.H.A.**, Molecular analysis of the Chlamydomonas nuclear gene encoding PsbW and demonstration that PsbW is a subunit of photosystem II, but not photosystem I, *Plant Mol. Biol.*, 52 (2003) 285-289.
- [21] **Shi, L.X., Lorkovic, Z.J., Oelmuller, R., Schroder, W.P.**, The low molecular mass PsbW protein is involved in the stabilization of the dimeric photosystem II complex in *Arabidopsis thaliana*, *J. Biol. Chem.*, 275 (2000) 37945-37950.
- [22] **Rokka, A., Suorsa, M., Saleem, A., Battchikova, N., Aro, E.M.**, Synthesis and assembly of thylakoid protein complexes: multiple assembly steps of photosystem II, *Biochem. J.*, 388 (2005) 159-168.
- [23] **Thidholm, E., Lindstrom, V., Tissier, C., Robinson, C., Schroder, W.P., Funk, C.**, Novel approach reveals localisation and assembly pathway of the PsbS and PsbW proteins into the photosystem II dimer, *FEBS Lett.*, 513 (2002) 217-222.
- [24] **Granvogel, B., Zoryan, M., Ploescher, M., Eichacker, L.A.**, Localization of 13 one-helix integral membrane proteins in photosystem II subcomplexes, *Anal. Biochem.*, 383 (2008) 279-288.
- [25] **Sessions, A., Burke, E., Presting, G., Aux, G., McElver, J., Patton, D., Dietrich, B., Ho, P., Bacwaden, J., Ko, C., Clarke, J.D., Cotton, D., Bullis, D., Snell, J., Miguel, T., Hutchison, D., Kimmerly, B., Mitzel, T., Katagiri, F., Glazebrook, J., Law, M., Goff, S.A.**, A high-throughput Arabidopsis reverse genetics system, *Plant Cell*, 14 (2002) 2985-2994.
- [26] **Alonso, J.M., Stepanova, A.N., Leisse, T.J., Kim, C.J., Chen, H., Shinn, P., Stevenson, D.K., Zimmerman, J., Barajas, P., Cheuk, R., Gadriab, C., Heller, C., Jeske, A., Koesema, E., Meyers, C.C., Parker, H., Prednis, L., Ansari, Y., Choy, N., Deen, H., Geralt, M., Hazari, N., Hom, E., Karnes, M., Mulholland, C., Ndubaku, R., Schmidt, I., Guzman, P., Aguilar-Henonin, L., Schmid, M., Weigel, D., Carter, D.E., Marchand, T., Risseuw, E., Brogden, D., Zeko, A., Crosby, W.L., Berry, C.C., Ecker, J.R.**, Genome-wide insertional mutagenesis of *Arabidopsis thaliana*, *Science*, 301 (2003) 653-657.
- [27] **Noren, H., Svensson, P., Andersson, B.**, Auxiliary photosynthetic functions of *Arabidopsis thaliana* - Studies in vitro and in vivo, *Bioscience Rep.*, 19 (1999) 499-509.
- [28] **Porra, R.J., Thompson, W.A., Kriedemann, P.E.**, Determination of accurate extinction coefficients and simultaneous-equations for assaying chlorophyll a and chlorophyll b extracted with 4 different solvents - Verification of the concentration of chlorophyll standards by atomic-absorption spectroscopy, *Biochim. Biophys. Acta*, 975 (1989) 384-394.
- [29] **Arellano, J.B., Schroder, W.P., Sandmann, G., Chueca, A., Baron, M.**, Removal of nuclear contaminants and of nonspecifically photosystem II bound copper from photosystem II preparations, *Physiol. Plant.*, 91 (1994) 369-374.
- [30] **Schagger, H., Vonjagow, G.**, Native electrophoresis of membrane-proteins for detection of alterations in human complex I, complex II, complex III, complex IV and complex V, *Biol Chem H-S*, 372 (1991) 552-552.

- [31] **Cline, K., Mori, H.**, Thylakoid delta pH-dependent precursor proteins bind to a cpTatC-Hcf106 complex before Tha4-dependent transport, *J. Cell Biol.*, 154 (2001) 719-729.
- [32] **Peter, G.F., Takeuchi, T., Philip Thornber, J.**, Solubilization and two-dimensional electrophoretic procedures for studying the organization and composition of photosynthetic membrane polypeptides, *Methods*, 3 (1991) 115-124.
- [33] **Maxwell, K., Johnson, G.N.**, Chlorophyll fluorescence - a practical guide, *J. Exp. Bot.*, 51 (2000) 659-668.
- [34] **Koblizek, M., Kaftan, D., Nedbal, L.**, On the relationship between the non-photochemical quenching of the chlorophyll fluorescence and the photosystem II light harvesting efficiency. A repetitive flash fluorescence induction study, *Photosynth Res.*, 68 (2001) 141-152.
- [35] **Damkjaer, J.T., Kereiche, S., Johnson, M.P., Kovacs, L., Kiss, A.Z., Boekema, E.J., Ruban, A.V., Horton, P., Jansson, S.**, The photosystem II light-harvesting protein Lhcb3 affects the macrostructure of photosystem II and the rate of state transitions in Arabidopsis, *Plant Cell*, 21 (2009) 3245-3256.
- [36] **Demeter, S., Vass, I., Horvath, G., Laufer, A.**, Charge accumulation and recombination in photosystem II studied by thermo-luminescence. 2. Oscillation of the C-band induced by flash excitation, *Biochim. Biophys. Acta*, 764 (1984) 33-39.
- [37] **Keskitalo, J., Bergquist, G., Gardestrom, P., Jansson, S.**, A cellular timetable of autumn senescence, *Plant Physiol.*, 139 (2005) 1635-1648.
- [38] **Kovacs, L., Damkjaer, J.T., Kereiche, S., Illoia, C., Ruban, A.V., Boekema, E.J., Jansson, S., Horton, P.**, Lack of the light-harvesting complex CP24 affects the structure and function of the grana membranes of higher plant chloroplasts, *Plant Cell*, 18 (2006) 3106-3120.
- [39] **Mamedov, F., Danielsson, R., Gadjeva, R., Albertsson, P.A., Styring, S.**, EPR characterization of photosystem II from different domains of the thylakoid membrane, *Biochemistry*, 47 (2008) 3883-3891.
- [40] **Danielsson, R., Albertsson, P.A., Mamedov, F., Styring, S.**, Quantification, of photosystem I and II in different parts of the thylakoid membrane from spinach, *Biochim. Biophys. Acta*, 1608 (2004) 53-61.
- [41] **Haldrup, A., Jensen, P.E., Lunde, C., Scheller, H.V.**, Balance of power: a view of the mechanism of photosynthetic state transitions, *Trends Plant Sci.*, 6 (2001) 301-305.
- [42] **Havaux, M., Dall'Osto, L., Cuine, S., Giuliano, G., Bassi, R.**, The effect of zeaxanthin as the only xanthophyll on the structure and function of the photosynthetic apparatus in *Arabidopsis thaliana*, *J. Biol. Chem.*, 279 (2004) 13878-13888.
- [43] **de Bianchi, S., Dall'Osto, L., Tognon, G., Morosinotto, T., Bassi, R.**, Minor antenna proteins CP24 and CP26 affect the interactions between photosystem II Subunits and the electron transport rate in grana membranes of Arabidopsis, *Plant Cell*, 20 (2008) 1012-1028.
- [44] **Keller, D., Bustamante, C.**, Theory of the interaction of light with large inhomogenous molecular aggregates 2. Psi-type circular dichroism, *J Chem Phys*, 84 (1986) 2972-2980.
- [45] **Garab, G., Wells, S., Finzi, L., Bustamante, C.**, Helically Organized Macroaggregates of Pigment Protein Complexes in Chloroplasts - Evidence from Circular Intensity Differential Scattering, *Biochemistry*, 27 (1988) 5839-5843.
- [46] **Finzi, L., Bustamante, C., Garab, G., Juang, C.B.**, Direct observation of large chiral domains in chloroplast thylakoid membranes by differential polarization microscopy, *P Natl Acad Sci USA*, 86 (1989) 8748-8752.
- [47] **Boekema, E.J., van Breemen, J.F.L., van Roon, H., Dekker, J.P.**, Arrangement of photosystem II supercomplexes in crystalline macrodomains within the thylakoid membrane of green plant chloroplasts, *J. Mol. Biol.*, 301 (2000) 1123-1133.
- [48] **Schwenkert, S., Umate, P., Dal Bosco, C., Volz, S., Mlcochova, L., Zoryan, M., Eichacker, L.A., Ohad, I., Herrmann, R.G., Meurer, J.**, PsbI affects the stability, function, and phosphorylation patterns of photosystem II assemblies in tobacco, *J. Biol. Chem.*, 281 (2006) 34227-34238.
- [49] **Bjorkman, O., Demmig, B.**, Photon yield of O<sub>2</sub> evolution and chlorophyll fluorescence characteristics at 77K among vascular plants of diverse origins, *Planta*, 170 (1987) 489-504.

# Role of PsbW protein in macro-organisation

- [50] **Stirbet, A., Govindjee,** On the relation between the Kautsky effect (chlorophyll a fluorescence induction) and Photosystem II: Basics and applications of the OJIP fluorescence transient, *J. Photochem. Photobiol. B: Biol.*, 104 (2011) 236-257.
- [51] **Lavergne, J., Trissl, H.W.,** Theory of fluorescence induction in photosystem II - Derivation of analytical Expressions in a model including exciton-radical-pair equilibrium and restricted energy-transfer between photosynthetic units, *Biophys. J.*, 68 (1995) 2474-2492.
- [52] **Rutherford, A.W., Crofts, A.R., Inoue, Y.,** Thermo-luminescence as a probe of photosystem II photochemistry - the origin of the flash-induced glow peaks, *Biochim. Biophys. Acta*, 682 (1982) 457-465.
- [53] **Allen, J.F., Forsberg, J.,** Molecular recognition in thylakoid structure and function, *Trends Plant Sci.*, 6 (2001) 317-326.
- [54] **Ruban, A.V., Johnson, M.P.,** Dynamics of higher plant photosystem cross-section associated with state transitions, *Photosynth Res.*, 99 (2009) 173-183.
- [55] **Bellafore, S., Barneche, F., Peltier, G., Rochaix, J.D.,** State transitions and light adaptation require chloroplast thylakoid protein kinase STN7, *Nature*, 433 (2005) 892-895.
- [56] **Bonardi, V., Pesaresi, P., Becker, T., Schleiff, E., Wagner, R., Pfannschmidt, T., Jahns, P., Leister, D.,** Photosystem II core phosphorylation and photosynthetic acclimation require two different protein kinases, *Nature*, 437 (2005) 1179-1182.
- [57] **Vainonen, J.P., Hansson, M., Vener, A.V.,** STN8 protein kinase in *Arabidopsis thaliana* is specific in phosphorylation of photosystem II core proteins, *J. Biol. Chem.*, 280 (2005) 33679-33686.
- [58] **Rintamaki, E., Kettunen, R., Aro, E.M.,** Differential D1 dephosphorylation in functional and photodamaged photosystem II centers - Dephosphorylation is a prerequisite for degradation of damaged D1, *J. Biol. Chem.*, 271 (1996) 14870-14875.
- [59] **Hagman, A., Shi, L.X., Rintamaki, E., Andersson, B., Schroder, W.P.,** The nuclear-encoded PsbW protein subunit of photosystem II undergoes light-induced proteolysis, *Biochemistry*, 36 (1997) 12666-12671.
- [60] **Barber, J.,** Influence of surface-charges on thylakoid structure and function, *Annu. Rev. Plant Physiol. Plant Mol. Biol.*, 33 (1982) 261-295.
- [61] **Swiatek, M., Kuras, R., Sokolenko, A., Higgs, D., Olive, J., Cinque, G., Muller, B., Eichacker, L.A., Stern, D.B., Bassi, R., Herrmann, R.G., Wollman, F.A.,** The chloroplast gene *ycf9* encodes a photosystem II (PSII) core subunit, PsbZ, that participates in PSII supramolecular architecture, *Plant Cell*, 13 (2001) 1347-1367.
- [62] **Umate, P., Schwenkert, S., Karbat, I., Dal Bosco, C., Mlcochova, L., Volz, S., Zer, H., Herrmann, R.G., Ohad, I., Meurer, J.,** Deletion of PsbM in tobacco alters the Q(B) site properties and the electron flow within photosystem II, *J. Biol. Chem.*, 282 (2007) 9758-9767.
- [63] **Umate, P., Fellerer, C., Schwenkert, S., Zoryan, M., Eichacker, L.A., Sadanandam, A., Ohad, I., Herrmann, R.G., Meurer, J.,** Impact of PsbTc on forward and back electron flow, assembly, and phosphorylation patterns of photosystem II in tobacco, *Plant Physiol.*, 148 (2008) 1342-1353.
- [64] **Garcia-Cerdan, J.G., Sveshnikov, D., Dewez, D., Jansson, S., Funk, C., Schroder, W.P.,** Antisense inhibition of the PsbX protein affects PSII integrity in the higher plant *Arabidopsis thaliana*, *PCP*, 50 (2009) 191-202.
- [65] **Henmi, T., Iwai, M., Ikeuchi, M., Kawakami, K., Shen, J.R., Kamiya, N.,** X-ray crystallographic and biochemical characterizations of a mutant photosystem II complex from *Thermosynechococcus vulcanus* with the *psbTc* gene inactivated by an insertion mutation, *J. Synchrotron Radiat.*, 15 (2008) 304-307.

## 3.9 Supplementary Information



**Figure Supplementary Information 3.1.** Photograph of wild-type *Col-O* (WT), *PsbW* knock-out (*koPsbW*) and *PsbW* antisense (*asPsbW*) plants grown in Murashige and Skoog media agar plates showing that deleting or decreasing *PsbW* has no visible effect on phenotype.

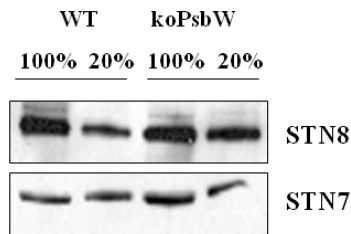


**Figure Supplementary Information 3.2.** Immunodetection of protein kinases *STN7* and *STN8* in thylakoid membranes of dark-adapted leaves harvested from wild-type and *koPsbW*. 100% corresponds to 5  $\mu$ g of chlorophyll.

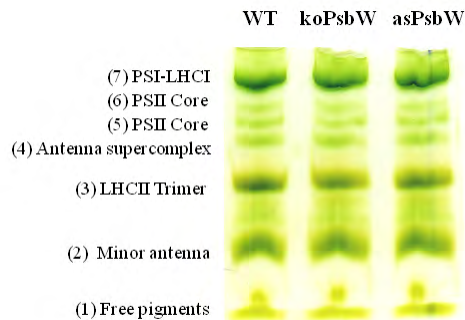


**Figure Supplementary Information 3.3.** Characterization of the thylakoid membrane chlorophyll-containing protein complexes isolated from WT, *asPsbW* and *koPsbW*. Separation of the protein complexes in the thylakoid membrane by non-denaturing Deriphat-PAGE. Bands were identified according to [1]. Loading corresponds to 15  $\mu$ g of total chlorophyll.

# *Role of PsbW protein in macro-organisation*

**Table Supplementary Information 3.1.**

Fluorescence Illumination (PAR) <sup>1</sup>	Wild-type		koPsbW	
	100	500	100	500
ΦPSII	0.73 ± 0.01 <sup>2</sup>	0.52 ± 0.01	0.69 ± 0.01	0.47 ± 0.05
qP	0.95 ± 0.01	0.78 ± 0.03	0.95 ± 0.01	0.78 ± 0.02
NPQ	0.26 ± 0.02	0.91 ± 0.07	0.23 ± 0.01	0.96 ± 0.30

<sup>1</sup>Illumination units are  $\mu\text{mol photons m}^{-2} \text{s}^{-1}$ .

<sup>2</sup>Errors reported are plus and minus 1 standard deviation (n=5).

The photosynthetic properties of koPsbW plants were examined in more detail by measuring other fluorescence parameters [2], including the operational PSII quantum yield (ΦPSII), photochemical quenching (qP) and non-photochemical quenching (NPQ) (Table 3.1). ΦPSII defines the efficiency to use absorbed light energy for PSII photochemistry under continuous illumination. Under photon flux densities of 100 and 500  $\mu\text{mol m}^{-2} \text{s}^{-1}$ , ΦPSII was slightly lower in the koPsbW plants than in wild-type (Table 3.1), possibly due to a slower rate of PSII linear electron transport in the mutant. However, the qP parameter, indicating the proportion of open PSII reaction centers under continuous illumination, was not considerably different in the koPsbW plants compared to wild-type. Similarly, NPQ, which is related to the antenna heat dissipation, was unchanged in koPsbW compared with wild type plants under these conditions as well as under illumination of 900  $\mu\text{mol m}^{-2} \text{s}^{-1}$  (data not shown).

**Table Supplementary Information 3.2.**

	Wild-type	koPsbW
<b>EPR measurements<sup>1</sup></b>		
TyrD <sup>ox</sup>	100%	92%
S <sub>2</sub> state multiline signal	100%	47%
Q <sub>A</sub> Fe <sup>2+</sup> signal	100%	72%
Cytb <sub>559</sub> ox/red	40/60%	45/55%

<sup>1</sup>Induction and measurements of EPR signals were performed according to [3]. TyrD<sup>ox</sup> signal is normalised against chlorophyll, whilst the S<sub>2</sub> state multiline and Q<sub>A</sub>Fe<sup>2+</sup> signals were based on Photosystem II (TyrD<sup>ox</sup>). Oxidized (ox) and reduced (red) represent the low and high potential forms of Cytb<sub>559</sub> respectively.

Experimental error in the measurements is ± 5%.

EPR analysis of the electron transport components of PSII showed that neither TyrD<sup>ox</sup> nor the amount of oxidized and reduced Cytb<sub>559</sub> is changed in koPsbW plants. However, the Q<sub>A</sub>Fe<sup>2+</sup> interaction signal was decreased, in agreement with the thermoluminescence analysis (Fig. 3.8). Interestingly, the S<sub>2</sub> state multiline EPR signal of the water-oxidizing complex showed significant (50%) differences in

amplitude between wild-type and koPsbW preparations, most probably due to the double effect of less reducible  $Q_A$  and more mixed S state composition in the mutant before the signal induction.

[1] **de Bianchi, S., Dall'Osto, L., Tognon, G., Morosinotto, T., Bassi, R.**, Minor antenna proteins CP24 and CP26 affect the interactions between photosystem II Subunits and the electron transport rate in grana membranes of Arabidopsis, *Plant Cell*, 20 (2008) 1012-1028.

[2] **Maxwell, K., Johnson, G.N.**, Chlorophyll fluorescence - a practical guide, *J. Exp. Bot.*, 51 (2000) 659-668.

[3] **Mamedov, F., Danielsson, R., Gadjieva, R., Albertsson, P.A., Styring, S.**, EPR characterization of photosystem II from different domains of the thylakoid membrane, *Biochemistry*, 47 (2008) 3883-3891.

# Chapter 4

## ***The role of light-harvesting complex II in the macro-organisation of thylakoid membranes, as revealed by circular dichroism spectroscopy in vivo***

Tünde Tóth<sup>1,2</sup>, Neha Rai<sup>1</sup>, Attila Bóta<sup>3</sup>, Wolfgang P. Schröder<sup>4</sup>, Győző Garab<sup>1</sup>,  
Herbert van Amerongen<sup>2</sup>, Peter Horton<sup>5</sup>, László Kovács<sup>1</sup> *In preparation*

*1 Institute of Plant Biology, Biological Research Centre, Hungarian Academy of Sciences,  
Szeged, Hungary*

*2 Laboratory of Biophysics, Wageningen University, Wageningen, The Netherlands*

*3 Department of Biological Nanochemistry, Research Centre of Natural Sciences,  
Hungarian Academy of Sciences, Budapest, Hungary*

*4 Department of Chemistry, Umea Plant Science Centre (UPSC), Umea University, Umea,  
Sweden*

*5 Department of Molecular Biology and Biotechnology, University of Sheffield, Sheffield,  
United Kingdom*

### 4.1 Abstract

The chloroplast thylakoid membrane is a hierarchically ordered self-organised structure. Photosystem II (PSII) complexes localised in the grana thylakoids are associated with light-harvesting antenna complexes (LHCII) to form supercomplexes. Electron-microscopy studies have revealed that population of PSII supercomplexes can assemble into ordered arrays. However, the extent and importance of these PSII arrays *in vivo* have not been clarified, partly due to their substantial instability. Circular dichroism (CD) spectroscopy is a potentially useful non-invasive technique for studying the presence and properties of various macrostructures *in vivo*. Granal thylakoid membranes exhibit intense, non-conservative, psi-type CD bands, originating from long-range chiral order of chlorophyll and carotenoid chromophores, due to the presence of protein macrodomains. In order to gain insight into the origin of these psi-type CD bands and to correlate them with the macro-organization of protein complexes, we compared more than a dozen plant species from different habitats and taxonomic positions, and also studied the effect of altered membrane organization induced by mutations or modified environmental conditions. We show that all examined species share the main spectral features, exhibiting psi-type CD bands at around (+)506, (-)674 and (+)688 nm, but the relative intensities of these bands vary in a broad range between species. CD spectroscopy on intact leaves with different thylakoid protein compositions has also revealed that the formation of chiral macrodomains depends on the presence of PSII-LHCII supercomplexes and, in particular, on the protein composition of the light-harvesting antenna system. These data, along with earlier studies, demonstrate that CD spectroscopy can provide important information on the macro-organization of pigment-protein complexes in the leaves under physiological conditions.

### 4.2 Introduction

In oxygenic photosynthetic organisms photosynthetic energy conversion occurs in and around the thylakoid membranes. The thylakoids are unique assemblies of protein, pigment and lipid molecules arranged into a hierarchic, self-organized structure [1]. Photosynthetic energy conversion is performed by coordinated action of the membrane-associated Photosystem I (PSI), Photosystem II (PSII), the cytochrome *b<sub>6</sub>/f* complex and the ATP synthase. These evolutionarily well-conserved complexes show high sequence homology between cyanobacteria and higher plants. In order to increase the light-harvesting efficiency of the photosystems, they are associated with light harvesting antennae, which show

## Role of LHCII in thylakoid organisation

remarkable variability in nature. While cyanobacteria and red algae possess outer light-harvesting antenna complexes, the phycobilisomes, which are extrinsically connected to the photosystems, green algae and higher plants contain membrane-embedded light-harvesting complexes (LHCs). In green algae and higher plants the photosynthetic complexes are accommodated in the thylakoid membranes. PSII is found mainly in the stacked grana layers, whereas PSI is localized in the unstacked stroma membranes and the grana end-membranes [2, 3]. In these organisms the photosynthetic pigment-protein complexes are assembled into supercomplexes, comprised of core complexes and outer antennae, in order to optimise their functions [4, 5]. Most of the core proteins are encoded by the chloroplast genome, while the proteins of the LHC are nuclear-encoded [6]. Both PSI and PSII core protein-complexes contain only Chl *a* and carotenoids, while LHCI and LHCII proteins also contain Chl *b*.

In the PSI supercomplex of vascular plants the monomeric PSI core is associated with LHCI proteins encoded by the *lhca1-lhca5* genes. Four LHCI proteins form two functional heterodimers (Lhca1/4 and Lhca2/3), which are attached to PSI in a belt-shape organization [7, 8].

The PSII core complex consists of the reaction centre (RC) and the inner antenna proteins CP43 and CP47, along with several low molecular weight proteins. The core possesses a conservative structure for all oxygen-evolving organisms, but the outer antennae of PSII are much more dynamic and diverse [9]. The Chl *a/b*-containing LHCII proteins are encoded by a multi-gene family [10, 11]. In the PSII supercomplexes of higher plants the dimeric PSII cores are associated with two copies of each minor LHCII component (CP29, CP26 and CP24) and two to four LHCII trimers, depending on the physiological conditions [12]. The apoproteins of CP29, CP26 and CP24 are encoded by the *lhcb4*, *lhcb5* and *lhcb6* genes, respectively. The LHCII trimers are composed of the *lhcb1*, *lhcb2* and *lhcb3* gene products, but the exact ratio of these proteins in the trimers varies [13]. In the PSII supercomplex there are two high- and two medium-affinity binding sites for LHCII trimers, and the trimers bound to them are called S and M trimers, respectively [14]. Not all of these binding sites are necessarily occupied. According to the occupancy of these binding sites different types of PSII supercomplexes can be distinguished: C<sub>2</sub>S<sub>2</sub> when only the S trimers are present, and C<sub>2</sub>S<sub>2</sub>M<sub>1</sub> or C<sub>2</sub>S<sub>2</sub>M<sub>2</sub>, depending on the number of M trimers bound to the supercomplex [12]. Recent results indicate that *Arabidopsis thaliana* contains typically C<sub>2</sub>S<sub>2</sub>M<sub>1</sub> or C<sub>2</sub>S<sub>2</sub>M<sub>2</sub> complexes; however, a pool of additional, 'extra' LHCII trimers is also present, varying between one to four trimers in response to the intensity of growth light [15]. In the green alga *Chlamydomonas reinhardtii* the PSII supercomplex structure is different from the

one described for vascular plants. In this organism subunits of the LHCII trimers are encoded by *lhcbM1-M9* genes, and the cells also contain CP26 and CP29 proteins but no CP24. In the PSII supercomplex of *Chlamydomonas* an additional, so-called N trimer can be found at the position corresponding to that of CP24 in higher plants [16].

Cryo electron microscopy and negative staining electron microscopy of partially solubilised thylakoid membranes uncovered semi-crystalline structures in grana thylakoids [14, 17, 18]: about 7-10% of the recorded micrographs reveal PSII supercomplexes in long-range ordered domains [15, 19, 20]. These macro-arrays comprise long, parallel rows of PSII-LHCII supercomplexes, in which the PSII supercomplex subunits join together in a specific way. It was also shown that PSII arrays of adjacent membranes are connected via their stromal sides [14, 21]. The angle between the PSII rows in the two membranes has specific values [17], probably to warrant optimal overlap between the LHCII trimers. Moreover, under certain conditions the distance between the thylakoid membranes at the luminal side does not allow the luminal extrinsic PSII subunits of the adjacent membranes directly opposing to each other [17, 21]. To some extent this space limitation can also determine the relative position of PSII complexes in membrane pairs that are separated by the lumen, which, together with the order between stacked layers, might impose order on the entire granum.

In spite of this general organisation, structural diversity is present at every organisational level of the thylakoid membranes. Although the main features of PSII-LHCII supercomplexes and their higher associations are quite ubiquitous among green algae and higher plants, the antenna proteins of PSII vary in composition and macroassembly even within the same phylum. The evolutionary adaptation of species to different environmental conditions can be manifested at lower taxonomic levels. LHCs are encoded by several highly homologous but distinct genes belonging to the same multi-gene family. The different LHC components are represented at a high genetic redundancy in the genomes of various species [10, 22-24]. The expression of these genes varies per species and depends on the environmental conditions [13, 25-27]. Slight variations in the protein composition might result in altered supramolecular organisation of the photosynthetic complexes [17]. The various types of supercomplexes form ordered arrays with different spacing and dimensions [14, 17, 28]. The small- or large-spaced semi-crystalline domains superimposed at the adjacent layers of stacked membranes assume well-defined relative orientations. Modified macro-organisation can modulate the photosynthetic functions of the thylakoid membrane [29]. The diversity of these supramolecular structures indicates their role in the adaptation to

## Role of LHCII in thylakoid organisation

the natural habitats of different species and in the acclimation of plants to particular environments. Recent observations demonstrate that different environmental conditions favour the formation of certain types of macro-organisation [15, 30, 31], but the physiological relevance of these macro-structures has not been clarified yet. However, the investigation of the thylakoid membrane supramolecular organisation is quite challenging due to its substantial instability. The *in vivo* presence of these PSII macrodomains observed by electron microscopy is still under debate. For instance, low temperature and some other factors can induce artificial aggregation of proteins *in vitro* [32, 33]. However, based on the instability of these macro-structures to invasive sample preparations, a higher extent of semi-crystalline domains *in vivo* seems to be also plausible.

For these reasons, non-invasive spectroscopic methods that provide information on the macro-organisation of the complexes are of particular value. Circular dichroism (CD) spectroscopy is a useful tool to monitor the structural changes of pigment protein complexes *in vivo*. CD is defined as the difference between the absorption of left- and right-handed circularly polarised light by asymmetric (chiral) molecules and structures [34]. CD spectroscopy is widely used to study structure of photosynthetic pigment-containing complexes with Chl and carotenoid content [35-37]. The CD signal in the visible spectral region, resulting from short-range excitonic interactions of chromophores, is characteristic for isolated pigment-protein complexes, and it is sensitive to minor variations in the distance and relative orientation of the interacting transition dipoles [34, 38]. CD spectroscopy is also suitable for monitoring pigment-pigment interactions between adjacent subunits [39-41], and therefore CD is capable of indicating variations in the association of certain complexes within their supramolecular assembly, e.g. the oligomerisation state of LHCII [38, 42, 43]. CD technique has proven to be useful in the investigation of more complex structures, such as thylakoid membranes, as well. The presence of intense, anomalously shaped, non-conservative bands at 690 and 510 nm in isolated chloroplasts was first reported by Faludi-Daniel *et al.* [44]. It was detected only in granal mesophyll chloroplasts of maize, but not in the agranal bundle sheath chloroplasts of the same leaves [44-46]. Small chloroplast fragments also lack anomalously intense CD and show only the less intense bands of pigment-pigment excitonic interactions [47] between photosynthetic complexes. The prominent CD signal dominating the spectrum of whole chloroplasts could not be recomposed from the CD spectra of small chloroplast fragments or the known pigment-protein complexes [47]. Large particle-containing samples, like chloroplast suspensions, show intense light scattering, which in principle might also contribute to the strong CD signals.

Several studies proved that anomalously intense CD is mainly due to the inherent structural organisation of thylakoid membranes, and the distortion effect of light scattering is negligible [45]. The properties of the intense CD signal are characteristic for the so-called psi-type (polymer- and salt-induced) CD that relates to large asymmetrically long-range ordered aggregates with a high density of chromophores and sizes commensurate with the wavelength of the absorbed light [48, 49]. Based on these literature data the presence of psi-type CD in thylakoid membrane is attributed to long-range ordered macrodomains of Chl-containing protein complexes [50], though its exact origin in terms of molecular structures has not been elucidated yet. It is not clear which proteins participate in the formation of these long-range ordered structures and what the specific role is of different subunits in the self-organisation of the chiral macrodomains.

The aim of the present work is to establish a CD-based method for fingerprinting various macrodomain structures in chloroplast thylakoid membranes *in vivo*. We used different plants, growth conditions and mutants with varying amounts of light-harvesting complexes in order to gain further insight into the origin of the psi-type CD bands *in vivo* in intact leaves, and to correlate them with the macro-organization of protein complexes. Our data revealed that the formation of chiral macrodomains depends on the presence of PSII-LHCII supercomplexes and, most prominently, on the protein composition of the light harvestin antenna.

## 4.2 Materials and methods

### *Growth conditions*

*Arabidopsis thaliana* wild-type *Col-0* (WT), *chl1* [51, 52], *npq1* [53], *npq2* [53], *aba4* [54], *lut2* [55], *kolhcb6* [28], *kolhcb5* [56], *aslhcb2* [57], *kopsbW* [58] plants and barley (*Hordeum vulgare*) plants were grown at 150  $\mu\text{mol photons m}^{-2} \text{s}^{-1}$ , 8/16 h day/night regime at 22/18 °C day/night temperature. Experiments were performed on *Arabidopsis thaliana* and barley plants at an age of eight and two weeks, respectively. Maize (*Zea mays*) plants were grown under intermittent-light conditions by providing 2 min illumination every two hours. Lincomycin-treated maize seedlings were hydroponically grown in ¼ strength Hoagland solution. Plants were grown in the dark for five days, then exposed to continuous light at a photon flux density of 25  $\mu\text{mol m}^{-2} \text{s}^{-1}$  for four days. The nutrient solution was supplemented with 100  $\mu\text{g ml}^{-1}$  lincomycin 16 h prior to the start of the illumination [59]. *Chlamydomonas reinhardtii* WT (CC-124) strain and the chlorophyll-deficient

# Role of LHCII in thylakoid organisation

*tla3* mutant [60] were cultivated in TAP medium [61] at 26 °C, with horizontal shaking (100 rpm) under continuous light (150  $\mu\text{mol photons m}^{-2} \text{s}^{-1}$ ).

## *Thylakoid isolation*

Leaf tissue was homogenised by Ultra-Turrax (3-5 short pulses) in buffer containing 50 mM Tricine, 400 mM Sorbitol, 5 mM  $\text{MgCl}_2$  and 5 mM KCl (pH 7.5), then filtered through four layers of cheese cloth and the homogenate was centrifuged at 3000 g for 5 min. The pellet was washed with buffer containing 50 mM Tricine, 5 mM  $\text{MgCl}_2$  and 5 mM KCl (pH 7.5) and resuspended in the homogenisation buffer.

## *Chlorophyll determination*

Pigment content of thylakoid membranes was determined in 80% acetone according to Porra [62]. Leaf pigments were extracted by N,N-dimethylformamide (DMF) and estimated as described in [63].

## *Protein analysis*

Maize leaf discs of 11 mm diameter were frozen in liquid nitrogen, ground to a fine powder, and then solubilised in 500  $\mu\text{L}$  2x Laemmli buffer. Homogenates were incubated at 90 °C for 5 min and at 37 °C for 20 min. Proteins were separated by 15% denaturing SDS-PAGE [64]. Equal volumes of the samples were loaded onto each lane. The proteins were blotted onto nitrocellulose membranes with a semidry blotting system using methanol-containing buffer (25 mM TRIS, 192 mM glycine, 20% methanol). The nitrocellulose membranes were blocked using 5% milk powder in TBST buffer (10 mM TRIS pH 8.0, 150 mM NaCl, 0.1% Tween 20) for 2 h and incubated with primary antibodies in TBST buffer for 2 h. The membranes were washed three times for 5 min in TBST buffer and incubated with goat anti-rabbit IgG horseradish peroxidase conjugate (Millipore) at a 1:5000 dilution in TBST buffer for 2 h. Immunoblotted membranes were incubated with ECL plus horseradish peroxidase substrate reagent (GE Healthcare Bio-Sciences) for 5 min. The resulting chemiluminescence was detected on Hyperfilm ECL photographic film (GE Healthcare Bio-Sciences). Developed films were digitized with Epson Perfection V700 scanner.

## *Circular dichroism spectroscopy*

CD spectra were recorded with a JASCO J-815 dichrograph between 400 and 800 nm at 100 nm/min scan speed. Measurements were carried out at room

temperature, using 3 nm band-pass and 1 nm step size. The chlorophyll concentration of thylakoid membranes and *Chlamydomonas reinhardtii* cell suspensions were adjusted to 20  $\mu\text{g ml}^{-1}$  and measured in a cuvette with a 1 cm optical path length. Intact leaves supported by a flat cell were placed perpendicularly to the optical path. To improve the signal-to-noise ratio, leaves were infiltrated with distilled water prior to the measurements and three scans were averaged. For baseline correction DMF bleached leaves were used [63]. CD spectra were normalised to total Chl content or to the Chl  $Q_y$  absorption band. Amplitudes of the (+)688 nm, (-)674 nm and (+)506 nm psi-type CD bands were calculated as the difference of the CD signal at 688 to 800 nm and 506 to 620 nm, respectively.

### 4.3 Results

#### *CD fingerprints of isolated thylakoid membranes*

The CD spectrum of thylakoid membranes isolated from higher plants (*Arabidopsis*) is complex because of the superposition of CD signals with different physical origins (Fig. 4.1). The visible region of the spectrum is dominated by the so-called psi-type bands. The positive band at around 691 nm and the negative band at around 675 nm [44] originate from Chl *a* molecules associated with macrodomains of the photosynthetic complexes [50]. The band at around 509 nm must be arising from carotenoids of long-range ordered structure, which absorb in this spectral region. The accompanying conservative minor bands below 500 nm, as well as the signal at around 650 nm, originate from short-range excitonic interactions [34]. Partial solubilisation of the thylakoid membranes with a very mild detergent treatment (up to 0.1 %  $\beta$ -DM) is sufficient to completely abolish the psi-type CD bands (Fig. 4.1), while this detergent treatment exerted only marginal effects on the excitonic CD signals [65]. However, the pre-treatment of the thylakoid membranes by 1% glutaraldehyde, which is capable to cross-linking the neighbouring protein subunits, substantially decreases the detergent sensitivity of the psi-type signal. Accordingly, the difference in the CD spectra of untreated and detergent-treated thylakoid membranes (in the absence of cross-linker) provides the CD fingerprint of large, long-range ordered, chiral pigment-protein domains [50].

#### *CD signal in vivo*

The CD spectrum of intact *Arabidopsis* leaves is shown in Figure 4.1. The main features of the spectrum is very similar to that of an *Arabidopsis* stacked thylakoid membrane suspension (Fig. 4.1), in agreement with the earlier observation

# Role of LHCI in thylakoid organisation

that in intact leaves no distortion or artefact results from the structural elements of leaf tissues [28].

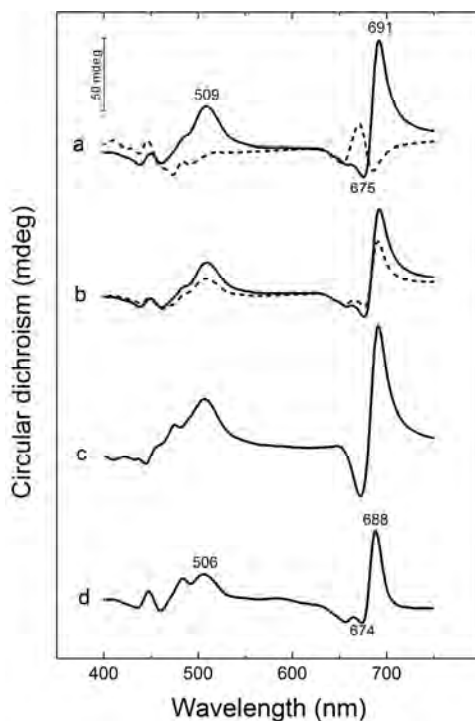


**Figure 4.1.** CD spectra of thylakoid membrane suspensions and detached leaf of wild type *Arabidopsis thaliana* plants. Spectra represent typical records of (a) intact (solid line) and 0.1%  $\beta$ -dodecyl-maltoside ( $\beta$ -DM) solubilised (dashed line) thylakoid membranes, (b) thylakoid membranes pre-treated with 1% glutaraldehyde in the absence (solid line) and presence (dashed line) of 0.1%  $\beta$ -DM, (c)  $\Delta$ CD, obtained as the difference spectrum of intact and solubilised thylakoid membranes and (d) the CD spectrum of intact leaf. The CD spectra were normalised to the Chl  $Q_y$  absorption band.

According to their peak positions and directions in *Arabidopsis* leaves, the psi-type CD bands in the ranges of 688-691, 667-675 and 505-512 nm are designated (+)688, (-)674 and (+)506 bands, respectively. The CD spectra measured for detached leaves of various plant species (e.g. *Arabidopsis thaliana*, *Hordeum vulgare*, *Zea mays*, *Hedera helix*, *Alocasia macrorrhiza*) and *Chlamydomonas reinhardtii* cells share the same overall features, namely the strong (+)688, (-)674 and (+)506 nm psi-type CD bands, only the relative ratios of these peaks vary (Fig. 4.2, see more species in Fig. Supplementary Information 4.1). However, in some cases, e.g. in *Hedera* and *Alocasia* the isolation of intact thylakoid membranes is rather difficult and the spectra vary with isolation methods and buffer compositions.

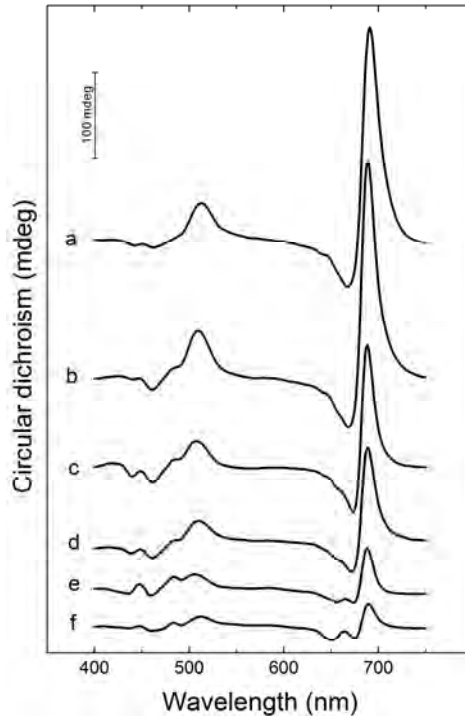


**Figure 4.2.** CD spectra of detached leaves of various plant species and the green alga *Chlamydomonas reinhardtii*. CD spectra were measured on detached leaves of (a) *Alocasia macrorrhiza*, (b) *Hedera helix*, (c) *Hordeum vulgare*, (d) *Zea mays*, (e) *Arabidopsis thaliana* leaves and from (f) *Chlamydomonas reinhardtii* cells. The CD spectra were normalised to the maximum of Chl  $Q_y$  absorption band.

The similarity between the CD spectra of leaves and algal cells with thylakoid membranes demonstrates that the *in vivo* macro-organization of pigment-protein complexes is rather similar in all these plants, despite the considerable variability that most probably reflect different *in vivo* macrodomain organisation. The main features of the CD spectra are characterised by the amplitude of the (+)688, (-)674, and (+)506 nm psi-type CD bands, normalised to the  $Q_y$  Chl absorption band, and by the (+)688/(-)506 nm and (+)688/(-)674 nm band ratios. Since the different units of Chl concentration used for leaves ( $\mu\text{g Chl}/\text{cm}^2$ ) and alga suspensions ( $\mu\text{g Chl}/\text{ml}$ ) do not allow the Chl-based comparison of spectra, we normalised the data to the  $Q_y$  Chl absorption band. The amplitudes of psi-type CD bands were defined as the difference from the reference wavelengths: 800 nm for the (+)688 and (-)674 nm bands and 620 nm for the (-)506 nm band. We use these parameters to compare the CD fingerprint of the leaves in various species (Table 4.1).

# Role of LHCI in thylakoid organisation

**Table 4.1.** Quantitative analysis of circular dichroism spectral data obtained from leaves of various plant species and from intact *Chlamydomonas reinhardtii* cells. The CD values of the (+)688, (-)674 and (+)506 nm psi-type bands are normalised to Chl  $Q_y$  absorption and given in mdeg/OD<sub>680</sub>.

Sample	(+)688	(-)674	(+)688/(+)506	(+)688/(-)674	Chl <i>a/b</i>
<i>A. macrorrhiza</i>	260 ± 75	49 ± 23	5.09 ± 0.4	5.10 ± 1.10	2.86 ± 0.16
<i>H. helix</i>	258 ± 43	54 ± 9	4.28 ± 0.4	5.74 ± 0.37	2.76 ± 0.09
<i>Hordeum vulgare</i>	149 ± 17	53 ± 3	4.3 ± 0.46	2.78 ± 0.20	2.81 ± 0.1
<i>Zea mays</i>	110 ± 12	44 ± 7	3.77 ± 0.44	2.52 ± 0.34	4.14 ± 0.26
<i>Gingko biloba</i>	33 ± 8	9 ± 2	3.65 ± 0.46	3.20 ± 1.34	3.33 ± 0.13
<i>Oxalis triangularis</i>	447 ± 54	111 ± 15	9.13 ± 6.44	4.03 ± 0.39	2.23 ± 0.07
<i>Nephrolepis exaltata</i>	104 ± 34	34 ± 5	5.2 ± 2.92	3,11 ± 1,00	2.64 ± 0.14
<i>Spinacia oleracea</i>	37 ± 8	14 ± 3	2.75 ± 0.29	2.78 ± 1.03	3.73 ± 0.16
<i>A. thaliana</i>	51 ± 4	9 ± 2	2.65 ± 0.16	6.92 ± 2.30	3.48 ± 0.03
<i>C. reinhardtii</i>	28 ± 11	12 ± 4	2.0 ± 0.5	2.20 ± 0.20	2.4 ± 0.0

Our results show that the value of (+)688 nm changes in a broad range between various species, e.g. leaves of *Arabidopsis* (51.3±4.5 mdeg) and spinach (37.4±8.12 mdeg) give low amplitudes, whereas those of *Alocasia* and *Hedera* show high values (290±71 and 258±43 mdeg, respectively) relative to the respective main ( $Q_y$ ) Chl absorption band. However, the (+)506 and (-)674 nm psi-type bands change at different extent resulting in modified (+)688 to (+)506 and (+)688 to (-)674 nm ratio. For instance the (+)688/(-)506 value is almost twice higher in *Alocasia* than in *Arabidopsis*. The (+)688/(-)674 ratio is quite low in *Chlamydomonas*, maize and barley, but rather high in *Arabidopsis*. The data of Chl *a/b* ratio were obtained from the same leaves of which the CD spectra were recorded. We could not observe apparent correlation between the Chl *a/b* ratio and the amplitudes of any psi-type CD.

## *Effects of antenna and core enrichment on the CD signal*

To shed light on the specific roles of different pigment-protein complexes in the formation of the chiral macrodomains that give rise to the psi-type CD bands we compared the CD spectra of maize leaves with thylakoid membranes enriched in either LHCs or core complexes of the two photosystems. LHC enrichment was achieved by lincomycin treatment (LMT) of maize seedlings, lincomycin is an antibiotic that specifically inhibits protein synthesis in the chloroplast, resulting in the suppression of chloroplast-encoded photosystem core complexes [59]. By contrast, maize seedlings growing in intermittent light (IML) suppress the accumulation of LHC in the thylakoid membranes due to the limited Chl *b* availability, causing accumulation of the core complexes [66].

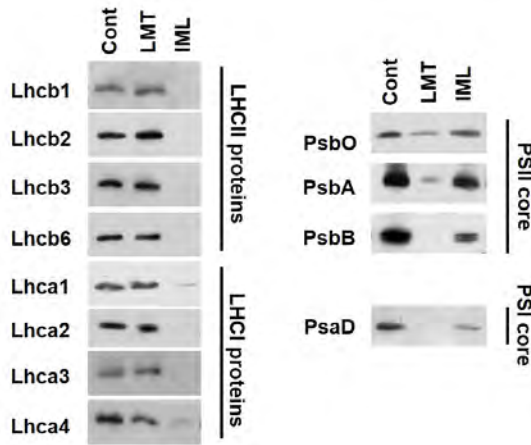


**Figure 4.3.** Analysis of protein composition of control, lincomycin treated (LMT) and intermittent light grown (IML) maize leaves. Immunodetection of photosynthetic proteins of control, LMT and IML samples were obtained from extracts of whole leaves with equal leaf area. Immunoblotting with antibodies against LHCII proteins (Lhcb1, Lhcb2, Lhcb3, Lhcb6), LHCI proteins (Lhca1, Lhca2, Lhca3, Lhca4), PSII core (PsbO, PsbA, PsbB) and PSI core proteins (PsaD) were performed.

Immunoblot analyses (Fig. 4.3) demonstrated that in LMT plants there were no detectable changes in the amounts of LHC components on Chl base, while PSII core proteins (PsbA, PsbC, CP43, PsbO) and the PSI core protein, PsaD were present only in trace amounts or were even undetectable.

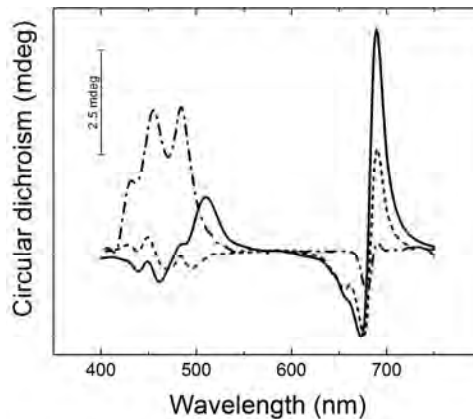


**Figure 4.4.** CD spectra of control, lincomycin treated (LMT) and intermittent light grown (IML) maize leaves. Different lines represent the average CD spectra of control (solid line), LMT (dashed line) and IML (dash-dot line) maize leaves. The CD spectra were normalised to the total Chl content per unit area.

## Role of LHCII in thylakoid organisation

In IML-grown maize samples, however, we could detect only very low levels of Lhca1 and 4 proteins, but not other LHC proteins. The level of the PSII core proteins (PsbA and PsbO) does not show a noticeable difference, and only a small decrease in the amounts of PsbB and PsaD proteins was detected. The CD spectrum of the LHCII-enriched LMT plant leaves exhibits no (+)506 nm psi-type CD and suppresses (to approx. 50%) (+)688 nm psi-type CD signals relative to the control maize leaves (Fig. 4.4). The IML-grown leaves do not show psi-type CD bands, only Chl a excitonic bands in the red, and mainly carotenoid bands in the Soret region. We have to note that the Car/Chl ratio is increased in the IML-grown leaves, resulting in the enhancement of carotenoid bands relative to the Chl excitonic bands. Freeze-fracture electron microscopy pictures confirm the efficient enrichment of LMT and IML thylakoid membranes in LHC and core complexes, respectively (Fig. Supplementary Information 4.2). The large and small particles observed in fractured surfaces of control thylakoid membranes can be identified as PSII core and LHCII complexes/aggregates. In LMT thylakoids we could detect mainly small particles, while only large particles were observed in the IML samples. In some cases the freeze-fracture procedure resulted in cross fractured chloroplasts that reveal granum and stroma membranes in untreated, continuous light-grown control samples. However, the LMT samples show large stacked membrane fractions and almost no stroma thylakoids, whereas in IML samples we could not observe stacked membrane regions at all.

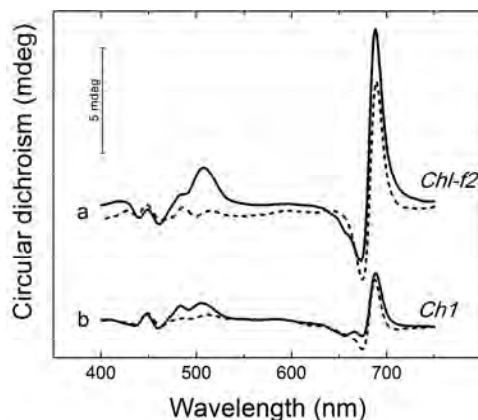


**Figure 4.5.** CD spectra of leaves of wild-type and chlorophyll-b-deficient barley and *Arabidopsis thaliana* plants. Upper graphs (a) represent the CD spectra obtained from barley WT (solid line) and Chl b-deficient *Chlorina-f2* (dashed line) mutant leaves. Lower graphs (b) show the CD spectra of WT (solid line) and Chl b-deficient *Ch1* (dashed line) *Arabidopsis thaliana* leaves. The CD spectra were normalised to the total Chl content per unit area.

Since it has been shown by earlier studies [67] that the granal organisation of thylakoid membranes in vascular plants is a prerequisite for the appearance of psi-

type CD in chloroplasts, we looked for other model systems in which the depletion of LHC components is not accompanied by the disappearance of stacked membrane structures. The *Arabidopsis* *chl1* and barley *chlorina-f2* mutants, impaired in Chl b synthesis, have been reported to lack LHCs but to retain the granal structures of WT plants [68, 69]. Figure 4.5 shows the CD spectra of detached leaves of the barley and *Arabidopsis* Chl b-deficient mutants. Both mutants exhibit relatively strong (+)688 and (-)674 nm psi-type CD bands, but virtually none or very weak (+)506 nm band as compared to the corresponding WT leaves.

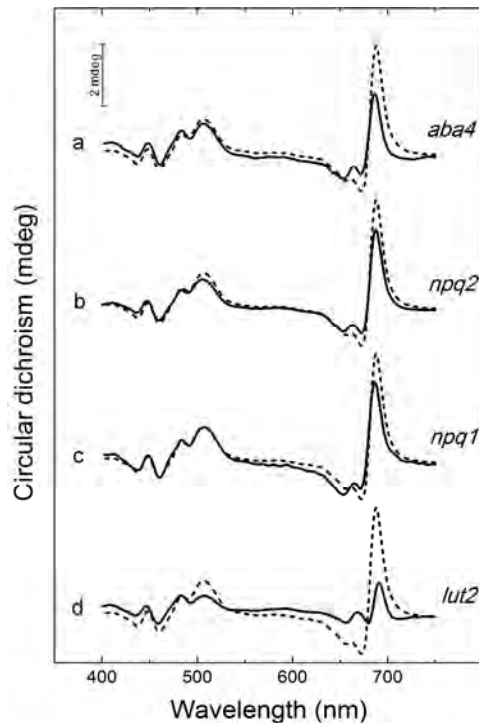


**Figure 4.6.** Circular dichroism spectra of leaves of *Arabidopsis thaliana* wild type and mutants impaired in their xanthophyll biosynthetic pathways. For better comparison, the mutant spectra (solid lines) - (a) *aba4*, (b) *npq2*, (c) *npq1* and (d) *lut2* - are overlaid with the spectrum of WT (dashed lines). The CD spectra were normalised to the total Chl content per unit area.

### *Effect of xanthophyll composition on the CD spectra*

The pigment composition of the core complexes and LHCs are different. Both the core complexes and LHCII contain Chl *a* and thus can contribute to the (+)688 nm psi-type CD, which originates from Chl *a*. By contrast, only the core complexes contain  $\beta$ -carotene, while xanthophylls (lutein, neoxanthin, violaxanthin

# Role of LHCII in thylakoid organisation

and zeaxanthin) are found only in LHCs. According to the peak positions we can assume that the blue, (+)506 nm, psi-type band originates from long-range-ordered carotenoid arrays. Therefore, by identifying the carotenoid species that are involved in the formation of the (+)506 nm psi-type band we might be able to elucidate the origin of this band and assign it to the core or the LHC complexes. To this end, we measured the CD spectra of *Arabidopsis* mutants devoid of one or two of the four xanthophyll species occurring in LHCs (Fig. 4.6).

The *lut2* mutant lacks lutein, whereas *aba4*, *npq1* and *npq2* are deficient in neoxanthin, zeaxanthin and both neoxanthin and violaxanthin, respectively. As shown in Figure 4.6, only slight decrease of the psi-type CD bands were observed in *aba4*, *npq2* and *npq1* mutants, while in *lut2* mutant both positive psi-type bands were strongly reduced relative to the WT. Although the amplitudes of the psi-type CD bands decreased to various extents, the (+)506 nm psi-type CD band was present in all xanthophyll mutants examined. Interestingly, the Chl related (+)688 nm band was stronger affected by the elimination of xanthophylls than the carotenoid related one.

**Table 4.2. Quantitative analysis of circular dichroism spectral data obtained from *Arabidopsis thaliana* leaves of wild-type plants and mutants deficient in various PSII proteins. The CD amplitudes of the psi-type bands are normalised to [Chl (a+b)] and given in mdeg/[ $\mu\text{g Chl}/\text{cm}^2$ ]. Data are expressed as the mean for 9 samples  $\pm$  SD.**

Sample	(+)688 nm	(+)506 nm	(-)674 nm	(+)688/(-)674
WT	2.55 $\pm$ 0.25	0.97 $\pm$ 0.12	0.46 $\pm$ 0.11	2.65 $\pm$ 0.16
<i>kopsbW</i>	1.5 $\pm$ 0.35**	0.68 $\pm$ 0.1**	0.42 $\pm$ 0.19	2.2 $\pm$ 0.2**
<i>kolhcb6</i>	0.48 $\pm$ 0.2**	1.35 $\pm$ 0.1**	0.39 $\pm$ 0.12	0.35 $\pm$ 0.11**
<i>kolhcb5</i>	1.51 $\pm$ 0.39**	0.83 $\pm$ 0.11*	0.39 $\pm$ 0.16	1.81 $\pm$ 0.34**
<i>aslhcb2</i>	0.63 $\pm$ 0.11**	0.56 $\pm$ 0.08**	0.54 $\pm$ 0.09	1.14 $\pm$ 0.15**

Statistically significant difference with respect to the wild type sample determined using the Student's t test at level of  $P < 0.05$  \* or  $P < 0.01$  \*\*.

## *Effect of PSII supercomplex composition on the CD spectra*

Recently, we have demonstrated that in an *Arabidopsis* knock-out mutant (*kopsbW*) lacking the PsbW protein, a low molecular weight PSII core component, the stability of the PSII-LHCII supercomplex decreases strongly even if the PSII core and LHCII components are present at the same level as in the WT [58]. In the CD spectrum of *kopsbW* leaves both positive (+)688 and (+)506 nm psi-type CD bands are present, but with a significant lower peak height than observed in WT leaves (Fig. 4.7 and Table 4.2).

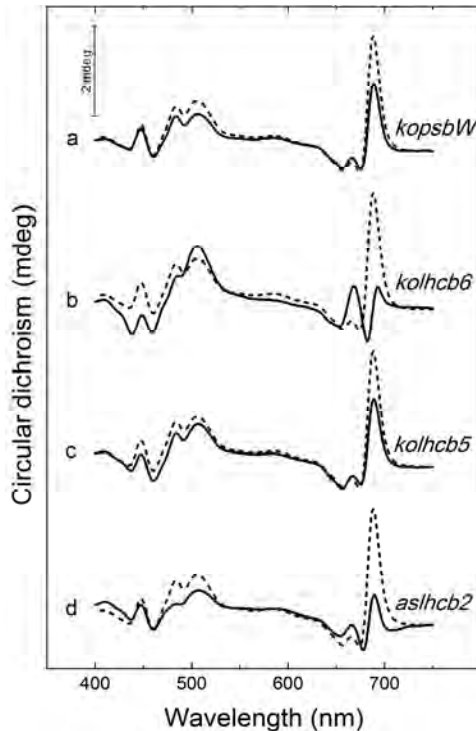


**Figure 4.7. Circular dichroism spectra of wild type *Arabidopsis thaliana* and mutants deficient in various PSII supercomplex protein components.** Spectra of WT leaves (dashed lines) are overlaid with those of mutants (solid lines) (a) *kopsbW*, (b) *kolhcb6*, (c) *kolhcb5* and (d) *aslhcb2*. The spectra were normalised to the total Chl content per unit area.

The decrease of the (+)688 nm peak is stronger, as reflected by the intensity-ratio of the two psi-type bands, (+)688/(+)506. This ratio is decreased from 2.65 in the WT to 2.2 in *kopsbW* plants (Table 4.2). In order to study the specific role of different LHCII proteins in the thylakoid membrane macro-organisation we compared the CD spectra of genetically modified plants lacking different LHCII components (Fig. 4.7 and Table 4.2). In *kolhcb5* *Arabidopsis* plants, devoid of Lhcb5 (CP26), a decrease of the (+)688 nm psi-type CD is observed, while the (+)506 nm band remains at a similar level as for the WT, resulting in a strong decrease of the (+)688/(+)506 value to 1.81. The depletion of Lhcb6 (CP24) leads to almost complete elimination of the (+)688 nm psi-type CD band and significantly increases the (+)506 nm band (Fig. 4.7 and Table 4.2), similarly to earlier results obtained with *kolhcb6* leaves [28]. Accordingly, in CP24 deficient plants the (+)688/(+)506 ratio drastically decreases to a value of 0.35. In the *aslhcb2* line, in which antisense suppression efficiently decreases the level of Lhcb1 and Lhcb2 proteins, the main components of trimeric

# Role of LHCII in thylakoid organisation

LHCII, both the (+)688 and (+)506 nm psi-type CD bands decrease. However, in *aslhcb2* plants the (+)688/(+)506 ratio also changes, indicating a more pronounced effect on the red (+)688 psi-type CD band (Fig. 4.7 and Table 4.2).

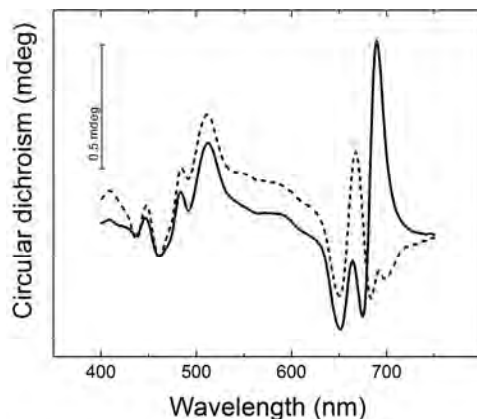


**Figure 4.8.** Circular dichroism spectra of the wild type and a mutant with truncated antenna size (*tla3*) of *Chlamydomonas reinhardtii*. Average spectra of WT (solid lines) and antenna-truncated *tla3* (dashed line) cells were normalised to the total Chl content of the suspension.

In order to further investigate the relation between the antenna size and the CD signal, the *Chlamydomonas reinhardtii tla3* mutant with truncated light-harvesting antenna was also examined. The *tla3* cells are deficient in the CrCpSRP43 protein, which is important for thylakoid membrane biogenesis and formation of the Chl *a/b* light-harvesting antenna. The lack of CrCpSRP43 leads to drastic decrease of the antenna size relative to the amount of the RCs [60]. The CD spectrum of *tla3* cells shows strongly diminished (+)688 nm psi-type CD band, while the amplitude of the (+)506 nm band seems unaffected.

## 4.4 Discussion

### *Basic properties of psi-type CD signals*

The so-called psi-type CD signals, ‘anomalously’ shaped, intense bands at around (-)678 nm, and (+)690 and (+)510 nm with long tails outside the main absorbance bands [44], are assigned to large, chirally ordered macroassemblies of LHCII-containing macrodomains embedded in the thylakoid membranes [50]. The

magnitudes of the psi-type CD bands are proportional to the size of the chiral macroaggregates with long-range order of chromophores [70].

In native membranes protein-protein interactions can easily be disrupted by detergents, high temperature or chaotropic agents. Commonly used  $\beta$ -dodecyl-maltoside can completely abolish the psi-type CD at a concentration of 0.1 % (Fig. 4.1). This is 10-20 times lower than the concentration routinely used for the isolation of photosynthetic complexes, e.g. by non-denaturing gel electrophoresis and sucrose density gradient centrifugation and for the preparation of negative staining electron microscopy samples. These isolation techniques mostly retain the PSII core and LHCII complexes and even a considerable amount of intact PSII-LHCII supercomplexes. This effect of detergents on the CD signal can be alleviated by pre-treatment of the thylakoid membrane with glutaraldehyde that cross-links the proteins (Fig. 4.1). In detergent-solubilised samples the excitonic bands remain unaffected and the difference spectra of intact and solubilised samples exhibit intense CD bands with only minor contributions from short-range excitonic interactions between about 450 and 480 nm (see [65]). These data confirm that long-range ordered protein domains, which are organised mainly by weak protein-protein interactions, [71] give rise to the intense CD bands of thylakoid membranes.

### *CD signal in vivo*

Due to the fact that protein-protein interactions in the macrodomains are weak, it is often difficult to maintain the intact thylakoid structure in an isolated sample. The CD spectrum of thylakoid membranes purified from the same plant material strongly depends on both the isolation methods and buffer composition. Changes in the pH [72], ionic strength [44, 71], concentration of divalent cations [71] and osmotics [71] in the isolation media result in different CD spectra. The physiological values of these parameters are often unknown, and it is not clear which buffer composition mimics best the *in vivo* environment of the thylakoid membrane. Here we confirm the presence of chromophore-containing macrodomain structures by a non-invasive CD spectroscopy technique, measuring the psi-type CD under physiological conditions in intact leaves and algal cells (Fig. 4.2) in line with the literature data [28, 58, 67, 73, 74]. The main features of CD spectra obtained from leaves are comparable to those of thylakoid membranes implying *in vivo* presence of a similar macro-organisation leading to the psi-type CD (Fig. 4.2). All Chl *a/b* protein containing species examined in this study share the main features of psi-type CD with slight variations in the intensity and the relative contributions from the three psi-type CD bands, suggesting common principles in the supramolecular organisation of photosynthetic complexes in the thylakoid membrane. By the use of

## Role of LHCII in thylakoid organisation

CD spectroscopy from intact cells or leaves we can get structural information on the *in vivo* organisation of thylakoid membranes even from species (e.g. *Alloccasia* and *Hedera*) where the isolation of intact thylakoid membrane has not been successful so far.

### *Role of grana stacking in generating psi-type CD signal*

The fact that psi-type CD requires membrane stacking [44, 67] indicates that the Chl binding proteins (PSII core and or LHCII components) localized in the grana are probably those that participate in the formation of the long-range ordered protein assemblies giving rise to psi-type CD signals. In good agreement with this notion, our data show that plant species that generally possess large grana (barley, maize, *Hedera*) exhibit the most intense psi-type CD signal, as normalized to the Chl absorption. Vice versa, *Chlamydomonas* cells and *Arabidopsis* leaves, possessing less extended grana regions, have the smallest psi-type CD bands (Table 4.1). The fact that bigger grana represent more stacked membrane surface can explain the more intense psi-type CD signal in certain species.

On the other hand, Garab *et al.* [71] demonstrated that increasing the  $Mg^{2+}$  concentration, which substantially enhances membrane stacking, enlarges the 674 nm negative band while influences the positive psi-type bands (+)688, (+)506 nm to a lesser extent. The independent behaviour of the positive and negative bands suggests different origins of these signals [75, 76], but for all kinds of psi-type CD observed in plant thylakoid membranes the presence of stacking is a prerequisite [44, 49, 67, 74, 77, 78]. Accordingly, in the species with larger grana the negative psi-type band was also increased substantially (Fig. 4.2). In addition, the genetically modified *Arabidopsis* and *Chlamydomonas* lines lacking various LHCII components exhibit marked differences in their CD spectra (Figs. 4.7 and 4.8), although the electron microscopy studies of these mutants revealed no obvious differences in membrane stacking and the general ultrastructure of grana [28, 56, 58, 79]. In line with these observations, our measurements do not show significant differences in the (-)674 nm psi-type CD band (Table 4.2), which is closely associated with membrane stacking [71]. As pointed out above, the negative band correlates better with the membrane stacking, whereas the positive bands are influenced mainly by the lateral organisation of chlorophyll-binding proteins in the membrane plane. The positive bands only indirectly depend on membrane stacking, since stacking can stabilise the lateral organisation of protein complexes [80]. Psi-type CD signals can only be interpreted on the basis of three dimensional chiral structures [49]. Laterally arranged (2D) domains can be organised transversally into 3D structures, which gives rise to psi-type CD. A correlation between the orientations of PSII-LHCII

semi-crystalline domains of adjacent layers in stacked membranes was found by Dekker *et al.* [17]. This determined orientation of PSII-LHCII domains in stacked membrane layers might be sufficient for ensuring the 3D organisation necessary for the appearance of psi-type CD. Furthermore, the luminal protrusion of PSII core, together with narrow luminal distance, sterically limits the localisation of PSII supercomplexes and the orientation of PSII domains on opposite sides of the lumen. This transversal asymmetry may extend through several stacked layers of the multilamellar membrane systems in the grana, resulting in chiral 3D structures, an effect that can contribute to the psi-type CD signals. This, in turn, may explain how bigger grana typically result in stronger psi-type signals. It needs to be emphasized, however, that alterations in the lateral organisation of protein complexes might also lead to the decrease of some of the psi-type bands in a mutant without noticeable change in the granal membrane ultrastructure [28].

### *Role of PSII supercomplex in the psi-type CD signals*

It has been demonstrated that lamellar aggregates of isolated LHCII exhibit psi-type CD bands [70, 81, 82]. Since these *in vitro* aggregates generate negative bands, they cannot produce the dominant positive bands of the CD spectra obtained *in vivo*. However, LHCII may form aggregates in its native membrane environment, giving rise to the positive psi-type CD. In lincomycin-treated maize leaves, which are deficient in core complexes but enriched in LHCII (Fig. 4.4), the (+)688 nm positive band is present although at considerably lower intensity, whereas the 506 nm band is absent. This observation suggests that LHCII alone can give rise to the positive psi-type CD *in vivo*, but its fingerprint is different from the CD fingerprint of native samples.

However, it cannot be ruled out that the sign-inversion in the psi-type CD of LHCII aggregates, is related to different arrangements of LHCII, since *in vitro* in stacked 2D lamellae the trimers assume a flip-flop orientation [83]. On the other hand, the depletion of LHCII only partially abolishes the red psi-type CD in the Chl *b*-less mutants of *Arabidopsis* and barley (Fig. 4.5). The presence of the red (+)688 nm peak in the CD spectra of these core-enriched membranes indicates that LHCII-deficient core complexes can form long-range ordered structures that give rise to CD fingerprints resembling those of LHCII-enriched membranes. Although both LHCII and core complexes alone can contribute to the psi-type CD (Figs. 4.4 and 4.5), the CD spectra of native membranes cannot be recomposed from the spectra of the two complexes. The blue (+)506 nm band is absent in samples containing only core or only LHCII. Hence, psi-type CD, in its full extent, requires the co-existence of the the core and LHCII complexes.

## Role of LHCII in thylakoid organisation

We recently demonstrated that in the absence of the PsbW protein the stability of PSII-LHCII complexes decreases, and that a significant amount of supercomplexes dissociates into core and LHCII without noticeable changes in the protein composition of the thylakoid membranes [58]. The (+)688 nm red and (+)506 nm blue positive psi-type CD bands concomitantly decrease in the CD spectrum of the *kopsbW* mutant, as compared to that of WT plants (Fig. 4.7).

From the results above we conclude that the blue psi-type CD band most probably originates from the PSII core complex associated with LHCII. Hence, the CD fingerprint of native samples, characterised by the presence of both blue and red positive psi-type CD bands, appears to require the presence of PSII-LHCII supercomplexes, but the small, randomly distributed supercomplexes themselves are still not sufficient for generating psi-type CD, as shown by the theory of psi-type CD [49].

The (+)506 nm psi-type CD is in the spectral range of carotenoid absorption. While the Chl composition of LHCII and core complexes partially overlaps, the carotenoid compositions of the two complexes are different. The core complex contains only  $\beta$ -carotene, while LHCII comprises various xanthophylls. In the presence of at least two of the five xanthophyll species present in LHCs, LHCII proteins can fold and at least partially fulfil their structural role [55, 84]. The (+)506 nm psi-type CD band is present in all examined mutants lacking one or two xanthophyll species (Fig. 4.6). It is known that most of the xanthophylls can efficiently replace each other [85] maintaining the normal protein structure, except in the absence of lutein, which is important for a stable trimeric LHCII [55, 85]. If such replacement would be responsible for the maintenance of the psi-type CD spectrum one might expect at least some changes in the (+)506 nm signal. We could not, however, observe any shift in the position of this CD band. Although in the *lut2* mutant the blue CD band decreases, the Chl *a* related (+)688 nm band decreases even greater extent. It has been reported that in the *lut2* mutant the amount of LHCII trimers and, consequently, the number of PSII-LHCII supercomplexes decreases [55]. The fact that the red psi-type CD changes more in all xanthophyll-deficient mutants suggests that the observed changes in the blue psi-type CD most probably reflect the altered structure of LHCII and PSII-LHCII supercomplex, caused by the lack of the required xanthophyll rather than by direct contribution of this xanthophyll to the blue psi-type CD band. Nevertheless, we cannot exclude the possibility that the blue psi-type CD is maintained via replacement of one xanthophyll by another. If we rule out the role of all xanthophylls in the formation of the (+)506 nm CD band then we can assume that this band originates from the  $\beta$ -

carotene of the core complex (Fig. 4.5), but only when PSII is associated with LHCII.

### *Role of long-range order of PSII in the psi-type CD spectra*

Electron microscopy of negatively stained thylakoid membranes revealed the presence of large semi-crystalline domains consisting of long parallel rows of PSII-LHCII supercomplexes [17, 86]. These semi-crystalline arrays might be important constituents of the 3D chiral macrodomains that give rise to the psi-type CD signals. It is estimated that approximately 7-10% of the total amount of PSII-LHCII is involved in the semi-crystalline domains [15, 19]. Kiss *et al.* [87] reported that in a PsbS-overexpressing *Arabidopsis* mutant the amount of PSII-LHCII semi-crystalline domains decreased, as compared to the WT, in contrast to the increase observed in PsbS-deficient plants. In PsbS mutant plants the amplitude of the psi-type CD signal changed in parallel with the size of the PSII arrays. However, the negative staining technique involves partial solubilisation of the thylakoid membranes with detergent, which might destabilise the semi-crystalline domains. If this is the case then the observed PSII-LHCII semi-crystalline domains are just fragments of larger long-range ordered protein assemblies existing before detergent treatment. Our experiments demonstrate that the psi-type CD is drastically reduced when thylakoid membranes are treated or leaves are infiltrated with dodecyl-maltoside at the same detergent concentration that is used for negative staining.

It has been shown that the antenna composition of PSII-LHCII supercomplexes determines the structure of semi-crystalline domains [28, 56, 57, 88]. Alteration of macrodomain structure can modify the long-range interactions of pigments incorporated in the building blocks of macrodomains and eventually modulate the psi-type CD fingerprint of the thylakoid membrane [28, 58]. It is in accordance with our assumption that the core complex can be organised into a long-range ordered structure capable of generating blue psi-type CD only via association with LHCII, as reflected by the lack of blue psi-type CD for the LHCII deficient Chl *b*-less mutant.

In WT *Arabidopsis* the dominating type of PSII-LHCII supercomplexes is the so-called C<sub>2</sub>S<sub>2</sub>M<sub>2</sub> supercomplex, in which the dimeric core is associated with four LHCII trimers [88]. In the *kolhcb6* *Arabidopsis* mutant, deficient in CP24 protein, the supercomplex contains only the S-trimers, resulting in C<sub>2</sub>S<sub>2</sub> supercomplexes [28, 56] that build up a more densely packed semi-crystalline domain than C<sub>2</sub>S<sub>2</sub>M<sub>2</sub>. In agreement with our previous results [28] the CD fingerprint of *kolhcb6* plants profoundly differs from that of the WT. The red positive psi-type CD band is diminished while the blue peak is increased (Fig. 4.7, Table 4.2).

## Role of LHCII in thylakoid organisation

The decrease in the red/blue peak ratio ((+)/688/(+)/506) in *kolhcb6* plants can be explained by the notion that rearrangements of the protein subunits within macrodomains, without changing their relative amounts at cellular level, can modify their CD fingerprints. However, the more pronounced blue peak in *kolhcb6* mutant may be related to the relatively higher core content of C<sub>2</sub>S<sub>2</sub> semi-crystalline domains, as compared to the C<sub>2</sub>S<sub>2</sub>M<sub>2</sub> domain (C<sub>2</sub>/S<sub>2</sub> > C<sub>2</sub>/S<sub>2</sub>M<sub>2</sub>), in accordance with our suggestion that the blue peak mainly originates from a carotenoid pigment bound to the core complex.

The psi-type CD fingerprint of WT *Chlamydomonas* cells (Fig. 4.2) indicates a PSII-LHCII macro-organisation that is similar to that of higher plants, although this structure is not observed yet but hypothesised [16]. Moreover, the CD spectrum of the *Chlamydomonas* mutant *lla3*, characterised by truncated antenna size [60], resembles that of the C<sub>2</sub>S<sub>2</sub>-containing *kolhcb6* mutant of *Arabidopsis* (Figs. 4.7 and 4.8). The estimated antenna size of the mutant PSII is around 94 Chl/RC, which is 40% of that of the WT. This antenna size corresponds to the Chl content of a C<sub>2</sub>S<sub>2</sub> subunit, taking into consideration the Chl content of the PSII core, CP26, CP29 and the LHCII trimer [37, 89].

The *Arabidopsis* mutants, *aslhcb2* in which the level of Lhcb1 and Lhcb2 proteins are suppressed [57, 79] and *kolhcb5* that is depleted in the CP26 protein [56], retain the C<sub>2</sub>S<sub>2</sub>M<sub>2</sub> type semi-crystalline domain but with an altered structure. In the *aslhcb2* mutant the missing lhcb1/2 trimer is replaced by a trimer of the CP26 protein. This replacement provides a very similar, but not identical, macrodomain structure [57]. The variations of packing can be responsible of the observed changes in the intensity and ratio of the psi-type CD bands in these mutants (Fig 4.7, Table 4.2). It is remarkable that despite the very similar supercomplex organization the psi-type CD spectrum changes dramatically (Fig 4.7, Table 4.2). The alteration of LHCII composition changes the interaction between PSII supercomplexes (belonging to semi-crystalline domains) in adjacent membranes, resulting in a modified orientation of macrodomains in the adjacent membranes of stacked thylakoids [14, 17]. However, structural modifications of PSII supercomplex, resulting in small changes in lateral packing (2D organisation), still can be accompanied by more substantial changes in the relative orientation of semi-crystalline domains in adjacent layers (3D organisation) that is more difficult to detect by negative staining electron microscopy than by CD spectroscopy.

Goral and co-authors [19] characterised the macro-organisation of thylakoid membranes in various *Arabidopsis* antenna mutants by determining the nearest neighbour distance (NND) of PSII in the thylakoid membrane.

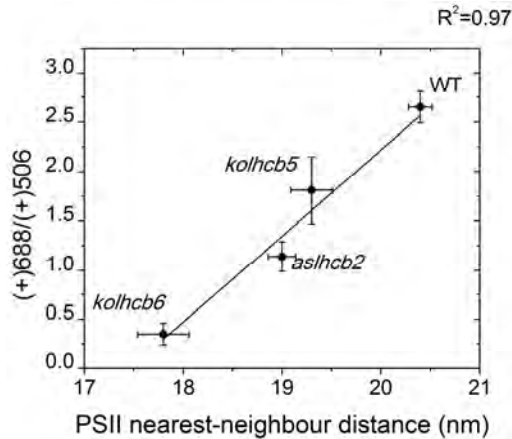


**Figure 4.9. Correlation of the psi-type CD peak ratios of wild type and LHCII mutants of *Arabidopsis thaliana* with the nearest-neighbour distance between PSII complexes.** The calculated ratio of the (+)688 nm to the (+)506 nm CD signal is shown as a function of PSII centre-to-centre nearest-neighbour distance obtained from [19].

Interestingly, the ratios of the two positive peaks in the psi-type CD signal ((+)688/(+)506) that we measured in leaves of WT *Arabidopsis* and the *kolhcb6*, *kolhcb5*, *aslhcb2* mutants show good correlation with the NND values, as determined by Goral *et al.* [19] for the thylakoid membranes of the corresponding mutants (Fig. 4.9).

The above findings indicate that the changes in PSII semi-crystalline domains are accompanied by changes in the CD signal of the thylakoid membranes *in vivo*. While the amount of PSII-LHCII domains influences the amplitude of the psi-type CD bands, the altered structure of the domains influences the ratio of the psi-type CD bands.

## 4.5 Conclusion

Using CD spectroscopy we demonstrated the *in vivo* presence of long-range ordered chiral macromolecules of Chl-containing pigment-protein complexes of the thylakoid membranes in a wide range of plants from a unicellular green algae to dicotyledonous and monocotyledonous angiosperms. The monitoring of the macro-organisation of thylakoid membrane proteins *in vivo* is of high importance since these delicate structures can undergo substantial structural changes during invasive sample preparation. CD spectroscopy can be easily applied on whole cells and leaves, and the psi-type CD bands give fingerprints of macro-structures in the native thylakoid membranes. These fingerprints can be quantitatively described as the chlorophyll-normalised amplitude ratios of the (+)688, (+)506 and (-)674 nm psi-

# Role of LHCII in thylakoid organisation

type bands. Changes of these parameters reflect alterations of the macro-organisation. The independent behaviour of the three psi-type bands upon structural reorganisation suggests that they originate from distinct macrodomains with different molecular organisations, i.e. from heterogeneity of macrodomains and/or from inherent structural variations in the macro-organisation of supercomplexes. The (+)688 and (-)674 bands are also observed in LHC- or core-depleted membranes. The (+)506 band appears only in the presence of PSII-LHCII supercomplex. The PSII-LHCII supercomplex per se does not give rise to psi-type CD, but long-range ordered PSII-LHCII semi-crystalline domains are thought to be responsible for generating the psi-type CD signals that are observed in native thylakoid membranes. The PSII core associated with LHCII can form unique structures with characteristic CD fingerprints. These fingerprints seems to depend largely on the composition of outer antenna complexes. Our data also demonstrate that CD spectroscopy is a potent non-invasive technique for fingerprinting the macroorganisation of thylakoid membranes *in vivo*.

## 4.6 Acknowledgement

This work was supported by the Sandwich PhD program of Wageningen University to T.T. and Social Renewal Operational Programmes (TAMOP-4.2.2/B-10/1-2010-0012, TAMOP-4.2.2.A-11/1/KONV-2012-0047), by a grant from the Hungarian Scientific Research Fund/National Office for Research and Technology (Grant No. 80345) and Hungarian National Innovation Office and A\*STAR Singapore (NIH-A\*STAR TET\_10-1-2011-0279) (to G.G.). The authors thank Terez Kiss for technical help with the electron microscopy measurements.

## 4.8 Reference list

- [1] Croce, R., van Amerongen, H., Natural strategies for photosynthetic light harvesting, *Nat. Chem. Biol.*, 10 (2014) 492-501.
- [2] Danielsson, R., Albertsson, P.A., Mamedov, F., Styring, S., Quantification, of photosystem I and II in different parts of the thylakoid membrane from spinach, *Biochim. Biophys. Acta*, 1608 (2004) 53-61.
- [3] Mustardy, L., Garab, G., Granum revisited. A three-dimensional model - where things fall into place, *Trends Plant Sci.*, 8 (2003) 117-122.
- [4] Croce, R., van Amerongen, H., Light-harvesting in photosystem I, *Photosynth Res.*, 116 (2013) 153-166.
- [5] van Amerongen, H., Croce, R., Light harvesting in photosystem II, *Photosynth Res.*, 116 (2013) 251-263.
- [6] Wollman, F.A., Minai, L., Nechushtai, R., The biogenesis and assembly of photosynthetic proteins in thylakoid membranes, *Biochim. Biophys. Acta*, 1411 (1999) 21-85.
- [7] Amunts, A., Toporik, H., Borovikova, A., Nelson, N., Structure determination and improved model of plant photosystem I, *J. Biol. Chem.*, 285 (2010) 3478-3486.

- [8] Ganeteg, U., Klimmek, F., Jansson, S., Lhca5 - an LHC-type protein associated with photosystem I, *Plant Mol. Biol.*, 54 (2004) 641-651.
- [9] Koziol, A.G., Borza, T., Ishida, K., Keeling, P., Lee, R.W., Durnford, D.G., Tracing the evolution of the light-harvesting antennae in chlorophyll a/b-containing organisms, *Plant Physiol.*, 143 (2007) 1802-1816.
- [10] Jansson, S., A guide to the Lhc genes and their relatives in Arabidopsis, *Trends Plant Sci.*, 4 (1999) 236-240.
- [11] Klimmek, F., Sjodin, A., Noutsos, C., Leister, D., Jansson, S., Abundantly and rarely expressed Lhc protein genes exhibit distinct regulation patterns in plants, *Plant Physiol.*, 140 (2006) 793-804.
- [12] Caffarri, S., Kouril, R., Kereiche, S., Boekema, E.J., Croce, R., Functional architecture of higher plant photosystem II supercomplexes, *EMBO J.*, 28 (2009) 3052-3063.
- [13] Mishra, Y., Jankanpaa, H.J., Kiss, A.Z., Funk, C., Schroder, W.P., Jansson, S., Arabidopsis plants grown in the field and climate chambers significantly differ in leaf morphology and photosystem components, *BMC Plant Biol.*, 12 (2012).
- [14] Kouril, R., Dekker, J.P., Boekema, E.J., Supramolecular organization of photosystem II in green plants, *Biochim. Biophys. Acta*, 1817 (2012) 2-12.
- [15] Kouril, R., Wientjes, E., Bultema, J.B., Croce, R., Boekema, E.J., High-light vs. low-light: Effect of light acclimation on photosystem II composition and organization in Arabidopsis thaliana, *Biochim. Biophys. Acta*, 1827 (2013) 411-419.
- [16] Drop, B., Webber-Birungi, M., Yadav, S.K.N., Filipowicz-Szymanska, A., Fusetti, F., Boekema, E.J., Croce, R., Light-harvesting complex II (LHCII) and its supramolecular organization in *Chlamydomonas reinhardtii*, *Biochim. Biophys. Acta*, 1837 (2014) 63-72.
- [17] Dekker, J.P., Boekema, E.J., Supramolecular organization of thylakoid membrane proteins in green plants, *Biochim. Biophys. Acta*, 1706 (2005) 12-39.
- [18] Kouril, R., Oostergetel, G.T., Boekema, E.J., Fine structure of granal thylakoid membrane organization using cryo electron tomography, *Biochim. Biophys. Acta*, 1807 (2011) 368-374.
- [19] Goral, T.K., Johnson, M.P., Duffy, C.D.P., Brain, A.P.R., Ruban, A.V., Mullineaux, C.W., Light-harvesting antenna composition controls the macrostructure and dynamics of thylakoid membranes in Arabidopsis, *Plant J.*, 69 (2012) 289-301.
- [20] Wientjes, E., Drop, B., Kouril, R., Boekema, E.J., Croce, R., During state 1 to state 2 transition in *Arabidopsis thaliana*, the photosystem II supercomplex gets phosphorylated but does not disassemble, *J. Biol. Chem.*, 288 (2013) 32821-32826.
- [21] Daum, B., Nicastro, D., Il, J.A., McIntosh, J.R., Kuhlbrandt, W., Arrangement of photosystem II and ATP synthase in chloroplast membranes of spinach and pea, *Plant Cell*, 22 (2010) 1299-1312.
- [22] Green, B.R., Pichersky, E., Kloppstech, K., Chlorophyll a/b-binding proteins: an extended family, *Trends Biochem. Sci.*, 16 (1991) 181-186.
- [23] Dunsmuir, P., The petunia chlorophyll a/b binding protein genes: a comparison of Cab genes from different gene families, *Nucleic Acids Res.*, 13 (1985) 2503-2518.
- [24] Stauber, E.J., Fink, A., Markert, C., Kruse, O., Johanningmeier, U., Hippler, M., Proteomics of *Chlamydomonas reinhardtii* light-harvesting proteins, *Eukaryot. Cell*, 2 (2003) 978-994.
- [25] Caffarri, S., Frigerio, S., Olivieri, E., Righetti, P.G., Bassi, R., Differential accumulation of Lhcb gene products in thylakoid membranes of *Zea mays* plants grown under contrasting light and temperature conditions, *Proteomics*, 5 (2005) 758-768.
- [26] Ballottari, M., Govoni, C., Caffarri, S., Morosinotto, T., Stoichiometry of LHCI antenna polypeptides and characterization of gap and linker pigments in higher plants photosystem I, *Eur. J. Biochem.*, 271 (2004) 4659-4665.
- [27] Timperio, A.M., Gevi, F., Ceci, L.R., Zolla, L., Acclimation to intense light implies changes at the level of trimeric subunits involved in the structural organization of the main light-harvesting complex of photosystem II (LHCII) and their isoforms, *Plant Physiol. Biochem.*, 50 (2012) 8-14.
- [28] Kovacs, L., Damkjaer, J.T., Kereiche, S., Illoia, C., Ruban, A.V., Boekema, E.J., Jansson, S., Horton, P., Lack of the light-harvesting complex CP24 affects the structure and function of the grana membranes of higher plant chloroplasts, *Plant Cell*, 18 (2006) 3106-3120.

# *Role of LHCI in thylakoid organisation*

- [29] Rumak, I., Mazur, R., Gieczewska, K., Koziol-Lipinska, J., Kierdaszuk, B., Michalski, W.P., Shiell, B.J., Venema, J.H., Vredenberg, W.J., Mostowska, A., Garstka, M., Correlation between spatial (3D) structure of pea and bean thylakoid membranes and arrangement of chlorophyll-protein complexes, *BMC Plant Biol.*, 12 (2012).
- [30] Kirchhoff, H., Haase, W., Wegner, S., Danielsson, R., Ackermann, R., Albertsson, P.A., Low-light-induced formation of semicrystalline photosystem II arrays in higher plant chloroplast, *Biochemistry*, 46 (2007) 11169-11176.
- [31] Johnson, M.P., Goral, T.K., Duffy, C.D.P., Brain, A.P.R., Mullineaux, C.W., Ruban, A.V., Photoprotective energy dissipation involves the reorganization of photosystem II light-harvesting complexes in the grana membranes of spinach chloroplasts, *Plant Cell*, 23 (2011) 1468-1479.
- [32] Semenova, G.A., Particle Regularity on Thylakoid Fracture Faces Is Influenced by Storage-Conditions, *Can J Bot*, 73 (1995) 1676-1682.
- [33] Tsvetkova, N.M., Apostolova, E.L., Brain, A.P.R., Williams, W.P., Quinn, P.J., Factors influencing PSII particle array formation in *Arabidopsis thaliana* chloroplasts and the relationship of such arrays to the thermostability of PSII, *Biochim. Biophys. Acta*, 1228 (1995) 201-210.
- [34] Parson, W., Nagarajan, V., Optical Spectroscopy in Photosynthetic Antennas, in: B. Green, W. Parson (Eds.) Light-Harvesting Antennas in Photosynthesis, *Springer Netherlands*, 2003, pp. 83-127.
- [35] Croce, R., Canino, G., Ros, F., Bassi, R., Chromophore organization in the higher-plant photosystem II antenna protein CP26, *Biochemistry*, 41 (2002) 7334-7343.
- [36] Pagano, A., Cinque, G., Bassi, R., In vitro reconstitution of the recombinant photosystem II light-harvesting complex CP24 and its spectroscopic characterization, *J. Biol. Chem.*, 273 (1998) 17154-17165.
- [37] Sandona, D., Croce, R., Pagano, A., Crimi, M., Bassi, R., Higher plants light harvesting proteins. Structure and function as revealed by mutation analysis of either protein or chromophore moieties, *Biochim. Biophys. Acta*, 1365 (1998) 207-214.
- [38] Georgakopoulou, S., van der Zwan, G., Bassi, R., van Grondelle, R., van Amerongen, H., Croce, R., Understanding the changes in the circular dichroism of light harvesting complex II upon varying its pigment composition and organization, *Biochemistry*, 46 (2007) 4745-4754.
- [39] Shubin, V.V., Tsuprun, V.L., Bezmertnaya, I.N., Karapetyan, N.V., Trimeric forms of the photosystem I reaction center complex pre-exist in the membranes of the cyanobacterium *Spirulina platensis*, *FEBS Lett.*, 334 (1993) 79-82.
- [40] Croce, R., Morosinotto, T., Castelletti, S., Breton, J., Bassi, R., The Lhca antenna complexes of higher plants photosystem I, *Biochim. Biophys. Acta*, 1556 (2002) 29-40.
- [41] Subramanyam, R., Jolley, C., Brune, D.C., Fromme, P., Webber, A.N., Characterization of a novel photosystem I-LHCI supercomplex isolated from *Chlamydomonas reinhardtii* under anaerobic (State II) conditions, *FEBS Lett.*, 580 (2006) 233-238.
- [42] Peterman, E.J.G., Hobe, S., Calkoen, F., vanGrondelle, R., Paulsen, H., vanAmerongen, H., Low-temperature spectroscopy of monomeric and trimeric forms of reconstituted light-harvesting chlorophyll a/b complex, *Biochim. Biophys. Acta*, 1273 (1996) 171-174.
- [43] Jackowski, G., Kacprzak, K., Jansson, S., Identification of Lhcb1/Lhcb2/Lhcb3 heterotrimers of the main light-harvesting chlorophyll a/b-protein complex of Photosystem II (LHC II), *Biochim. Biophys. Acta*, 1504 (2001) 340-345.
- [44] Faludi-Daniel, A., Demeter, S., Garay, A.S., Circular dichroism spectra of granal and agranal chloroplasts of maize, *Plant Physiol.*, 52 (1973) 54-56.
- [45] Garab, G., Faludidaniel, A., Sutherland, J.C., Hind, G., Macroorganization of chlorophyll a/b light-harvesting complex in thylakoids and aggregates - Information from circular differential scattering, *Biochemistry*, 27 (1988) 2425-2430.
- [46] Garab, G., Linear and circular dichroism, in: J.H.A.J. Ames (Ed.) Photosynthesis, Biophysical Techniques in Photosynthesis, *Kluwer Academic Publishing, Dordrecht*, 1996, pp. 11-14.
- [47] Gregory, R.P.F., Borbely, G., Demeter, S., Faludi-Daniel, A., Chiroptical properties of chlorophyll protein complexes separated on deriphat polyacrylamide-gel, *Biochem. J.*, 202 (1982) 25-29.

- [48] **Keller, D., Bustamante, C., Maestre, M.F., Tinoco, I.**, Model computations on the differential scattering of circularly polarized-light (Cids) by dense macromolecular particles, *Biopolymers*, 24 (1985) 783-797.
- [49] **Keller, D., Bustamante, C.**, Theory of the interaction of light with large inhomogenous molecular aggregates 2. Psi-type circular dichroism, *J Chem Phys*, 84 (1986) 2972-2980.
- [50] **Garab, G., van Amerongen, H.**, Linear dichroism and circular dichroism in photosynthesis research, *Photosynth Res.*, 101 (2009) 135-146.
- [51] **Havaux, M., Dall'Osto, L., Bassi, R.**, Zeaxanthin has enhanced antioxidant capacity with respect to all other xanthophylls in Arabidopsis leaves and functions independent of binding to PSII antennae, *Plant Physiol.*, 145 (2007) 1506-1520.
- [52] **Kim, E.H., Li, X.P., Razeghifard, R., Anderson, J.M., Niyogi, K.K., Pogson, B.J., Chow, W.S.**, The multiple roles of light-harvesting chlorophyll a/b-protein complexes define structure and optimize function of Arabidopsis chloroplasts: A study using two chlorophyll b-less mutants, *Biochim. Biophys. Acta*, 1787 (2009) 973-984.
- [53] **Niyogi, K.K., Grossman, A.R., Bjorkman, O.**, Arabidopsis mutants define a central role for the xanthophyll cycle in the regulation of photosynthetic energy conversion, *Plant Cell*, 10 (1998) 1121-1134.
- [54] **North, H.M., De Almeida, A., Boutin, J.P., Frey, A., To, A., Botran, L., Sotta, B., Marion-Poll, A.**, The Arabidopsis ABA-deficient mutant *aba4* demonstrates that the major route for stress-induced ABA accumulation is via neoxanthin isomers, *Plant J.*, 50 (2007) 810-824.
- [55] **Dall'Osto, L., Lico, C., Alric, J., Giuliano, G., Havaux, M., Bassi, R.**, Lutein is needed for efficient chlorophyll triplet quenching in the major LHClI antenna complex of higher plants and effective photoprotection in vivo under strong light, *BMC Plant Biol.*, 6 (2006).
- [56] **de Bianchi, S., Dall'Osto, L., Tognon, G., Morosinotto, T., Bassi, R.**, Minor antenna proteins CP24 and CP26 affect the interactions between photosystem II Subunits and the electron transport rate in grana membranes of Arabidopsis, *Plant Cell*, 20 (2008) 1012-1028.
- [57] **Ruban, A.V., Wentworth, M., Yakushevskaya, A.E., Andersson, J., Lee, P.J., Keegstra, W., Dekker, J.P., Boekema, E.J., Jansson, S., Horton, P.**, Plants lacking the main light-harvesting complex retain photosystem II macro-organization, *Nature*, 421 (2003) 648-652.
- [58] **Garcia-Cerdan, J.G., Kovacs, L., Toth, T., Kereiche, S., Aseeva, E., Boekema, E.J., Mamedov, F., Funk, C., Schroder, W.P.**, The PsbW protein stabilizes the supramolecular organization of photosystem II in higher plants, *Plant J.*, 65 (2011) 368-381.
- [59] **Gaspar, L., Sarvari, E., Morales, F., Szigeti, Z.**, Presence of 'PSI free' LHClI and monomeric LHClI and subsequent effects on fluorescence characteristics in lincomycin treated maize, *Planta*, 223 (2006) 1047-1057.
- [60] **Kirst, H., Garcia-Cerdan, J.G., Zurbriggen, A., Ruehle, T., Melis, A.**, Truncated photosystem chlorophyll antenna size in the green microalga *Chlamydomonas reinhardtii* upon deletion of the TLA3-CpSRP43 gene, *Plant Physiol.*, 160 (2012) 2251-2260.
- [61] **Gorman, D.S., Levine, R.P.**, Cytochrome f and plastocyanin: their sequence in the photosynthetic electron transport chain of *Chlamydomonas reinhardtii*, *Proceedings of the National Academy of Sciences of the United States of America*, 54 (1965) 1665-1669.
- [62] **Porra, R.J.**, The chequered history of the development and use of simultaneous equations for the accurate determination of chlorophylls a and b, *Photosynth Res.*, 73 (2002) 149-156.
- [63] **Inskeep, W.P., Bloom, P.R.**, Extinction coefficients of chlorophyll a and chlorophyll b in N,N-dimethylformamide and 80 percent acetone, *Plant Physiol.*, 77 (1985) 483-485.
- [64] **Laemmli, U.K.**, Cleavage of structural proteins during the assembly of the head of Bacteriophage T4, *Nature*, 227 (1970) 680-685.
- [65] **Lambrev, P.H., Varkonyi, Z., Krumova, S., Kovacs, L., Miloslavina, Y., Holzwarth, A.R., Garab, G.**, Importance of trimer-trimer interactions for the native state of the plant light-harvesting complex II, *Biochim. Biophys. Acta*, 1767 (2007) 847-853.

# *Role of LHCI in thylakoid organisation*

- [66] **Tzinias, G., Argyroudiakoyunoglou, J.H., Akoyunoglou, G.**, The effect of the dark interval in intermittent light on thylakoid development - Photosynthetic unit formation and light-harvesting protein accumulation, *Photosynth Res.*, 14 (1987) 241-258.
- [67] **Faludi-Daniel, A., Mustardy, L.A.**, Organization of chlorophyll a in the light-harvesting chlorophyll a/b protein complex as shown by circular dichroism - liquid crystal-like domains, *Plant Physiol.*, 73 (1983) 16-19.
- [68] **Goodchild, D., Highkin, H.R., Boardman, N.K.**, Fine structure of chloroplasts in a barley mutant lacking chlorophyll b, *Exp. Cell Res.*, 43 (1966) 684-&.
- [69] **Murray, D.L., Kohorn, B.D.**, Chloroplasts of Arabidopsis thaliana homozygous for the ch-1 locus lack chlorophyll b, lack stable LHCP II and have stacked thylakoids, *Plant Molecular Biology Reporter*, 16 (1991) 71-79.
- [70] **Barzda, V., Mustardy, L., Garab, G.**, Size dependency of circular dichroism in macroaggregates of photosynthetic pigment-protein complexes, *Biochemistry*, 33 (1994) 10837-10841.
- [71] **Garab, G., Kieleczawa, J., Sutherland, J.C., Bustamante, C., Hind, G.**, Organization of pigment protein complexes into macrodomains in the thylakoid membranes of wild-type and chlorophyll b-less mutant of barley as revealed by circular dichroism, *Photochem. Photobiol.*, 54 (1991) 273-281.
- [72] **Jajoo, A., Szabo, M., Zsiros, O., Garab, G.**, Low pH induced structural reorganization in thylakoid membranes, *Biochim. Biophys. Acta*, 1817 (2012) 1388-1391.
- [73] **Demeter, S., Mustardy, L., Machowicz, E., Gregory, R.P.F.**, Development of intense circular dichroism signal during granum formation in greening etiolated maize, *Biochem. J.*, 156 (1976) 469-472.
- [74] **Goss, R., Garab, G.**, Non-photochemical chlorophyll fluorescence quenching and structural rearrangements induced by low pH in intact cells of *Chlorella fusca* (Chlorophyceae) and *Mantoniella squamata* (Prasinophyceae), *Photosynth Res.*, 67 (2001) 185-197.
- [75] **Cseh, Z., Rajagopal, S., Tsonev, T., Busheva, M., Papp, E., Garab, G.**, Thermo-optic effect in chloroplast thylakoid membranes. Thermal and light stability of pigment arrays with different levels of structural complexity, *Biochemistry*, 39 (2000) 15250-15257.
- [76] **Finzi, L., Bustamante, C., Garab, G., Juang, C.B.**, Direct observation of large chiral domains in chloroplast thylakoid membranes by differential polarization microscopy, *P Natl Acad Sci USA*, 86 (1989) 8748-8752.
- [77] **Buchel, C., Garab, G.**, Organization of the pigment molecules in the chlorophyll a/c light-harvesting complex of *Pleurochloris meiringensis* (Xanthophyceae). Characterization with circular dichroism and absorbance spectroscopy, *J. Photochem. Photobiol. B: Biol.*, 37 (1997) 118-124.
- [78] **Szabo, M., Lepetit, B., Goss, R., Wilhelm, C., Mustardy, L., Garab, G.**, Structurally flexible macro-organization of the pigment-protein complexes of the diatom *Phaeodactylum tricornutum*, *Photosynth Res.*, 95 (2008) 237-245.
- [79] **Andersson, J., Wentworth, M., Walters, R.G., Howard, C.A., Ruban, A.V., Horton, P., Jansson, S.**, Absence of the Lhcb1 and Lhcb2 proteins of the light-harvesting complex of photosystem II - effects on photosynthesis, grana stacking and fitness, *Plant J.*, 35 (2003) 350-361.
- [80] **Garab, G., Mustardy, L.**, Role of LHCP II-containing macrodomains in the structure, function and dynamics of grana, *Aust. J. Plant Physiol.*, 26 (1999) 649-658.
- [81] **Miloslavina, Y., Lambrev, P.H., Javorfi, T., Varkonyi, Z., Karlicky, V., Wall, J.S., Hind, G., Garab, G.**, Anisotropic circular dichroism signatures of oriented thylakoid membranes and lamellar aggregates of LHCP II, *Photosynth Res.*, 40 (2011) 178-179.
- [82] **Simidjiev, I., Barzda, V., Mustardy, L., Garab, G.**, Isolation of lamellar aggregates of the light-harvesting chlorophyll a/b protein complex of photosystem II with long-range chiral order and structural flexibility, *Anal. Biochem.*, 250 (1997) 169-175.
- [83] **Standfuss, J., Kuhlbrandt, W.**, The three isoforms of the light-harvesting complex II - Spectroscopic features, trimer formation, and functional roles, *J. Biol. Chem.*, 279 (2004) 36884-36891.

- [84] **Dall'Osto, L., Cazzaniga, S., North, H., Marion-Poll, A., Bassi, R.**, The Arabidopsis *aba4-1* mutant reveals a specific function for neoxanthin in protection against photooxidative stress, *Plant Cell*, 19 (2007) 1048-1064.
- [85] **Croce, R., Weiss, S., Bassi, R.**, Carotenoid-binding sites of the major light-harvesting complex II of higher plants, *J. Biol. Chem.*, 274 (1999) 29613-29623.
- [86] **Boekema, E.J., van Breemen, J.F.L., van Roon, H., Dekker, J.P.**, Arrangement of photosystem II supercomplexes in crystalline macrodomains within the thylakoid membrane of green plant chloroplasts, *J. Mol. Biol.*, 301 (2000) 1123-1133.
- [87] **Kiss, A.Z., Ruban, A.V., Horton, P.**, The PsbS protein controls the organization of the photosystem II antenna in higher plant thylakoid membranes, *J. Biol. Chem.*, 283 (2008) 3972-3978.
- [88] **Boekema, E.J., van Roon, H., van Breemen, J.F.L., Dekker, J.P.**, Supramolecular organization of photosystem II and its light-harvesting antenna in partially solubilized photosystem II membranes, *Eur. J. Biochem.*, 266 (1999) 444-452.
- [89] **Loll, B., Kern, J., Saenger, W., Zouni, A., Biesiadka, J.**, Towards complete cofactor arrangement in the 3.0 angstrom resolution structure of photosystem II, *Nature*, 438 (2005) 1040-1044.

# Role of LHCII in thylakoid organisation

## 4.9 Supplementary Information

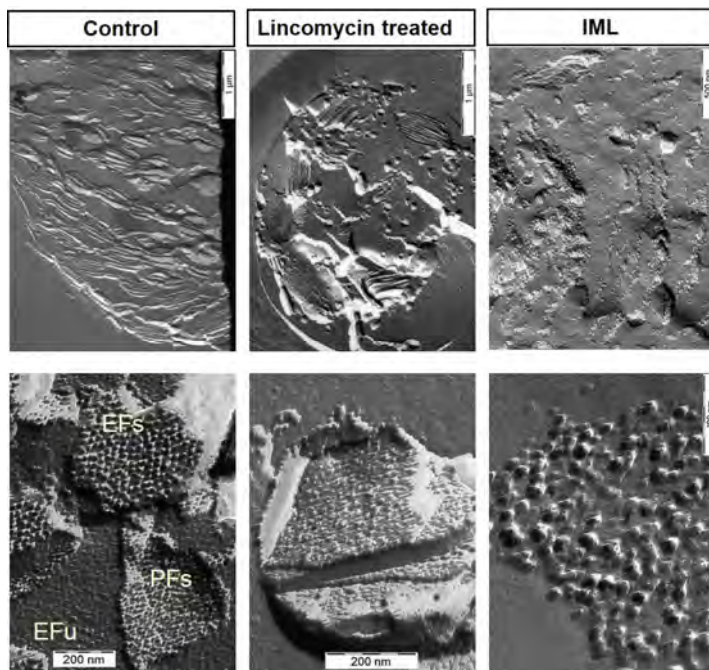


**Figure Supplementary Information 4.1.** Freeze etching electron micrographs of control, lincomycin treated and intermittent light-grown maize thylakoids at various magnification.

For freeze-fracture freshly isolated chloroplasts were prepared. Droplets of 1–2  $\mu\text{L}$  from the samples containing 30% glycerol were pipetted onto the gold holders which were then immediately plunged into liquid-nitrogen-cooled partially solidified Freon for freezing. The fracturing was carried out at  $-110\text{ }^{\circ}\text{C}$  in a Balzers freeze-fracture device (Balzers AG, Vaduz, Liechtenstein). The freeze-fractured faces were etched for 30 s at  $-100\text{ }^{\circ}\text{C}$ , followed by unidirectional platinum/carbon coating at an angle of  $45^{\circ}$ . Replicas of the samples were removed by the submersion into distilled water and subsequently cleaned with commercial detergent solution and then examined using a JEOL JEM-100 CX II (Japan) electron microscope.

## Chapter 5

***Cadmium exerts its toxic effects on  
photosynthesis via a cascade mechanism  
in the cyanobacterium, *Synechocystis*  
PCC 6803***

T. Tóth, O. Zsiros, M. Kis, G. Garab, L. Kovács (2012) Cadmium exerts its toxic effects on photosynthesis via a cascade mechanism in the cyanobacterium, *Synechocystis* PCC 6803. *Plant Cell & Environment* 35:2075-2086

*Institute of Plant Biology, Biological Research Centre, Hungarian Academy of Sciences, PO Box 521, H-6726, Szeged, Hungary*

# *Effect of cadmium on photosynthesis*

---

## **5.1 Abstract**

Despite intense research, the mechanism of  $\text{Cd}^{2+}$  toxicity on photosynthesis is still elusive because of the multiplicity of the inhibitory effects and due to different barriers in plants. The quick  $\text{Cd}^{2+}$  uptake in *Synechocystis* PCC 6803 permits the direct interaction of cadmium with the photosynthetic machinery and allows the distinction between primary and secondary effects. We show that the  $\text{CO}_2$ -dependent electron transport is rapidly inhibited upon exposing the cells to  $40 \mu\text{M Cd}^{2+}$  (50% inhibition in ~15 min). However, during this time we observe only symptoms of photosystem I acceptor side limitation and a build of an excitation pressure on the reaction centres, as indicated by light-induced P700 redox transients,  $\text{O}_2$  polarography and changes in chlorophyll a fluorescence parameters. Inhibitory effects on photosystem II electron transport and the degradation of the reaction centre protein D1 can only be observed after several hours, and only in the light, as revealed by chlorophyll a fluorescence transients, thermoluminescence and immuno blotting. Despite the marked differences in the manifestations of these short- and long-term effects they exhibit virtually the same  $\text{Cd}^{2+}$  concentration dependence. These data strongly suggest a cascade mechanism of the toxic effect, with a primary effect in the dark reactions.

## **5.2 Introduction**

Cadmium is one of the most toxic environmental pollutants and several studies focus on the mechanism of action of this element. For a long time cadmium was regarded as a toxic heavy metal without any biological function. Some recent discoveries revealed that plants can require  $\text{Cd}^{2+}$  at trace amounts for optimal growth [1]. Although cadmium is a relatively rare element in the Earth crust [2] human activities can increase its concentration to toxic level. Cadmium is introduced into the terrestrial environment from mining, non-ferrous metal production, phosphate fertilizers, and manure that can increase the  $\text{Cd}^{2+}$  concentration up to a few hundred mg/kg soil at industrialized or intensely cultivated areas. In addition, cadmium input to the aquatic environment is through discharge of industrial waste, surface run-off, and deposition. This elevated  $\text{Cd}^{2+}$  concentration can result in the uptake and accumulation of  $\text{Cd}^{2+}$  in different organisms to toxic levels.  $\text{Cd}^{2+}$  exerts severe physiological effects in most living organisms also because it has a relatively long biological half-time, e.g. in human it is estimated to be between 25-50 years depending on age [3]. Due to this long half time plants and animals can easily accumulate  $\text{Cd}^{2+}$  in their organs. Plants and phytoplankton possess high  $\text{Cd}^{2+}$  accumulating capacities [4]. Since the  $\text{Cd}^{2+}$  that is incorporated into plants or aquatic cells is transferred to higher trophic levels of the food chain, consecutive

accumulation at every trophic level, the so-called biomagnifications, can increase the  $\text{Cd}^{2+}$  concentration in the consumers much above the  $\text{Cd}^{2+}$  concentration found in the environment.

The photosynthetic apparatus of various photoautotroph organisms appear to be particularly susceptible to this heavy metal pollutant. In spite of the intense research on  $\text{Cd}^{2+}$  effects on photosynthesis the mechanism of  $\text{Cd}^{2+}$  toxicity is still elusive and the reported results are often contradictory. The toxic effect of  $\text{Cd}^{2+}$  on photosynthesis is very complex and apparently different mechanisms are involved.  $\text{Cd}^{2+}$  can interact with proteins by reacting with their active groups [5, 6] or replacing metal cations ( $\text{Zn}^{2+}$ ,  $\text{Cu}^{2+}$ ,  $\text{Ca}^{2+}$ ) in metallo-proteins [6, 7]. Heavy metals can generate reactive oxygen species by Fenton's reaction although in this respect  $\text{Cd}^{2+}$  is rather inert. Many proteins involved in photosynthetic and related processes contain  $\text{Zn}^{2+}$  (e.g. carbonic anhydrases) and sulfhydryl groups (e.g. glyceraldehyde-3-phosphate dehydrogenase, ribulose-5-phosphate kinase, fructose-1,6-bisphosphatase), which may make photosynthesis one of the main targets to  $\text{Cd}^{2+}$ .

The primary target of  $\text{Cd}^{2+}$  inhibition is still not identified and it is not clear which are the direct and indirect effects. Both the donor [8, 9] and acceptor sides of PSII [8, 10] have been demonstrated to suffer damage upon  $\text{Cd}^{2+}$  exposure *in vitro*, but these results have not been confirmed by *in vivo* experiments. Recently, PSI acceptor side and FNR were also suggested as the primary target [7] but in these experiments the authors used unrealistically high, millimolar to molar  $\text{Cd}^{2+}$  concentrations. In other studies, the effect of  $\text{Cd}^{2+}$  on the dark reactions of photosynthesis was emphasised [11, 12]. The contradictory observations may originate from differences in the experimental conditions, particularly in the applied  $\text{Cd}^{2+}$  concentration, the duration of  $\text{Cd}^{2+}$  exposure and the way the  $\text{Cd}^{2+}$  was administered. Also, the mechanism of  $\text{Cd}^{2+}$  toxicity can be different in various organisms. In case of terrestrial plants cadmium is typically taken up from the soil by the root system, from where it is transported to the assimilatory tissues of leaves and can reach the chloroplasts. The transport of cadmium from the soil to the chloroplast via different tissues is delayed by several barriers. Active defensive mechanisms such as the expression of metal sequestering proteins and the accumulation of  $\text{Cd}^{2+}$  in the vacuole, sequesters a considerable amount of  $\text{Cd}^{2+}$  away from potential targets [13]. To affect photosynthesis, the remaining  $\text{Cd}^{2+}$  must be transported to the leaves from the root via xylem transport. By the time the  $\text{Cd}^{2+}$  could accumulate significantly in the chloroplast, secondary effects induced in the roots can already influence the photosynthetic machinery, e.g. the iron deficiency caused by the inhibition of the metal transport leading to a disturbed metal homeostasis that can suppress the chlorophyll and metalloprotein synthesis [14].

# *Effect of cadmium on photosynthesis*

---

In contrast to terrestrial plants, aquatic organisms can readily take up  $\text{Cd}^{2+}$  from water.  $\text{Cd}^{2+}$  has high water solubility compared to other transition metals, which ensures high mobility to  $\text{Cd}^{2+}$  in marine and fresh water environments and consequently promotes its wide distribution in aquatic ecosystems. The species of phytoplankton and higher plants submerged to water take up metals via the whole surface of their body. They possess very narrow cuticle and thin cell wall and thus there is no need for long transport mechanisms between different tissues and organs.  $\text{Cd}^{2+}$  has a quick access to the chloroplast or, in cyanobacteria, the thylakoid membranes, and can rapidly exert effects on photosynthesis. Hence, while in terrestrial plants the secondary effects of  $\text{Cd}^{2+}$  can dominate above the direct effects on photosynthesis, in aquatic photosynthetic organisms direct effects can play the major role, at least in the first phase of  $\text{Cd}^{2+}$  inhibition. The cadmium induced effects comparable to responses observed in cyanobacteria can be obtained in higher plants only in isolated protoplasts or chloroplasts [15].

Cyanobacteria are important part of phytoplankton that support all aquatic ecosystems and are known to be highly sensitive to cadmium. Cyanobacteria possess high  $\text{Cd}^{2+}$  binding capacity and rapid uptake, which make these organisms employable in phytoremediation to eliminate  $\text{Cd}^{2+}$  from polluted areas [16]. The enhanced  $\text{Cd}^{2+}$  tolerance is a pre-requisite for such kind of biotechnological application and requires a detailed understanding of the inhibitory mechanism of  $\text{Cd}^{2+}$ . To this end, in the present study, we investigated direct and indirect effects of  $\text{Cd}^{2+}$  on photosynthesis of the cyanobacterium *Synechocystis* PCC 6803.

## **5.3 Materials and Methods**

### *Organism and culture conditions*

*Synechocystis* PCC 6803 cells were grown photoautotrophically in BG11 medium supplemented with 20 mM N-(2-hydroxyethyl)piperazine)-N'-ethanesulfonic acid (HEPES)-NaOH (pH 7.5), at 30 °C under continuous illumination at 25  $\mu\text{mol photons m}^{-2} \text{ s}^{-1}$  photon flux density. Cultures were aerated on a horizontal shaker at 100 r.p.m. The Chl concentration was determined according to [17]. Different concentrations of  $\text{CdCl}_2$  (5, 10, 20, 40, 100, 200  $\mu\text{M}$ ) were applied during the exponential phase of the cell culture.

### *Measurement of photosynthetic activities*

Photosynthetic oxygen-evolving activity of intact cells was measured with a Clark-type oxygen electrode (Hansatech Instruments, Kings Lynn, UK) at saturating intensity of 2000  $\mu\text{mol photons m}^{-2} \text{s}^{-1}$  white light at 30 °C. The PSII dependent Hill reaction was recorded in the presence of 1 mM para-benzoquinone (pBQ). The reaction from  $\text{H}_2\text{O}$  to PSI was followed in the presence of 1 mM methyl viologen (MV). For all polarography measurements the same amount of sample equivalent to 2  $\mu\text{g mL}^{-1}$  chlorophyll was loaded into the sample holder.

### *Measurement of chlorophyll a fluorescence transients*

Chlorophyll a fluorescence transient emission was detected with a Handy PEA instrument (Hansatech Instruments, UK). For the measurements, the sample (equivalent to 20  $\mu\text{g}$  chlorophyll) was filtered onto a filter paper disk. Synechocystis cells were dark adapted for 3 min before the measurements then the cells were illuminated with continuous light (650 nm peak wavelength, 3000  $\mu\text{mol photons m}^{-2} \text{s}^{-1}$  maximum photon flux density) provided by an array of three light-emitting diodes focused on a circle of 5 mm diameter of the sample surface. The first reliably measured point of the fluorescence transient is at 20  $\mu\text{s}$ , which was taken as  $F_0$ .

Maximum and effective quantum yield measurements of PSII were carried out by using a Pulse-Amplitude-Modulation chlorophyll fluorometer (PAM-101); 1 cm optical pathlength was used and the chlorophyll concentration of the sample was 2  $\mu\text{g mL}^{-1}$ . The actinic light was given by 102-L (Walz) red LED light sources with 650 nm peak wavelength, 40  $\mu\text{mol photon m}^{-2} \text{s}^{-1}$  maximum photon flux density. To measure the maximal fluorescence 1 s long, 3000  $\mu\text{mol photons m}^{-2} \text{s}^{-1}$  maximum photon flux density pulse was used. During the illumination the maximal fluorescence ( $F_m'$ ) was measured every 200 seconds.

### *Measurement of the oxidation–reduction kinetics of P700*

The light-induced redox changes of P700 were monitored by measuring the absorbance changes at 820 nm with a Dual PAM-100 chlorophyll fluorometer (Heinz Walz, Germany). The sample (equivalent to 20  $\mu\text{g}$  chlorophyll) was filtered onto a filter paper disk and cells were dark adapted for 3 min before the measurements. In order to determine the amount of total photooxidisable P700, 10 s far-red preillumination followed by a 200 ms long pulse with 1000  $\mu\text{mol photons m}^{-2} \text{s}^{-1}$  maximum photon flux density was used. The rate of the cyclic electron transport was characterised by the time constants ( $\tau$ ) of the re-reduction of  $\text{P700}^+$  after

# *Effect of cadmium on photosynthesis*

---

preillumination. The decay kinetics was recorded with 5 ms time resolution and fitted with a single exponential.

## *Thermoluminescence measurements*

Thermoluminescence measurements were carried out in a home-built apparatus [18]. For the measurement the sample (equivalent to 20  $\mu\text{g}$  chlorophyll) was filtered onto a filter paper disk. After 3 min dark adaptation at 30  $^{\circ}\text{C}$  in the sample holder the cells were excited at -20  $^{\circ}\text{C}$  by a saturating single-turnover flash. Immediately after excitation, the sample was cooled down to -30  $^{\circ}\text{C}$  and the emitted thermoluminescence was measured during heating of the sample in the dark at a heating rate of 20  $^{\circ}\text{C min}^{-1}$ . The Q TL band was detected in the presence of 10  $\mu\text{M}$  DCMU.

## *Polypeptide analysis*

For detailed measurements of D1 content after the different treatments, cells with the same chlorophyll content were homogenized in 250  $\mu\text{L}$  2x Laemmli buffer, and the homogenates were incubated at 90  $^{\circ}\text{C}$  for 5 min followed by a 20 min long incubation at 37  $^{\circ}\text{C}$ . D1 protein of the whole cell extract was separated and analysed by immunoblotting as described by [19].

## **5.4 Results**

Toxic effect of  $\text{Cd}^{2+}$  on the cyanobacterium *Synechocystis* PCC 6803 is demonstrated by measuring the growth rate of algal cultures exposed to various  $\text{CdCl}_2$  concentrations in the range between 5 and 100  $\mu\text{M}$  (Fig. 5.1). The increase of cell density and chlorophyll concentration were followed for 3 days. Even at the lowest applied concentration, at 5  $\mu\text{M}$ ,  $\text{Cd}^{2+}$  significantly suppressed the growth rate (Fig. 5.1 A); above 100  $\mu\text{M}$  the cell propagation was completely halted. The chlorophyll content of the cultures showed similar changes (Fig. 5.1 B). In the presence of 5  $\mu\text{M}$   $\text{Cd}^{2+}$ , the increase of chlorophyll concentration was retarded to the same extent as the increase of cell density; at higher concentrations, they did not increase at all. It is interesting to note that despite the complete inhibition of cell propagation at 10  $\mu\text{M}$   $\text{Cd}^{2+}$  we did not observe any decrease in the cell density and pigment content even at four times higher concentration of  $\text{Cd}^{2+}$  during the three days exposition of the cells to  $\text{Cd}^{2+}$ . Further, the ratio of chlorophyll content to cell density remained unchanged at all examined concentrations. These data strongly suggest that although the cells are not able to divide they still keep their viability at least for three days in the presence of  $\text{Cd}^{2+}$  in the solution. This conclusion is further

supported by viability test (Fig. Supplementary Information 5.1), which has shown that the cells keep their division ability similar to the untreated control even after 12 h  $\text{Cd}^{2+}$  treatment if the cells are subsequently washed with  $\text{Cd}^{2+}$ -free culture medium and transferred to agar plates containing BG11 medium.

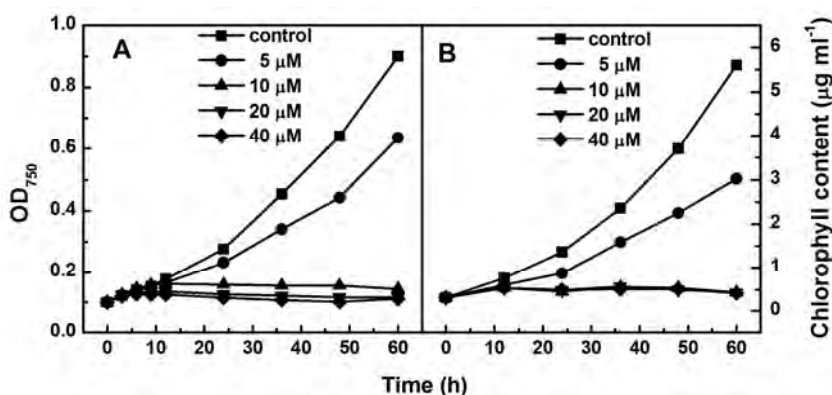


**Figure 5.1.** Variations in the cell density, measured as the OD at 750 nm (A), and the chlorophyll content (B) in *Synechocystis* culture as a function of time after the  $\text{Cd}^{2+}$  treatment at different  $\text{CdCl}_2$  concentrations, as indicated.

The high  $\text{Cd}^{2+}$  sensitivity of the photosynthetic electron transport in *Synechocystis* cells in vivo is demonstrated in Figure 5.2, data similar to our previous work [20].  $\text{Cd}^{2+}$  at 40 μM concentration brings about a complete block in the whole chain electron transport in about half an hour. In order to localize the primary site of inhibition in the photosynthetic electron transport we investigated the effect of cadmium on the photosynthetic activity of intact cells in the presence of artificial electron acceptors, pBQ and MV (Fig. 5.2). It can be seen, however, that neither the pBQ nor the MV dependent Hill reaction rates showed significant decrease even 60 min after the  $\text{Cd}^{2+}$  treatment; by this time the whole chain electron transport had been already completely blocked. In the presence of pBQ and MV respectively, the PSII dependent oxygen evolution and the PSII+PSI electron transport activity, which is independent from ferredoxin and the reduction of  $\text{NADP}^+$ , can be assessed. Hence, these data show that the site of inhibition is to be found at or beyond the ferredoxin binding site in PSI.

The oxidation-reduction kinetics of PSI reaction centre, P700, provides useful information about PSI functions in vivo. The polyphasic oxidation kinetics of P700 upon illumination by actinic red light (Fig. 5.3) can be detected in control

# Effect of cadmium on photosynthesis

sample by measuring the absorption change at 820 nm [21]. The first, fast phase of oxidation is related to the reduction of ferredoxin.

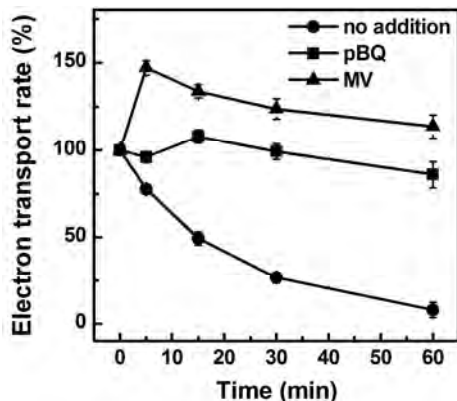


**Figure 5.2.** Effect of  $40 \mu\text{M CdCl}_2$  on the rate of electron transport in the absence and presence of artificial electron acceptors ( $1 \text{ mM pBQ}$  or  $1 \text{ mM MV}$ ) in *Synechocystis* cells as a function of time after the  $\text{Cd}^{2+}$  treatment in presence of the growth light ( $25 \mu\text{mol photons m}^{-2} \text{ s}^{-1}$  white light). The data are given in percentage of the corresponding control values. The activities corresponding to 100% for the untreated cells are about 200, 150 and  $350 \mu\text{mol O}_2 \text{ mg}^{-1} (\text{chl}) \text{ h}^{-1}$ , for whole chain electron transport, MV and pBQ dependent Hill reactions, respectively. Values are given as means  $\pm$  SD ( $n=3$ ).

It is followed by a temporary reduction and finally a few minutes long oxidation occurs in the last phase, which is attributed to the Calvin-Benson cycle. In the sample treated with  $40 \mu\text{M CdCl}_2$  the initial fast phase is still present after 1 h incubation, but the slow kinetic component is missing, suggesting the suppressed capacity of the Calvin-Benson-cycle.

By monitoring the reduction kinetics of P700 after FR illumination, the PSI cyclic electron transport can be tested, which is related to the PSI acceptor side function; since PSI is preferentially excited by FR light, the contribution of PSII to the re-reduction of  $\text{P700}^+$  is negligible [22]. After the illumination of the cells with FR light, a fast re-reduction occurs at a rate proportional to the rate of cyclic ET, and can be characterized by the time constant of the dark reduction. It can be seen that comparable decay time was observed in dark adapted control and  $40 \mu\text{M CdCl}_2$  treated samples (Table 5.1).

**Table 5.1.** The effect of cadmium on the time constant ( $\tau$ ) of re-reduction of  $\text{P700}^+$  kinetics

	$\tau$ (ms $\pm$ SD)	
	dark-adapted	light-adapted
Control	$280 \pm 21$	$143 \pm 2$
$40 \mu\text{M CdCl}_2$ treated	$261 \pm 9$	$59 \pm 5$

After 5 min preillumination by actinic light the cyclic ET in both samples is enhanced as the result of accumulation of NADPH during illumination. In the presence of  $\text{Cd}^{2+}$ , preillumination proved to be more effective in enhancing the re-reduction rate of  $\text{P700}^+$  compared to the control, which suggests an increased NADPH/NADP ratio in  $\text{Cd}^{2+}$  treated samples.

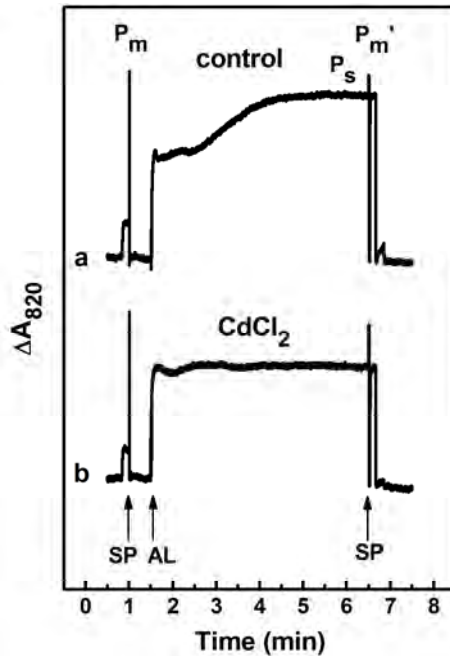


**Figure 5.3.** Kinetics of P700 oxidation recorded as absorbance changes at 820 nm in control (a) (60 min dark adapted) and  $\text{Cd}^{2+}$  treated (b) ( $40 \mu\text{M CdCl}_2$ , 60 min dark) cells. Before the 5 min long actinic light (AL:  $50 \mu\text{mol photons m}^{-2} \text{s}^{-1}$ )  $P_m$ , and at its end  $P_m'$  were obtained with a saturation pulse (SP). Arrows indicate the onset of AL and SPs.

In order to further clarify the site of inhibition in the whole chain electron transport, i.e. the site of inhibition of  $\text{O}_2$  evolution in the absence of artificial electron acceptors, we also performed chlorophyll fluorescence analysis (Fig. 5.4). The time constant of re-reduction of  $\text{P700}^+$  was determined from the kinetics of the absorbance change at 820 nm after far red illumination in intact cells. The kinetic traces were recorded on dark- and light-adapted (5 min,  $50 \mu\text{mol photons m}^{-2} \text{s}^{-1}$ ) cells with and without incubation with  $40 \mu\text{M CdCl}_2$  for 60 min. Values are given as means  $\pm$  SD ( $n=3$ ).

During illumination with non-saturating light intensity the electron acceptors of PSII become partly reduced through a complex kinetics and finally

# Effect of cadmium on photosynthesis

reach a steady-state level with fluorescence intensity ( $F_s$ ), a value between the maximal fluorescence ( $F_m$ ) and the original fluorescence ( $F_o$ ) levels.

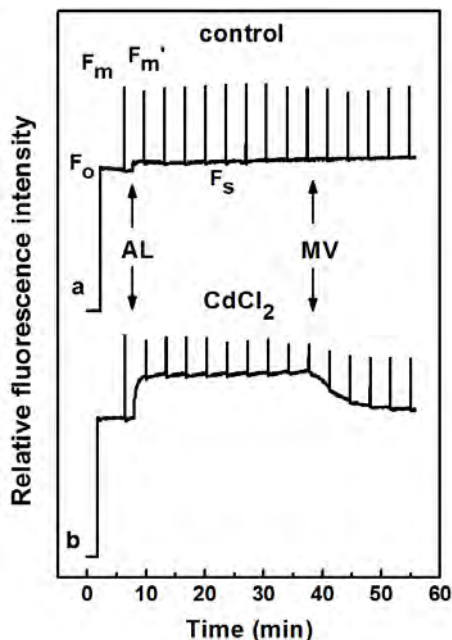


**Figure 5.4.** Chlorophyll a fluorescence induction transients in control (a) (60 min dark-adapted) and  $Cd^{2+}$ -treated (b) (40  $\mu M$   $CdCl_2$ , 60 min dark incubated) *Synechocystis* cells.  $F_o$  and  $F_m$  were obtained before the actinic light (AL: 50  $\mu mol$  photons  $m^{-2} s^{-1}$  red light) was applied.  $F_m'$  values were determined at every third minutes. After 30 min illumination 1 mM methyl viologen (MV) was added. Arrows indicate the onset of AL and the addition of MV.

The  $F_s$  level depends on the applied actinic light intensity. The untreated control and the cells preincubated with 40  $\mu M$   $Cd^{2+}$  for 1 hour in the dark exhibit the same  $F_o/F_m$  values of about 0.4, which is characteristic to dark adapted *Synechocystis* cells [23-25]. In light adapted state the maximal fluorescence,  $F_m'$ , and the  $F_s$  parameters can be used to determine the effective quantum yield of PSII by using the  $\Phi_{PSII}=1-F_o/F_m'$  formula [26]. It can be seen that after illumination of the samples at a photon flux density of 40  $\mu mol$  photons  $m^{-2} s^{-1}$  actinic red light, significantly lower  $\Phi_{PSII}$  can be obtained from  $Cd^{2+}$  treated sample than in the control. The decrease of  $\Phi_{PSII}$  upon  $Cd^{2+}$  treatment is mainly due to the elevation of  $F_s$  value while the decrease of  $F_m'$  is negligible. The addition of 1 mM MV restores  $F_s$  to the control level, which indicates a PSI acceptor side limitation.

In order to identify the possible long-term effects of  $Cd^{2+}$  on the photosystems, functional parameters of PSI and PSII were followed for several

hours. In longer timescale, the  $F_v/F_m$  and the amount of the maximum photooxidisable P700 ( $P_m$ ) parameters were monitored. The activity of PSI ( $P_m$ ) did not show significant changes during the studied time interval; in contrast, a continuous decrease in PSII maximal quantum yield can be observed (Fig. 5.5). The tendency of  $F_v/F_m$  (around 0.4 in control cells) to decrease became pronounced after 4 h of the  $Cd^{2+}$  treatment and in approximately 12 h, a very low value (around 0.15) was detected.

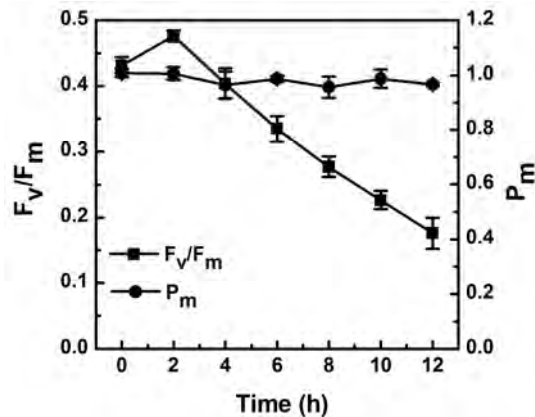


**Figure 5.5.** Maximal quantum yield of PSII ( $F_v/F_m$ ) and the relative amount of the maximal photooxidisable P700 ( $P_m$ ) as a function of time after the addition of 40  $\mu M$   $CdCl_2$  to *Synechocystis* cells. Values are given as means  $\pm$  SD ( $n=3$ ).

The effect of  $Cd^{2+}$  on PSII was further examined by thermoluminescence. Thermoluminescence is a suitable technique to examine the charge separation and stabilization in PSII [27]. In cyanobacterial cells thermoluminescence signal can be induced by a saturating single turnover flash at  $-20$  °C. The arising B band, with a maximum at around 30 °C, originates from charge recombination between the  $S_2$  state of the water splitting enzyme and the reduced secondary quinone acceptor ( $Q_B$ ) of PSII. In the presence of DCMU the so called Q band can be observed. This band originates from charge recombination between the reduced primary PSII acceptor  $Q_A$  and the  $S_2$  state of the water splitting enzyme and exhibits a maximum at around 10 °C. Due to the reduced PSII activity in  $Cd^{2+}$  treated cells, the amplitudes of both the B and the Q bands decreased parallel during  $Cd^{2+}$  treatment (Fig. 5.6). The band positions did not shift suggesting unperturbed redox potential of PSII acceptors and donors involved in the charge recombination process.

## Effect of cadmium on photosynthesis

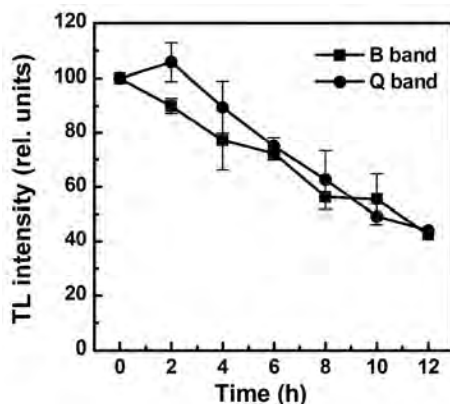


**Figure 5.6.** Changes of the amplitudes of the B and Q thermoluminescence bands in *Synechocystis* cells as a function of time following the 40  $\mu\text{M}$   $\text{CdCl}_2$  treatment. The samples were excited with a single turnover saturating flash at  $-20^\circ\text{C}$  in the absence and presence of 10  $\mu\text{M}$  DCMU for the B and Q bands, respectively. Data are given as percentage of the untreated control. Values are given as means  $\pm$  SD ( $n=3$ ).

In order to check the possible RC protein degradation, we measured the amounts of PSII RC protein D1 in control and  $\text{Cd}^{2+}$  treated sample at different time intervals after the treatment. As shown in Figure 5.7,  $\text{Cd}^{2+}$  treatment decreased the D1 protein level by about 50 % in 5 h.

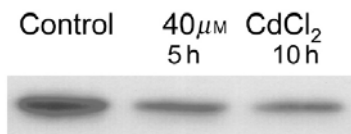


**Figure 5.7.** Immunoblot analysis of D1 protein in control and 40  $\mu\text{M}$   $\text{CdCl}_2$  treated *Synechocystis* cells. The loaded sample in each lane corresponds to 0.15  $\mu\text{g}$  of total chlorophyll.

Effect of cadmium on the photosynthetic activity was also recorded under different light conditions. The treatment was carried out either in the dark or under growth light conditions. The whole chain electron transport and the PSII dependent oxygen evolution ( $\text{H}_2\text{O} \rightarrow \text{pBQ}$ ) were examined (Fig. 5.8). The fast, short-term inhibition in the NADPH dependent whole chain electron transport was observed equally in the dark and in the light. In contrast, the long-term PSII activity decrease was avoided in the dark and evolved only in cells exposed to  $\text{Cd}^{2+}$  in the light.

The rate of inactivation of PSII RC under environmental stresses depends on the balance between the damage and repair mechanisms of the RC proteins. Chloramphenicol inhibits the protein translation at the ribosomes and allows following the net protein damage without recovery processes.

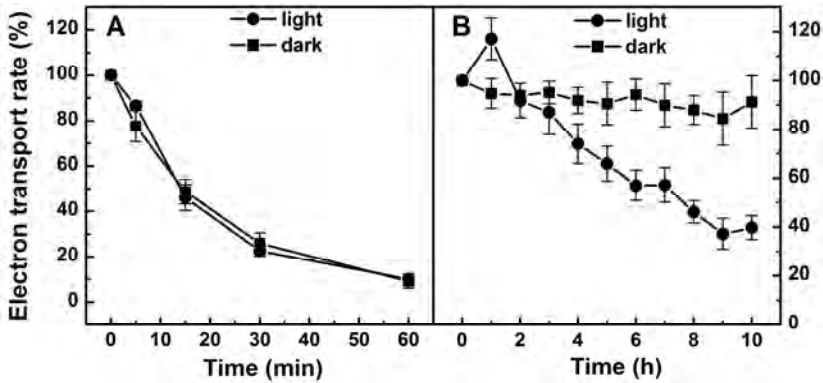


**Figure 5.8.** Time courses of the short-term (60 min (A)) and long-term (10 h (B)) effects of CdCl<sub>2</sub> on *Synechocystis* cells incubated in the presence of 40 μM CdCl<sub>2</sub> in the dark and in the growth light (25 μmol photons m<sup>-2</sup> s<sup>-1</sup> white light). In A and B respectively, the rates of the whole chain electron transport, H<sub>2</sub>O→pBQ Hill reaction were measured. Values are given as means ± SD (n=3).

We have investigated the effect of chloramphenicol on maximal efficiency of PSII in the presence and absence of Cd<sup>2+</sup> at different light intensities (Fig. 5.9). The chloramphenicol treatment induced a decrease in F<sub>v</sub>/F<sub>m</sub> as a function of time in a light intensity dependent way. In the presence of Cd<sup>2+</sup> the effect of chloramphenicol was enhanced at all applied light intensities. The loss of PSII function was faster with increasing light intensities and the extent of inhibition was greater than that chloramphenicol induced alone, although the Cd<sup>2+</sup> decreased the F<sub>v</sub>/F<sub>m</sub> at the same rate as in the presence or absence of chloramphenicol.

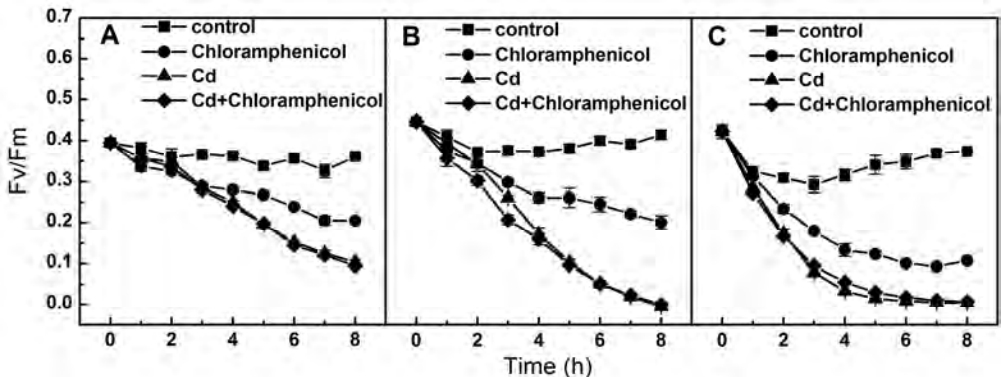


**Figure 5.9.** Long term effect of cadmium on the F<sub>v</sub>/F<sub>m</sub> in the presence of chloramphenicol at different light intensities. *Synechocystis* cells were incubated in the presence or absence of 40 μM CdCl<sub>2</sub> and 200 μg mL<sup>-1</sup> chloramphenicol at 50 (A), 100 (B) and 250 (C) μmol photons m<sup>-2</sup> s<sup>-1</sup> white light.

# *Effect of cadmium on photosynthesis*

Concentration dependences of different responses to  $\text{Cd}^{2+}$  treatment, i.e. the short-term effect, the fast inhibition of the whole-chain electron transport, and the long-term effect, the slow decline of PSII effective quantum yield and the slow the decrease in  $F_v/F_m$  parameter (PSII maximal quantum yield), were compared. Interestingly, the concentration dependences did not differ from each other and the half-maximal inhibition ( $I_{50}$ ) in all cases required the same  $\text{Cd}^{2+}$  concentration, about 20  $\mu\text{M}$  (Fig. 5.10). The derived  $I_{50}$  values,  $19.3 \pm 2.1$  (SE,  $n=6$ ) for  $F_v/F_m$ ,  $14.8 \pm 4.1$  (SE,  $n=5$ ) for  $\Phi_{\text{PSII}}$  and  $20.2 \pm 3.8$  (SE,  $n=6$ ) for ETR respectively do not differ significantly at  $P > 0.05$ .

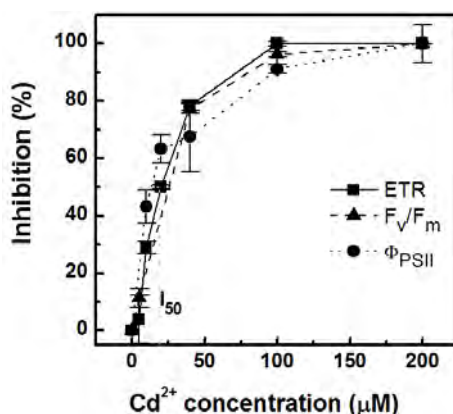


**Figure 5.10.** Cadmium concentration dependences of the inhibition of the maximal ( $F_v/F_m$ ) and the effective ( $\Phi_{\text{PSII}}$ ) quantum yield of PSII and of the suppression of the whole-chain electron transport activity (ETR). The values are given as the percentage of maximal inhibition.  $I_{50}$  value refers to the concentration inducing 50 % inhibition. Values are given as means  $\pm$  SD ( $n=3$ ).

## **5.5 Discussion**

In photosynthetic organisms, photosynthesis is one of the main targets of the toxic effects of  $\text{Cd}^{2+}$  [28]. In plants, the slow uptake rate and delayed accumulation of  $\text{Cd}^{2+}$  may mask the primary effects on the photosynthetic apparatus. Therefore, the primary and secondary inhibitory effects on photosynthesis are not separated, resulting in a rather complex inhibitory pattern, with different  $\text{Cd}^{2+}$  concentration dependences.

In aquatic plants, algae and cyanobacteria the cells are more directly exposed to  $\text{Cd}^{2+}$ , which is thus capable to inhibit the photosynthetic processes drastically in considerably shorter time than in terrestrial plants. Despite the fact that there is no known biological function for cadmium, these photosynthetic organisms take up  $\text{Cd}^{2+}$  in considerable quantity in a relatively short time (less than 5 min) (see

Fig. 5.2), cf. also on *Spirulina pratensis* [16] and on *Synechocystis aquatilis* [29]. Hence, in cyanobacteria the primary effects of  $\text{Cd}^{2+}$  toxicity can be manifested fast enough to discriminate between the fast primary and the slower, secondary effects.

In our experiments *Synechocystis* proved to be very sensitive to  $\text{Cd}^{2+}$  treatment (Fig. 5.1) and already a few  $\mu\text{M}$   $\text{Cd}^{2+}$  drastically decreased the photosynthetic activity after a short time of incubation (Fig. 5.2). Comparable sensitivity to our observations was recorded in the marine cyanobacterium *Synechocystis aquatilis* [29] and in the freshwater cyanobacterium *Microcystis aeruginosa* [30], where, however, a few  $\mu\text{M}$  of  $\text{Cd}^{2+}$  was able to induce significant changes only in two hours. In some other cyanobacterial species, e.g. in *Synechococcus* much higher  $\text{Cd}^{2+}$  concentrations engendered even weaker response [31]. Possible reasons for the lower response are the  $\text{Cd}^{2+}$  adsorption on the cell wall or a more effective operation of inactivation mechanisms, e.g. by induction of chelator proteins [13]. In *Scenedesmus armatus* and *Chlamydomonas reinhardtii* also lower cadmium sensitivity of photosynthetic processes was detected [32]. In these green algae few hundred micromolar  $\text{Cd}^{2+}$  caused similar magnitude inhibition of photosynthesis as in our experiments. In the case of higher plants the applied  $\text{Cd}^{2+}$  concentrations often are unrealistically high.

By using *Synechocystis* cells, we could establish the sequence of different responses to  $\text{Cd}^{2+}$ . In this organism, the fast uptake and the applied  $\text{Cd}^{2+}$  concentrations combined with different light conditions ensures the narrow overlap between different responses provoked by  $\text{Cd}^{2+}$ . In the first step, inhibition of the whole chain electron transport can be observed in a few minutes after the addition of  $\text{Cd}^{2+}$  to the cell culture; in about an hour, with  $40 \mu\text{M}$   $\text{CdCl}_2$ , the  $\text{CO}_2$  dependent  $\text{O}_2$  evolution is fully blocked (Fig. 5.2). Nevertheless, the cells retain their viability even after 12 h  $\text{Cd}^{2+}$  treatment (Fig. Supplementary Information 5.1) despite the complete halt of photosynthetic processes and cell division. This shows that suppression of photosynthesis at the  $\text{Cd}^{2+}$  concentration applied in our experiments is a specific, direct effect rather than arising from a general decline of cell metabolism. In the green alga, *Chlamydomonas reinhardtii* the predominant proportion of cadmium was localized in chloroplasts [33], supporting the notion that photosynthetic processes are the prime targets of  $\text{Cd}^{2+}$  toxicity. Further, the cadmium tolerant mutant of *Chlamydomonas reinhardtii* exhibits an impaired photosynthesis also in the absence of  $\text{Cd}^{2+}$ , suggesting that photosynthesis is more sensitive target of  $\text{Cd}^{2+}$  toxicity than any other metabolic process in green algae [28].

In *Synechocystis aquatilis*  $\text{Cd}^{2+}$  uptake has been shown to occur via active transport [29]. We observed that the fast effect of  $\text{Cd}^{2+}$ , i.e. the inhibition of the whole chain ET occurs at the same rate in the dark as under growth light intensity

## *Effect of cadmium on photosynthesis*

---

(Fig. 5.8 A), suggesting that oxidative phosphorylation can be sufficient for the uptake and it does not demand photophosphorylation.

The insensitivity of MV dependent O<sub>2</sub> uptake and the PSII dependent (H<sub>2</sub>O→pBQ) O<sub>2</sub> evolution to Cd<sup>2+</sup> (Fig. 5.2) can rule out the possibility that the primary site of inhibition is localised in PSII or PSI or the intersystem electron transport components. These data are consistent with literature data [30] and show that the fast inhibition of ET must be localized downstream of PSI acceptor side.

The first possible target of Cd<sup>2+</sup> in terms of the sequence of ET is the ferredoxin-NADP reductase (FNR). Inhibition of FNR by Cd<sup>2+</sup> has been reported by [7], though these results are from in vitro measurements and 5 mM Cd<sup>2+</sup> resulted in only 50 % inhibition. Taking into account that in our case, in vivo, a few μM was sufficient for an essentially full inhibition, the role of FNR as the primary target can be ruled out. This conclusion is consistent with our results on P700 kinetic measurements, where the presence of Cd<sup>2+</sup> does not cause any change in the initial phase of light induced P700 oxidation assigned to ferredoxin activity (Fig. 5.3) [21]. After far red illumination, which preferentially excites PSI, the re-reduction of P700<sup>+</sup> is mainly due to PSI driven cyclic electron transport [34]. In the dark adapted state, the rates of cyclic electron transport, determined from the A<sub>820</sub> transients were essentially identical in the control and the Cd<sup>2+</sup> treated cells (Table 5.1). In light adapted state the rate of re-reduction of P700<sup>+</sup> increases due to the accumulation of reducing power on the acceptor side of PSI [35]. The enhanced acceleration of the re-reduction of P700<sup>+</sup> in Cd<sup>2+</sup> treated cells indicates enhanced NADPH accumulation, which requires the presence of active FNR.

On the basis of the above observations it is clear that the primary site of inhibition must be found beyond PSI, i.e. at later events of photosynthesis, which include the reduction of CO<sub>2</sub> and related processes. Our observation that Cd<sup>2+</sup> interferes with the slow phase of the light induced oxidation kinetics of P700 (Fig. 5.3), which is known to be related to the Calvin-Benson cycle [21], is in perfect agreement with this conclusion. It can be assumed that the main target of Cd<sup>2+</sup> toxicity is one of the enzymes having role in CO<sub>2</sub> fixation since some of the enzymes, e.g. Rubisco, contain free thiol (-SH) groups, which can interact easily with Cd<sup>2+</sup> [5, 36]. The changes in the ratio of the metabolites originating from the Rubisco catalysed reactions observed after cadmium treatment suggest activity decrease of the enzyme [37]. These observations are not direct indicators of the Rubisco operation, and the effect of decreased substrate level on the enzyme activity cannot be excluded. Another possible site of inhibition can be found in the enzymes of the CO<sub>2</sub> concentrating mechanism (CCM), which is also coupled to CO<sub>2</sub> fixation. CCM has basic role in the operation of the Rubisco in aquatic photosynthetic

organisms since it ensure the necessary CO<sub>2</sub> in sufficiently high concentrations in the microenvironment of the enzyme for the domination of carboxylation processes [38]. The key enzymes of CCM are the carbonic anhydrases (CA), which are localised together with Rubisco in the carboxysomes. They are also potential targets to Cd<sup>2+</sup>, since a Zn ion, coordinated in its active centre can be replaced by Cd<sup>2+</sup> [12]. In vitro studies on human carbonic anhydrase showed that the Zn<sup>2+</sup> replacement by Cd<sup>2+</sup> was accompanied by the loss of enzyme activity [39]. In the absence of the CCM key enzyme, CA, the cells cannot provide the conditions necessary for the operation of the Rubisco [40]. Decrease of Rubisco activity at the same rate as the decrease of the CA has been published in the literature [29, 37]. In our previous work, perturbed angular correlation of  $\gamma$ -rays (PAC) spectroscopy measurements have shown in vivo that in *Synechocystis* cells in the presence of 40  $\mu$ M CdCl<sub>2</sub>, fast, 20-30 min incubation causes a specific binding of Cd<sup>2+</sup> to a CA like protein [20]. Further, it has been reported [41] that in presence of Cd<sup>2+</sup> the synthesis of a novel carbonic anhydrase enzyme that contains Cd<sup>2+</sup> in its catalytic centre instead of Zn<sup>2+</sup> is induced in the marine diatom *Thalassiosira weissflogii*; the physiological role of this CA is not completely clarified yet but it might indicate that the Zn<sup>2+</sup> containing isoform is sensitive to Cd<sup>2+</sup> [41].

Until four hours after the addition of Cd<sup>2+</sup>, the thermoluminescence (Fig. 5.6) and chlorophyll fluorescence transient (Fig. 5.5) measurements show no significant changes in PSII functions, and PSI activity (Fig. 5.5) remains unaffected even after 12 h of the start of the treatment. In contrast to the maximal efficiency, the operative efficiency of PSII in light adapted state ( $\Phi$ PSII) is decreasing in the sample preincubated with 40  $\mu$ M CdCl<sub>2</sub> (Fig. 5.4). The reason of this decrease is mainly due to the reduced number of open reaction centres (increase of the F<sub>s</sub>), rather than the decrease of the intrinsic maximum quantum yield of PSII (decrease of F<sub>m</sub>'). This is supported by the fact that the PSII effective quantum yield can be restored to the control value by the addition of PSI electron acceptor, MV (1 mM), to the cells. In other terms, the increased F<sub>s</sub> can be explained by the combined effect of illumination and the block of ET beyond PSI.

In the second phase of the response to Cd<sup>2+</sup> treatment, the activity of PSII (the maximal quantum efficiency) and the primary photochemical processes of PSII (Figs. 5.5 and 5.6) show gradual decrease as a function of time. These decreases and the pBQ dependent O<sub>2</sub> evolution (Fig. 5.8 B circle) are manifested after four hours incubation in the presence of cadmium. In the literature two target sites, at which PSII inactivation occurs upon cadmium treatment, have been proposed in higher plants. Several authors suggested donor side effect as the origin of the Cd<sup>2+</sup> induced decrease in PSII activity [9, 11, 22, 42], while others proposed the inactivation of the

## *Effect of cadmium on photosynthesis*

PSII RCs [10, 43]. It is also suggested that the photoactivation of PSII RC is inhibited by cadmium at low concentrations due to a competition between  $\text{Cd}^{2+}$  and  $\text{Ca}^{2+}$  for the  $\text{Ca}^{2+}$  binding site that hampers the assembly the PSII with functional donor side [9].

Our thermoluminescence results do not support a specific inactivation of the water splitting complex. Both the B and Q TL bands depend on  $\text{S}_2$  states of the WOC. Although the parallel decrease of these two bands would suggest the inactivation of donor side but in this case the TyrZ and TyrD redox-active residuals of the heterodimer RC proteins would replace the  $\text{S}_2$  state of water splitting enzyme in the charge recombination processes, which should increase the C band and the AT band originating from  $\text{TyrZ}^+/\text{Q}_\text{A}^-$  and  $\text{TyrD}^+/\text{Q}_\text{A}^-$  charge recombinations, respectively [44]; however, neither the appearance of AT band nor the enhancement of C band were observed (Fig. Supplementary Information 5.3), similarly to our previous results [20]. Hence, our TL data reflect the inactivation of RCs rather than specific donor side effect. These results are in good agreement with the data from chl a fluorescence transient measurements where the same gradual long-term decrease of  $F_m$  was observed both in the absence and presence of DCMU (Fig. Supplementary Information 5.4).  $F_m$  in DCMU treated sample does not depend on the WOC as long as the RC is active since a single electron provided by TyrZ or TyrD is sufficient to fully reduce  $\text{Q}_\text{A}$ . Hence, the decrease of  $F_m$  in the presence DCMU reflects the impairment of RCs. Immunoblot analysis (Fig. 5.7) also shows that the amount of D1 protein decreases together with PSII fluorescence and thermoluminescence, further supporting our assumption that the decrease of PSII activity is due to the inactivation of the RC rather than the impairment of PSII donor side.

In contrast to the short-term effect, which occurs at the same rate in the dark as in light, the long-term  $\text{Cd}^{2+}$  induced inhibition on PSII activity, i.e. the decrease of  $\text{O}_2$  evolving capacity in the presence of pBQ and the decline of  $F_v/F_m$  were observed in cells which were kept in light after the  $\text{Cd}^{2+}$  treatment (Fig. 5.8). The extent of PSII inactivation was greater with increasing light intensity (Fig. 5.9). It is well established that even moderate light can promote ROS formation under stress conditions [45]. The direct ROS formation ability of  $\text{Cd}^{2+}$  via Fenton's reaction is rather low but it might produce ROS indirectly in the presence of light by blocking the electron transport because of the limitation of  $\text{CO}_2$  fixation and the increased excitation pressure on PSII [46, 47]. This is indicated by the elevated  $F_s$  level that can be alleviated by the addition of MV (Fig. 5.4) serving as an artificial PSI electron acceptor.

It is generally accepted that the ROS generated under stress conditions can directly inactivate the photochemical reaction center of PSII [48]. This model has

been recently challenged by a new scheme in which ROS inhibit the repair of photodamaged PSII by suppressing primarily the synthesis of proteins de novo [49, 50]. The damage of RC can be monitored separately from its recovery in the presence of protein synthesis inhibitors like chloramphenicol [51]. Our observation that  $\text{Cd}^{2+}$  enhances the rate of PSII inactivation measured in the presence of chloramphenicol (Fig. 5.9) shows that  $\text{Cd}^{2+}$  promotes the direct inhibition of PSII RC. Although, the  $\text{Cd}^{2+}$  itself suppresses the PSII maximum efficiency in the same extent as in the presence of chloramphenicol indicating that the recovery of PSII is not efficient during  $\text{Cd}^{2+}$  stress. The limited recovery may be due to the retarded de novo protein synthesis. The last step of PSII recovery from photodamage is the photoactivation of PSII RC. Since it has been shown that in *Chlamydomonas reinhardtii*  $\text{Cd}^{2+}$  directly inhibits this step of recovery at low concentrations [9], we cannot rule out that the hampered photoactivation may also contribute to the lack of efficient recovery in  $\text{Cd}^{2+}$  treated *Synechocystis* cells, as well.

Comparison of the concentration dependence of short- and long term  $\text{Cd}^{2+}$  effects followed the pattern and resulted in approximately the same  $I_{50}$  value despite the differences in the inhibitory sites and times required for the inhibition (Fig. 5.10). This strongly suggests that all the above effects originate from the same primary effect. Evidently, the short-term effect, the fast inhibition of electron transport must be considered the primary inhibitory effect, which then can be held responsible for the long-term effects, the slowly evolving secondary effects affecting PSII.

Based on the data presented in this work and our previous results, together with data available in the literature, we propose that the multiphase effect of  $\text{Cd}^{2+}$  on the photosynthesis of *Synechocystis* cells primarily stems from a single site of inhibition and is extended via a cascade mechanism according to the following scheme:  $\text{Cd}^{2+}$  is able to penetrate through the cell wall and to accumulate in the cells even at low environmental concentrations; it inhibits the dark phase of the photosynthesis via specifically binding to (an) enzyme(s) of the Calvin-Benson cycle and/or that involved in the  $\text{CO}_2$  concentrating mechanism. Inhibition of carbon fixation decreases the consumption of ATP and NADPH, which in turn, in the presence of light, increases the ATP/ADP and NADPH/NADP ratios. This engenders the block of the electron transport; this, combined with the effect of simultaneous illumination, can bring about an elevated excitation pressure on PSII. The over-reduction of electron transport components can increase the probability of charge recombination between  $\text{P680}^+$  and reduced pheophytin that produce the excited state of the reaction centre,  $\text{P680}^*$  and thus can induce the production of reactive oxygen species [52, 53]. The ROS accumulation decreases the D1 protein

# *Effect of cadmium on photosynthesis*

level directly or indirectly by blocking the protein synthesis and recovery of the PSII RCs that finally leads to the impairment of the reaction centre functions. At the same time, via an independent mechanism, the Cd<sup>2+</sup> may enhance the PSII inactivation by suppressing the photoactivation of PSII.

## 5.6 Acknowledgements

This work was supported by grants from Hungarian Research Fund (OTKA, CNK-8345 and OTKA, 68692), Social Renewal Operational Program (TÁMOP-4.2.2/B-10/1-2010-0012) and Hungary-Romania Cross-Border Co-operation Program (HURO/0901/270/2.2.2.)

## 5.7 Reference list

- [1] Liu, M.Q., Yanai, J.T., Jiang, R.F., Zhang, F., McGrath, S.P., Zhao, F.J., Does cadmium play a physiological role in the hyperaccumulator *Thlaspi caerulescens*?, *Chemosphere*, 71 (2008) 1276-1283.
- [2] Shiller, A.M., Boyle, E.A., Variability of dissolved trace-metals in the Mississippi river, *Geochim. Cosmochim. Acta*, 51 (1987) 3273-3277.
- [3] Wagner, G.J., Accumulation of cadmium in crop plants and its consequences to human health, *Advances in Agronomy*, Vol 51, 51 (1993) 173-212.
- [4] Conway, H.L., Sorption of arsenic and cadmium and their effects on growth, micronutrient utilization, and photosynthetic pigment composition of *Asterionella formosa*, *J Fish Res Board Can*, 35 (1978) 286-294.
- [5] Clijsters, H., Van Assche, F., Inhibition of photosynthesis by heavy metals, *Photosynth Res.*, 7 (1985) 31-40.
- [6] Vanassche, F., Clijsters, H., Effects of metals on enzyme-activity in plants, *Plant Cell and Environment*, 13 (1990) 195-206.
- [7] Grzyb, J., Waloszek, A., Latowski, D., Wieckowski, S., Effect of cadmium on ferredoxin : NADP<sup>+</sup> oxidoreductase activity, *J. Inorg. Chem.*, 98 (2004) 1338-1346.
- [8] Sigfridsson, K.G.V., Bernat, G., Mamedov, F., Styring, S., Molecular interference of Cd<sup>2+</sup> with photosystem II, *Biochim. Biophys. Acta*, 1659 (2004) 19-31.
- [9] Faller, P., Kienzler, K., Krieger-Liszkay, A., Mechanism of Cd<sup>2+</sup> toxicity: Cd<sup>2+</sup> inhibits photoactivation of photosystem II by competitive binding to the essential Ca<sup>2+</sup> site, *Biochim. Biophys. Acta*, 1706 (2005) 158-164.
- [10] Atal, N., Saradhi, P.P., Mohanty, P., Inhibition of the chloroplast photochemical-reactions by treatment of wheat seedlings with low concentrations of cadmium - Analysis of electron-transport activities and changes in fluorescence yield, *PCP*, 32 (1991) 943-951.
- [11] Krupa, Z., Oquist, G., Huner, N.P.A., The effects of cadmium on photosynthesis of *Phaseolus vulgaris* - A fluorescence analysis, *Physiol. Plant.*, 88 (1993) 626-630.
- [12] Aravind, P., Prasad, M.N.V., Carbonic anhydrase impairment in cadmium-treated *Ceratophyllum demersum* L. (free floating freshwater macrophyte): toxicity reversal by zinc, *J Anal Atom Spectrom*, 19 (2004) 52-57.
- [13] Cobbett, C., Goldsbrough, P., Phytochelatins and metallothioneins: Roles in heavy metal detoxification and homeostasis, *Annu. Rev. Plant Biol.*, 53 (2002) 159-182.
- [14] Siedlecka, A., Baszynski, T., Inhibition of electron flow around photosystem I in chloroplasts of Cd-treated maize plants is due to Cd-induced iron-deficiency, *Physiol. Plant.*, 87 (1993) 199-202.
- [15] Greger, M., Ogren, E., Direct and indirect effects of Cd<sup>2+</sup> on photosynthesis in sugar-beet (*Beta vulgaris*), *Physiol. Plant.*, 83 (1991) 129-135.

- [16] **Rangsayatorn, N., Upatham, E.S., Kruatrachue, M., Pokethitiyook, P., Lanza, G.R.**, Phytoremediation potential of *Spirulina (Arthrospira) platensis*: biosorption and toxicity studies of cadmium, *Environ. Pollut.*, 119 (2002) 45-53.
- [17] **Arnon, D.I., McSwain, B.D., Tsujimoto, H.Y., Wada, K.**, Photochemical activity and components of membrane preparations from blue-green algae. I. Coexistence of two photosystems in relation to chlorophyll a and removal of phycocyanin, *Biochim. Biophys. Acta*, 357 (1974) 231-245.
- [18] **Demeter, S., Vass, L., Horvath, G., Laufer, A.**, Charge accumulation and recombination in photosystem II studied by thermo-luminescence. 2. Oscillation of the C-band induced by flash excitation, *Biochim. Biophys. Acta*, 764 (1984) 33-39.
- [19] **Bajkan, S., Varadi, G., Balogh, M., Domonkos, A., Kiss, G.B., Kovacs, L., Lehoczki, E.**, Conserved structure of the chloroplast-DNA encoded D1 protein is essential for effective photoprotection via non-photochemical thermal dissipation in higher plants, *Mol. Genet. Genomics*, 284 (2010) 55-63.
- [20] **Sas, K.N., Kovacs, L., Zsiros, O., Gombos, Z., Garab, G., Hemmingsen, L., Danielsen, E.**, Fast cadmium inhibition of photosynthesis in cyanobacteria in vivo and in vitro studies using perturbed angular correlation of gamma-rays, *JBIC*, 11 (2006) 725-734.
- [21] **Harbinson, J., Hedley, C.L.**, Changes in P700 oxidation during the early stages of the induction of photosynthesis, *Plant Physiol.*, 103 (1993) 649-660.
- [22] **Bernat, G., Appel, J., Ogawa, T., Roegner, M.**, Distinct roles of multiple NDH-1 complexes in the cyanobacterial electron transport network as revealed by kinetic analysis of P700(+) reduction in various *ndh*-deficient mutants of *Synechocystis sp.* strain PCC 6803, *J. Bacteriol.*, 193 (2011) 292-295.
- [23] **Campbell, D., Hurry, V., Clarke, A.K., Gustafsson, P., Oquist, G.**, Chlorophyll fluorescence analysis of cyanobacterial photosynthesis and acclimation, *Microbiol. Mol. Biol. Rev.*, 62 (1998) 667-683.
- [24] **Laczko-Dobos, H., Ughy, B., Toth, S.Z., Komenda, J., Zsiros, O., Domonkos, I., Parducz, A., Bogos, B., Komura, M., Itoh, S., Gombos, Z.**, Role of phosphatidylglycerol in the function and assembly of photosystem II reaction center, studied in a *cdsA*-inactivated PAL mutant strain of *Synechocystis sp.* PCC6803 that lacks phycobilisomes, *Biochim. Biophys. Acta*, 1777 (2008) 1184-1194.
- [25] **Hackenberg, C., Engelhardt, A., Matthijs, H.C., Wittink, F., Bauwe, H., Kaplan, A., Hagemann, M.**, Photorespiratory 2-phosphoglycolate metabolism and photoreduction of O<sub>2</sub> cooperate in high-light acclimation of *Synechocystis sp.* strain PCC 6803, *Planta*, 230 (2009) 625-637.
- [26] **Baker, N.R., Harbinson, J., Kramer, D.M.**, Determining the limitations and regulation of photosynthetic energy transduction in leaves, *Plant Cell and Environment*, 30 (2007) 1107-1125.
- [27] **Ducruet, J.M., Vass, I.**, Thermoluminescence: experimental, *Photosynth Res.*, 101 (2009) 195-204.
- [28] **Nagel, K., Voigt, J.**, Impaired photosynthesis in a cadmium-tolerant *Chlamydomonas* mutant strain, *Microbiol. Res.*, 150 (1995) 105-110.
- [29] **Pawlik, B., Skowronski, T., Ramazanow, Z., Gardestrom, P., Samuelsson, G.**, pH-dependent cadmium transport inhibits photosynthesis in the cyanobacterium *Synechocystis aquatilis*, *Environ. Exp. Bot.*, 33 (1993) 331-337.
- [30] **Zhou, W.B., Juneau, P., Qiu, B.S.**, Growth and photosynthetic responses of the bloom-forming cyanobacterium *Microcystis aeruginosa* to elevated levels of cadmium, *Chemosphere*, 65 (2006) 1738-1746.
- [31] **Tumova, E., Sofrova, D.**, Response of intact cyanobacterial cells and their photosynthetic apparatus to Cd<sup>2+</sup> ion treatment, *Photosynthetica*, 40 (2002) 103-108.
- [32] **Tukaj, Z., Bascik-Remisiewicz, A., Skowronski, T., Tukaj, C.**, Cadmium effect on the growth, photosynthesis, ultrastructure and phytochelatin content of green microalga *Scenedesmus armatus*: A study at low and elevated CO<sub>2</sub> concentration, *Environ. Exp. Bot.*, 60 (2007) 291-299.
- [33] **Nagel, K., Adelmeier, U., Voigt, J.**, Subcellular distribution of cadmium in the unicellular green alga *Chlamydomonas reinhardtii*, *J. Plant Physiol.*, 149 (1996) 86-90.

# *Effect of cadmium on photosynthesis*

- [34] **Chow, W.S., Hope, A.B.**, Electron fluxes through photosystem I in cucumber leaf discs probed by far-red light, *Photosynth Res.*, 81 (2004) 77-89.
- [35] **Cornic, G., Bukhov, N.G., Wiese, C., Bligny, R., Heber, U.**, Flexible coupling between light-dependent electron and vectorial proton transport in illuminated leaves of C-3 plants. Role of photosystem I-dependent proton pumping, *Planta*, 210 (2000) 468-477.
- [36] **Štiborova, M.**, Cd<sup>2+</sup> ions affect the quaternary structure of ribulose-1,5-bisphosphate carboxylase from barley leaves, *Biochemie und Physiologie der Pflanzen*, 183 (1988) 371-378.
- [37] **Siedlecka, A., Krupa, Z., Samuelsson, G., Oquist, G., Gardestrom, P.**, Primary carbon metabolism in *Phaseolus vulgaris* plants under Cd/Fe interaction, *Plant Physiol. Biochem.*, 35 (1997) 951-957.
- [38] **Kaplan, A., Reinhold, L.**, CO<sub>2</sub> concentrating mechanisms in photosynthetic microorganisms, *Annu. Rev. Plant Physiol. Plant Mol. Biol.*, 50 (1999) 539-+.
- [39] **Bauer, H., Nagele, M., Comploj, M., Galler, V., Mair, M., Unterpertinger, E.**, Photosynthesis in cold-acclimated leaves of plants with various degrees of freezing tolerance, *Physiol. Plant.*, 91 (1994) 403-412.
- [40] **Moroney, J.V., Husic, H.D., Tolbert, N.E., Kitayama, M., Manuel, L.J., Togasaki, R.K.**, Isolation and characterization of a mutant of *Chlamydomonas reinhardtii* deficient in the CO<sub>2</sub> concentrating mechanism, *Plant Physiol.*, 89 (1989) 897-903.
- [41] **Lane, T.W., Saito, M.A., George, G.N., Pickering, I.J., Prince, R.C., Morel, F.M.M.**, A cadmium enzyme from a marine diatom, *Nature*, 435 (2005) 42-42.
- [42] **Krupa, Z., Skorzynska, E., Maksymiec, W., Baszynski, T.**, Effect of cadmium treatment on the photosynthetic apparatus and its photochemical activities in greening radish seedlings, *Photosynthetica*, 21 (1987) 156-&.
- [43] **Jegerschold, C., Arellano, J.B., Schroder, W.P., Vankan, P.J.M., Baron, M., Styring, S.**, Copper(II) inhibition of electron-transfer through photosystem II studied by EPR spectroscopy, *Biochemistry*, 34 (1995) 12747-12754.
- [44] **Vass, I.**, The history of photosynthetic thermoluminescence, *Photosynth Res.*, 76 (2003) 303-318.
- [45] **Huner, N.P.A., Maxwell, D.P., Gray, G.R., Savitch, L.V., Krol, M., Ivanov, A.G., Falk, S.**, Sensing environmental temperature change through imbalances between energy supply and energy consumption: Redox state of photosystem II, *Physiol. Plant.*, 98 (1996) 358-364.
- [46] **Long, S.P., Humphries, S., Falkowski, P.G.**, Photoinhibition of photosynthesis in nature, *Annu. Rev. Plant Physiol. Plant Mol. Biol.*, 45 (1994) 633-662.
- [47] **Korniyev, D., Logan, B.A., Holaday, A.S.**, Excitation pressure as a measure of the sensitivity of photosystem II to photoinactivation, *Funct. Plant Biol.*, 37 (2010) 943-951.
- [48] **Keren, N., Berg, A., VanKan, P.J.M., Levanon, H., Ohad, I.**, Mechanism of photosystem II photoinactivation and D1 protein degradation at low light: The role of back electron flow, *P Natl Acad Sci USA*, 94 (1997) 1579-1584.
- [49] **Murata, N., Takahashi, S., Nishiyama, Y., Allakhverdiev, S.I.**, Photoinhibition of photosystem II under environmental stress, *Biochim. Biophys. Acta*, 1767 (2007) 414-421.
- [50] **Nishiyama, Y., Allakhverdiev, S.I., Murata, N.**, Protein synthesis is the primary target of reactive oxygen species in the photoinhibition of photosystem II, *Physiol. Plant.*, 142 (2011) 35-46.
- [51] **Nishiyama, Y., Yamamoto, H., Allakhverdiev, S.I., Inaba, M., Yokota, A., Murata, N.**, Oxidative stress inhibits the repair of photodamage to the photosynthetic machinery, *EMBO J.*, 20 (2001) 5587-5594.
- [52] **Vass, I.**, Molecular mechanisms of photodamage in the photosystem II complex, *Biochim. Biophys. Acta*, 1817 (2012) 209-217.
- [53] **Vass, I.**, Role of charge recombination processes in photodamage and photoprotection of the photosystem II complex, *Physiol. Plant.*, 142 (2011) 6-16.

## 5.8 Supplementary Information

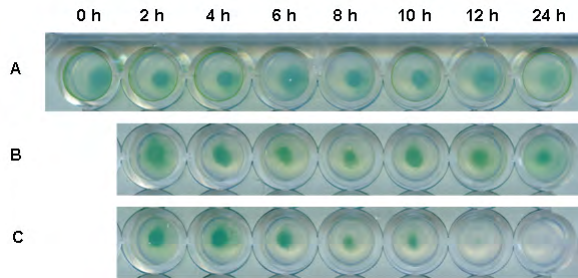


**Figure Supplementary Information 5.1.** Effect of  $\text{Cd}^{2+}$  on the viability of *Synechocystis* cells. Cells were incubated without (A) and with  $40 \mu\text{M CdCl}_2$  (B, C) and at various times aliquots were taken and centrifuged; then the cells were resuspended in Cd-free (A and B) and in  $40 \mu\text{M CdCl}_2$  containing cultivation medium (C) and equal volumes were loaded into the wells of tissue culture plates filled with agar containing BG11 medium. The photo was taken after 3 days incubation under growth conditions.

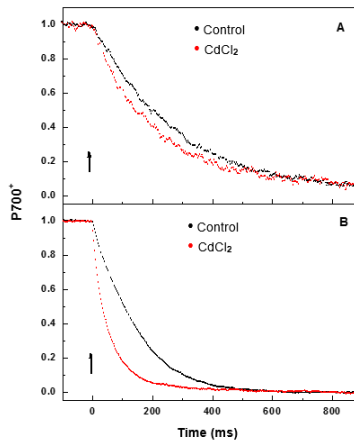


**Figure Supplementary Information 5.2.** Re-reduction kinetics of  $\text{P700}^+$  after far-red illumination in control ( $\bullet$ ) and  $\text{Cd}^{2+}$  pretreated ( $40 \mu\text{M CdCl}_2$ , 1 h) ( $\bullet$ ) *Synechocystis* cells before (A) and after (B) 5 min illumination with  $37 \mu\text{mol photon m}^{-2} \text{s}^{-1}$  actinic light. Arrows indicate the cessation of far-red light.

# Effect of cadmium on photosynthesis

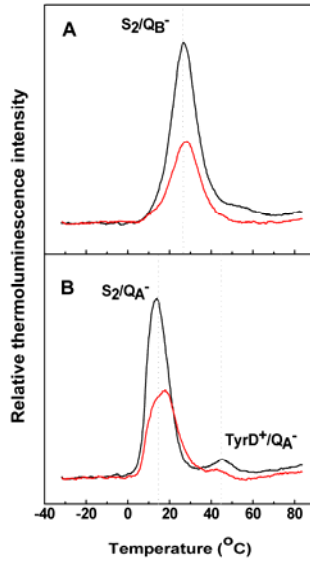


**Figure Supplementary Information 5.3.** Thermoluminescence glow curves of control (black curves) and CdCl<sub>2</sub> treated (red curves) (40 μM CdCl<sub>2</sub> for 10 h under growth light) *Synechocystis* cells. The B band (A) (originating from the S<sub>2</sub>/Q<sub>B</sub><sup>-</sup> charge recombination) and the Q band (B) (originating from the S<sub>2</sub>/Q<sub>A</sub><sup>-</sup> charge recombination) were measured in the absence and presence of 10 μM DCMU, respectively. The samples were excited with a single turnover saturating flash at -20 °C.

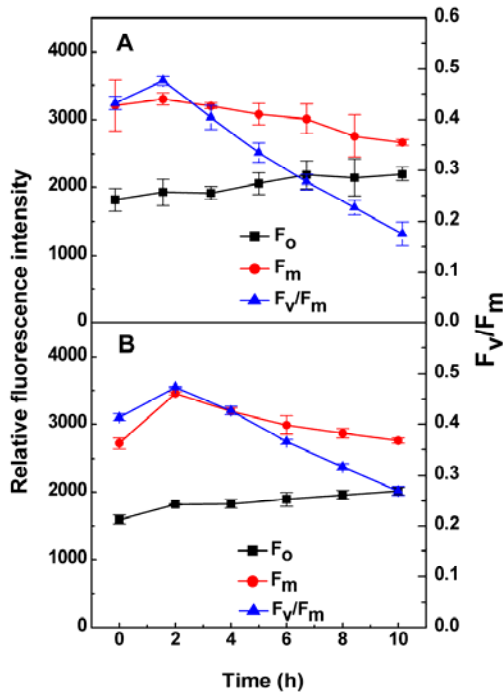


**Figure Supplementary Information 5.4.** Effect of 40  $\mu\text{M}$   $\text{CdCl}_2$  on the chlorophyll a fluorescence transient parameters ( $F_o$ ,  $F_m$  and  $F_v/F_m$ ) as a function of the time of Cd-treatment in the absence (A) and presence (B) of 10  $\mu\text{M}$  DCMU. Values are given as means  $\pm$  SD ( $n=3$ ).

## **Chapter 6**

### ***General discussion***

## 6.1 Introduction

Photosynthesis is a physico-chemical process that converts light energy into chemical energy, where pigment-protein complexes are responsible for the capture of light. The general importance of photosynthesis has been recognized long ago, but in the last decades its potential application as renewable energy source has further increased the interest in this field. The photosynthetic apparatus is an amazingly efficient system [1, 2] with the capacity to adapt rapidly to altered conditions. Understanding which external and internal factors to what extent determine the efficiency of the various photosynthetic processes is also important for industrial applications.

In this thesis *in vivo* techniques were preferentially applied to obtain a “realistic” picture about the physiological processes and structural organisation of the various elements.

## 6.2 Carotenoids in cyanobacterial thylakoid membrane

Carotenoids, the most widespread naturally occurring pigments, have important structural and functional roles in photosynthesis [3, 4]. The carotenoids serve as regulating factors in adaptation to altered conditions and the carotenoid composition is dynamically changed depending on the environment. They can contribute to the light harvesting [5, 6], play a structure-stabilizing role in pigment-protein complexes [7], influence the membrane fluidity [8], take part in photoprotection [9-12] and influence the membrane integrity [13]. We mostly focused on the structural roles and their consequences on energy transfer processes (**Chapter 2**). In this thesis the photosynthetic apparatus of wild-type cells and several carotenoid biosynthesis mutants of *Synechocystis* PCC 6803 are compared. We found that the carotenoid composition influences the structure of the carotenoid-containing photosystems as well as the phycobilisome (PBS) antennae, which are believed to contain no carotenoids.

Complete carotenoid deficiency results in the almost complete suppression of photosystem II (PSII) and the presence of photosystem I as monomers instead of trimers. The carotenoid-deficiency-induced effects leading to the decrease of PSII content are discussed in detail by Sozer *et al.* [7]. The same authors suggested that PSI is in monomeric form in the absence of carotenoids [7]. We confirmed the dominance of PSI monomeric form also by *in vivo* measurements in carotenoid deficient cells. It was previously demonstrated that the presence of PsaL protein [14] and one phosphatidyl-glycerol molecule [15] is a prerequisite for PSI trimer formation. Based on the PSI crystal structure some of the  $\beta$ -carotenes, localised at

the trimerisation domain, were proposed to stabilise the PSI trimer [16]. Our results show that the stable interaction of the PsaL protein with the PSI monomer requires carotenoids, most probably  $\beta$ -carotenes. In spite of the fact that only  $\beta$ -carotene is modelled in the crystal structure of photosystems, the lack of the main xanthophyll fraction (echinenone, zeaxanthin) lowers the stability of photosystem II dimers and slightly increases the photosystem I monomer/trimer ratio.

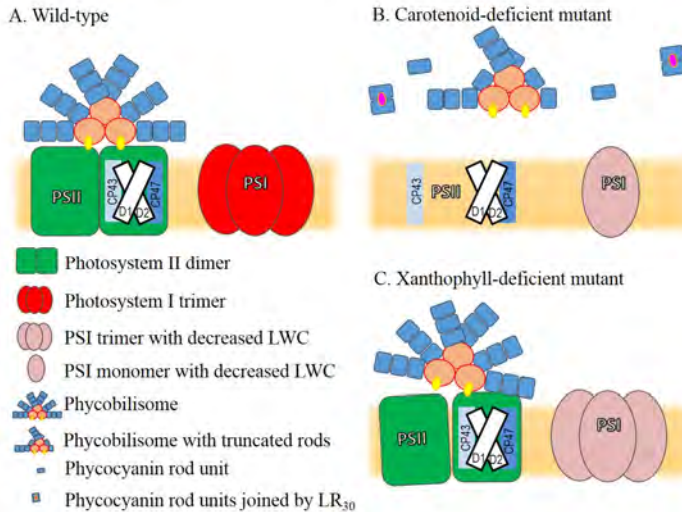


**Figure 6.1.** Schematic model of the photosynthetic complexes of wild type and carotenoid deficient mutant *Synechocystis PCC 6803* cells.

Surprisingly, the xanthophyll deficiency also strongly decreases the fluorescence emitted by long-wavelength chlorophylls. These effects of xanthophyll deficiency on the photosystems might indicate some previously unknown stabilizing role by the xanthophylls which are localised in close vicinity of the photosystems. It is evident that during isolation often some xanthophylls are co-purified with PSI [17] or PSII [18]. Our experiments also prove that the lack of carotenoids evokes a high level of unconnected PBS rod units co-existing with phycobilisomes with shorter radial rods. The fact that there is no indication of the presence of carotenoids in the PBS structure suggests the possibility of an indirect carotenoid effect on PBS. Based on the composition of the unconnected rod fractions we propose that dissociation of the rods occurs after the assembly of the phycobilisomes. The balance of continuous assembly and disassembly of PBSs are shifted towards the breakdown in the absence of Cars leading to a decreased steady-state level of PBSs and the appearance of unconnected phycocyanin rod units as degradation products.

## 6.3 Macro-organisation of thylakoid membrane in higher plants

In plant chloroplasts the unique thylakoid organisation requires specialised adaptation mechanisms. In plant thylakoids PSI and PSII are localised separately in the stroma and grana membranes, respectively. Both PSI and PSII are associated with light-harvesting antenna complexes forming supercomplexes [19]. In line with the previous prediction of macrodomains in the grana membranes [20-22] the granal thylakoids contain PSII semi-crystalline domains that form long parallel rows of PSII-LHCII supercomplexes [19, 23, 24]. It seems that the position of the PSII complexes within the PSII domains depends on the antenna composition of the PSII supercomplexes [19, 24-26], but it is not completely clear which factors determine the PSII macro-organisation.

Due to the large size and the relative instability of the plant PSII supercomplex its crystallisation was not successful until now. A molecular model of PSII supercomplexes was obtained by fitting the electron microscopy negative-staining picture of the supercomplex using the crystal structure of the cyanobacterial PSII core complex and the crystal structure of LHCII [27, 28]. However, the exact position of some small molecular weight proteins is still undetermined [29]. PsbW is a PSII-associated, 6.1 kDa peptide with one transmembrane helix [30, 31], but its exact role was not clear until recently. It was demonstrated that this protein is incorporated into the PSII supercomplex at a later step of the assembly [32]. In this thesis (**Chapter 3**) we investigated the role of the PsbW protein in PSII organisation in *Arabidopsis thaliana*. We have demonstrated that the decrease or loss of PsbW destabilizes the supercomplex of PSII. Although PsbW was originally believed to stabilise the PSII homodimer [33] our results support an earlier proposal that PsbW is rather important for the association of LHCII to the PSII core [31]. In the absence of the PsbW protein no PSII-LHCII supercomplexes could be isolated, which strongly suggests that the PsbW protein is located close to the minor antenna of the PSII complex, similarly as was expected from earlier results [31, 32]. Electron-microscopy analysis of the PsbW-deficient mutant revealed only random aggregates of PSII instead of the formation of semi-crystalline arrays in the wild type. However, with the use of CD spectroscopy we were able to detect, although at a reduced level, a psi-type CD signal, originating from long-range ordered pigment-protein complexes *in vivo*, which suggests that the macro-organisation is not completely abolished in the PsbW deficient mutant. The altered structure evokes several functional changes, which help to understand the role of the PSII macrodomains. Our results propound that these arrays are formed in order to optimise the energy

transfer between the PSII complexes and the interaction between the PSII and the plastoquinone pool. In our experiments the PSII macro-organisation also seems to influence the regulation of the energy distribution via state transitions by influencing the plastoquinone pool and the phosphorylation of PSII proteins. Our findings are in agreement with the idea that the ordered arrays are important, especially at low light intensity, in grana thylakoids to avoid diffusion problems in the crowded membrane [26, 34]. Moreover, the lack of PsbW decreases the efficiency of the repair cycle of PSII complexes.

The PSII domain organisation also dynamically varies depending on the environmental conditions [19, 24, 26, 34-36] and therefore a fast, non-invasive method is required for its investigation.

Circular dichroism (CD) spectroscopy is potentially a suitable method, since it is able to monitor the pigment-pigment interactions between adjacent protein subunits [37-39] and capable to indicate variations in the association of the pigment-protein complexes [40, 41]. In this thesis (**Chapter 4**) we confirm that CD spectroscopy is a sensitive technique to detect changes in PSII macrodomain structure and to compare the macrodomain organisation of various species. The intense, non-conservative psi-type CD bands exhibited by granal thylakoid membranes are indicating the long-range order of chlorophyll and carotenoid chromophores ensured by protein macrodomains. Previous observations suggested that each psi-type CD bands of granal thylakoid have different origin [42-44]. However, the exact structure giving rise to the *in vivo* psi-type signal in thylakoid membrane has not been demonstrated, only hypothesised [45, 46].

Our results show that the presence of chiral macrodomains observed in intact leaves requires the presence of both PSII and LHC complexes. However, the co-existence of PSII and LHCIIs in itself appeared to be insufficient, these complexes also need to be associated into supercomplexes and further to PSII domains in order to generate the psi-type CD signals. Based on our observations we confirm that the formation of the long-range ordered macrodomains, which exhibit the psi-type CD signal are mainly determined by LHCI [43, 47, 48]. By manipulating the PSII antenna constitution we show that LHCI composition determines the detailed structure of the PSII supercomplexes, and thus the geometry of the PSII-LHCI domains. The altered structure of the domains influences the amplitude of the psi-type CD bands and it is accompanied by a different ratio of the psi-type CD bands. In photosynthesis research there are some model organisms that are preferentially used to study plant photosynthesis (e.g., *Arabidopsis thaliana* and spinach), and therefore most of our knowledge is obtained from only a few species. Here we have compared several plant species and show that the examined plant

species share the main spectral features of the psi-type CD bands originating from the long-range order of chlorophyll and carotenoid chromophores in the protein macrodomains, whereas changes in the ratio of the psi-type CD bands suggest differences in their fine structure.

## 6.4 Toxic effects of cadmium on cyanobacterial photosynthetic processes

Although being a very flexible and responsive process, under extreme conditions even photosynthesis is no longer able to adapt to the altered environmental factors. Due to industrial activity the local concentrations of some toxic heavy metals have dramatically increased in some areas. Heavy metals are capable to inhibit the photosynthetic processes relatively fast even at low concentrations [49-52]. In this thesis we studied the effect of cadmium ( $\text{Cd}^{2+}$ ) on the cyanobacterial strain *Synechocystis* PCC 6803 (Chapter 5).

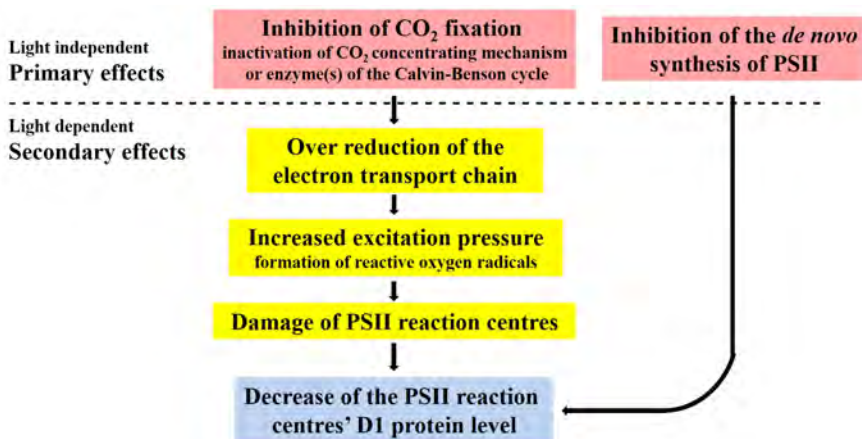


**Figure 6.2.** The proposed cascade mechanism that describes the cadmium-induced changes in the photosynthetic apparatus of *Synechocystis* PCC 6803.

Cyanobacteria are capable to uptake cadmium relatively fast from the surrounding solution [53], and therefore we were able to separate the fast, primary effects from slower secondary ones. Here we show that the CO<sub>2</sub>-dependent electron transport is rapidly inhibited upon exposing the *Synechocystis* PCC 6803 cells to low (40  $\mu\text{M}$ )  $\text{Cd}^{2+}$  concentration due to the dark events of photosynthesis, which include the reduction of CO<sub>2</sub> and related processes. Such an effect can be explained by the inhibition of an enzyme of the Calvin-Benson cycle or the CO<sub>2</sub>-concentrating mechanism. Our findings are in good agreement with results demonstrating that  $\text{Cd}^{2+}$

can inactivate different metal-containing enzymes, including the carbonic anhydrase, by replacing the zinc ion [54]. The block of the whole electron-transport chain creates excitation pressure on the reaction centres. After several hours, and only in the light, we observe the inhibitory effects of  $\text{Cd}^{2+}$  on PSII activity and the degradation of the PSII reaction centre protein D1. It is known that the excitation pressure enhances the production of reactive oxygen species (ROS). We propose that the increased production of ROS is mostly responsible for the degradation of D1 protein, although inhibition of D1 synthesis to a certain extent also seems to contribute. The  $\text{Cd}^{2+}$ -concentration dependence of short- and long-term effects are the same, strongly suggesting that the two effects are not independent. We propose a cascade mechanism for the toxic effects of  $\text{Cd}^{2+}$  (Fig 6.2), in which as a first step the dark reaction of photosynthesis is inhibited and the increased excitation pressure together with the insufficient synthesis of PSII complexes results in the decrease of PSII centres.

## 6.5 Summary

The thylakoid membrane has a hierarchically ordered well-organised structure containing pigment-protein complexes that capture the light energy and convert it into chemical energy. Its highly dynamic structure is capable to continuously respond to the altered environmental conditions, e.g., light quality and quantity, temperature changes and nutrient availability. Having detailed knowledge about the photosynthetic apparatus and its regulating factors is of paramount importance for the potential use of photosynthesis as alternative energy source or for removing toxic pollutants.

Here we provide (**Chapter 2**) new information about the role of various carotenoid molecules for the structure and energy transfer capacity of photosynthetic complexes in cyanobacteria. Our results demonstrate that besides the known structural importance of carotenoids they are also required for the oligomerisation of photosystems and for maintaining the structure of the phycobilisome light-harvesting antenna complex. These findings help to better understand the carotenoid-dependent fine tuning of the cyanobacterial thylakoid membrane organisation. The macro-organisation of the thylakoid membranes has been studied intensively over the last decades and part of this thesis (**Chapter 3 and 4**) focuses on the PSII macro-organisation in the chloroplast thylakoid membrane of plants.

In **Chapter 3** the general importance of a small-molecular-weight protein, PsbW is demonstrated for the organisation of the PSII supercomplexes and the formation of the parallel rows of PSII and the accompanying psi-type circular dichroism signal.

In **Chapter 4** we describe a new, circular dichroism (CD) based fingerprinting method to study the PSII macrodomain organization. CD is a potentially powerful method to follow the dynamic changes of the pigment-protein complex organisation of chloroplast membranes *in vivo*.

In **Chapter 5** cadmium-induced toxic effects on photosynthetic processes are investigated. The observed changes can be merged into a cascade mechanism model. Such detailed knowledge of toxic events is crucial for the effective use of cyanobacteria to remove the cadmium pollution from water.

In conclusion, this thesis contributes to our knowledge about the structure and dynamics of the photosynthetic apparatus at various organisation levels.

## 6.6 Reference list

- [1] van Amerongen, H., Croce, R., Light harvesting in photosystem II, *Photosynth Res.*, 116 (2013) 251-263.
- [2] Croce, R., van Amerongen, H., Light-harvesting in photosystem I, *Photosynth Res.*, 116 (2013) 153-166.
- [3] Domonkos, I., Kis, M., Gombos, Z., Ughy, B., Carotenoids, versatile components of oxygenic photosynthesis, *Prog. Lipid Res.*, 52 (2013) 539-561.
- [4] Takaichi, S., Carotenoids in algae: Distributions, biosyntheses and functions, *Mar. Drugs*, 9 (2011) 1101-1118.
- [5] Polivka, T., Frank, H.A., Molecular factors controlling photosynthetic light harvesting by carotenoids, *Accounts of chemical research*, 43 (2010) 1125-1134.
- [6] Martiskainen, J., Kananavicius, R., Linnanto, J., Lehtivuori, H., Keranen, M., Aumanen, V., Tkachenko, N., Korppi-Tommola, J., Excitation energy transfer in the LHCII trimer: from carotenoids to chlorophylls in space and time, *Photosynth Res.*, 107 (2011) 195-207.
- [7] Sozer, O., Komenda, J., Ughy, B., Domonkos, I., Laczko-Dobos, H., Malec, P., Gombos, Z., Kis, M., Involvement of carotenoids in the synthesis and assembly of protein subunits of photosynthetic reaction centers of *Synechocystis sp* PCC 6803, *PCP*, 51 (2010) 823-835.
- [8] Gruszecki, W.I., Strzalka, K., Carotenoids as modulators of lipid membrane physical properties, *Biochim. Biophys. Acta*, 1740 (2005) 108-115.
- [9] Wilson, A., Ajlani, G., Verbavatz, J.M., Vass, I., Kerfeld, C.A., Kirilovsky, D., A soluble carotenoid protein involved in phycobilisome-related energy dissipation in cyanobacteria, *Plant Cell*, 18 (2006) 992-1007.
- [10] Dall'Osto, L., Lico, C., Alric, J., Giuliano, G., Havaux, M., Bassi, R., Lutein is needed for efficient chlorophyll triplet quenching in the major LHCII antenna complex of higher plants and effective photoprotection *in vivo* under strong light, *BMC Plant Biol.*, 6 (2006).
- [11] Pogson, B.J., Rissler, H.M., Genetic manipulation of carotenoid biosynthesis and photoprotection, *Phil. Trans. R. Soc. B*, 355 (2000) 1395-1403.
- [12] Mohamad, S.B., Yousef, Y.A., Melo, T.B., Javorfi, T., Partali, V., Sliwka, H.R., Razi Naqvi, K., Singlet oxygen quenching by thione analogues of canthaxanthin, echinenone and rhodoxanthin, *J. Photochem. Photobiol. B: Biol.*, 84 (2006) 135-140.
- [13] Mohamed, H.E., van de Meene, A.M.L., Roberson, R.W., Vermaas, W.F.J., Myxoxanthophyll is required for normal cell wall structure and thylakoid organization in the cyanobacterium, *Synechocystis sp* strain PCC 6803, *J. Bacteriol.*, 187 (2005) 6883-6892.
- [14] Chitnis, V.P., Chitnis, P.R., PsaL subunit is required for the formation of photosystem I trimers in the cyanobacterium *Synechocystis sp* PCC 6803, *FEBS Lett.*, 336 (1993) 330-334.

- [15] **Domonkos, I., Malec, P., Sallai, A., Kovacs, L., Itoh, K., Shen, G.Z., Ughy, B., Bogos, B., Sakurai, I., Kis, M., Strzalka, K., Wada, H., Itoh, S., Farkas, T., Gombos, Z.**, Phosphatidylglycerol is essential for oligomerization of photosystem I reaction center, *Plant Physiol.*, 134 (2004) 1471-1478.
- [16] **Grotjohann, I., Fromme, P.**, Structure of cyanobacterial photosystem I, *Photosynth Res.*, 85 (2005) 51-72.
- [17] **Bautista, J.A., Rappaport, F., Guergova-Kuras, M., Cohen, R.O., Golbeck, J.H., Wang, J.Y., Beal, D., Diner, B.A.**, Biochemical and biophysical characterization of photosystem I from phytoene desaturase and  $\zeta$ -carotene desaturase deletion mutants of *Synechocystis* sp PCC 6803, *J. Biol. Chem.*, 280 (2005) 20030-20041.
- [18] **Bautista, J.A., Tracewell, C.A., Schlodder, E., Cunningham, F.X., Brudvig, G.W., Diner, B.A.**, Construction and characterization of genetically modified *Synechocystis* sp. PCC 6803 photosystem II core complexes containing carotenoids with shorter  $\pi$ -conjugation than beta-carotene, *J. Biol. Chem.*, 280 (2005) 38839-38850.
- [19] **Dekker, J.P., Boekema, E.J.**, Supramolecular organization of thylakoid membrane proteins in green plants, *Biochim. Biophys. Acta*, 1706 (2005) 12-39.
- [20] **Faludi-Daniel, A., Bialek, G.E., Horvath, G., Sz-Rozsa, Z., Gregory, R.P.**, Differential light-scattering of granal and agranal chloroplasts and their fragments, *Biochem. J.*, 174 (1978) 647-651.
- [21] **Demeter, S., Mustardy, L., Machowicz, E., Gregory, R.P.F.**, Development of intense circular dichroism signal during granum formation in greening etiolated maize, *Biochem. J.*, 156 (1976) 469-472.
- [22] **Garab, G., Wells, S., Finzi, L., Bustamante, C.**, Helically Organized Macroaggregates of Pigment Protein Complexes in Chloroplasts - Evidence from Circular Intensity Differential Scattering, *Biochemistry*, 27 (1988) 5839-5843.
- [23] **Miller, K.R.**, A particle spanning the photosynthetic membrane, *Journal of ultrastructure research*, 54 (1976) 159-167.
- [24] **Kouril, R., Dekker, J.P., Boekema, E.J.**, Supramolecular organization of photosystem II in green plants, *Biochim. Biophys. Acta*, 1817 (2012) 2-12.
- [25] **Kovacs, L., Damkjaer, J.T., Kereiche, S., Illoia, C., Ruban, A.V., Boekema, E.J., Jansson, S., Horton, P.**, Lack of the light-harvesting complex CP24 affects the structure and function of the grana membranes of higher plant chloroplasts, *Plant Cell*, 18 (2006) 3106-3120.
- [26] **Kouril, R., Wientjes, E., Bultema, J.B., Croce, R., Boekema, E.J.**, High-light vs. low-light: Effect of light acclimation on photosystem II composition and organization in *Arabidopsis thaliana*, *Biochim. Biophys. Acta*, 1827 (2013) 411-419.
- [27] **Nield, J., Orlova, E.V., Morris, E.P., Gowen, B., van Heel, M., Barber, J.**, 3D map of the plant photosystem II supercomplex obtained by cryoelectron microscopy and single particle analysis, *Nat. Struct. Biol.*, 7 (2000) 44-47.
- [28] **Caffarri, S., Kouril, R., Kereiche, S., Boekema, E.J., Croce, R.**, Functional architecture of higher plant photosystem II supercomplexes, *EMBO J.*, 28 (2009) 3052-3063.
- [29] **Shi, L.X., Hall, M., Funk, C., Schroder, W.P.**, Photosystem II, a growing complex: updates on newly discovered components and low molecular mass proteins, *Biochim. Biophys. Acta*, 1817 (2012) 13-25.
- [30] **Thidholm, E., Lindstrom, V., Tissier, C., Robinson, C., Schroder, W.P., Funk, C.**, Novel approach reveals localisation and assembly pathway of the PsbS and PsbW proteins into the photosystem II dimer, *FEBS Lett.*, 513 (2002) 217-222.
- [31] **Granvogl, B., Zoryan, M., Ploescher, M., Eichacker, L.A.**, Localization of 13 one-helix integral membrane proteins in photosystem II subcomplexes, *Anal. Biochem.*, 383 (2008) 279-288.
- [32] **Rokka, A., Suorsa, M., Saleem, A., Battchikova, N., Aro, E.M.**, Synthesis and assembly of thylakoid protein complexes: multiple assembly steps of photosystem II, *Biochem. J.*, 388 (2005) 159-168.
- [33] **Shi, L.X., Lorkovic, Z.J., Oelmuller, R., Schroder, W.P.**, The low molecular mass PsbW protein is involved in the stabilization of the dimeric photosystem II complex in *Arabidopsis thaliana*, *J. Biol. Chem.*, 275 (2000) 37945-37950.

- [34] **Kirchhoff, H., Haase, W., Wegner, S., Danielsson, R., Ackermann, R., Albertsson, P.A.**, Low-light-induced formation of semicrystalline photosystem II arrays in higher plant chloroplast, *Biochemistry*, 46 (2007) 11169-11176.
- [35] **Tsvetkova, N.M., Apostolova, E.L., Brain, A.P.R., Williams, W.P., Quinn, P.J.**, Factors influencing PSII particle array formation in *Arabidopsis thaliana* chloroplasts and the relationship of such arrays to the thermostability of PSII, *Biochim. Biophys. Acta*, 1228 (1995) 201-210.
- [36] **Kirchhoff, H., Tremmel, I., Haase, W., Kubitscheck, U.**, Supramolecular photosystem II organization in grana thylakoid membranes: Evidence for a structured affangement, *Biochemistry*, 43 (2004) 9204-9213.
- [37] **Shubin, V.V., Tsuprun, V.L., Bezmertnaya, I.N., Karapetyan, N.V.**, Trimeric forms of the photosystem I reaction center complex pre-exist in the membranes of the cyanobacterium *Spirulina platensis*, *FEBS Lett.*, 334 (1993) 79-82.
- [38] **Croce, R., Morosinotto, T., Castelletti, S., Breton, J., Bassi, R.**, The Lhca antenna complexes of higher plants photosystem I, *Biochim. Biophys. Acta*, 1556 (2002) 29-40.
- [39] **Subramanyam, R., Jolley, C., Brune, D.C., Fromme, P., Webber, A.N.**, Characterization of a novel photosystem I-LHCI supercomplex isolated from *Chlamydomonas reinhardtii* under anaerobic (State II) conditions, *FEBS Lett.*, 580 (2006) 233-238.
- [40] **Peterman, E.J.G., Hobe, S., Calkoen, F., vanGrondelle, R., Paulsen, H., vanAmerongen, H.**, Low-temperature spectroscopy of monomeric and trimeric forms of reconstituted light-harvesting chlorophyll a/b complex, *Biochim. Biophys. Acta*, 1273 (1996) 171-174.
- [41] **Georgakopoulou, S., van der Zwan, G., Bassi, R., van Grondelle, R., van Amerongen, H., Croce, R.**, Understanding the changes in the circular dichroism of light harvesting complex II upon varying its pigment composition and organization, *Biochemistry*, 46 (2007) 4745-4754.
- [42] **Miloslavina, Y., Lambrev, P.H., Javorfi, T., Varkonyi, Z., Karlicky, V., Wall, J.S., Hind, G., Garab, G.**, Anisotropic circular dichroism signatures of oriented thylakoid membranes and lamellar aggregates of LHCII, *Photosynth Res.*, 40 (2011) 178-179.
- [43] **Garab, G., Kieleczawa, J., Sutherland, J.C., Bustamante, C., Hind, G.**, Organization of pigment protein complexes into macrodomains in the thylakoid membranes of wild-type and chlorophyll b-less mutant of barley as revealed by circular dichroism, *Photochem. Photobiol.*, 54 (1991) 273-281.
- [44] **Cseh, Z., Rajagopal, S., Tsonev, T., Busheva, M., Papp, E., Garab, G.**, Thermo-optic effect in chloroplast thylakoid membranes. Thermal and light stability of pigment arrays with different levels of structural complexity, *Biochemistry*, 39 (2000) 15250-15257.
- [45] **Garab, G.**, Hierarchical organization and structural flexibility of thylakoid membranes, *Biochim. Biophys. Acta*, 1837 (2014) 481-494.
- [46] **Garab, G., van Amerongen, H.**, Linear dichroism and circular dichroism in photosynthesis research, *Photosynth Res.*, 101 (2009) 135-146.
- [47] **Garab, G., Mustardy, L.**, Role of LHCII-containing macrodomains in the structure, function and dynamics of grana, *Aust. J. Plant Physiol.*, 26 (1999) 649-658.
- [48] **Faludi-Daniel, A., Mustardy, L.A.**, Organization of chlorophyll a in the light-harvesting chlorophyll a/b protein complex as shown by circular dichroism - liquid crystal-like domains, *Plant Physiol.*, 73 (1983) 16-19.
- [49] **Nagajyoti, P.C., Lee, K.D., Sreekanth, T.V.M.**, Heavy metals, occurrence and toxicity for plants: a review, *Environ Chem Lett*, 8 (2010) 199-216.
- [50] **Clijsters, H., Van Assche, F.**, Inhibition of photosynthesis by heavy metals, *Photosynth Res.*, 7 (1985) 31-40.
- [51] **Pandey, N., Sharma, C.P.**, Effect of heavy metals  $\text{Co}^{2+}$ ,  $\text{Ni}^{2+}$  and  $\text{Cd}^{2+}$  on growth and metabolism of cabbage, *Plant Sci.*, 163 (2002) 753-758.
- [52] **Kucera, T., Horakova, H., Sonska, A.**, Toxic metal ions in photoautotrophic organisms, *Photosynthetica*, 46 (2008) 481-489.

[53] **Pawlik, B., Skowronski, T., Ramazanow, Z., Gardstrom, P., Samuelsson, G.**, pH-dependent cadmium transport inhibits photosynthesis in the cyanobacterium *Synechocystis aquatilis*, *Environ. Exp. Bot.*, 33 (1993) 331-337.

[54] **Sas, K.N., Kovacs, L., Zsiros, O., Gombos, Z., Garab, G., Hemmingsen, L., Danielsen, E.**, Fast cadmium inhibition of photosynthesis in cyanobacteria in vivo and in vitro studies using perturbed angular correlation of gamma-rays, *JBIC*, 11 (2006) 725-734.

# Chapter 7

## *Algemene discussie*

## 7.1 Introductie

Fotosynthese is een fysisch-chemisch proces waarbij lichtenergie wordt omgezet in chemische energie en waarbij pigment-eiwitcomplexen verantwoordelijk zijn voor het invangen van licht. Het belang van fotosynthese is reeds lang geleden onderkend, terwijl in de laatste decennia de aandacht voor het fenomeen verder is toegenomen, vanwege de mogelijkheid om fotosynthese te gebruiken bij het op duurzame wijze opwekken van energie. Het fotosynthese-apparaat is een bijzonder efficiënt werkend systeem [1, 2] dat zich razendsnel kan aanpassen aan veranderende omstandigheden. Begrip van welke externe en interne factoren in welke mate bijdragen aan de efficiëntie van de verschillende fotosynthetische processen is ook van belang voor industriële toepassingen.

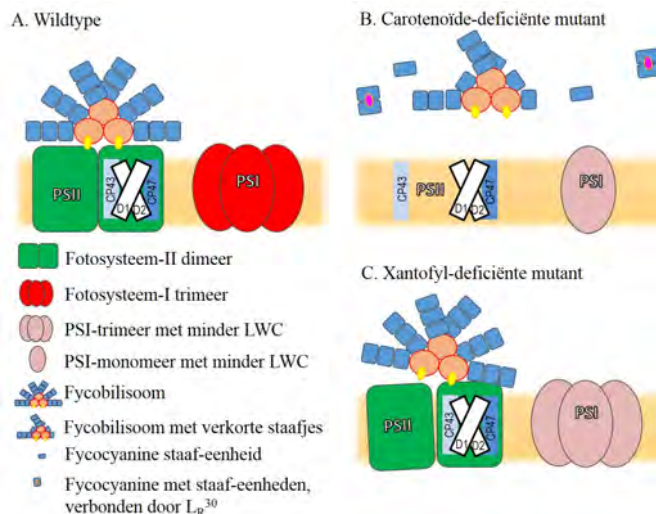
In dit proefschrift zijn bij voorkeur *in vivo*-methodes gebruikt om een “realistisch” beeld te verkrijgen van de fysiologische processen en de structurele organisatie van de verschillende betrokken elementen.

## 7.2 Carotenoïden in het thylakoïdmembraan van cyanobacteriën.

Carotenoïden, de meest wijdverspreide pigmenten in de natuur, spelen belangrijke structurele en functionele rollen bij de fotosynthese [3, 4]. Carotenoïden spelen een regulerende rol bij aanpassing aan veranderende omstandigheden, en de carotenoïdensamenstelling verandert op een dynamische wijze afhankelijk van de omgeving. Ze kunnen een bijdrage leveren aan het “oogsten van licht” [5, 6], een rol spelen bij het stabiliseren van de structuur van pigment-eiwitcomplexen [7], de membraanfluiditeit beïnvloeden [8], deelnemen aan fotoprotectie [9-12], en de intactheid van het membraan beïnvloeden [13]. We hebben ons voornamelijk toegelegd op de structurele functies en de consequenties daarvan voor energieoverdrachtsprocessen (**Hoofdstuk 2**). In dit proefschrift worden het fotosynthetisch apparaat van wildtype cellen en van verschillende carotenoïde-biosynthesemutanten van *Synechocystis* PCC 6803 met elkaar vergeleken. We hebben geobserveerd dat de carotenoïdesamenstelling de structuur van zowel fotosystemen die carotenoïden bevatten als de antennes van het fycobilisoom (PBS), dat waarschijnlijk geen carotenoïden bevat, beïnvloedt.

Het volledig ontbreken van carotenoïden heeft tot gevolg dat fotosysteem II (PSII) bijna volledig afwezig is en dat fotosysteem I zich niet meer in trimere, maar monomere vorm manifesteert. Sozer *et al.* hebben op uitgebreide wijze de effecten van carotenoïdedeficiëntie beschreven, die tot een daling van het aantal PSII-

systemen leiden [7]. Dezelfde auteurs hebben gesuggereerd dat PSI zich in afwezigheid van carotenoïden in een monomere toestand bevindt [7]. We hebben nu ook door middel van *in vivo*-metingen in carotenoïde-deficiënte cellen vastgesteld dat PSI zich daar voornamelijk in een monomere toestand bevindt. Eerder is aangetoond dat de aanwezigheid van het PsaL-eiwit [14] en één fosfatidylglycerolmolecuul [15] vereist zijn voor de vorming van een PSI trimeer. Op basis van de kristalstructuur van PSI is gesuggereerd dat sommige bèta-carotenen die aanwezig zijn in het trimerisatiegebied, de trimere PSI-structuur stabiliseren [16]. Ons onderzoek toont aan dat voor de stabiele interactie van het PsaL-eiwit met het PSI-monomeer carotenoïden vereist zijn, hoogstwaarschijnlijk bèta-carotenen. Ondanks het gegeven dat alleen bèta-carotenen in de kristalstructuur van fotosystemen zijn gemodelleerd, verlaagt het ontbreken van de voornaamste xantofylfractie (echinenon, zeaxanthine) de stabiliteit van PSII-dimeren en verhoogt het enigszins de PSI monomeer/trimeer-verhouding.



**Figuur 7.1.** Schematisch model van de fotosynthesecomplexen van wildtype en carotenoïde-deficiënte mutanten van *Synechocystis PCC 6803*

Op verrassende wijze leidt de xantofyl-deficiëntie ook tot een sterke afname van de fluorescentie die door de lange-golflengte chlorofylmoleculen wordt uitgezonden. Deze onverwachte effecten van xantofyl-deficiëntie op de fotosystemen zouden wel eens kunnen wijzen op een voorheen onbekende stabiliserende rol van de xantofylen die zich vlakbij de fotosystemen bevinden. Het is duidelijk dat gedurende de isolatie-procedure vaak enkele xantofylen worden “opgezuiverd” samen met PSI [17] of PSII [18]. Onze experimenten bewijzen ook dat het gebrek aan carotenoïden leidt tot een hoog niveau niet-gebonden PBS-staaf-

eenheden in combinatie met fycobilisomen met korte radiële staafjes. Het feit dat niets lijkt te wijzen op de aanwezigheid van carotenoïden in de PBS-structuur, suggereert de mogelijkheid van een indirect effect van carotenoïden op PBS. Op basis van de samenstelling van de niet-gebonden staafjes-fracties, concluderen wij dat dissociatie van de staafjes plaatsvindt nadat de fycobilisomen zijn geassembleerd. De balans tussen de voortdurende assemblage en de-assemblage van fycobilisomen verschuift naar de-assemblage in de afwezigheid van Cars, hetgeen leidt tot een afgenomen steady-state PBS-niveau en de verschijning van ongebonden fycocyanine staaf-eenheden als afbraakproduct.

### **7.3 Macro-organisatie van het thylakoïdmembraan in hogere planten.**

In plant-chloroplasten vraagt de unieke organisatie van het thylakoïdmembraan om gespecialiseerde aanpassingsmechanismen. In deze thylakoïdmembranen bevinden PSI en PSII zich afzonderlijk respectievelijk in de stroma- en grana-membranen. Zowel PSI als PSII zijn geassocieerd met “licht-oogstende” antenne-complexen die supercomplexen vormen [19]. In lijn met de eerdere voorspelling van macrodomeinen in grana-membranen [20-22], bevatten de grana-thylakoïden semi-kristallijne PSII-domeinen die lange, parallelle rijen van PSII-LHCII supercomplexen vormen [19, 23]. Hij lijkt erop dat de positie van de PSII-complexen binnen de PSII-domeinen afhangt van de antennesamenstelling van de PSII-supercomplexen [19, 24-26], maar het is niet geheel duidelijk door welke factoren de macro-organisatie van PSII wordt bepaald.

Vanwege de aanzienlijke grootte en betrekkelijke instabiliteit van het PSII-supercomplex in planten, is men er nog niet in geslaagd dit complex te kristalliseren. Een moleculair model van het PSII-supercomplex is verkregen door de “negative-staining”-afbeelding van het supercomplex, verkregen door middel van elektronenmicroscopie, te fitten, gebruikmakende van de kristalstructuur van het PSII-kerncomplex van cyanobacteriën en de kristalstructuur van LHCII [27, 28]. De positie van enkele kleinere eiwitten is echter nog niet precies vastgesteld [29]. PsbW is een PSII-gebonden peptide met een moleculair gewicht van 6.1 kDa en één transmembraanhelix [30, 31], waarvan de precieze rol tot voor kort niet was opgehelderd. Het is inmiddels aangetoond dat dit eiwit in een later stadium van de assemblage wordt ingebouwd in het PSII-supercomplex [32]. In dit proefschrift (**Hoofdstuk 3**) wordt de rol van het PsbW-eiwit in de PSII-organisatie in *Arabidopsis thaliana* beschreven. We hebben aangetoond dat de afname of het volledige verlies van PsbW het PSII-supercomplex destabiliseert. Hoewel in eerste

instantie werd gedacht dat PsbW het PSII-homodimeer stabiliseert [33], zijn onze resultaten in lijn met de vroegere gedachte dat PsbW van belang is bij de associatie van LHCII met de PSII-kern [31]. In de afwezigheid van het PsbW-eiwit konden geen PSII-LHCII-supercomplexen worden geïsoleerd, wat er sterk op wijst dat het PsbW-eiwit zich bevindt in de nabijheid van de kleine antenne van het PSII-complex, hetgeen ook al door eerdere resultaten werd gesuggereerd [31, 32]. Een studie van de PsbW-deficiënte mutant door middel van elektronenmicroscopie liet slechts willekeurig geaggregeerd PSII zien, in plaats van een semi-kristallijne rangschikking in het wildtype. Door middel van CD-spectroscopie zijn we er echter in geslaagd om een psi-type CD-signaal (hoewel met een lage intensiteit) te detecteren, hetgeen wijst op geordende pigment-eiwitcomplexen *in vivo* over grotere afstanden en dus suggereert dat macro-organisatie in de PsbW-deficiënte mutant niet geheel afwezig is. De veranderde structuur induceert verscheidene functionele veranderingen, die ons helpen om de rol van PSII-macrodomeinen te begrijpen. Onze resultaten brengen het beeld naar voren dat deze rangschikking ontstaat om de energieoverdracht tussen PSII-complexen, en de interactie tussen PSII en de plastoquinonen, te optimaliseren. In onze experimenten lijkt de macro-organisatie van PSII ook de regulatie van de energieverdeling door middel van toestandsovergangen te beïnvloeden, doordat het een invloed heeft op de plastoquinonen en de fosforylering van PSII-eiwitten. Onze bevindingen zijn in lijn met de idee dat de geordende rangschikkingen belangrijk zijn in grana-thylakoïden, met name bij een lage lichtintensiteit, om problemen met diffusie in het overvolle membraan te voorkomen [26, 34]. Bovendien leidt het gebrek aan PsbW tot een minder efficiënte PSII-reparatiecyclus.

De organisatie van PSII-domeinen verandert ook op dynamische wijze, afhankelijk van omgevingsfactoren [19, 25, 26, 34-36], en daarom is een snelle, niet-invasieve methode nodig om deze organisatie te bestuderen.

Circulair-dichroïsmespectroscopie (CD) is mogelijk een geschikte methode, omdat het de pigment-pigmentinteracties tussen naburige eiwit-sub-eenheden kan volgen [37-39] en variaties in de associatie van pigment-eiwitcomplexen kan aanwijzen [40, 41].

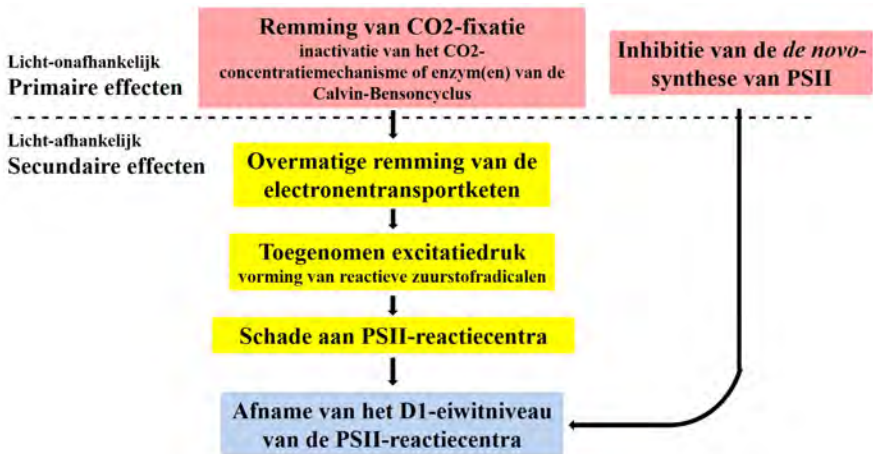
In dit proefschrift (**Hoofdstuk 4**) wordt gedemonstreerd dat CD-spectroscopie inderdaad een gevoelige methode is om veranderingen in de structuur van PSII-macrodomeinen te detecteren, en de organisatie van macrodomeinen tussen verschillende soorten te vergelijken. De intense, niet-conservatieve, psi-type CD-lijnen die afkomstig zijn van grana-thylakoïden, weerspiegelen de lange-afstandsordening van chlorofyl en carotenoïdechromoforen, opgelegd door eiwit-macrodomeinen. Eerdere waarnemingen leken erop te wijzen dat psi-type CD-

spectra van grana-thylakoïden een andere oorsprong hadden [42-44]. De precieze structuur die *in vivo* aan het psi-type signaal in thylakoïdmembranen ten grondslag ligt, is nooit vastgesteld, maar slechts gepostuleerd [45, 46].

Onze resultaten laten zien dat de aanwezigheid van chirale macrodomeinen, waargenomen in intacte bladeren, de aanwezigheid van zowel PSII als LHC-complexen vereist. De co-existentie van PSII en LHCII's is op zichzelf echter niet voldoende om psi-type CD-signalen te genereren; deze complexen dienen tegelijkertijd te zijn geassocieerd tot supercomplexen en verder tot PSII-domeinen. Op basis van onze waarnemingen kunnen we bevestigen dat de vorming van de lange-afstand-geordende macrodomeinen, die het psi-type CD-signaal geven, vooral zijn bepaald door LHCII [43, 47, 48]. Door de PSII-antennesamenstelling te manipuleren laten we zien dat de LHCII-samenstelling de precieze structuur van de PSII-supercomplexen bepaalt, en dus de geometrie van de PSII-LHCII-domeinen. De veranderde domeinstructuur beïnvloedt de amplitude van de psi-type CD-signalen, en tegelijkertijd ontstaat een andere verhouding tussen de psi-type CD-intensiteiten. In het onderzoek naar fotosynthese in planten wordt bij voorkeur een aantal modelorganismen gebruikt (bijv. *Arabidopsis thaliana* en spinazie) en daarom is onze kennis merendeels afkomstig van slechts een klein aantal soorten. Hier vergelijken we meerdere plantensoorten met elkaar en laten zien dat de onderzochte plantensoorten de voornaamste spectrale kenmerken van de psi-type CD-signalen, afkomstig van lange-afstands-ordening van chlorofyl en carotenoïdechromoforen in eiwit-macrodomeinen, met elkaar delen, terwijl veranderingen in de verhouding van de psi-type CD-signalen suggereren dat er verschillen zijn in de fijnstructuur.

### 7.4 Vergiftigingseffecten van cadmium op fotosyntheseprocessen in cyanobacteriën

Hoewel het een zeer flexibel en responsief proces is, kan zelfs de fotosynthese zich onder extreme omstandigheden niet meer aanpassen aan de veranderde omgevingsfactoren. Vanwege industriële activiteiten is in sommige gebieden de concentratie van enkele giftige zware metalen sterk gestegen. Zware metalen kunnen het fotosyntheseproces snel remmen, zelfs bij lage concentraties [49-52]. In dit proefschrift wordt het effect van cadmium ( $\text{Cd}^{2+}$ ) op de cyanobacterie-streng *Synechocystis sp. PCC 6803* beschreven (**Hoofdstuk 5**).



**Figuur 7.2.** Het voorgestelde cascademechanisme dat de cadmium-geïnduceerde veranderingen in het fotosynthese-apparaat van *Synechocystis PCC 6803* beschrijft.

Cyanobacteriën zijn in staat om cadmium relatief snel op te nemen uit de oplossing waarin ze zich bevinden [53] en daarom konden wij de snelle, primaire effecten scheiden van de langzamere, secundaire effecten. We laten zien dat het CO<sub>2</sub>-afhankelijke elektronentransport snel wordt geremd na blootstelling van *Synechocystis PCC 6803* aan lage (40 μM) Cd<sup>2+</sup>-concentraties vanwege de fotosynthetische donkerprocessen, waaronder de reductie van CO<sub>2</sub> en gerelateerde processen. Een dergelijk effect kan worden verklaard door de remming van een enzym uit de Calvin-Bensoncyclus of het CO<sub>2</sub>-concentratiemechanisme. Onze bevindingen zijn in lijn met resultaten die aantonen dat Cd<sup>2+</sup> verschillende metaalhoudende enzymen kan inactiveren, waaronder carboanhydrase, doordat het de plaats van het zink-ion inneemt [54]. Het blok van de gehele elektronentransportketen creëert excitatiedruk op de reactiecentra. Na enkele uren, en alleen in het licht, nemen we de remmende effecten van Cd<sup>2+</sup> op de PSII-activiteit waar als ook de degradatie van het PSII-reactiecentrumeiwit D1. Het is bekend dat excitatiedruk de vorming van reactieve zuurstofverbindingen doet toenemen. Wij stellen voor dat met name de toegenomen productie van reactieve zuurstofverbindingen verantwoordelijk is voor de degradatie van het D1-eiwit, hoewel remming van D1-synthese ook tot op zekere hoogte lijkt bij te dragen. De afhankelijkheid van korte- en langetermijneffecten op Cd<sup>2+</sup>-concentratie is gelijk, hetgeen er sterk op wijst dat de twee effecten niet onafhankelijk zijn. We stellen een cascademechanisme voor dat de vergiftigingseffecten van Cd<sup>2+</sup> beschrijft (Fig. 7.2), waarin allereerst de fotosynthetische donkerreactie wordt geremd, waarna de

toegenomen excitatiedruk samen met ontoereikende synthese van PSII-complexen leidt tot een afname in PSII-centra.

## **7.5 Samenvatting**

Het thylakoïdmembraan heeft een hiërarchisch geordende structuur waarin zich pigment-eiwitcomplexen bevinden die lichtenergie invangen en omzetten in chemische energie. De structuur is buitengewoon dynamisch en is in staat om zich voortdurend aan te passen aan veranderende omgevingsfactoren, zoals lichtkwaliteit en -kwantiteit, veranderingen in temperatuur en in de beschikbaarheid van voedingsstoffen. Gedetailleerde kennis van het fotosynthese-apparaat en bijbehorende regulatiemechanismen is van essentieel belang wanneer men het fotosyntheseproces zou willen gaan gebruiken als duurzame energiebron of om vervuilende stoffen op te ruimen.

Hier (**Hoofdstuk 2**) verschaffen we nieuwe informatie over de rol van verschillende carotenoidemoleculen voor de structuur en energieoverdrachts capaciteit van fotosynthese-complexen in cyanobacteriën. Onze resultaten tonen aan dat carotenoiden, naast hun bekende structurele rol, ook nodig zijn bij de oligomerisatie van fotosystemen en voor de instandhouding van de structuur van het “licht-oogstende” fycobilisoom-antennecomplex. Deze bevindingen helpen ons om de carotenoïde-afhankelijke fine-tuning van de organisatie van het thylakoïdmembraan in cyanobacteriën beter te begrijpen. De macro-organisatie van de thylakoïdmembranen is gedurende de afgelopen decennia intensief bestudeerd, en een deel van dit proefschrift (**Hoofdstuk 3 en 4**) focust op de macro-organisatie van PSII in het thylakoïdmembraan van chloroplasten van planten.

In **Hoofdstuk 3** wordt het algemeen belang van PsbW, een eiwit met een laag moleculair gewicht, voor de organisatie van de PSII-supercomplexen en de vorming van parallelle rijen PSII, en het ontstaan van het bijbehorende psi-type circulair-dichroïsmesignaal, aangetoond.

In **Hoofdstuk 4** beschrijven we een nieuwe, circulair-dichroïsme-gebaseerde fingerprintingmethode om de organisatie van PSII-macrodomeinen te bestuderen. CD is een potentieel krachtige methode om dynamische veranderingen in de organisatie van pigment-eiwitcomplexen van chloroplastmembranen *in vivo* te volgen.

In **Hoofdstuk 5** onderzoeken we cadmium-geïnduceerde vergiftigingseffecten op het fotosynthetisch proces. De waargenomen veranderingen zijn gevat in een cascademodel. Gedetailleerde kennis van vergiftiging is cruciaal

wanneer men effectief gebruik wil maken van cyanobacteriën om cadmiumverontreiniging uit water te verwijderen.

Concluderend: dit proefschrift draagt bij aan onze kennis over de structuur en dynamiek van het fotosynthese-apparaat op verschillende organisatieniveaus.

# ***Acknowledgement***

First of all my sincerest thanks go to my supervisor Herbert van Amerongen and to my co-supervisors Győző Garab and László Kovács for giving me the opportunity to work in this exciting scientific field.

Thank you, Herbert for encouraging me to think independently and for providing enormous help in writing of the manuscripts and my thesis.

Laci, special thanks to you for supervising me, starting from my master thesis, introducing me to such a wide range of techniques and being always patient with me. I am glad that we worked together during these years and we had all those interesting discussions.

I wish to thank you, Győző, for the chance to join your group and your support during these years.

I would like to express my gratitude to all of my collaborators including Zoltán Gombos, Wolfgang Schröder, Alfred Holzwarth and to their groups. I enjoyed the exciting experiments and discussions we had together.

Thanks to all my colleagues, especially Arie van Hoek, Volha Chukhutsina, Ildikó Domonkos, Rob Koehorst and Ottó Zsiros.

I would like to acknowledge the financial support I had from the Wageningen University for the Sandwich PhD fellowship and the Hungarian Academy of Sciences and the Social Renewal Operational Program (TÁMOP-4.2.2/B-10/1-2010-0012) for financing the Hungarian part of my PhD studies.

My warmest thanks to my parents, who have always given me moral support and to my friends, who have made these years unforgettable.

# ***List of Publications***

T. Tóth, V. Chukhutsina, I. Domonkos, J. Komenda, B. Ughy, M. Kis, Z. Lenárt, G. Garab, Z. Gombos, L. Kovács, H. van Amerongen. Carotenoid deficiency induces structural and functional changes in the phycobilisomes and photosystems of *Synechocystis* PCC 6803. *In preparation*

T. Tóth, N. Rai, A. Bóta, W. P. Schröder, G. Garab, H. van Amerongen, P. Horton, L. Kovács. The role of light-harvesting complex II in the macro-organisation of thylakoid membranes studied by circular dichroism spectroscopy in vivo. *In preparation*

T. Tóth, O. Zsiros, M. Kis, G. Garab, L. Kovács (2012) Cadmium exerts its toxic effects on photosynthesis via a cascade mechanism in the cyanobacterium, *Synechocystis* PCC 6803. *Plant Cell & Environment* 35:2075-2086

J. G. García-Cerdán, L. Kovács, T. Tóth, S. Kereiche, E. Aseeva, E. J. Boekema, F. Mamedov, C. Funk, W. Schröder (2011) The PsbW protein stabilizes the supramolecular organization of photosystem II in higher plants. *The Plant Journal* 65:368-381

## **Others:**

S. Nellaepalli, O. Zsiros, T. Tóth, V. Yadavalli, G. Garab, R. Subramanyam, L. Kovács (2014) Heat- and light-induced detachment of the light harvesting complex from isolated photosystem I supercomplexes. *Journal of Photochemistry and Photobiology B: Biology* 137:13-20

R. Ünneper, O. Zsiros, K. Sólymosi, L. Kovács, P. Lambrev, T. Tóth, R. Schweins, D. Posselt, N. K. Székely, L. Rosta, G. Nagy, G. Garab (2014) The ultrastructure and flexibility of thylakoid membranes in leaves and isolated chloroplasts as revealed by small-angle neutron scattering. *Biochimica et Biophysica Acta* In press doi: 10.1016/j.bbabi.2014.01.017

S. Krumova, S. Laptinok, L. Kovács, T. Tóth, A. van Hoek, G. Garab and H. van Amerongen (2010) Digalactosyl-diacylglycerol-deficiency lowers the thermal stability of thylakoid membranes. *Photosynthesis Research* 105:229-242

T. Tóth, Volha V. Chukhutsina, S. Krumova, Z. Gombos, H. van Amerongen (2010) Fluorescence lifetime imaging microscopy of *Synechocystis* WT cells – Variation in photosynthetic performance of individual cells in various strains of sp. PCC 6803. *Proceedings of the 15th International Conference on Photosynthesis. Photosynthesis Research for Food, Fuel and the Future; Advanced Topics in Science and Technology in China 2013*, pp 139-142

**Education Statement of the Graduate School**  
**Experimental Plant Sciences**

The Graduate School  
**EXPERIMENTAL  
PLANT  
SCIENCES**



**Issued to:** Tünde Tóth  
**Date:** 3 September 2014  
**Group:** Biophysics, Wageningen University & Research Centre

<b>1) Start-up phase</b>	<u>date</u>
▶ <b>First presentation of your project</b> The overall organization of thylakoid membranes - LHClI and lipid mutants	Mar 10, 2010
▶ <b>Writing or rewriting a project proposal</b> Writing a review or book chapter	
▶ <b>MSc courses</b>	
▶ <b>Laboratory use of isotopes</b>	

*Subtotal Start-up Phase*      1.5 credits\*

<b>2) Scientific Exposure</b>	<u>date</u>
▶ <b>EPS PhD student days</b> EPS PHD Student day, Leiden	Nov 29, 2013
▶ <b>EPS theme symposia</b> EPS Theme 3 'Metabolism and Adaptation', Wageningen	Mar 11, 2014
EPS Theme 1 'Developmental Biology of Plants', Wageningen	Jan 24, 2014
▶ EPS Theme 4 'Genome Biology', Wageningen	Dec 13, 2013
▶ <b>NWO Lunteren days and other National Platforms</b> NWO-ALW Meeting Experimental Plant Sciences, Lunteren	Apr 14-15, 2014
▶ <b>Seminars (series), workshops and symposia</b> Light Harvesting Processes, Banz, Germany	Apr 07-11, 2013
Photons for Fuel & LaserLaB Symposium, Amsterdam, The Netherlands	Dec 07, 2012
Photoprotection in cyanobacteria, Paris, France	Jun 14-15, 2012
Biophysica seminar series, WUR, Laboratory of Biophysics	2010
Seminar series Institute of Plant Biology, Szeged	2009, 2011
Visegrad Cooperation network meeting, Tata, Hungary	Feb 15-18, 2010
13th All India Cell Biology Conference and Workshop on Cell Cycle Regulation, Hyderabad, India	Dec 10-13, 2009
▶ <b>Seminar plus</b>	
▶ <b>International symposia and congresses</b> Harvest Marie Curie ITN final meeting, Chania, Greece	Sep 22-24, 2013
The 16th International Congress on Photosynthesis -Light harvesting satellite, St Louis, USA	Aug 08-11, 2013
8th EBSA European Biophysics Congress, Budapest, Hungary	Aug 23-27, 2011
Harvest Marie Curie ITN meeting, Venice, Italy	Sep 22-24, 2010
▶ <b>Presentations</b> Presentation: EPS Theme 3 'Metabolism and Adaptation', Wageningen	Mar 11, 2014
Presentation: Harvest Marie Curie ITN final meeting, Crete, Greece	Sep 22-24, 2013
Poster: The 16th International Congress on Photosynthesis -Light harvesting satellite, St Louis, USA	Aug 08-11, 2013
Poster: Light Harvesting Processes, Banz, Germany	Apr 07-11, 2013
Poster: Photons for Fuel & LaserLaB Symposium, Amsterdam, The Netherlands	Dec 07, 2012
Poster: 8th EBSA European Biophysics Congress, Budapest, Hungary	Aug 23-27, 2011
Poster: XXXIII. All India Cell Biology Conference and Workshop on Cell Cycle Regulation, Hyderabad, India	Dec 10-13, 2009
Poster: IX. Congress of the Hungarian Society of Plant Biology, Szeged, Hungary	Jul 07-09, 2008
▶ <b>IAB interview</b>	
▶ <b>Excursions</b>	

*Subtotal Scientific Exposure*      20.0 credits\*

<b>3) In-Depth Studies</b>	<u>date</u>
▶ <b>EPS courses or other PhD courses</b> Protected Plants of Hungary and the European Union, Universitas Scientiarum Szegedediensis	Sep -Dec 2011
EBSA Biophysics course on: Membrane Biophysics and Lipid/Protein Interaction, Arcachon, France	Jun 06-11, 2010
PhD lecture course on Fluorescence Sensing by Alexander Demchenko, Pécs, Hungary	14-19 Sep 14-19, 2009
FEBBS Practical Course Structure, Folding and Dynamics of Proteins and Their Complexes, Budapest, Hungary	Sep 02-09, 2009
Role of lipids in photosynthetic organisms, Universitas Scientiarum Szegedediensis	Sep-Dec 2009
Molecular Cell Biology I. -II., Universitas Scientiarum Szegedediensis	Sep 2009-Jun 2010
▶ <b>Journal club</b>	
▶ <b>Individual research training</b> Training at the laboratory of Prof. Alfred Holzwarth, Mülheim ad Ruhr, Germany	Sep 01-Sep30, 2013
Training at the laboratory of Dr. Mark Aurel Schoettler, Potsdam, Germany	Apr 15-Jun 28, 2012
Training at the laboratory of Dr. Rajagopal Subramanyam, Hyderabad, India	Nov 13-Dec 26, 2009
Training at the laboratory of Prof. Wolfgang Schröder, Umea, Sweden	Jul 15- Jul 25, 2009

*Subtotal In-Depth Studies*      13.8 credits\*

<b>4) Personal development</b>	<u>date</u>
▶ <b>Skill training courses</b> The Essentials of Scientific Writing and Presenting (EPS)	Dec 2013
Business aspects of Biotechnology, Universitas Scientiarum Szegedediensis, Hungary	Sep-Dec 2011
Training Course English Scientific Writing, Venice, Italy	Sep 24-26, 2010
▶ <b>Organisation of PhD students day, course or conference</b>	
▶ <b>Membership of Board, Committee or PhD council</b>	

*Subtotal Personal Development*      3.3 credits\*

<b>TOTAL NUMBER OF CREDIT POINTS*</b>	<b>38.6</b>
---------------------------------------	-------------

Herewith the Graduate School declares that the PhD candidate has complied with the educational requirements set by the Educational Committee of EPS which comprises of a minimum total of 30 ECTS credits

\* A credit represents a normative study load of 28 hours of study.